

MECHANICS
of
AIRCRAFT STRUCTURES

*This book is produced in full compliance
with the government's regulations for con-
serving paper and other essential materials.*

Mechanics

Aircraft Structures

PUBLISHED FORMERLY UNDER THE TITLE
STRUCTURAL DESIGN OF METAL AIRPLANES

BY

JOHN E. YOUNGER

*Professor and Chairman of Mechanical Engineering, University
of Maryland; Formerly Senior Aeronautical Engineer,
Wright Field; Consulting Aeronautical Engineer;
Chairman of Aviation Division, A.S.M.E.*

SECOND EDITION
THIRD IMPRESSION

McGRAW-HILL BOOK COMPANY, INC.
NEW YORK AND LONDON
1942

MECHANICS OF AIRCRAFT STRUCTURES

COPYRIGHT, 1935, 1942, BY THE
MCGRAW-HILL BOOK COMPANY, INC.

PRINTED IN THE UNITED STATES OF AMERICA

*All rights reserved. This book, or
parts thereof, may not be reproduced
in any form without permission of
the publishers.*

THE MAPLE PRESS COMPANY, YORK, PA.

*To Those
Pioneers in Aeronautical Development
Who Set the Pace of Progress
at*

WRIGHT FIELD

*and
Who Now Have Become the Country's Leaders
in Designing, Building, and Flying
the World's Finest
Airplanes*

PREFACE

"When we predict that great air liners will ply the upper regions of the stratosphere at incredible speeds, with great comfort and absolute safety, we are not making a broad guess. We know that this is certainly something we shall see in our own generation. While we feel certain that such developments as these will occur, we do not claim that these extremes will be obtained by virtue of *our present materials, our present types of engines, our present types of propellers, our present types of structures, or our present knowledge of aerodynamics, aviation psychology, and aviation medicine.* There of course will be progress in all these phases which, on the basis of our present knowledge, we cannot now conceive of. In one of our schools now, there may be a young engineer who will someday revolutionize our present conception of the aircraft engine and, like young Otto or Diesel, open new possibilities for power development. Possibly in our schools there is another young engineer who may some day show us how to combine metals to produce materials that will far surpass anything that the world now dreams of. Undoubtedly, new methods for cheaper production of known materials will be discovered. New ideas of fabrication now beyond our comprehension will certainly make our present methods appear as crude as the methods of twenty years ago appear to us now.

"We naturally think in terms of ideas that have germinated and then been cultivated by intensive research until they have grown into our everyday life.

"The germination of new methods, ideas, and principles very often originates with young people in the course of the research required for their graduation from a university or for higher degrees. These young people have more imagination than older ones who are limited by their experiences. *They*, not knowing that a thing cannot be done, go ahead and do it.

"*Always remember that a high standard of airplane design can never be higher than the standard of its designing engineers.* Our aeronautical engineers of the present generation are good, but the

engineers of the next generation must be much better. The engineers of the next generation are now students." Quotation from a paper presented by the author upon the receipt of the Spirit of St. Louis Gold Medal, 1941, "For Meritorious Service in the Advancement of Aeronautics."

This quotation expresses the spirit of this text—a faith in the capacity of the younger generation to be critical and dissatisfied with our present methods and to seek constantly for improvement—for that way progress lies.

About 40 per cent of this text is a revision of "Structural Design of Metal Airplanes." It was found necessary because of our great progress and expansion in airplane construction to limit the text strictly to the mechanics of the structure, the treatment of the broad field of design being kept to a minimum.

The author gratefully acknowledges the cooperation of the many aeronautical firms and governmental agencies in supplying material for this text (credit is given for specific contributions throughout the book) and the valuable assistance of J. C. Hege in the preparation of many of the illustrations and design charts and of Ruth Gladys Sauer in the preparation of the manuscript.

JOHN E. YOUNGER.

UNIVERSITY OF MARYLAND,
COLLEGE PARK, MD.,
June, 1942.

CONTENTS

	PAGE
PREFACE	vii
CHAPTER	
I. Design Requirements.	1
II. Materials of Fabrication	17
III. Summary of Basic Stress Formulas.	32
IV. Structures, Past, Present, Future	57
V. Properties of Structural Sections.	83
VI. Fundamentals of Structural Analyses.	102
VII. Beams, Columns, and Beam Columns	130
VIII. Continuous Beams and Continuous Beam Columns	162
IX. Analysis of Torsion Members	178
X. Elementary Principles of Design of Sheet-metal Construction	196
XI. Design of Flat Reinforced Plate Structures	227
XII. Design of Curved Reinforced Plate Structures.	241
XIII. Design of Thin-walled Columns and Stringers.	269
XIV. Torsional Rigidity of Wing Box Beams.	287
XV. Introduction to Cantilever-wing Analysis.	300
XVI. Design of Thin-sheet Wing Webs	316
XVII. Introduction to Shear Lag	329
XVIII. Problems in Fuselage Design	338
XIX. Pressure-cabin Structural Design	352
XX. Wing Flutter and Other Structural Vibrations.	366
XXI. Riveting in Aircraft Construction	375
INDEX,	391

MECHANICS OF AIRCRAFT STRUCTURES

CHAPTER I

DESIGN REQUIREMENTS

1:1. Structural and Aerodynamic Efficiency.—In airplane design, we should constantly bear in mind that any airplane represents a compromise between aerodynamical and structural efficiency. For example, a monoplane with a very thin wing section might be, for certain flight conditions, an ideal type of

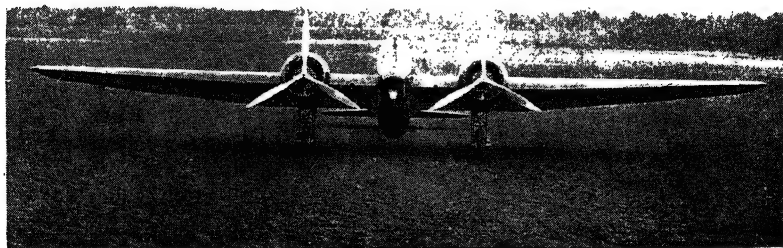


FIG. 1:1.—Martin Army Model XB-10. First high-speed bomber. Pioneering design in all-metal stressed-skin construction in the United States. (Courtesy of the Glenn L. Martin Company.)

airplane, yet it would be structurally impractical to build, for the weight would be prohibitive. While the braced-wing airplane is probably the most efficient structurally, it is inefficient aerodynamically because of the drag of the bracing which is exposed to the air stream. Structurally the efficiency ratio may be expressed as the *ratio of strength to weight*. Aerodynamically, the efficiency ratio is expressed as the *ratio of lift to drag*.

The present trend of design is to give precedence to aerodynamic efficiency. This trend offers a real challenge to the ingenuity of future structural designers.

1:2. General Specifications.—Design elements that the engineer must consider may be listed as follows:

I. LOADS TO BE CARRIED

1. *Crew.*—Pilot, assistant pilot, radio operator, mechanics, and attendants.
2. *Fuel and oil.*—Depend upon range of operation.
3. *Equipment.*—Instruments, radio, lavatories, seats, and other accommodations.
4. *Pay load.*—Passengers, mail, baggage, and express.

II. PERFORMANCE DESIRED

1. *Cruising speed.*—This item depends upon the purpose of the airplane. Economy may be the deciding factor in some cases; in other cases, such as for high-speed passenger transportation, high speed is the criterion.
2. *Landing speed.*—It is desirable from the standpoint of safety to have the landing speed as low as possible.
3. *Rate of climb.*—This enhances safety after take-off.

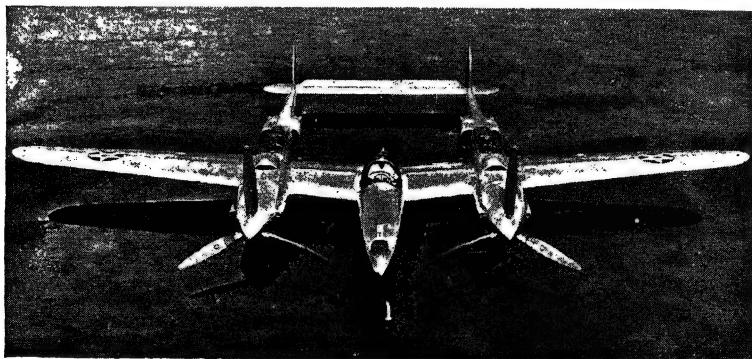


FIG. 1:2.—The P-38 Interceptor Pursuit, the U.S. Army Air Corps plane believed to be the fastest in the world. (Courtesy of Lockheed Aircraft Corporation.)

4. *Service ceiling.*—This is important in clearing mountain ranges and low weather disturbances.
5. *Range.*—This determines fuel load.
6. *Maneuverability.*—This is a major requirement in fighting planes.

III. POWER PLANT AVAILABLE

1. *Power to be used.*
2. *Number of power units.*
3. *Type of engine.*—Air-cooled, water-cooled, or chemically cooled.
4. *Geared or direct drive.*
5. *Supercharged or nonsupercharged.*

IV. TYPE OF PROPELLER

1. *Material*.—Wood, fiber, duralumin, or steel.
2. *Arrangement*.—Two-bladed, three-bladed, or four-bladed; controllable pitch, constant speed.

V. STRUCTURAL ARRANGEMENT

1. *Biplane or monoplane*.—There is a variation of opinion as to the merits of each of these.

2. *Disposition of tail surfaces*.—This depends upon general structure—whether monoplane, biplane, etc. For single-engined ships, the monoplane

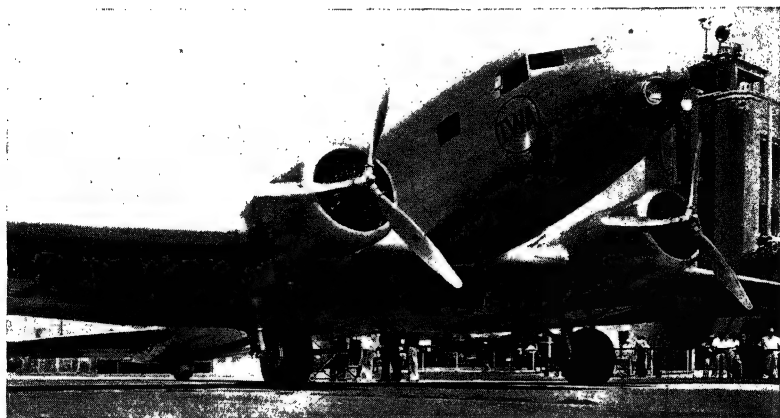


FIG. 1:3.—Douglas Air Liner; all-metal stressed-skin construction. (Courtesy of Transcontinental and Western Air.)

tail is generally used. For multi-engined ships, two or three fins and rudders are often necessary.

3. *Landing-gear arrangement*.—Retractable or otherwise.
4. *Fuselage*.—Shape and arrangement.
5. *Cabin*.—Interior arrangement.

VI. FACTOR OF SAFETY AND DEGREE OF RELIABILITY

Government requirements ensure certain safety precautions. The designer should, however, especially in the design of transport airplanes, consider safety as the first prerequisite in design.

VII. AERODYNAMIC CONSIDERATIONS

1. *Fineness ratio*.—Performance characteristics are improved by a "clean" design. This consists in eliminating protuberances as much as possible and forming or streamlining those which must be outside.

2. *Stability*.—Probably, in time, no airplane will be considered satisfactory that is not positively stable laterally, directionally, and longitudinally under all flight conditions.

3. *Controllability*.—This implies the proper design of controls and control surfaces.

VIII. WEIGHT

Weight saving is said to be the principal worry of aeronautical engineers. This implies careful and accurate structural design.

IX. MATERIALS

The principal materials now used are wood, steel, plastics, aluminum alloys, steel alloys, and magnesium alloys.

1:3. Special Requirements.—For each purpose of an airplane there is a specific set of requirements for its design. As an example of such requirements, consider those for a transport airplane. A brief summary of the major specifications presents its own story of the complex nature of the problem. It is impossible to list these in order of importance, since opinions differ as to the most important considerations. Similar lists may be prepared for other types of airplanes.

SPECIAL REQUIREMENTS FOR THE DESIGN OF TRANSPORT AIRPLANES

1. *Minimum first cost*—requiring a minimum of capital invested.
2. *Small size*—requiring a minimum amount of housing facilities. This again reduces the capital invested. Note that “small” is relative.
3. *Simplicity of construction and assembly*—to permit quick and adequate servicing.
4. *Rugged structure and power plants*—requiring a minimum of repair and maintenance and permitting a maximum number of hours per day in the air.
5. *Maximum structural strength*—to sustain the most severe aerodynamical load that may be imposed in the air or in landing or take-off conditions in bad fields.
6. *Minimum gross weight*—for maximum performance in climb and ceiling, etc.
7. *Minimum parasite resistance*—for a maximum cruising speed.
8. *Reasonable wing loading*—for a not too excessive landing speed and good performance and handling qualities at the altitudes at which the airplane may be operated.
9. *Maximum of power available*—for the allowable gross weight; also, for best climb and take-off speed.
10. *Maximum of comfort for passengers*.
11. *Maximum of comfort for pilots*—good vision from the cockpit and logical arrangement of controls and instruments.

12. *Adequate and easily accessible cargo space*—for pay load other than
13. *Adequate gas capacity*—sufficient to make longest probable trip against a probable prevailing head wind.
14. *Installation of best available aids to navigation*—including radio.

1:4. Ultimate-strength Requirement.—The ultimate strength of materials is the basis of structural-strength analyses in this country. This requirement is the outgrowth of early attempts to produce theoretically the breaking-strength loads that were obtained by static testing of airplanes. This requirement imposes a heavy burden on the stress analyst because no theoretical process of analysis has been devised for calculating stresses above the proportional limit of the material. The mathematical theory of elasticity, in which field we find our engineering formulas, is based on Hooke's law of the *proportionality of stress and strain* and hence does not apply above the proportional limit of the material. The student is warned that the value of the modulus of elasticity is constant only below the proportional limit of the material.

1:5. Flexibility, Rigidity, and Strength.—Except for the last few years, practically no consideration has been given, in government requirements, to the flexibility and rigidity of the component parts of aircraft. However, as one of our prominent engineers recently stated, "The problem of designing a structure so that there will be sufficient rigidity to resist all vibratory or fluttering influences is a problem which is really more difficult than the strength problem."

There is a great deal of difference between *rigidity* and *strength*. A structure may be very rigid, yet very weak. It may be very strong, yet very flexible. Numerous engine-mount designs have proved sufficiently strong but quite flexible—so flexible, in fact, that the operations of the engines were very unsatisfactory. Flexibility, in this particular case, may be desirable; yet we should recognize the fact that the question of flexibility does occur and is a very important consideration.

The design of the mountings of engines so that they will have the proper degree of flexibility illustrates the importance of this problem. If the engine is built rigidly into the nacelle or into the fuselage, quite naturally, then, all the vibratory stress will be transmitted directly to the airplane structure. On the other

hand, if the engine is attached to the fuselage through the medium of springs or rubber bearings, the engine will oscillate as a unit and the stress will not be transmitted directly to the airplane structure. In the first case, that of the rigid structure, the stress in the structure that is required to hold the engine will be excessive. On the other hand, in the case of the flexibly mounted engine, the vibrations on the engine will be so great that parts of the engine may actually be shaken off. Cases have been

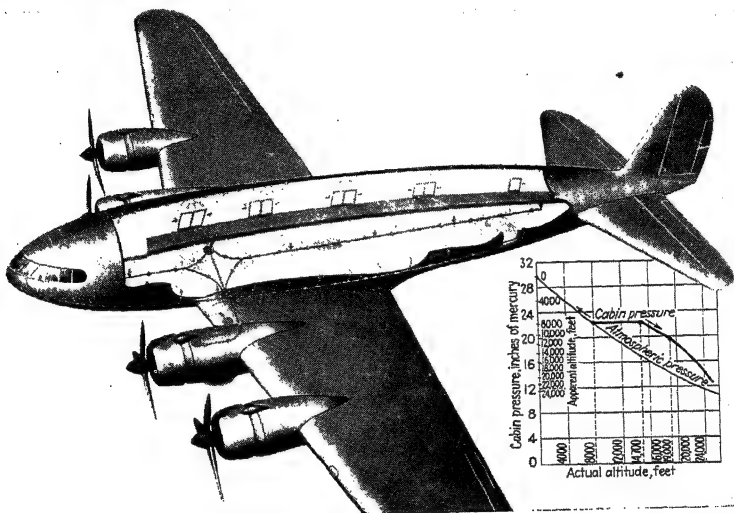


FIG. 1:4.—The Boeing Stratoliner, the first pressure (supercharged) cabin airplane to be used in commercial service. (Courtesy of the Boeing Airplane Company.)

known where the magneto and the carburetor and other accessories have been thrown off. In designing the supports for the engine, this question has to be decided, and we must strike a happy medium among the problems of *strength*, *flexibility*, and *rigidity*.

1:6. Weight as Affected by Size.—The weight of geometrically similar bodies varies as the cube of corresponding dimensions. For example, if a cubical block is doubled in size, that is, if each edge is doubled in length, its volume and weight will be eight times the volume and weight of the original block. Likewise, an airplane doubled in size will be eight times as heavy, assuming,

of course, that geometrical similarity is maintained. An airplane doubled in size, however, has only four times the wing area. Assume, for example, a 1,400-lb. airplane with an effective wing area of 100 sq. ft. and a wing loading of 14 lb. per square foot. If the airplane is doubled in size, its weight will be 11,200 lb. and its effective wing area will be 400 sq. ft. The wing loading will therefore be 28 lb. per square foot.

1:7. Pressure Cabins.—The trend in military operations and transport travel is toward higher altitudes. During 1935 to

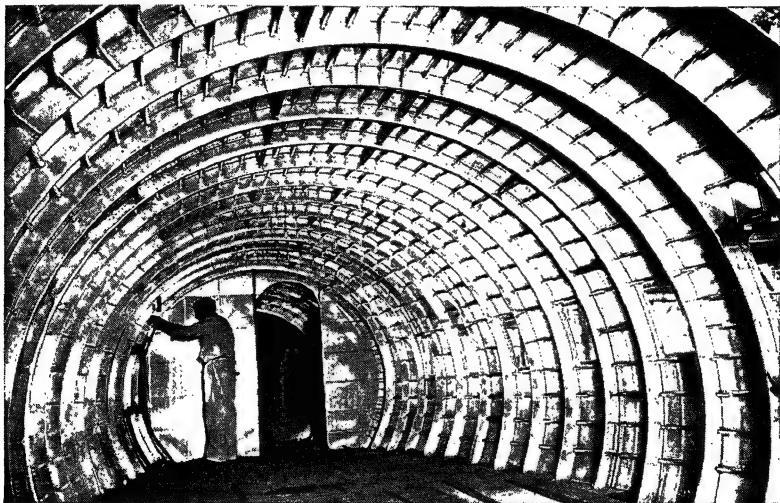


FIG. 1:5.—Fuselage structure of Curtiss Wright Model No. 20, designed for pressurization. (Courtesy of Curtiss Wright Corporation.)

1938 the U.S. Army Air Corps developed the XC-35, the first successful pressure- (supercharged) cabin airplane. In 1938, the Air Corps was awarded the Collier Trophy for this development.

At present, pressure cabins are used in both military and commercial airplanes.

Figure 1:4 shows the altitude conditioning in the Boeing Stratoliner, the first pressure-cabin airplane to be operated commercially. The diagram depicts the ventilating system in the sealed cabin of the 33-passenger ship. Fresh air is drawn through the leading edge of each wing, compressed by two engine-driven superchargers, and circulated through the cabin. Spent air is discharged through an exhaust chamber below deck.

The graph shows the cabin pressure at various altitudes in comparison with the actual atmospheric pressure. The graph is based on operation at a pressure differential of $2\frac{1}{2}$ lb. per square inch between inside and outside air.

Cabin supercharging, or *pressurization*, as it is sometimes called, opens an entirely new field for the structural designer. The author has given the new problems introduced by pressurization special consideration in Chap. XIX.

1:8. High Speeds.—Increasingly high speeds of aircraft impose new problems on the structural designer. The tendency is toward minimum thicknesses for wings, increased wing loading, satisfactory vibration and flutter characteristics, and the retention of wing-surface smoothness at all air loads.

Table 1:1 shows a study made by F. Flader and E. R. Child, engineers of the Curtiss Airplane Division of the Curtiss Wright Corporation, on what we may expect of airplanes as the speed is increased.

TABLE 1:1.—STUDY OF HIGH-SPEED AIRPLANES

Airplane designation.		A-1	B-1	C-1
Gross weight, lb.	6,000	11,200	15,800	20,600
Power, hp.	1,150	2,300	3,450	4,600
Wing area, sq. ft.	110	167.5	211	252
Tail surface area, sq. ft.,	39	59.5	75	89.5
Span, ft.	28	34.6	39	42.6
Length, ft.	22	31.9	36	38.4
Wing loading.	54	67	75	82
Stalling speed, m.p.h.	84	93	99	103
Maximum speed, m.p.h.	482	520	545	563

Note the increase of wing loading from 54 lb. per square foot to 82 lb. per square foot. The present maximum wing loading is between 40 and 50 lb. per square foot. Also note the increase of the stalling speed.

1:9. Loads Imposed on an Aircraft Structure.—It is quite obvious that, to design the structure of an airplane, it is necessary to know the loads which will be imposed upon the structure in order that we may determine the stresses in the members and hence determine the sizes of the members to carry the loads. A general classification of these loads is as follows:

1. *Air loads* on the main part of the structure, such as the wing and the fuselage, and upon the control surfaces, such as ailerons, elevators, and rudders.

2. *Static loads* other than air loads, such as loads in handling, taxiing, and landing.

3. *Dynamic loads*—any loads that involve the acceleration of the parts or of the complete airplane. These accelerations, of course, are encountered in maneuvers such as looping, spinning, diving, and landing.

1:10. Strength Criterion of Design.—What are the design conditions pertaining to air loads, static loads, and dynamic loads



FIG. 1:6.—The final assembly department is where the engines and planes are assembled to the fuselage. Subassemblies such as making up dashboards, installing radios, and checking hydraulic landing-gear operations take place in this department. As the planes roll off the end of this line, they are flown from the runway to the Buffalo Municipal Airport, where they are accepted by the pilots of the U. S. Air Corps. (Courtesy of Curtiss Airplane Division, Curtiss Wright Corporation.)

that would produce a satisfactory type of structure in the airplane? This is not an easy question to decide. As a matter of fact the question has never been definitely decided. It is probably the most discussed of all problems of design. The criteria set down by the Civil Aeronautics Administration, the Army Air Corps, and the Navy Bureau of Aeronautics

were evolved after years of practical experience, industry, and careful consideration on the part of a great many aeronautical engineers; they probably represent a fairly accurate picture of the loads that are actually imposed upon the airplane in flight. These conditions number approximately 15 to 20. That is, to satisfy the government agencies, it is necessary to analyze an airplane structure for strength on the basis of approximately 15 to 20 conditions. The design of each member in the structure is ordinarily based upon the maximum load, positive or negative, that may be incurred by that member under any one of the conditions of operation. It is quite obvious, also, that, if an airplane is designed for the exact condition of loading which may be incurred in flight, there may be a possibility of a slight weakness in some material of construction or a weakness due to corrosion or some other cause, so that the strength of the airplane may drop below the standard for which it is designed. Thus these conditions should also be provided for in the criterion of design.

1:11. Other Types of Loads.—Other types of loads that may be allowed for in a design are:

1. Unsymmetrical wing loading as in a "barrel roll."
2. Effect of air gusts.
3. Engine torque.
4. Stabilizer and elevator loads.
5. Fin and rudder loads.
6. Drop in a "pancake" landing.
7. Gyroscopic effect of propeller and engine.
8. Vibration of engine, propeller, or other parts.
9. Wing fluttering, tail fluttering, etc.
10. Pressure-cabin loads.

1:12. Load Factors.—In stress analyzing the average engineering structure, the maximum load that may occur on the structure is first determined. This maximum load is then multiplied by a certain *factor* which produces a *design load*. This factor is designated as the *factor of safety*. In aircraft work, we have no such factor as defined. If we should use a factor of safety, as defined, it is quite obvious that the airplane would be so heavy that it would not fly properly. Instead of a factor of safety in aeronautical engineering, we use what we call a *factor of loading*. In using this factor of loading, the loads in the members are determined for normal maneuvers, that is, level flight or

normal landing conditions. These loads are then multiplied by the factor of loading to determine the design load. Load factors as used today are based mostly upon experience and very little upon theory. The problem of load factors is probably the most outstanding aeronautical engineering problem yet to be solved. The most fundamental question arising in the design of a new airplane is: How much stronger than the actual strength required for normal operating conditions shall we make the structural parts of this airplane?

1:13. Distribution of Air Loads.—The distribution and magnitude of air loads on wings, fins, and control surfaces for design maneuvers are, of course, the basis for design for flight conditions. An enormous amount of experimental work has been done to find a rational basis for determining the air loads. The student is advised to study reports on such air-load experiments and to compare their findings with the government handbook requirements. The field of study is one that properly belongs to books on aerodynamics rather than to books on structures.

1:14. Classification of Airplane-design Work.—Airplane-design work may be classified under three main heads, namely:

- A. Design.
 - 1. Project design.
 - 2. Detailed design.
- B. Stress analysis.
 - 1. Stress analysis of the primary structure.
 - 2. Stress analysis of secondary parts.
- C. Drafting.
 - 1. Layout.
 - 2. Detailed.

Actual design work is generally carried out under the direction of a project engineer who is directly responsible to the chief engineer of the factory. Project-design work is usually handled by a graduate aeronautical engineer and includes not only structural design but also aerodynamic and economical design problems. The detailed design is usually performed by a draftsman qualified for this work. Detailed design consists of the design of small parts.

Stress analyses are usually performed by stress-analysis experts under the supervision of a competent engineer. Drafting, of course, is performed by competently trained draftsmen.

An analysis of the aircraft manufacturing industry in this country shows that the aeronautical engineering positions are divided approximately as follows:

Aircraft-manufacturing Personnel	Per Cent
1. Aerodynamic engineers.....	3
2. Structural engineers.....	8
3. Project engineers.....	3
4. Weight-control engineers.....	4
5. Preliminary designers.....	2
6. Layout designers.....	8
7. Detail designers.....	50
8. Draftsmen, blueprinters, etc.....	22
Total.....	100

Workers numbered 2 to 7 above require an intimate knowledge of the fundamental principles of aircraft structural design and stress analysis. This group includes 75 per cent of the entire personnel, draftsmen and blueprinters being classed as engineers. If this last division is omitted, the structural-design group constitutes about 97 per cent of all aeronautical engineers.

1:15. Specifications.—A proposed job of airplane design first comes to the attention of the engineer in the form of *specifications*. The proposed airplane may be of conventional design, or it may be new and a radical departure from conventional models. Thus a general outline of procedure may not be applicable in every case, but it will at least give some ideas of the steps that are to be followed in the design. The object of the airplane and its characteristics are set forth in the specifications for the job; for example, the order may be for a very high speed mail-plane, a low-speed freight plane, a high-altitude plane, or a small sport plane. These specifications being assigned, we proceed as follows:

1:16. Structural Characteristics.—We determine the characteristics of the ship in regard to the structure; that is, we determine whether the airplane should be a biplane or monoplane, whether it is to be of wood and fabric construction or all metal, etc. These characteristics may also be specified in the order. When these characteristics are determined for the required specifications, we must then decide upon the power plant.

1:17. Power Plant.—Power plants are not designed for any specific airplane; consequently, we must buy our power plants to fit our job. Of all the power plants that are available we must

determine the most desirable for the particular job, taking into consideration the characteristics of the power plant, the cost, etc.

1:18. Preliminary Sketches.—When the size and characteristics of the motor or motors are determined, then it is desirable to make a *preliminary sketch* of the airplane, incorporating all the principal parts. In this sketch the engineer should give careful consideration to the artistic appearance of the job. In general an airplane that is nicely streamlined and pleases the eye is also high in efficiency.

It is obvious that these preliminary drawings may be changed and that we may not be able to build the airplane as pleasing to the eye as the preliminary drawings indicate; we vary, however, as little as possible from the preliminary sketch of the job in order to incorporate the proper structural characteristics.

Obviously the structural and aerodynamic features must be satisfied, as they are of primary importance. The finished product should be a judicious compromise among the *artistic*, *aerodynamic*, and *structural*.

1:19. Preliminary Weight Estimate.—It is quite obvious that the strength of the structure will determine the weight of the structure. The weight of the structure, to a great extent, will determine the strength requirement. Each depends upon the other. There is no direct solution of the problem. At first we can determine only approximately what the weight of the structure will be; when we calculate the actual size of the members in the structure, so that we may determine the actual weight of the structure, we must revise our preliminary weight estimate. Now, for the purpose of making the preliminary weight estimate, we have the benefit of the experience of designers who have made a study of weight. For example, we have data available, assuming we are designing a conventional type of airplane, on the proportional weight of the fuselage to the total weight, the proportional weight of the empennage, etc. Consequently we can form some judgment as to the proper distribution of the total weight of the airplane among the component parts. The total of these distributed weights equals the weight of the airplane as originally predetermined or estimated (see handbooks for weight estimates).

1:20. Airfoil-section Requirements.—With the preliminary weight estimate made, we can then determine the airfoil section

required to carry this weight and execute the desired performance in regard to the speed, the lift, the rate of climb, etc. Having determined the airfoil section, we then carry out preliminary calculations for the dimensions of the wing, such as the aspect ratio, area of the wings, and other characteristics pertaining to the wing structure.

1:21. Preliminary Drawing.—We now make a preliminary side-view sectional drawing of the airplane for the purpose of obtaining the relative location of the airplane parts, cargo, and personnel; these will include the wings, engine, pilot, passengers, tail surfaces, landing gear, etc.

1:22. Preliminary Installation Drawing.—The next step is to complete the side-view drawing, in which we designate the location of instruments, gas tanks, fighting equipment (if it is a military plane), mail quarters (if a mailplane), etc.

1:23. Detailed Weight Estimate.—We are now ready for a more detailed weight estimate. In this weight estimate, we include such things as the instruments and other small items in the airplane which, for simplicity in calculations, would not be included in the first preliminary weight estimate, except under general headings.

It is good procedure to increase the detailed weight estimate by about 5 per cent to account for small items neglected in the estimate.

1:24. Balance Analysis.—The center of gravity of the airplane must be located with a definite relationship to the center of lift of the wings. This requires a balance analysis. With reference to a V - (vertical-) and H - (horizontal-) axes coordinate system, with the origin fixed relative to the airplane, we may find, by the application of the principle of moments, \bar{V} and \bar{H} , the coordinates of the center of gravity, thus,

$$(1:1)$$

and

$$(1:2)$$

in which W is the weight of the part under consideration and H and V are the coordinates of the center of gravity of the part.

1:25. Revised Side-view Drawing and Balance Diagram.—We next revise the side-view drawing and balance diagram, more

accurately locating the landing gear, wings, etc. It is apparent that, when the balance diagram, which also includes the wings and landing gear, is completed, it may be found more desirable to move the wings and landing gear than it is to move some part of the airplane structure or some part of the useful load. We may find it desirable to move the wings backward or forward slightly to ensure that balance and stability are properly maintained.

1:26. Design and Location of Ailerons and Tail Surfaces.—

This problem is mostly a study in aerodynamics at this stage of the design. Data are available in texts and handbooks on the size, proportion, shape, and other features of airfoils affecting the stability and control of the airplane.

1:27. Final Three-view Drawing.—With the principal design details of the general layout determined, a final three-view drawing may be made. Certain complications may arise, however, which may necessitate later changes in these drawings.

1:28. Estimation of Performance.—With the weights, sizes, and shapes now practically fixed, it is desirable to make a careful check of the performance to see that the specifications have been met.

1:29. Determination of Characteristics of Wing Structure.—

It is necessary to determine, first, the air loading on the wings in the required loading conditions, and then the loads in the assumed structural parts of the wing, before the exact design of the parts can be made. The general type of construction may probably be determined by specification. It remains for the designer to determine sizes and other details. This requires a stress analysis.

1:30. Determination of the Characteristics of the Fuselage Structure.—The general type of construction of the fuselage may be determined by specifications. It is probable, at least, that the type and general plan have been determined before this stage is reached. It is necessary, therefore, for the designer to determine sizes and other details. This requires a stress analysis.

1:31. Determination of the Characteristics of Tail-surface Structures and Ailerons.—In general, the types of these structures would have been determined previously; consequently, only the sizes, special arrangements, and details must be determined at this stage. This too requires a stress analysis.

1:32. Detail Design of All Structures.—The jobs may be listed as follows:

1. Wing ribs with fittings.
2. Wing spars with joints and fittings.
3. Trussing in the wings and between the wings.
4. Wing tips.
5. Fuselage bulkheads.
6. Fuselage, wing fittings, door and window reinforcements, pilot's compartment.
7. Ribs, longerons, stringers, bulkhead rings.
8. Stabilizer and fin.
9. Chassis and tail wheel.
10. Control surfaces: ailerons, elevators, rudders.
11. Control-surface controls with fittings.
12. Engine controls with fittings.
13. Electric wiring.
14. Passenger-compartment furnishing and equipment.
15. Hydraulic system.
16. Pressure-cabin equipment.

CHAPTER II

MATERIALS OF FABRICATION

2:1. General Requirements.—The materials mostly used in airplane construction are woods, plastic plywood, aluminum alloys, magnesium alloys, and strong alloys of steel. The materials are in general adaptable to aircraft construction in the order of their density and the weight of the airplane. For example, wood and plastic plywood are most suitable for very light structures such as soaring gliders and light training airplanes. Aluminum alloys are more appropriate for heavier airplanes such as our present transports and fighting airplanes. As the speed and wing loadings of our airplanes increase, requiring that the structure become heavier, strong alloy steels become more adaptable.

At present there is a tendency to build an airplane entirely of one material. Structurally this is inefficient. Some day we may expect to see composite airplane structures in which the material is selected for each part according to the suitability of its characteristics.

A designer must know the characteristics of his materials particularly with reference to

a. Physical properties such as strength in tension, compression, and shear; stiffness as indicated by the modulus of elasticity; toughness, hardness, fatigue strength, and weight.

b. Mechanical properties for ease of fabrication such as ductility, malleability, thermal expansion, and machinability.

c. Chemical properties with respect to durability, weldability, corrosion resistance, and uniformity of composition.

2:2. Aluminum Alloys.—The importance of aluminum and aluminum alloys in aircraft construction is demonstrated by their use. The structural weight of several successful military and transport airplanes is divided as follows:

	Per Cent
Aluminum alloys (non-heat-treatable).....	5 - 8
Aluminum alloys (heat-treatable).....	70 -80
Steel, low alloy.....	14 -18
Nickel alloys of steel, corrosion resistant.....	2 - 3
Copper alloys.....	0.3- 0.5
Miscellaneous materials.....	1 - 2

TABLE 2.1.—ALUMINUM-BASE ALLOYS*

Classification	Specifications					Chemical composition					
	Federal	U.S. Army or Air Corps	U.S. Navy	S.A.E.	Manufacturer's No.	Aluminum	Copper	Magnesium	Manganese	Iron	Silicon
Sheet and plate	QQ-A-561	57-151-1	47A2	25	2S	99.0	0.20	0.2-0.75	1.0-1.5	0.70	0.60
	QQ-A-359		47A4	29	3S	97.0	3.5-4.5	0.2-0.75	0.4-1.0		
	QQ-A-353		47A3	26	17S	92.0	3.5-4.5	0.2-0.75	0.4-1.0		
		57-152-2	47A6	24	17 Alclad	92.0	3.8-4.9	1.25-1.75	0.3-0.9		
		57-152-6	47A10	24	24 Alclad	92.0	3.8-4.9	1.25-1.75	0.3-0.9		
		11067	47A8	28	51S	97.0		0.6			1.0
	QQ-A-318	11072	47A11		52S	Rem.	0.10	2.2-2.8	0.10	FE + SI = 0.45 (max.)	†
	QQ-A-334		47A12		53S (72S)3S	Rem.	0.10	1.1-1.4		0.35	
Bar, rod, wire, and shapes	QQ-A-411		46A3	25	2S						
	QQ-A-366		46A6	29	3S						
	QQ-A-351		46A4	26	17S						
		57-152-5	46A9	24	24S						
			46A11		52S						
	QQ-A-331		46A10		53S						
Tubing	WW-T-783		44T19	25	2S						
	WW-T-788		44T20	29	3S						
		11069	44T21	20	4S						
		10235	44T28	26	17S						
	WW-T-786		44T32	24	24S						
		57-187-3	44T30		52S						
			44T30		53S						
Flexible tubing		10236	49T12		3S						
		10236	49T12		52S						
Forgings	QQ-A-367	57-153	M277	26	14S	Rem.	3.9-5.0	0.2-0.75	0.4-1.2	1.0	0.5-1.2
	QQ-A-367	57-153	46A7		17S	92.0	3.5-4.5	0.2-0.75	0.4-1.0	1.0	0.75
	QQ-A-367	57-153		27	18S	Rem.	3.5-4.5	0.45-0.9	0.20	1.0	0.90
	QQ-A-367	57-153	46A7		25S	92.0	3.9-5.0	0.03	0.4-1.2	1.0	0.5-1.2
	QQ-A-367	57-153			32S	Rem.	0.5-1.3	0.8-1.3	0.02	1.0	11.5-13.5
	QQ-A-367	57-153			A51S	96.5	0.25	0.45-0.80	0.20	1.0	0.6-1.2
	QQ-A-367	57-153	46A7		X73S	Rem.	0.90	0.75-1.00	0.20	1.0	0.7

TABLE 2:1.—ALUMINUM-BASE ALLOYS.*—(Continued).

Classification	Specifications					Chemical composition					
	Federal	U.S. Army or Air Corps	U.S. Navy	S.A.E.	Manufacturer's No.	Aluminum	Copper	Magnesium	Manganese	Iron	Silicon
Rivets and rivet wire		25526	43R5		A17S	Rem.	2.0-3.0	0.2-0.5	0.20	1.0	0.80
Welding rod	QQ-R-571 QQ-R-571		46R1 46R1		43S 99%	92.5 99.0	0.60	0.02	0.20	1.00	4.5-6.0
Wire-metal spray		10285			99%	99.0					
Sand castings		11311	46A1	35	43	93.0	0.10	0.05	0.07	0.80	4.5-6.0
		11312			108	Rem.	3.5-4.5	0.03	0.30	1.0	3.5
		57-72-1	M212	39	142	90.0	3.8-4.5	1.2-1.8	0.30	0.80	0.50
		57-72-5	46A1	38	195	92.0	4.0-5.0	0.03	0.30	1.20	1.20
		11310			212	Rem.	7.0-8.5		0.30	1.40	1.0-1.5
		57-72-4	46A1		214	94.0	0.05	3.5-4.5	0.60	0.50	0.40
		11309	M186	324	220	88.0	0.20	9.5-1.10	0.30	0.30	0.20
		11307	M212	322	355	91.0	1.0-1.5	0.4-0.6	0.30	0.50	4.5-5.5
		11308	46A1	323	356	Rem.	0.20	0.2-0.4	0.03	0.50	6.5-7.5
		57-93-1 57-93-1		307 305	85 13	Rem. Rem.	3.5-4.5 0.60	0.10 0.10	0.30 0.30	2.25 2.00	4.5-5.5 11-13
Magnesium-base Alloys											
Sheet		M111			M-AM3S§		0.05	Rem.	1.20		0.30
Bars and forgings		M126			J-AMC57S§	5.8-7.2		Rem.	0.15		0.50
Sand castings		57-74-1 57-74-1			G-AM240§ H-AM265§ AM403	9-11 5.3-6.7	0.05 0.05	89.0 Rem.	0.10 1.20		0.50 0.50 0.30

TABLE 2.1.—ALUMINUM-BASE ALLOYS. *—(Continued)

Classification	Chemical composition			Temper	Mechanical properties						
	Nickel	Zinc	Chromium		Ultimate strength, lb./sq. in.	Yield strength, lb./sq. in.	Elongation, per cent	Compressive strength, lb./sq. in.	Shear strength, lb./sq. in.	Brinell hardness, 500 kg.	Fatigue rev. bend. 500×10^6 cycles
Sheet and plate				$\frac{1}{2}$ hard	16,000	14,000	3.0				
				$\frac{3}{4}$ hard	19,500	17,000	3.0				
				H.T.	55,000	32,000	15.0				
				H.T.	50,000	27,000	13.0				
				H.T.	62,000	40,000	12.0				
Bar, rod, wire, and shapes				H.T.	56,000	37,000	12.0				
			0.25	H.T. and aged	45,000	35,000	8.0				
			0.15-0.35	$\frac{1}{2}$ hard	34,000	24,000	4.0				
		0.03	0.2-0.3	H.T. and aged	35,000	28,000	8.0				
		0.03		$\frac{1}{2}$ hard	16,000	14,000	20.0	17,000	11,000†	32	7,000†
				$\frac{3}{4}$ hard	19,500	18,000	20.0	19,500	14,000†	40	9,500
				H.T.	55,000	30,000	18.0	55,000	30,000	100	13,000
				H.T.	62,000	40,000	16.0	65,000	35,000	105	14,000
				$\frac{1}{2}$ hard	34,000	29,000	10.0		21,000†	67	19,000†
				H.T. and aged	32,000	25,000	16.0		24,000†	80	11,000†
Tubing				$\frac{1}{2}$ hard	16,000	14,000	9.0				
				$\frac{3}{4}$ hard	19,500						
				$\frac{1}{2}$ hard	32,000		10.0				
				H.T.	55,000	40,000	16.0				
				H.T.	62,000	42,000	16.0				
Flexible tubing				$\frac{1}{2}$ hard	34,000	24,000	5.0				
				H.T. and aged	35,000	28,000	16.0				
Forgings				H.T.	65,000	50,000	10.0	70,000	45,000†	130	15,000
			0-0.25	H.T.	55,000	30,000	16.0	55,000	36,000	90	13,000
				H.T.	55,000	35,000	10.0	45,000			
			T1-0.20	H.T.	55,000	30,000	16.0	55,000	35,000†	90	14,000
			0.15-0.35	H.T.	52,000	40,000	5.0	50,000	38,000†	110	14,000
				H.T.	43,000	34,000	12.0	45,000	23,000	90	10,500†
				H.T.	48,000	38,000	12.0		34,000	95	15,500
				H.T.							

TABLE 2:1.—ALUMINUM-BASE ALLOYS.*—(Continued)

Classification	Chemical composition			Temper	Mechanical properties						
	Nickel	Zinc	Chromium		Ultimate strength, lb./sq. in.	Yield strength, lb./sq. in.	Elongation, per cent	Compressive strength, lb./sq. in.	Shear strength, lb./sq. in.	Brinell hardness, 500 kg.	Fatigue rev. bend, 500 X 10 ⁶ cycles
Rivets and rivet wire								25,000			
Welding rod		0.20									
Wire-metal spray											
Sand castings	1.7-2.3			As cast	17,000	7,000	3.0	25,000	14,000†	40	5,000
				As cast	19,000		1.0	62,000	20,000†	55	8,500†
				H.T.	32,000	20,000		77,000	32,000†	100	8,000
				H.T.	32,000	18,000	3.0	50,000	30,000†	80	9,000
				As cast	19,000			64,000	20,000†	65	7,500†
				As cast	22,000	10,000	6.0	45,000	18,000	50	5,000
Die castings	0.03			H.T.	42,000	22,000	12.0	72,000	33,000†	75	7,500
				H.T.	32,000	20,000	1.0	65,000	30,000†	92	7,500
				H.T.	30,000	20,000	3.0	50,000	22,000	90	8,000
				As cast	32,000	18,000	2.0			60	17,000†
			0.75		33,000	16,000	1.5			80	15,000†
			0.75								
Magnesium-base Alloys											
Sheet			Annealed	35,000	15,000	12.0			48		
Bars and forgings		1.5	Extruded	40,000	26,000	12.0	64,000	20,500†	55	14,000	
Sand castings	0.03	0.30 2.5-3.5	H.T.	30,000	18,000	1.0	54,000	21,000§	65	9,000§	
			H.T. and aged	32,000	16,000	2.0	50,000	18,000§	62	10,000§	
	0.03		As cast	12,000		3.0					

* Ref. 1. See references listed at the end of the chapter.

† Not less than 45 per cent or more than 65 per cent of magnesium content.

‡ Aluminum Company of America.

§ Dow Chemical Company.

oped by the Society of Automotive Engineers (S.A.E.). For these steels the first digit has the following meaning:

1. Carbon steel.
2. Nickel steel.
3. Nickel-chromium steel.
4. Molybdenum steel.
5. Chromium steel.
6. Chrome-vanadium steel.
7. Tungsten steel.
8. Not yet assigned to any steel.
9. Silicomanganese steel.

For the alloy steels, the second digit signifies the average percentage of the alloying element. The remaining successive digits are the average points (0.01 per cent) of carbon content. For example:

Steel 1025 is a carbon steel with 25 points or 0.25 per cent carbon.

Steel 51236 is a chromium steel with an average of 12 per cent chromium and 0.36 per cent carbon.

2:7. Steel Alloys : Chrome-Molybdenum Steel (see Table 2:3). S.A.E. X-4130 has fulfilled the requirements of the aircraft industry for a steel that is easily fabricated by welding in the normalized condition without appreciable loss in strength and that is capable of being heat-treated to develop a wide range of mechanical properties. It is used extensively for structures, axles, tail-wheel knuckles, and stamped and forged fittings. For heavy sections, high tensile properties cannot be obtained consistently except by quenching in water. Because this may cause cracks in fittings of variable cross section, S.A.E. 4140 is more generally used for such parts. Welding is questionable if the carbon limit exceeds 0.38 per cent unless the base metal is preheated.

2:8. Stainless Steel (see Table 2:4).—Stainless steel is any one of a series of iron-base alloys containing enough chromium (at least 11 per cent) to be highly resistant to corrosion. The first commercial alloy of the series is said to have been made in 1914 by Harry Brearley, who introduced about 13 per cent of chromium to a 0.30 per cent carbon steel. This alloy, after certain heat-treatments, has excellent resistance to atmospheric corrosion and to the staining action of a number of acids and salts. Brearley's discovery centered attention on the power

TABLE 2:3.—MECHANICAL PROPERTIES AND MATERIALS OF ALLOY STEELS, X-4130*

		Normalized plate tube and bar—0.188 in. thick and under (X-4130)	Near welding when welded after heat-treatment (X-4130 special)	Normalized tubes—0.188 in. thick and under (X-4130 special)
Specification:				
Army.....		57-180-2D for tubing		
Navy.....		Round tubing 44T18 Straight tubing 44T17		
Tension:				
F_{tu}	Ultimate stress, lb./sq. in.	95,000	84,000	100,000
F_{ty}	Yield stress, lb./sq. in.	75,000		85,000
F_{tp}	Proportional limit, lb./sq. in.			
E	Modulus of elasticity, lb./sq. in.	29,000,000	29,000,000	29,000,000
	Elongation in 2 in., %			12
Compression:				
F_{cu}	Ultimate (block) stress, lb./sq. in.	95,000	76,000	100,000
F_{cy}	Yield stress, lb./sq. in.	75,000		85,000
F_{cp}	Proportional limit, lb./sq. in.			
F_{co}	Column yield stress, lb./sq. in.	79,500		90,100
E_c	Modulus of elasticity, lb./sq. in.	29,000,000	29,000,000	29,000,000
Shear:				
F_{su}	Ultimate stress, lb./sq. in.	55,000	52,500	58,000
F_{st}	Torsional modulus of rupture, lb./sq. in.	80,000	73,500	84,000
F_{sp}	Proportional limit (torsion), lb./sq. in.	40,000		
G	Modulus of rigidity (torsion), lb./sq. in.	11,000,000	11,000,000	11,000,000
Bearing:				
F_{br}	Ultimate stress, lb./sq. in.	140,000	130,000	147,000
Fatigue:				
F_{bs}	Bending endurance limit (300,000,000 cycles of completely reversed stress), lb./sq. in.	45,000		

* specific weight = 0.2833 lb./cu. in. or 490 lb./cu. ft.

* Ref. 9.

of chromium to confer corrosion resistance when used as an alloying element in steel.

Since 1914, metallurgists have developed other varieties of stainless steel, which differ widely in their characteristics. The

variety of most importance to aircraft designers is that popularly known as 18-8, which contains approximately 18 per cent of chromium, 8 per cent of nickel, and relatively low carbon, the balance being chiefly iron. Modifications of this alloy containing small percentages of columbium, titanium, molybdenum, and selenium also are used.

TABLE 2:4.—PHYSICAL PROPERTIES THAT RECENTLY PUBLISHED DATA SHOW CAN BE OBTAINED IN 18-8 CHROMIUM-NICKEL STAINLESS STEEL¹
(0.10 maximum per cent carbon)

Physical properties	Annealed	Cold-rolled
Tensile strength, lb./sq. in.	80,000–95,000	120,000–185,000 (maximum can exceed 200,000)
Yield strength at 0.2% set, lb./sq. in.	35,000–45,000	80,000–140,000
Modulus of elasticity in tension and compression, lb./sq. in.	28,000,000–29,000,000	28,000,000–29,000,000
Modulus of elasticity in shear	9,500,000	9,500,000
Endurance limit, lb./sq. in.	35,000	93,000(150,000 U.T.S.)
Weight per cubic inch....	0.286	0.284
Specific gravity.....	7.92	7.86
Melting range, deg. F....	2,550–2,590	2,550–2,590
Melting range, deg. C....	1,400–1,420	1,400–1,420

¹ Ref. 6.

2:9. Magnesium Alloys (see Table 2:5).—Magnesium is not as yet used extensively as a structural material; but when it is alloyed with aluminum, manganese, zinc, silver, and occasionally other elements such as silicon and cadmium, its mechanical properties are greatly improved and the strength-weight ratio compares favorably with that of other structural materials. These alloys have the lowest density of any of the commercial metals that are available for airplane construction. The tensile properties of the cast alloys compare favorably with many aluminum alloys, and it would be possible to replace the latter with a saving in weight of approximately 35 per cent, except for the lower modulus of elasticity, Brinell hardness, and notch sensitivity. Equal rigidity can generally be obtained by larger fillets, thicker well-supported flanges, and reinforcing ribs, and

TABLE 2:5.—MAGNESIUM ALLOYS¹

	Sheet (condi- tion A)	Sheet (condi- tion H)	Round seamless tubing	Round and square shapes up to 1½ in.	Struc- tural shapes	Round and square shapes up to 1½ in.	Struc- tural shapes	Round and square shapes up to 1½ in.	Struc- tural shapes	Sand casting (condi- tion H.T.) H.T.A.)	Sand casting (condi- tion H.T.A.)	Sand casting as cast	Die cast- ing
Specification:	11317	11317	11318	11320	11320	11320	11320	11320	11320	57-74-1	57-74-1	57-74-1	113119
Army			(grade 1)	(grade 1)	(grade 1)	(grade 1)	(grade 2)	(grade 2)	(grade 2)	(grade 1)	(grade 1)	(grade 2)	
Navy			M-366 (alloy 8)			M-366 (alloy 11)				M-112	M-112	M-112	
Tension:										(alloy 4)	(alloy 4)	(alloy 11)	
Ultimate stress, lb./ sq. in.	28,200	32,000	36,000	40,000	38,000	32,000	30,000	32,000	30,000	32,000	34,000	12,000	31,000
Yield stress, lb./sq. in.		24,000	17,000	26,000	23,000	20,000	16,000	20,000	16,000	10,000	16,000		
Proportional limit, lb./sq. in.													
Modulus of elasticity, lb./sq. in.	6,500,000	6,500,000	6,500,000	6,500,000	6,500,000	6,500,000	6,500,000	6,500,000	6,500,000	6,000,000	6,000,000	6,000,000	
Elongation in 2 in., %	12	4	7	12	10	5	3	5	3	7	3	3	2

¹ Ref. 1.

the lower hardness counteracted by using bushed holes, larger washers under boltheads, and similar methods for increasing the bearing area. Notch sensitivity is compensated for by the same methods as those used for increasing the rigidity and by avoiding sharp edges. The castings are serviceable for wheels, engine housings, brackets, and similar parts.

2:10. Plastics and Plywood (see Table 2:6 and Ref. 1).—*Plastics* are defined as moldable materials manufactured from organic compounds. This broad definition has been used to include plywood, steamed ash, and impregnated wood, but it would be preferable to avoid the use of the term for materials that are in common use under other more descriptive names. The organic plastics have been classified according to their behavior under temperature changes.

a. Thermoplastic-temperature-flow Relationship Is Reversible.—Plastics in this class can be remolded with the application of moderate heat and pressure, which permits the fabrication of shapes by the airplane builder without expensive molding equipment.

b. Thermosetting-temperature-flow Relationship Is Irreversible.—The plastic in the final stage is infusible and cannot be remolded. Plastics are available in the form of powder, liquid, semiconverted, and completely converted solids. Conversion to a usable solid form generally requires the application of heat and pressure under controlled conditions; only in special cases is this operation undertaken by the airplane manufacturer. In the case of the thermoplastic airplane dopes, solidification proceeds under normal conditions by the evaporation of solvents and plasticizers.

Thermoplastic materials that are being used in the aircraft industry are cellulose nitrate and acetate, acrylates, vinyl acetals, and styrene. These are used as coatings or fillers in combination with other materials to produce artificial leather and laminated glass and directly in the form of cast or rolled sheet and molded shapes for windows, handles, knobs, and small accessories. Polystyrene is used in the ring lighting of instruments on account of its heat resistance and ability to transmit light.

The *thermosetting resin* is phenol formaldehyde, which is used for electrical parts, instrument and gear cases, pulleys, propeller chafing bands, gears, and miscellaneous parts requiring

TABLE 2.6.—PLASTICS—AVERAGE VALUES¹

Type	Grade	Spec. No.	Specific gravity	Moisture absorption 24 hr., per cent	Tensile strength, lb./sq. in.	Flexural strength, lb./sq. in.	Compressive strength, lb./sq. in.	Modulus of elasticity, lb./sq. in. $\times 10^5$	Thermal expansion per deg. C. $\times 10^{-5}$	Resistance to heat continuous, deg. F.	Light transmission, per cent		Burning rate
											Orig.	Exp. ¹	
Phenol formaldehyde	Laminated paper base	71-484	1.4	1.3	9,500	16,000	35,000	12.5	2	260	Opaque	..	Very low
	Fabric base	71-484	1.4	1.7	10,000	20,000	38,000	10	3	280	Opaque	..	Very low
	Macerated fabric	71-484	1.4	1.5	6,500	11,000	26,000	300	Opaque	..	Very low
	Molded—no filler	71-484	1.3	0.2	7,500	14,000	8.5	250	70	..	Very low
Methyl methacrylate	Cast sheet	12014	1.2	0.4	8,500	10,000	8,000	4	8.5	125	94	90	Slow
Cellulose acetate	Roll sheet	12025	1.3	2.5	8,400	6,000	10,000	2.3	13	140	82	73	Slow
Cellulose nitrate	Roll sheet	12008	1.5	1.5	6,000	2.5	10	...	75	16	Very high
Styrene	Cast sheet	1.1	0.0	7,000	7,000	13,000	5	7.5	155	85	..	Slow
Vinyl acetals	Sheet	1.1	1.3	9,000	11,000	Opaque
Cellulose fiber	Hard vulcanized	40231	1.05	35.0	7,000	13,000	25,000	Opaque

TABLE 2.7.—COMPARISON OF APPROXIMATE PHYSICAL PROPERTIES OF REINFORCED PLASTICS, WOOD, AND METALS

Material	Weight, lb./ cu. ft.	Specific gravity	Tensile strength, lb./ sq. in.	Ratio of tensile strength to speci- fic gravity, lb./ sq. in.	Com- pressive strength, lb./ sq. in.	Ratio of com- pressive strength to speci- fic gravity, lb./ sq. in.	Modulus of elastic- ity in tension (E_t), lb./ sq. in.	Ratio of E_t to specific gravity, lb./ sq. in.	Modulus of elastic- ity in com- pres- sion (E_c), lb./ sq. in.	Ratio of E_c to specific gravity lb./ sq. in.	Coeffi- cient of thermal expansion per deg. F.
Stainless steel (18-8).....	490	7.85	185,000	23,600	150,000*	19,100	29,000,000	3,700,000	29,000,000	3,700,000	0.0000066
Chrome-molybdenum steel (heat- treated).....	490	7.85	180,000	22,900	150,000*	19,100	29,000,000	3,700,000	29,000,000	3,700,000	0.0000066
Aluminum alloy (24ST).....	174	2.80	62,000	22,100	40,000*	14,300	10,300,000	3,700,000	10,300,000	3,700,000	0.000012
Magnesium alloy (AM58S).....	113	1.81	46,000	25,400	35,000†	19,300	6,500,000	3,600,000	6,500,000	3,600,000	0.000016
Aircraft spruce (Douglas fir).....	27	0.43	10,000	23,300	5,000	11,600	1,300,000	3,000,000	1,300,000	3,000,000	
Birch plywood.....	37	0.80	13,100	16,400	5,700	7,100	1,400,000	1,800,000	1,400,000	1,800,000	
Birch-reinforced resin.....	78	1.27	27,700	21,800	22,800	18,000	3,400,000	2,700,000	2,300,000	1,800,000	
Paper-reinforced resin.....	85	1.37	19,000	14,000	30,000	22,000	1,200,000	900,000	600,000	400,000	
Fabric-reinforced resin.....	85	1.37	10,000	7,200	40,000	29,000	1,000,000	700,000	600,000	400,000	
Cord-reinforced resin.....	85	1.37	25,000	18,700	27,000	20,100	5,900,000	4,300,000	600,000	400,000	

* Yield point in compression.

† Yield point in tension. Yield point in compression is substantially equal to yield point in tension for wrought alloys.

mechanical strength and hardness. With few exceptions the resin is mixed with fillers such as wood, flour, paper, and fabric. This permits a wide variation in specific gravity and mechanical and electrical properties. The airplane pulley is an excellent example of the use of a phenol formaldehyde plastic with fabric filler to produce a structural element. The resistance to splitting is increased if the filler follows the contour of the mold, similar to the flow lines in a forging, for the laminated construction is relatively weak in a direction perpendicular to the lay of the laminations. It is probable that a similar construction with the proper combination of resin and filler would be satisfactory for wheels and similar parts produced in quantity. Thermosetting plastic sheets have been used to a limited extent for the primary structure for gussets and reinforcing patches. They are superior to plywood because there is no shrinkage or swelling from changes in moisture content.

2:11. Comparison of Characteristics.—Table 2:7 gives a comparison of approximate values of several aircraft materials. The strength-weight ratio and the modulus of elasticity-weight ratio are important for aircraft structural design.

References

1. JOHNSON, J. B.: Materials for Airplane Construction, *Jour. Aeronautical Sciences*, March, 1939, pp. 185-202.
2. ANC-5 Handbook, "Strength of Aircraft Elements," Government Printing Office, Washington, D.C., October, 1940.
3. "Aluminum in Aircraft," a handbook by the Aluminum Company of America, Pittsburgh, 1941.
4. "Dowmetal Magnesium Alloys," a handbook on magnesium alloys by the Dow Chemical Company, Midland, Mich., 1940.
5. "Molybdenum Steels in Aircraft Construction," a handbook by the Climax Molybdenum Company, New York, 1941.
6. "Stainless Steel in Aircraft," a handbook by the Electro Metallurgical Company, New York, 1941.
7. "Republic Alloy Steels," a handbook by the Republic Steel Corporation, Cleveland, Ohio, 1941.
8. FISHBEIN, M.: Physical Properties of Synthetic Resin Materials, *N.A.C.A. Tech. Note* 694, March, 1939.
9. YOUNGER, JOHN E., Consulting Editor: "Aircraft Tubing Data," Sumner Tubing Company, Bridgeport, Pa., 1941.

CHAPTER III

SUMMARY OF BASIC STRESS FORMULAS

3:1. Applicability of Formulas.—The design of aircraft structures, which is fundamentally based on structural stress analysis, requires that the engineer possess a good basic knowledge of strength of materials. It is not, however, sufficient merely to remember or refer to the formulas in a handbook. An intelligent use of basic stress formulas in airplane stress analysis requires that the assumptions on which the formulas were derived be understood and appreciated. It is safe to say that in aircraft work hardly a fundamental formula of strength of materials is used under the same conditions for which it was derived. The aircraft structural engineer should learn early in his career to evaluate the applicability of a fundamental formula to his particular problem.

3:2. Approximate Formulas.—No structures formula is exact. At best, all our mathematical analyses are nothing more than estimates. Mathematics, of course, is exact; but our assumptions on which the analyses are based are always approximate, the assumed loads are only estimates, and the physical characteristics of the material vary considerably. This is not an argument *against* mathematics, but rather an argument *for* mathematics, because it is the only tool the engineer has for arriving at an estimate; and whether simple arithmetic or the calculus be used in arriving at an estimate, the principle is all the same. An engineer who knows his calculus as well as his addition and subtraction can find as much practical use for the former as for the latter.

It is the partial knowledge of mathematics that is dangerous; one who finds it difficult to understand the theory and application of multiplication would not fare very well in a position requiring the use of multiplication. The same applies to higher forms of mathematics.

An engineer must make mathematics his slave, rather than be a slave to his mathematics. He should learn to make it do

things he wants done and should, at all times, understand its limitations so that he may form a practical estimate of the answer.

In engineering, it is the *answer* that counts, regardless of how it was arrived at—by orthodox methods or by approximations. For example, consider the simple equation, $\sin x = x$, from which we are to find x . Not one in a hundred engineering students can solve the equation for x , yet a practical answer can be found in a minute or two by referring to a table or by drawing two curves and noting the intersection.

The author can cite instances in practice in which long complicated formulas were not so accurate as simple rules of thumb.

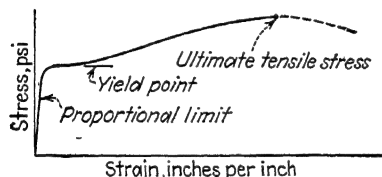


FIG. 3:1.—Stress-strain curve of a material having a definite yield point (such as low-carbon steel).

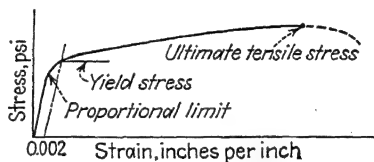


FIG. 3:2.—Stress-strain curve of materials not having a definite yield point (such as aluminum alloys, high-carbon alloy, and cold-worked steels).

Again the fault was not with the mathematics but with the engineer in blindly following the dictates of the “master” and in failing to understand the mathematical limitations.

3:3. Elastic Constants.—Practically all mathematical analyses of stresses and strains are based on Hooke’s law of the proportionality of stress and strain. Hence these formulas apply only below the proportional limit which for most aircraft materials is the elastic limit.

3:4. Modulus of Elasticity.—Within the proportional limit of the material, in tension,

$$E = \frac{\text{unit stress}}{\text{unit strain}} = \frac{P/A}{\delta/L} = \frac{PL}{A\delta} = \frac{f}{e} \quad (3:1)$$

This is the slope of the straight portions of the curves of Figs. 3:1 and 3:2.

If the force in equation (3:1) is compressive, E becomes E_c . Usually, $E_c = E$.

The *tangent modulus* E_t is the slope of the stress-strain diagram at a point corresponding to a given stress.

The secant modulus E_{sec} is the slope of a line drawn through the same point as for E_t and the origin.

The modulus of elasticity in shear (Fig. 3:3) is

$$E_s = \frac{\text{unit shear stress}}{\text{unit shear strain}} = \frac{S/A}{\delta/L} = \frac{SL}{A\delta} = \frac{f_s}{e} \quad (3:2)$$

in which $e = \delta/L$.

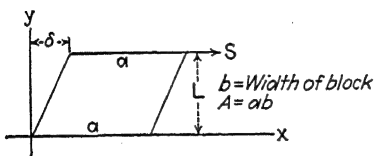


FIG. 3:3.—Shear modulus.

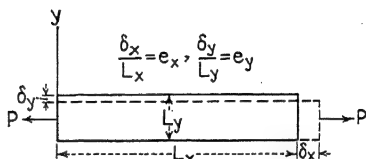


FIG. 3:4.

3:5. Poisson's Ratio.—In Fig. 3:4, the extensional strain e_x causes a compressional strain e_y . The following relationship represents an experimental fact. $e_y = -\mu e_x$ (3:3) in which μ is Poisson's ratio. For steel, μ is 0.25 approximately; for aluminum alloys, μ is about 0.30 and for usual analyses may be taken as such.

In equation (3:3) since, from (3:1), $e = \frac{J}{E}$, (3:4)

$$e_y = -\frac{\mu}{E} f_x \quad (3:5)$$

If a stress f_y (tension) also exists,

$$e_y = \frac{f_y}{E} - \frac{\mu f_x}{E} = \frac{1}{E} (f_y - \mu f_x) \quad (3:6)$$

Note that in this equation f is the unit stress (tension) in pounds per square inch and e is the unit strain in inches per inch.

Likewise,
$$e_x = \frac{1}{E} (f_x - \mu f_y) \quad (3:7)$$

3:6. Relationship between Constants.—The relationship between the constants E , E_s , and μ is expressed as follows:

$$E_s = \frac{E}{2(1 + \mu)} \quad (3:8)$$

Thus, for steel, $E_s = E/2(1 + 0.25) = \frac{2}{5}E$.

3:7. Calculated Stress and Allowable Stress.—There are two phases to every analysis of the strength of a structure, namely:

(1) the calculation of the stress in the member caused by a given applied load; (2) the calculation of the allowable stresses, that is, the stress or combination of stresses at which failure in the member occurs.

For example, the column stress (compressive) is the load P divided by the area A , that is, P/A ; but the *allowable* stress depends on the length of the column, the radius of gyration, and the modulus of elasticity of the material as in Euler's column formula.

Another example is the calculation of the stress in a thin-walled tube by the usual modulus-of-rupture formula,

$$f_b = \frac{M y}{I} = \frac{M}{Z} \quad (3:9)$$

The equation applies up to the point of wrinkling of the thin wall, it being assumed that the wrinkling stress is below the proportional limit. But how much is the allowable stress? This, of course, is the stress at which wrinkling occurs, which depends upon the thickness of the wall, the diameter of the tube, and the modulus of elasticity of the material. This is given by a formula of the form $f_a = KE(D/T)^n$.

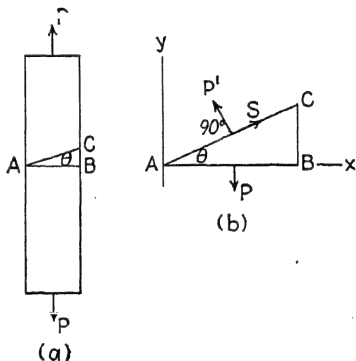


FIG. 3:5.—Shear caused by tension.

3:8. Shear Caused by Tension or Compression.—In Fig. 3:5a is shown a strip of metal of cross section A subjected to a tensile force P . We are to find the shear stress along the line AC inclined an angle θ to AB , which is perpendicular to the axis of the strip [see free-body diagram (Fig. 3:5b)].

$$\Sigma F_x = 0 = -P' \sin \theta + S \cos \theta \quad (3:10)$$

$$\Sigma F_y = 0 = -P + P' \cos \theta + S \sin \theta \quad (3:11)$$

Eliminating P' and solving for S , we have

$$S = \frac{1}{2} P \frac{\sin 2\theta}{\cos \theta} \quad (3:12)$$

But, letting A = area of cross section at AB ,

$$S = \frac{f_s A}{\cos \theta} \quad \text{and} \quad P = f_t A \quad (3:13)$$

Thus, substituting in (3:12),

$$f_s = \frac{1}{2}f_t \sin 2\theta \quad (3:14)$$

We have $f_{s(\max.)}$, when $\sin 2\theta = 1$, $\theta = 45$ degrees, thus,

3:9. Shear Caused by a Combined Tensile (or Compressive) and Shearing Load.—This type of stress occurs quite often in airplane structures. Figure 3:6a shows the shearing load S

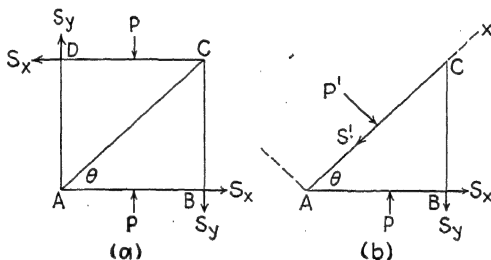


FIG. 3:6.—Shear caused by a normal (tension or compression) and a shearing load.

and the tensile load P acting on the block $ABCD$ of thickness t . Figure 3:6b shows the free-body diagram.

Summing the forces parallel to AC and those perpendicular to AC , we have

$$\Sigma F_x = 0 = -S' + S_x \cos \theta - S_y \sin \theta + P \sin \theta \quad (3:16)$$

$$\Sigma F_y = 0 = -P' + P \cos \theta - S_y \cos \theta - S_x \sin \theta \quad (3:17)$$

Let A be the area of cross section at AC ; then

$$P = Af_n \cos \theta, \quad S_x = Af_s \cos \theta, \quad S_y = Af_s \sin \theta, \\ S' = Af'_s, \quad \text{and} \quad P' = A \quad (3:18)$$

Thus, equations (3:16) and (3:17) become

$$f'_s = +\frac{1}{2}f_t \sin 2\theta + f_s \cos 2\theta \quad (3:19)$$

and

$$f_n \cos^2 \theta + f_s \sin 2\theta = f_n \sin \quad (3:20)$$

The maximum f'_s occurs when $df'_s/d\theta = 0$, and the maximum f'_n occurs when $df'_n/d\theta = 0$, which gives, for θ ,

$$\tan 2\theta_s = +\frac{f_n}{2f_s}, \text{ angle of max. shear} \quad (3:21)$$

and

$$\tan 2\theta_n = + \frac{2f_s}{f_n}, \text{ angle of max. normal} \quad (3:22)$$

The angles $2\theta_s$ and $2\theta_n$ are shown in Fig. 3:7*a* and *b*. From this figure, we compute the $\sin 2\theta$ and $\cos 2\theta$ for shear and normal

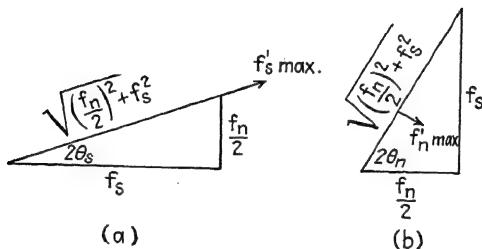


FIG. 3:7.

stress and substitute in equations (3:19) and (3:20) to obtain the formulas for maximum stresses.

For maximum shear,

$$\frac{f'_s \max}{f_s} = \frac{f_n}{2} \quad (3:23)$$

For maximum tension of compression,

$$f'_{n(\max)} = \frac{f_n}{2} + f'_s \quad (3:24)$$

The formulas of this article are for the calculation of stresses, on the assumption of Hooke's law. The formulas do not tell us how or at what loads the structure will fail, nor do they take into consideration the conditions of local buckling in thin sheet structures.

This brings up again the two phases of every strength analysis, (1) calculation of the stress due to an applied load, just considered, and (2) determination of the failing stress condition. The second phase is considered in the following article:

3:10. Allowable Combined Tensile (or Compressive) and Shear Stresses.—How and at what load a member of a structure will fail depends upon many factors, such as the characteristics of the material and the configuration of the structure. Assume that a member whose failing stress in tension is F_{tu} is subjected

to a tensile stress f_t ; what will be the allowable shear stress f_s , if F_{su} is the failing stress in pure shear? If we let

$$\text{and } \frac{J_s}{F_{su}} = \quad (3:25)$$

an empirical relationship may be expressed by the following formula:

$$R_1^N + R_2^M = 1 \quad (3:26)$$

It should be borne in mind, however, that this is purely empirical.

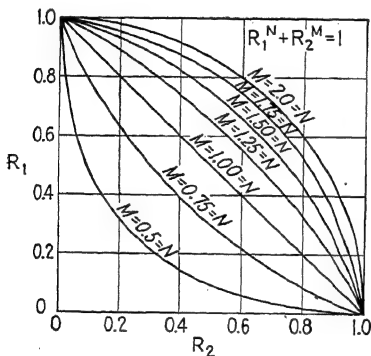


FIG. 3:8.

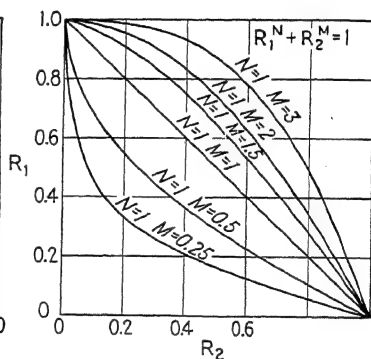


FIG. 3:9.

If there are three types of loading, obviously the following form may be used empirically:

$$R_1^N + R_2^M + R_3^O = 1 \quad (3:27)$$

Figures 3:8 to 3:12 present graphs of equation (3:26) for various values of N and M . For the particular problem, when the values of N and M are known from experimental data, the corresponding curve may be used for design. If the stresses f_t and f_s are calculated and F_{tu} and F_{su} are known, the stresses are safe if the left side of equation (3:26) is less than 1.

3:11. Modulus of Rupture.—The theoretical breaking strength of a beam subjected to bending is given by the formula

$$\frac{Mc}{I} \quad (3:28)$$

where f_b = stress in the outer fiber.

M = applied bending moment.

c = distance from the neutral axis of the cross-sectional area to the outermost fiber.

I = moment of inertia of the cross-sectional area with reference to the neutral axis.

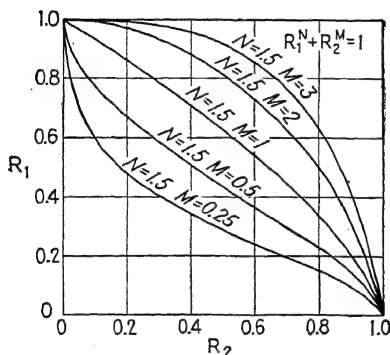


FIG. 3:10.

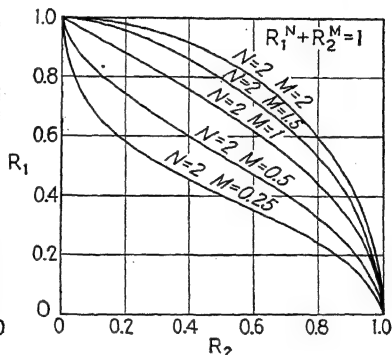


FIG. 3:11.

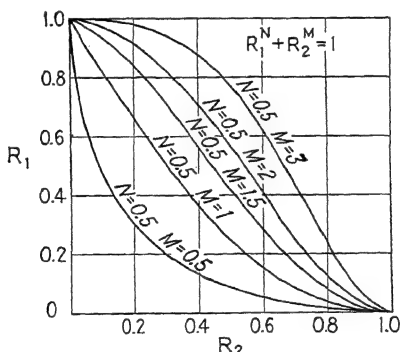


FIG. 3:12.

The student is advised to study the deviation of this formula with special reference to the *assumptions* on which the derivation is based. If the formula were valid beyond the elastic limit, the value of f_b for rupture would agree reasonably well with the ultimate strength of the material. However, since the formula is thus used incorrectly, the value of f_b is found to agree with neither the ultimate tensile strength nor the compressive strength of the material. *This value of f_b should be regarded, not as a*

physical constant, but as a figurative value, valuable mainly for comparative purposes. This figurative value is known as the modulus of rupture of the material.

3:12. Application of the Modulus-of-rupture Formula.—It may be noted that the modulus-of-rupture formula is useful only in applying results from *model tests* to the design of beams. This means that, for an accurate application of the formula, it is necessary to have the results of experiments on beams similar to the beams which are being used in airplane design. The fiber stress f_b that we are capable of developing in a beam will depend upon the configuration of the cross section of the beam. For example, let us consider Fig. 3:13, in which we have represented an I-beam and a box beam.

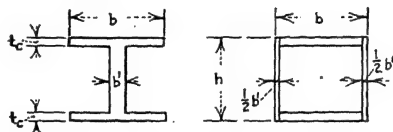


FIG. 3:13.—Standard dimensions of I-beam and box beam.

If these beams are subjected to a bending load, the question of *instability* enters, because of the thin webs and flanges. The fibers in the beam may not fail but they may buckle, developing thereby much less strength than they would develop if they were properly supported. It is therefore apparent that the fiber stress f_b allowed in beams of this type would be less than the fiber stress allowed in a solid beam.

In many types of beams in thin sheet-metal construction, the modulus of rupture is displaced by the compressive stress which causes buckling of the thin sheet in the outermost fibers of the compression flange of the beam. If we designate this buckling stress by

$\frac{P}{A}$ axial load
 area of cross section under compression

we have

$$\frac{P}{A} = \frac{Mc}{I} \quad (3:29)$$

In this case, P/A is a function of the modulus of elasticity of the material of the tube, the wall thickness, and the diameter. It represents the allowable stress, that is, the stress of failure,

which is wrinkling of the skin in this case. The Mc/I produces the calculated stress and holds good only up to the value of P/A .

If a composite beam of parts of the same material such as a semi-monocoque cantilever wing is built up of a combination of thick and thin sections of materials, the Mc/I formula holds only below the stress of failure of the weakest, usually the thinnest, part. However, if I of the cross section of the wing is recalculated, the weak parts being omitted, the formula is valid for computing the stresses of the remaining parts, up to the stress of failure of the next weakest parts. The process may then

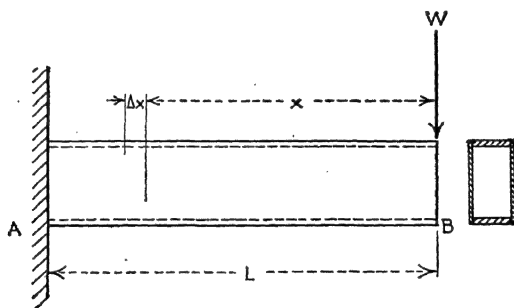


FIG. 3:14.

be repeated until the actual strength of the wing section is determined.

3:13. Calculation of Shear in the Web of a Beam.—In the consideration of the design of a wing beam, special attention must be given to the design of the thin web as in a box beam or in an I-beam. The load that occurs in the web of a wing beam is mostly shear. As a matter of fact, the webs of a wing beam are generally neglected in the calculation of tension and compression. They are thus designed exclusively for the resistance of the shear in the beam.

Consider the beam in Fig. 3:14, subjected to the bending moment

$$M = Wx \quad (3:30)$$

We have, as shown in Fig. 3:15, then, the total shearing load on the beam at A as F_1 , in which

$$F_1 = Wx_1 \quad (3:31)$$

Now at a section B we note that

$$V_s = \frac{F_s}{d} \quad (3:32)$$

and that the resultant shearing stress on the increment Δx is

$$F_s = F_1 - F_2 \quad (3:33)$$

or

$$F_s = \frac{-M_B}{d} \quad (3:34)$$

We note that the unit shear which we designate as f_s is equal to the total shear F_s divided by the area,

$$f_s = \frac{F_s}{b \Delta x} \quad (3:35)$$

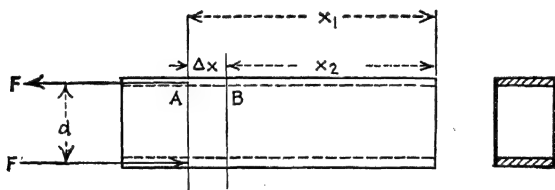


FIG. 3:15.

where b is the total width of the web material. Now, substituting the value of F_s from equation (3:34) into equation (3:35), we have

$$f_s = \frac{M_A - M_B}{bd \Delta x} = \frac{\Delta M}{bd \Delta x} \quad (3:36)$$

or, in the limiting form, we find f_s , for this particular case,

$$f_s = \frac{dM}{dx (db)} \quad \frac{V}{bd} \quad (3:37)$$

Now let us consider the general case for the solid beam. In Fig. 3:16, consider the section of a beam that is bent. At section A the moment is M_A ; at section B the moment is M_B . Now at A the total shearing stress at any point is

$$(3:38)$$

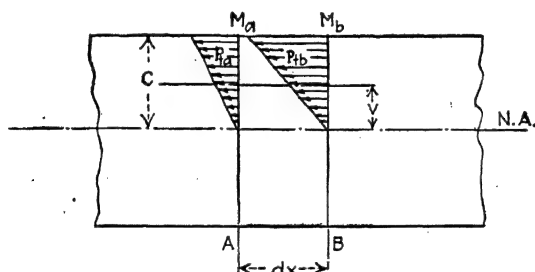
where P_t is the tensile or compressive load on an area dA of the cross section. Likewise,

$$F_b = \sum_v^c P_{tb} \quad (3:39)$$

The resultant shearing stress on the section of length dx is

$$F_A - F_B = \sum_v^c (P_{ta} - P_{tb}) \quad (3:40)$$

The unit shear in pounds per square inch of shearing surface is



g. 3:16.—Shear in a bent beam.

$$f_s = \frac{F_A - F_B}{dx} = \frac{b}{b} \frac{dx}{dx} \quad (3:41)$$

Note that

$$P_{ta} = f_a dA \quad (3:42)$$

and

$$P_{tb} = f_b dA \quad (3:43)$$

Now, from the modulus-of-rupture formula [equation 3:28], we have

$$f = \frac{Mv}{I} \quad (3:44)$$

so that

$$Mav \quad (3:45)$$

and

$$(3:46)$$

in which we assume the beam to be uniform in cross section.

Now, substituting the values of equations (3:45) and (3:46) in equations (3:42) and (3:43) and in turn substituting these values in equation (3:41), we have

$$\frac{dA - M_B v dA}{Ib dx} \quad (3:47)$$

And, since the difference between the two moments is the differential moment, we have expressed the equation in an integral form,

$$\overline{Ib} \int \frac{(M_A - M_B)v dA}{dx} = \frac{1}{\overline{Ib}} \int^c \frac{dM}{dx} v dA \quad (3:48)$$

Now, dM/dx is the shear on the beam at the point x , and this term is independent of the variable v ; therefore, this equation may be written

$$= \frac{V}{\overline{Ib}} \int^c v dA \quad (3:49)$$

where V is the total shear on the beam at the point x . The integral in equation (3:49) is the statical moment of an area above a line through the point at which we desire to obtain the shear; in general, this is the neutral axis of the beam above.

Let

$$\int^c v dA = Q \quad (3:50)$$

Thus

$$\overline{Ib} \quad (3:51)$$

3:14. Allowable Shear in Web of a Beam.—While equation (3:51) enables us to calculate the stress, it does not enable us to determine whether or not the webs will carry the stress. Thus, before the beam can be designed, it will be necessary for us to know what stress f_s may be allowed in the webs. Obviously, f_s will depend upon the buckling condition of the web; that is, if the web is very thin and not very well braced, it is quite obvious that it will buckle easily and very little shearing stress can be resisted. However, if the web is fairly thick and well braced, the shearing stress f_s may be fairly high. In certain cases of metal beams where thin webs are used, the shearing stress in the webs is resisted entirely by a diagonal tensile stress; in this

case it is necessary to brace the flanges of the beam by bulkheads to prevent the beam from collapsing.

The tensile lines in the thin web will assume approximately a 45-degree direction. Now it is quite obvious in this case that f_s is calculated not as a shear stress but as a tensile stress in the thin webs and as a shear stress in the rivets which attach the thin webs to the flanges.

3:15. Secondary Stress Due to Flexure.—The flexibility of an airplane structure alters very greatly the stress in the members of

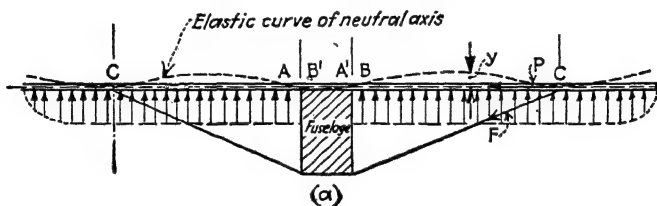


FIG. 3:17.—Secondary stresses in a wing beam.

the structure, and therefore it is of prime importance to be able to calculate the effect of the flexure in the members. *The stress due to a flexure of the structure is called a secondary stress.* In many instances the secondary stress in a wing beam and in other types of beams in an airplane structure is greater than the primary stress in the beam. This is particularly true when the beam acts not only as a beam but also as a column, as, for example, the wing beam in a biplane or in a braced monoplane. When the beam is bent by a side load and then an axial load is applied to the beam, a *secondary* stress is induced by this load, for example, as noted in Fig. 3:17. We have in this figure the flexure of the wing beam due to the flying load indicated by y . The axial load on this beam is a component P of the load in the flying wire. The secondary moment in this case is Py . If the deflection is very great, moment Py may be greater than the bending moment due to the air load.

3:16. Calculation of Flexure of a Beam.—Now let us consider the calculation of this flexure. At any point x along the beam, the beam has a certain radius of curvature. The radius of curvature ρ is given by the equation

$$\rho = \frac{[1 + (dy/dx)^2]^{3/2}}{d^2y/dx^2} \quad (3:52)$$

For small curvatures the term $(dy/dx)^2$ is assumed zero, so that

$$\rho = \frac{1}{d^2y/dx^2} \quad (3:53)$$

This equation is invariably used for deflection calculations, with accurate results. It remains, therefore, for us only to find the value of ρ , the radius of the curvature, in terms of known quantities

such as the bending moment, the modulus of elasticity, and the moment of inertia of the section. For this purpose, let us consider Fig. 3:18, which is a section of a beam that is bent. We have, from the definition of E ,

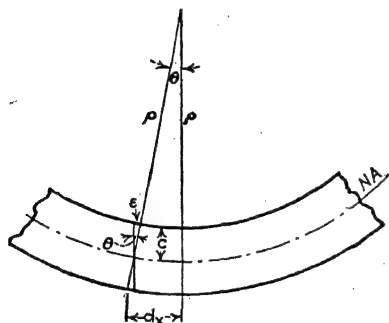


FIG. 3:18.—Radius of curvature of a bent beam.

$$J = \int \frac{y^2}{dx} \quad (3:54)$$

Now

$$\rho : dx = c : \epsilon \quad (3:55)$$

and from this equation we find that

$$\frac{\epsilon}{dx} = \frac{c}{\rho} \quad (3:56)$$

Now, substituting this value in equation (3:54), we find that

$$J = \int \frac{c^2}{\rho} \quad (3:57)$$

which, when substituted in equation (3:28), gives us

$$E \frac{c}{\rho} = \frac{Mc}{I} \quad (3:58)$$

from which

$$\frac{1}{\rho} = \frac{M}{EI} \quad (3:59)$$

or

$$I \frac{d^2y}{dx^2} \quad (3:60)$$

Now, in the application of formula (3:60), great care should be exercised to see that the conditions relative to the sign of these terms are correct. In some cases the definition of our convention of signs, unless very carefully observed, will produce erroneous results. In such a case, we should note that our conventions are matters of definition; the error involved might be, not an error of theory, but merely an error of definition.

3:17. Convention of Signs.—We assume a *positive load* with respect to the x and y coordinate plane as *upward* (Fig. 3:19a).



(a)

(b)

FIG. 3:19.—(a) Positive load; (b) positive shear.

We define a shear in the following manner: *If the section to the right shears downward, the shear is said to be positive.* For example, in Fig. 3:19b, the load W induces positive shear in the beam AB .

A *positive moment* is that moment which produces compression in the upper fiber of the beam. This requires that the radius of curvature for a positive moment shall be upward, that is, in the positive direction of y . These conventions are purely matters of definition; but, after the assumptions are made for a problem, we cannot change them for that problem. We also note that these conventions may not conform to the conventions of shear and bending moment, etc., in problems of statics; it should be understood that any connection between the two would be a matter of definition rather than a matter for logical thought.

3:18. Bending Moment Due to Distributed Load.—In Fig. 3:20 is a beam simply supported at the ends, subjected to a non-uniformly distributed load $f(u)$. We designate the section at

which the moment is to be determined by x . The length of the beam is L . We determine first the reaction R_a at A . In order to determine the reaction at A , we sum the moments about the point B as noted.

$$\Sigma M_B = 0 \quad (3:61)$$

Since the load is nonuniform, we divide it up into increments, the length of each increment being the fixed quantity Δu . We note

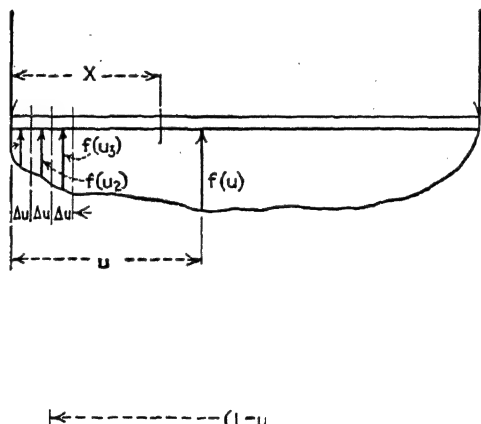


FIG. 3:20.—Bending moment for distributed load.

that the load for a length Δu is the load per unit length $f(u)$ times the length Δu . That is,

$$p = f(u) \Delta u \quad (3:62)$$

Now let us consider the first increment, that next to station A . Let us designate the average value of the unit load for the increment by $f(u_1)$. The total load is

$$p_1 = f(u_1) \Delta u \quad (3:63)$$

The moment due to this particular increment is (see Fig. 3:20b)

$$\Delta M_b = p_1(L - u_1) = f(u_1)(L - u_1) \Delta u \quad (3:64)$$

The moment at B , due to all the increments of loading, is

$$= f(u_1)(L - u_1) \Delta u + f(u_2)(L - u_2) \Delta u + f(u_3)(L - u_3) \Delta u + \dots - R_a L = 0 \quad (3:65)$$

Thus, we have from this equation, by approaching the limiting value du ,

$$\int_0^L f(u)(L - u) du \quad (3:66)$$

The bending moment at x , assuming the beam to be cut at the point x , and considering the cantilever extension to the left, is the sum of the bending moment due to the applied nonuniform load to the left of the section and to the concentrated reaction R_a . We therefore have

$$= -R_ax + \int_0^x f(u)(x - u) du \quad (3:67)$$

and in this case we use the negative sign in front of R_a because the load R_a causes an extension in the upper fiber of that portion of the beam. Now, substituting in equation (3:67) the value of R_a as found in equation (3:66), we have

$$= -\frac{x}{L} \int_0^L f(u)(L - u) du + \int_0^x f(u)(x - u) du \quad (3:68)$$

This equation applies to any type of loading; for example, if we assume the load to be uniform and equal to w , that is,

$$f(u) = w \quad (3:69)$$

we can evaluate the integrals of equation (3:68). Thus we find that

$$M_x = -\frac{x}{L} \int_0^L w(L - u) du + \int_0^x w(x - u) du \quad (3:70)$$

Integrating this, we get

$$M_x = -\frac{wL^2x}{2L} + \frac{wx^2}{2} - \frac{wx^3}{6} \quad (3:71)$$

3:19. Bending Moments at Ends of Bay.—In Fig. 3:21 is represented a simply supported beam subjected to an applied moment at each end, namely, M_a and M_b . Plot the vectors for these moments (see Fig. 3:22). These vectors, of course, would occur in a plane perpendicular to the plane of the page, but we may assume that we have rotated our axis so that the vectors

appear in the same plane. If M_b is zero, the moment in the beam, that due to M_a , is directly proportional to the distance from the point B . Likewise, the effect of the moment due to M_b would be proportional to the distance from A . Now the moment at x is the sum of the moments due to M_a and M_b as represented by the

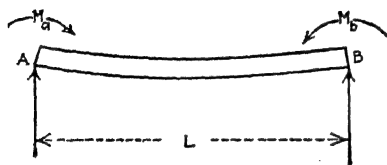


FIG. 3:21.—Bending moment at support.

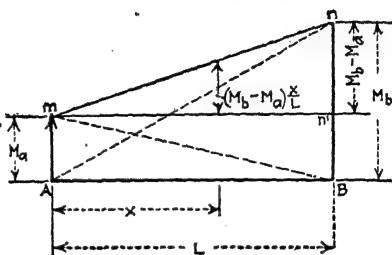


FIG. 3:22.—Variation of bending moment due to moments at supports.

line mn . The value of the moment at any point, it will be observed, is

$$= M_a + (M_b - M_a)x/L \quad (3:72)$$

3:20. General Moment Equation.—We find then that the total bending moment which may occur on the spars of an airplane is

$$M_x = M_a + \int_0^x f(u)(L - u) du + \int_0^x f(u)(x - u) du - Py \quad (3:73)$$

In this equation the M_a and the M_b are determined by the *three-moment equation* if the beam is continuous, or by the loading on the cantilever overhang in the portion in which the beam is discontinuous.

3:21. Relation between Load, Shear, Moment, and Deflection.—The relation between load, shear, bending moment, and deflection is useful in stress analyses in connection with struts that have side load and in connection with wing beams. We may note that the shear V is

$$V = \frac{dM}{dx} \quad (3:74)$$

The bending moment M is

$$M = \int \int w dx dx = \int V dx \quad (3:75)$$

And since

$$EI \frac{d^2 y}{dx^2} = M \quad (3:76)$$

we have the slope i ,

$$\frac{dy}{dx} = i = \int \int \int \frac{w \, dx \, dx \, dx}{EI} = \int \frac{M \, dx}{EI} \quad (3:77)$$

Likewise, the deflection is

$$y = \int \int \int \int \frac{w \, dx \, dx \, dx \, dx}{EI} = \int i \, dx \quad (3:78)$$

3:22. Differentiating the Moment Equation.—In general the reverse of the procedure in equations (3:74) to (3:78) would not be possible. For one reason, the loading may be composed of concentrated loads or other discontinuous types of loading so that we encounter discontinuous functions; for another reason, the constants of integration may be missing. For example, the operation $d^2 M/dx^2$, when applied to

$$M_x = -\frac{4L^2}{\pi^2} W_0 \cos \frac{\pi}{2L} x + C_1 x + C_2 \quad (3:79)$$

and to

$$M_x = -\frac{4L^2}{\pi^2} W_0 \cos \frac{\pi}{2L} x \quad (3:80)$$

will give the same loading curve,

$$w = W_0 \cos \frac{\pi}{2L} x \quad (3:81)$$

Equation (3:79) is the correct equation, in which C_1 and C_2 may be evaluated by the following two conditions:

$$\begin{array}{ll} \text{When } x = L, & \text{shear} = 0 \\ \text{When } x = L, & \text{moment} = 0 \end{array}$$

We may also note that, whereas, from a mathematical standpoint, these discontinuous functions may be apparently difficult, from a practical standpoint they offer the engineer no practical difficulty.

3:23. Integration of the Load Curve.—Note some of the applications of equations (3:74) to (3:78). Consider, for example, a cantilever beam, shown in Fig. 3.23, which is subjected to a

known distributed load that we may designate, as a function of u , as $f(u)$. Designate a portion of the beam at which point the bending moment, slope, or deflection is to be calculated as x . We notice, in this case, that we use two variables, u and x . The two variables may at certain times indicate the same point on the beam. However, the variable x indicates the point at which

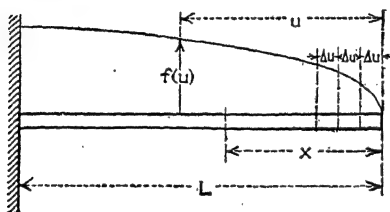


FIG. 3:23.—Distributed load for wing beam.

we are to determine the shear, the bending moment, or other qualities, while u indicates the portion of the load which is being considered in connection with the load. For example, suppose that we are to find the shear at point x_1 . x , then, is fixed as x_1 ; yet the shear at point x_1 will be the summation

of the loading $f(u)$ from $x = 0$ to $x = x_1$. This may be indicated as in equation (3:82),

$$V_x = f(u_1) \Delta u \quad \Delta u \quad (3:82)$$

where $f(u)$ = magnitude of the load per unit of length.

Δu = length into which the beam is divided.

We note in this case that

$$\Delta u = \frac{x}{n}$$

where $n = 1, 2, 3$, etc.

Equation (3:82) defines a definite integral which may be written

$$V_x = \int_0^x f(u) du \quad (3:83)$$

which, expressed in words, means that the shear at the point x is equal to the total load on the beam from $x = 0$ to $x = x_1$. For example, if, in equation (3:83), $f(u) = w$, we have

$$V_x = \int_0^x w du = wx \quad (3:84)$$

We note that the bending moment is

$$M_x = \Delta u [f(u_1)(x - u_1) + [f(u_2) \Delta u](x - u_2) + [f(u_3) \Delta u](x - u_3)] \quad (3:85)$$

or, expressed as an integral,

$$M_x = \int_0^x f(u)(x - u) du$$

Now, as an example of this, let us again assume the loading uniform, that is, $f(u)$ to be replaced by w . We have, therefore,

$$M = \int_0^x w(x - u) du = \left[wxu - w \frac{u^2}{2} \right]_0^x = \frac{wx^2}{2}$$

3:24. Evaluating the Beam Integrals.—Graphical methods have been devised for evaluating these integrals. However, one is less inclined to make a mistake, and possibly the solution is simplified, if use is made of the application of the definition of the definite integral, as, for example, in the following illustration pertaining to a cantilever beam:

In Fig. 3:24a we have plotted the load w to scale. In Fig. 3:24b we have plotted the shear to the proper scale. Now, in evaluating the integral graphically, we note that before we can start to plot the shear curve we must know the value of the shear at some point from which the curve is started. This is the graphical equivalent of evaluating the constant of integration. For example, at point O the value of the shear is not known, but at point C it is apparent that its value is zero. We start plotting the integral at point C where the shear is known, thus obtaining the shear curve BC . We note that the shear at any point x is the summation of the loading from A to x . That is, the value of the shear ordinate at the point x is the total sum of the loading from A to x . The negative value of the shear results, not from the integration, but from the definition of a positive shear. If the cantilever beam had been turned toward the left, by definition, the shear would have been positive.

In plotting the bending-moment curve, as noted in Fig. 3:24c, for the purpose of determining where the curve shall be started, we notice that the bending moment at E is known; that is, the bending moment at E is zero. We also note that, from the nature of the loading, the bending moment will be positive. We therefore have the bending-moment curve ED in c , in which the ordinate at any point x is the summation of the shear from C to x .

We note that in the slope curve the value of the slope is known at point O . We therefore start plotting the slope curve at station O , or $x = L$. We note that the values of the sums of the incre-

ments must be divided by EI in order to find the ordinate of the slope curve at any point x .

For the deflection curve we note that the value of the deflection is known at point O . At point O the deflection is zero. We

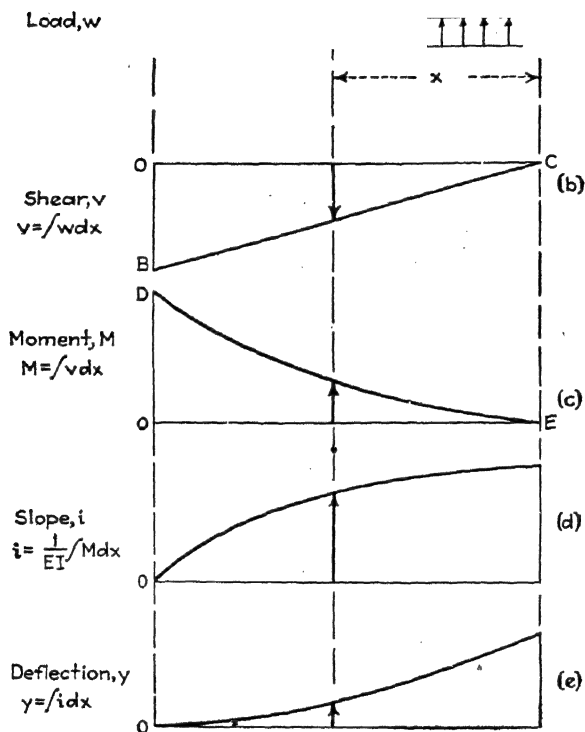


FIG. 3:24.—Relationship between beam load, shear, moment, slope, and deflection. therefore start our deflection curve at O . We notice in this case that the deflection is upward. The ordinate at any point is the summation of the slope up to the point x , but in this case the quantity is not divided by EI .

3:25. Allowable Compressive Stress.—The allowable compressive stress of a structural member depends upon many factors, such as the length of the member, the radius of gyration of the cross section of the member, the thickness of the walls, and the radius of curvature of the thin sheet used in its construc-

tion. If the length L is great as compared with the radius of gyration ρ of its cross section, the allowable stress P/A is purely a problem of stability, and the allowable stress is expressed accurately by Euler's formula. However, if the member is short, other factors predominate. For example, if the member is constructed of formed thin sheet, the sheet may wrinkle, the stress P/A it will carry depending on such factors as the thickness t of the sheet and the radius of curvature R of the cross section of the member.

If the ratio R/t is great, the allowable stress depends upon the stability of the structure and not upon the strength of the material.

If the L/ρ and the R/t of the member both are small, the factor of strength of the material enters into the problem; the smaller these values, the greater is the predomination of the fiber strength of the material.

Most generally the allowable compressive stress must be expressed empirically. Figure 3:25 shows the type of curves that may usually be made to fit the experimental data.

In this figure the stability factor is designated as B_s . The allowable stress curve is ABC . The two formulas expressing these curves are;

$$F_c = 1 - K_1 B_s^n \quad (3:86)$$

and

$$F_c = \frac{K_2}{B_s^m} \quad (3:87)$$

The dividing line between the two curves is called the *critical* B_s . Obviously the critical B_s must be known in order to determine which formula is to be used for the particular problem.

If the numerical values of F_c and B_s of two points on the curve B to C are known, these values may be successively substituted in equation (3:87), and the two resulting equations in m and K_2 may be solved simultaneously for the numerical values of m and K_2 .

Likewise, if the numerical values of F_c and B_s of two points on the curve A to B are known, these values may be successively

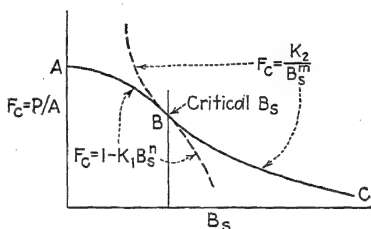


FIG. 3:25.

substituted in equation (3:86), and the resulting two equations solved simultaneously for the numerical values of n and K_1 .

The determination of the critical value of B_s is based upon the two facts: (1) that the curves coincide at B and (2) that the two curves are tangent at B .

Thus

$$1 - \quad (3:88)$$

and

$$\frac{d}{dB_s} \quad (3:89)$$

For numerical values of K_1 , K_2 , m , and n , either of these equations is sufficient to determine the critical value of B_s .

CHAPTER IV

AIRPLANE STRUCTURES, PAST, PRESENT, FUTURE

4:1. Progress in Structural Design.—Judging by our present standards of airplane construction, the airplanes of a quarter of a century ago were very crude affairs.

Likewise, judging by the standards of construction a quarter of a century hence, our present airplane structures are very crude affairs.

When airplanes were constructed entirely of wood and fabric, our factories were equipped solely for this type of construction.

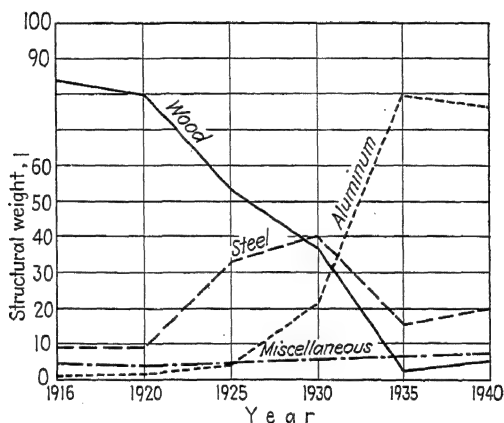


FIG. 4:1a.—Basic structural materials; total for all airplanes, U. S. Army Air Corps. (By J. B. Johnson, *Courtesy of Aviation.*)

Our national research efforts were directed according to the dictates of the requirements of wood and fabric construction. Structural engineers thought in terms of the mode of construction of the time, and engineering students were taught this type of construction.

When about 1920 (see Fig. 4:1a) steel tubular construction was introduced, there of course was considerable opposition to its use. The manufacturer required expensive new equipment, and the structural engineers had to revise their concepts of air-

plane structures and learn new methods of design. Many engineers were too stubborn or were not able to change over to the new methods of design and accordingly became as obsolete as the airplanes they once created. The emphasis in government research in due course changed from wood to steel. Every effort was made to improve the design of steel tubular structures.

About 1925 (see Fig. 4:1a) the aluminum-alloy thin-sheet (semi-monocoque) construction began to make its appearance. The intensive development program at Wright Field about 1925 to 1930 (see the dedication of this volume) and the subsequent development of the Martin XB-10 (see Fig. 1:1) changed the entire plan of airplane construction. The author, being closely associated with the development of this type of construction, can testify to the great opposition offered by many high officials in industry and government. After all, the older men in aircraft construction had spent the best part of their lives in learning to design better steel tubular airplanes. Research men had become authorities on steel tubular construction and were reluctant to shift to new types of structures. Many could see no good in the new type of construction because *they had learned to think in terms of the structures then in vogue.*

4:2. The Perfect Construction.—What is the perfect construction? Is it our present type of thin-sheet aluminum-alloy construction? As in the case of wood construction and steel tubular construction, every effort is now being made to improve the design of the present type of construction. All research programs on structures are planned for this sole object. Many engineers are convinced, just as in the case of wood and steel tubular construction, that we have at last found the ideal type.

What will be the next innovation? Is there any concerted effort being made to bring about another innovation in structures? Who wants it anyway? The manufacturer? The engineer? The research man? A change means extra expense and effort for all.

Older engineers are too prone to let things move along as they now are. It is the young engineers who are now in our engineering schools who will promote the next revolution in aircraft structures, but not if they are taught to think—as the older engineers now think—only in terms of our present knowledge of aircraft structures. The student engineer must learn to look

to the future, to think for himself, and to learn to use his imagination with respect to aircraft structures. He must resist all efforts to make him a "handbook engineer."

4.3. Structural Research.—Aircraft structural research may be divided into four divisions, as follows:

1. Development research.
2. Research on fundamental theory.
3. Design-data testing.
4. Static testing.

No one division is more important than another.

The purpose of *development research* is to promote new ideas in construction, new uses of materials, and new materials of fabrication.

The purpose of *research on fundamental theory* is to develop fundamental theory for the use of the designing engineer. This is assumed to be independent of material; then experimental conditions, such as application of loads, restraints, and the characteristics of the material or structure, must approach the assumed theoretical conditions. The development of Euler's formula is a good example of this type of research.

The purpose of *design-data testing* is to obtain data for immediate design. This type of research must take into consideration the variation in material and structural characteristics. The testing should simulate as nearly as possible the actual requirements in the airplane structure. The test specimens should be made from the regular stock materials used in aircraft construction. The results of this type of research are usually expressed as a graph. The plotted points are always scattered because there are considerable variations in the materials. Naturally the average curve of the data cannot be a design curve, because the strength of about half the structures tested is below this curve, and this condition may also be expected in airplane structures. For example, for S.A.E. 1025 steel the tensile design stress is 55,000 lb. per square inch, but tests on the S.A.E. steel tubes show that the tensile strength is never below 55,000 lb. per square inch and usually is about 65,000 to 85,000 lb. per square inch.

Research on fundamental theory and design-data testing overlap to some extent. Many research workers apparently do not recognize any distinction between the two.

The purpose of *static testing* is to check the design strength of a structure. Static testing usually produces, as a by-product, some excellent design data.

4:4. Predictions on Aircraft Construction.—Omitting motorless airplanes and low-powered commercial airplanes, the following lines of structural development will probably confront the aeronautical structural-engineering graduate:

1. *Composite structures*, steel, aluminum alloy, magnesium alloys, woods, and plastics, will be developed, the light materials for light structural parts requiring surface stability and the dense materials for heavy structural parts.

2. *Cast magnesium and aluminum-alloy structures*, even entire wing sections, will be developed.

3. *Riveting will be completely eliminated.*

4. *Spot welding will find an ultimate limited application.* It is not the answer to the problem of displacing rivets.

5. A method will be found for *edge-joining thin sheet* material without leaving a rough surface. Even now, very thin strips of steel can be rolled into the form of a tube and welded so accurately that the seam cannot be found by the naked eye.

6. *New high-strength alloys*, now considered impossible, will be developed.

7. *Alloys of beryllium* will be produced in production quantities, giving a ratio of strength and modulus of elasticity to density much greater than in present materials.

8. *Airplane outer surfaces* will be made *glassy smooth* and impervious to surface wrinkles.

9. *All structural joints will be welded.*

10. Practically all air-line and military airplanes will have *pressure cabins for high-altitude flying*. This introduces many new structural problems.

11. For certain types of airplanes, *pressed structural parts of plastics*, including entire sections of the airplane, will be developed.

12. *Uniformly tapered structural parts* such as tubes, extruded sections, and sheet will be made available commercially.

13. *Prefabricated cellular plates* for airplane surfaces will be developed (see, for example, Fig. 4:11).

4:5. Basic Factors in Wing Construction.—Structurally, wing design has been the most difficult problem in airplane structures. Some of the factors influencing wing design are as follows:

1. Minimum weight per square foot.

2. Minimum thickness for increased speed.

3. Maximum wing loading, limited by aerodynamic requirement.

4. Wing chord.

5. Wing span.

6. Wing material.

7. Functional requirements, such as housing of gas tanks, guns, and retractable wheels.

8. Stability requirements, to preclude wing flutter.
9. Stability of wing surface, to preclude wrinkling of the skin at a specified wing loading.
10. Rigidity in torsion and bending to ensure a constant angle of attack, and other forms of stability.

4:6. Wing-weight Variation.—Figure 4:1 shows a graphical study of some of these factors. Wing weight is plotted as a

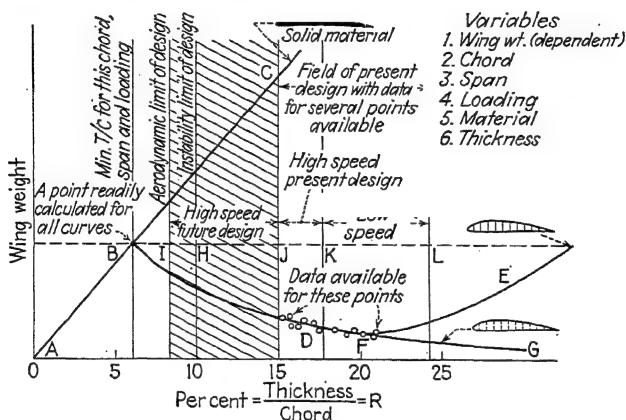


FIG. 4:1b.—A study of high-speed wings for future development.

function of the thickness-to-chord ratio for a fixed wing loading, wing span, chord, and material of construction. The following characteristics may be noted:

1. Curve *ABC* is the wing weight of a wing of solid structure, like a propeller blade of wood or forged aluminum alloy. As noted, for the material under consideration the minimum thickness-to-chord ratio possible is about 0.6. The point *B* can be determined by the application of the modulus-of-rupture formula, $f = MT/2I$, from which $I = MT/2f$. From this equality, the thickness T can be found (see Art. 5:11 for formula for I). The weight per unit length is the density of the material (pounds per cubic foot) multiplied by the volume of the wing per foot length.

2. Curves *BDE* and *BFG* represent two typical shell wing-weight curves. They both, of course, pass through point *B*.

3. The region *K* to *L* (thickness-to-chord ratios of about 0.175 up) represent the design of relatively low speed airplanes. Points on specific curves may be obtained from actual airplanes in this region. This is also true for airplanes in the present high-speed field *J* to *K*. The field *I* to *J* is the field for future developments—probably by engineering students who are now studying this text.

If a high-speed design is based on a former wing structure—the only variation being in the thickness—the point *B* may be

calculated and a parabola passed through *B* and the wing weight of the former wing structure to form a design weight curve. The accuracy should be fair.

4:7. Constants of Wing Design.—In wing-design estimates, it is desirable to know the variation of one factor in terms of another factor, all other factors remaining constant. For example, how does the weight vary with such factors as wing loading, material, span, and thickness? In the following articles, many useful relationships are derived.

4:8. Wing Weight.—Neglecting gas tanks, landing gear, etc., in the wings, the wing weight is composed of the weight of the main supporting structure and the weight of the nonsupporting structure. In shell wings the main supporting structure is the box section forming the central axis of the wing. This section represents the major portion of the structural wing weight. Without serious error—for estimating only—it may be assumed that the entire weight of the wing is proportional to the weight of the supporting structure.

Other factors being constant, the weight of a tube is proportional to the density ρ of the material and the thickness t of the wall. This is true also for a box beam without stringers or other forms of support.

In a box beam with stringers and other supports, we may assume an equivalent thickness t of skin such that the weight of the assumed unsupported box beam is the same as the weight of the actual supported box. Thus,

$$W = K_1 \rho t \quad (4:1)$$

where W = weight per square foot of projected area.

ρ = weight per cubic foot of the material.

t = thickness of the skin, in.

K_1 = a proportionality factor.

Thus, for similar wings, for the same thickness,

1. The steel wing will be $490/175 = 2.8$ times heavier than the aluminum-alloy wing.

2. The steel wing will be $490/113 = 4.32$ times heavier than the magnesium-alloy wing.

Also, for the same weight, the thicknesses will be as follows:

$$t_s = \frac{t_a}{2.8} = \frac{t_m}{4.32} \quad (4:2)$$

4:9. Moment of Inertia.—If the webs of a flat box beam of width b and depth d and flange thickness t are neglected, the moment of inertia (transverse) is

$$I = \frac{b d^3}{12} \quad (4:3)$$

The moment of inertia is proportional to the thickness of the skin. If the box beam has stringers, etc., t is the equivalent thickness as expressed in Art. (4:8).

For a thin-walled tube of radius r and thickness t , the transverse moment of inertia is

$$I = \pi r^3 t = K_3 t \quad (4:4)$$

Thus, for estimates, we may assume that the moment of inertia of the cross section of a wing box beam is proportional to an equivalent skin thickness t .

Solving for t in (4:3) and substituting in (4:1), we have

$$W = \frac{K_1}{K_2} \rho I = K_4 \rho I \quad (4:5)$$

that is, the weight of a thin-walled tube, such as a wing shell, is proportional to the amount of inertia of the cross section and to the density of the material.

4:10. Bending Moment and Wing Loading.—Upon measuring x from the tip of the (cantilever) wing, the shear at section x for a variable loading w is

$$V = \int_0^x C w \, dx \quad (4:6)$$

where C is the wing chord.

If the magnitude of the loading is increased by a constant n , then

$$V_n = n \int_0^x C w \, dx = nV \quad (4:7)$$

The bending moment at section x is

$$M = \int_0^x V \, dx = \int_0^x \int_0^x C w \, dx \, dx \quad (4:8)$$

If the magnitude of the loading is increased by a constant n , then

$$M_n = n \int_0^x \int_0^x C w \, dx \, dx = nM \quad (4:9)$$

Thus the shear and the bending moment on a cantilever wing are proportional to the magnitude of the loading.

Note that n may apply to C , the chord, as well as to w . Hence, the moment is also proportional to the chord of the wing.

4:11. Wing Rigidity in Bending.—The deflection of a cantilever wing is expressed by

If the magnitude of the loading is increased by a constant n , then

$$y_n = n \int_0^x \int_0^x \frac{M}{EI} dx dx = \quad (4:11)$$

Our conclusions are as follows:

1. For constant EI , the deflection of the wing is proportional to the loading.

2. For constant loading the deflection of the wing is inversely proportional to EI . That is,

$$y = \frac{K}{EI} \quad (4:12)$$

For the same weight of wing, from equation (4:5),

$$I = \frac{W}{\rho K_4} \quad (4:13)$$

Substituting this in equation (4:12), for constant moment and constant wing weight,

$$y = \frac{K}{EW/\rho K_4} = \frac{K_5 \rho}{EW} = K_6 \frac{\rho}{E} \quad (4:14)$$

If the deflection of the steel wing is 1, then

$$1 = \frac{490}{29,000,000}$$

or

$$K_6 = \frac{29,000,000}{490}$$

The deflection of the aluminum-alloy wing of the same weight is

$$y_a = \frac{29,000,000}{490} \times \frac{174}{10,000,000} = \frac{2.9}{2.82} = 1.03$$

The deflection of the magnesium-alloy wing of the same weight is

$$= \frac{29,000,000}{490} \times \frac{113}{6,500,000} = \frac{4.46}{4.32} = 1.03$$

Thus, it may be concluded that for the same weight of wing, for different materials, the rigidities will be about the same.

4:12. Bending Stress.—The bending stress is

$$M \frac{T}{2} \quad (4:15)$$

The allowable stress f_a , on the basis of instability, for light thin sheets is expressed by

$$f_a = KEt^2 \quad (4:16)$$

where t is the thickness of the material.

Equating equation (4:15), for constant M and T , to (4:16) and letting $M \frac{T}{2} = K_1$, we have

$$f_a = \frac{K_1}{I} = \quad (4:17)$$

Since $W = K_4 \rho I$ [equation (4:5)] and $I = W/K_4 \rho$, equation (4:17) becomes

$$\frac{K_4 K_1 \rho}{W} = KEt^2 \quad (4:18)$$

But, from equation (4:1),

$$t^2 = \frac{W^2}{E}$$

Thus, (4:18) becomes

$$\frac{K_4 K_1 \rho}{W} = \frac{EW^2}{E} \quad (4:19)$$

Thus,

$$W = K_7 \quad (4:20)$$

If W for steel is 1, then

$$\sqrt[3]{E_s} \quad (4:21)$$

Thus, for aluminum alloy,

$$W_a = \frac{\rho_s}{\rho_a} \sqrt[3]{\frac{E_s}{E_a}} = \frac{2.82}{2.82} = 0.51 \text{ as heavy as steel}$$

For magnesium alloy,

$$W_m = \frac{\sqrt[3]{4.46}}{4.32} = \frac{1.65}{4.32} = 0.38 \text{ as steel.}$$

And for plywood, approximately,

$$W_p = \frac{\sqrt[3]{30,000,000}}{490} = \frac{34}{490} = 0.07 \text{ as heavy as steel}$$

Note that this is on the basis of instability of thin sheets.

We may conclude, in general, that in similar light structures of thin material, in which instability is the strength criterion, *the lightest material has the advantage.*

On the basis of the proportional limit, for thicker sections in which we assume

$f_a = 90,000$ for chromium-molybdenum steel,

$f_a = 36,000$ for duralumin,

$f_a = 30,000$ for magnesium alloy,

we compute the weight ratio as follows:

From equations (4:15) and (4:5),

$$f_a = \frac{M}{2W} \frac{T}{\tau} \quad (4:22)$$

From this, if we let

$$\frac{MT}{2}$$

then

$$(4:23)$$

If W for steel is 1, then

$$W = \frac{f_{as}}{f_a} \frac{\rho}{\rho_s} = \frac{90,000}{490} \times \frac{\rho}{f_a} \quad (4:24)$$

Thus, for aluminum alloy,

$$W_a = \frac{90,000}{490} \times \frac{174}{36,000} - \frac{1}{2.82} \times \frac{90}{36} = \frac{90}{36} = 0.88$$

as heavy as steel

and for magnesium alloy,

$$W_m = \frac{90,000}{490} \times \frac{112}{30,000} = \frac{3}{1.25} = 0.69 \text{ as heavy as steel}$$

on the basis of ultimate strength, assuming

$f_a = 240,000$ for heat-treated steel.

$f_a = 125,000$ for chromium-molybdenum steel.

$f_a = 60,000$ for aluminum alloy.

$f_a = 43,000$ for magnesium alloy.

If, for heat-treated steel, $W = 1$, K_s in equation (4:24) becomes

$$K_s = \frac{240,000}{490}$$

Thus, for chromium-molybdenum steel,

$$\frac{W_{cs}}{W_s} = \frac{240,000}{490} \times \frac{490}{125,000} = 1.92$$

For aluminum alloy,

$$\frac{W_a}{W_s} = \frac{240,000}{490} \times \frac{174}{60,000} = \frac{4}{2.82} = 1.42$$

For magnesium alloy,

$$\frac{W_m}{W_s} = \frac{240,000}{490} \times \frac{112}{43,000} = \frac{5.45}{4.32} = 1.25$$

4:13. Variation of Weight with Wing Loading.—The moment M (w being the wing loading) is

$$M = Kw \tag{4:25}$$

where K is a constant. But

$$M = Mc \tag{4:26}$$

For constant f and c ,

$$M = K_1 I \tag{4:27}$$

Thus, equating (4:25) and (4:27),

$$Kw = K_1 I \quad (4:28)$$

But, from equation (4:5),

$$I = W \quad (4:29)$$

where W is the wing weight. Thus, equation (4:28) becomes

$$w = K_5 \frac{W}{\rho} \quad (4:30)$$

or

$$W = K_6 \rho w \quad (4:31)$$

Of course, if ρ is constant, the wing weight is proportional to the wing loading.

$$W = K_7 w \quad (4:32)$$

There are other elements, however, to be taken into consideration later. Fundamentally, however, we may consider the wing weight (cantilever) as *proportional to the wing loading*.

4:14. Variation of Wing Weight with Wing Thickness.—Letting T be the wing thickness,

$$f = \frac{M \frac{T}{2}}{I} = \frac{MT}{2I} \quad (4:33)$$

from which

$$T = \frac{2fI}{M} \quad (4:34)$$

For constant f and M ,

$$T = KI \quad (4:35)$$

However, I is proportional to the thickness t of the skin, and the wing thickness squared, T^2 [see equation (4:3.)]. Thus,

$$I = K_1 CT^2 t \quad (4:36)$$

The wing weight is approximately expressed:

$$W = \quad t = \quad (4:37)$$

Substituting in (4:36),

$$^2 \frac{W}{K_2 \rho} \quad (4:38)$$

Substituting equation (4:38) in equation (4:35),

$$T = \frac{WC}{\rho} \quad (4:39)$$

or

$$(4:40)$$

Thus, in general, the wing weight is inversely proportional to the thickness of the wing.

4:15. Variation of Wing Weight with Wing Span.—Let L be the semi-span of the monoplane wing. The bending moment at a distance x from the tip of the cantilever wing is proportional to x^2 , and the bending moment at the root section is proportional to L^2 . Thus,

$$M = KL^2 \quad (4:41)$$

We have noted [equation (4:25)] that the moment is proportional to the wing loading and [equation (4:31)] that the wing weight is proportional to the wing loading; hence, the wing weight is proportional to the square of the semi-span L . Thus, we may write

$$W = K_1 L^2 \quad (4:42)$$

4:16. General Variation of Wing Weights.—We have noted that the weight of a cantilever shell wing varies as follows:

1. Equation (4:31). Proportional to the wing loading w .
2. Equations (4:1), and (4:31). Proportional to the density of the material.
3. Equation (4:9) and explanation following. Proportional to the chord C of the wing.
4. Equation (4:23). Inversely proportional to the allowable stress f_a .
5. Equation (4:40). Inversely proportional to the thickness T and chord C .
6. Equation (4:42). Proportional to the square of the semi-span L .

Hence, we may write the general expression for wing weight,

$$W = K \frac{L^2}{T f_a C} \quad (4:43)$$

This equation checks dimensionally.

Expressed as a function of T/C , we have

$$W = K \frac{1}{T/C} \frac{1}{f_a/\rho} \frac{L}{C} wL \quad (4:44)$$

This relation may be stated as follows: The wing weight is inversely proportional to the *thickness-chord ratio* and the *strength-weight ratio* and proportional to the *aspect ratio*, the *wing loading*, and the *span*.

4:17. More Exact Equation of Wing Weights.—Equation (4:44) is parabolic as shown by curve *BDG*, Fig. 4:1*b*. It cannot, however, be made to pass through two points such as *B* and *D*, since it contains only one constant. If the ratio T/C is replaced by $(T/C)^n$, in which n is a constant, equation (4:44) remains dimensionally correct, and the curve can be made to pass through the two points *B* and *D* of Fig. 4:1*b*. The equation will undoubtedly become more exact. Thus,

$$W = K \cdot \frac{1}{\left(\frac{T}{C}\right)^n} \cdot \frac{1}{\frac{L}{\infty}} \cdot wL \quad (4:45)$$

[It should be emphasized that equation (4:45) merely expresses a general relationship for the study of future trends. It may

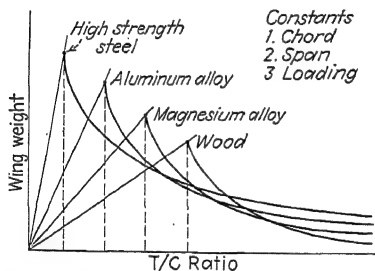


FIG. 4:2.—Typical curves of wing weight as a function of thickness to chord ratio for several materials.

serve as a starting point for developing a design wing-weight formula.]

In equation (4:45), f_a is a function of W . For example, for very light weights, f_a is mostly a function of the elastic stability of the material, giving an advantage to lightweight materials. On the other hand, for very heavy wings, heavy materials can be used in thick enough sections to develop ultimate strengths. The lighter materials would require, in this high-weight range, such thick sections that their efficiency would be reduced in practice.

The curves of Fig. 4:2, patterned after the curve *BDG* of Fig. 4:1 and calculated by formula 4:45, show the fundamental uses of materials in aircraft-wing construction. The relative magnitudes of weights are arbitrarily shown. They of course depend upon the strength-weight ratios assumed.

Simply expressed, the curves show

1. That for very light wings, such as soaring plane wings, a very light material such as wood has the advantage fundamentally.

2. That for very heavy wings, such as the wings required for a wing loading of 80 to 100 lb. per square foot and a T/C ratio of about 0.1, a high-strength dense material has the advantage fundamentally.

4:18. Wing Torsion as a Factor in Wing Weight.—In a mono-coque structure the torsional stress (shear) is given by the formula

where Q = torsion on the wing.

A = area circumscribed by the contour of the wing section.

t = thickness of the material.

q = torque per unit of length.

L = length of the semi-span.

We note the following:

- (1) q is proportional to the wing loading w and the chord C .

$$q = KwC \quad (4:47)$$

- (2) A is proportional to the product of the chord and the thickness t .

$$A = K_1TC \quad (4:48)$$

- (3) W , weight, is proportional to the thickness t of the skin and the periphery of the wing. Thus,

$$W = \rho tp \quad (4:49)$$

However, for thin wing sections, for all practical purposes, p is proportional to the chord C ; thus,

$$W = K_2t\rho C \quad (4:50)$$

Substituting (4:47) and (4:48) in equation (4:46), we have

$$S = \frac{KwCL}{2K_1TCt} \quad (4:51)$$

However, from (4:50),

$$tC = \frac{W}{\rho} \quad (4:52)$$

Thus,

$$S = \frac{KwCLK_2\rho}{2K_1TW} \quad (4:53)$$

Solving for W , we have

$$W = K_3 \frac{wCL}{TS} \quad (4:54)$$

$$\frac{w}{T/C} \frac{\rho}{S} \quad (4:55)$$

This equation is the same in form as equation (4:43) except that L is not squared.

4:19. Torsional Rigidity.—If θ is the angle of twist for a length L , we have (see Art. 9:12)

$$A = \frac{Qc}{\tau}$$

where $Q = qL$.

$$q = KwC. \quad (C = \text{wing chord})$$

Thus,

$$Q = KwCL \quad (4:57)$$

In these equations, w is the wing loading, L is the length of the semi-span, c is the periphery of the airfoil section, A is the area circumscribed by the airfoil section, E_s is the modulus of elasticity in shear, and t is the thickness of the skin.

From equation (4:48), $A = K_1TC$. Thus, equation (4:56) becomes

$$\theta = \frac{KwcCL^2}{4}$$

For a thin wing, c is practically $2C$; thus,

However, substituting equation (4:52) into equation (4:58), we have

$$\theta = K_3 \frac{wCL^2\rho}{T^2E_sW} \quad (4:59)$$

Solving for W ,

$$W = K_3 \frac{wCL^2\rho}{T^2E_s\theta} \quad (4:60)$$

$$= K_3 \frac{w}{(T/C)^2} \frac{\rho}{E_s} \frac{L^2}{C\theta} \quad (4:61)$$

For the same conditions except for the material, the angle θ is proportional to the ratio ρ/E_s and inversely proportional to the weight.

The *rigidity* is proportional to W and E_s/ρ .

4:20. Frequency of Vibration. Bending.—If we let f be the frequency, we have

$$n = \sqrt{\frac{EI_0g}{\rho A_0}} \quad (4:62)$$

where n is a constant for the wing section and I_0 and A_0 refer to the root section of the wing. If t is the thickness of the skin, I_0 is proportional to t , and the square of the thickness of the wing $T^2 \cdot A_0$, the area of the cross section of the metal, is proportional to the chord and to the thickness t . Thus, equation (4:62) may be expressed as follows:

$$\overline{E T^2 t} \quad (4:63)$$

But

$$W = K_1 C t \rho$$

Thus,

$$(4:64)$$

However, for the same weight, t is inversely proportional to ρ ; thus equation (4:64) becomes

$$\overline{E} \quad (4:65)$$

If we let f_s refer to steel, f_a to aluminum, and f_m to magnesium alloy, for constant T and L ,

$$\begin{aligned} \frac{f_s}{f_a} &= \sqrt{\frac{E_s/\rho_s}{E_a/\rho_a}} = \sqrt{\frac{30,000,000}{490}} \times \sqrt{\frac{174}{10,000,000}} \\ &= \sqrt{\frac{3 \times 174}{490}} \quad \frac{522}{1.03} \end{aligned}$$

Thus

$$\frac{f_s}{f_m} = \sqrt{\frac{30,000,000}{490}} \quad \frac{522}{6,500,000}$$

Thus for the same weight of wing the frequency of bending vibration will be approximately the same for all materials considered.

4:21. Torsional Frequency of Vibration.—The torsional frequency of vibration of a thin-walled tube is given by

$$f = \quad (4:66)$$

where M is the mass per unit length. M is proportional to W and C . Thus

$$M = KWC \quad (4:67)$$

When equation (4:66) is used for an airfoil-shaped tube, r may be replaced by $K_1 T$, in which T is the thickness and K_1 is a constant. Thus, equation (4:66) becomes

$$f = \frac{K_2}{L} \sqrt{\frac{E_s t T}{WC}} \quad (4:68)$$

However, the thickness t is inversely proportional to the allowable stress f_a ; thus, equation (4:68) becomes

$$(4:69)$$

Thus for the same weight of wing, W , and constant T/C and L , the frequency may be expressed

$$(4:70)$$

4:22. Composite Structures.—The three principal features to be taken into consideration in the design of composite wing structures are

1. Division of stress among members of different materials carrying loads.
2. Temperature stresses.
3. Electrolytic action.

4:23. Division of Stress.—If two materials must carry a load in parallel (equal deformations), the stresses are in proportion to the modulus of elasticity of each material. For example, if aluminum alloy and steel are used together, the stress in the aluminum alloy will be approximately one-third of that in the steel. If the proportional limit of the aluminum alloy is 40,000 lb. per square inch and that of the steel is 120,000 lb. per square inch, the proportional limits of the two materials will be reached at the same applied wing load. In design, it probably can be assumed that they work well together to the ultimate strength.

In the case of a plastic with steel, on the basis of an average modulus of elasticity of 1,500,000 lb. per square inch for plastics, the stress in the plastic will be one-twentieth that of steel. For example, if the proportional limit of the plastic is 6,000 lb. per square inch and that of steel is 120,000 lb. per square inch, the elastic limits of the materials will be reached at the same wing loading. For example, if the main supporting part of the wing

structure is steel, if the wing cover is a shell of plastic, and if the stress in the steel at a load factor of 2 is 20,000 lb. per square inch, the stress in the plastic cover will be 1,000 lb. per square inch. The plastic cover, to be satisfactory, must not wrinkle at this stress or at the maximum temperature stress. The attachment of the two materials must be such that there will be no failures in the attachments and no slippage between the materials.

4:24. Temperature Stresses.—The following table shows the coefficients of thermal expansion of various metals.

Material	Coefficient of Thermal Expansion per Degree Fahrenheit, C
Magnesium alloy.....	0.000016
Aluminum alloy.....	0.000012
Steel.....	0.0000066

Let C be the coefficient of expansion. Let the subscript s refer to steel and the subscript m refer to magnesium.

Example.—Assume 20 ft. (240 in.) of magnesium alloy and steel used in parallel, a change of temperature from 70 to -50°F. , and the same area of cross section. Find the stress.

The change of temperature is 120°F. The deformation of the steel unrestrained will be

$$\begin{aligned}\delta_s &= 120 \times 240 \times 0.0000066 \\ &= 0.19 \text{ in.}\end{aligned}$$

The deformation of the magnesium alloy unrestrained will be

$$\begin{aligned}\delta_m &= 120 \times 240 \times 0.000016 \\ &= 0.46 \text{ in.}\end{aligned}$$

The difference of deformation is

$$\Delta\delta = \delta_m - \delta_s = 0.46 - 0.19 = 0.27 \text{ in.}$$

On the assumption now that the materials are brought to the same length, the deformation of each metal will be inversely proportional to its modulus of elasticity.

Thus, $\Delta\delta_m/\Delta\delta_s = 30,000,000/6,500,000 = 4.62$. Thus,

$$\Delta\delta_m = 4.62 \Delta\delta_s.$$

Since $\Delta\delta_m + \Delta\delta_s = 0.27$ in., then $4.62 \Delta\delta_s + \Delta\delta_s = 0.27$ in. Thus, $5.62 \Delta\delta_s = 0.27$ in. $\Delta\delta_s = 0.27/5.62 = 0.048$ in., and $\Delta\delta_m = 0.27 - 0.048 = 0.222$ in.

The stress in the magnesium is

$$\begin{aligned} f_m &= \frac{E \Delta \delta_m}{L} = \frac{6,500,000 \times 0.222}{240} \\ &= 27,000 \times 0.222 \\ &= 6040 \text{ lb. per square inch} \end{aligned}$$

4:25. Temperature-stress Formula.—The deformation per unit length of each of two metals, for example, steel and magnesium, used together is

$$\delta_s = C_s t \quad (4:71)$$

and

$$\delta_m = C_m t \quad (4:72)$$

where t refers to the change in temperature in degrees Fahrenheit. The difference, that is, the relative free expansion, is

$$\delta = (\delta_m - \delta_s) = t(C_m - C_s) \quad (4:73)$$

If the metals are combined (as welded parallel), the relative strain becomes zero, and stresses are developed. If f is the stress,

$$f_s = E_s \Delta \delta_s \quad (4:74)$$

and

$$f_m = E_m \Delta \delta_m \quad (4:75)$$

where, as δ is used in (4:73),

$$\Delta \delta_s + \Delta \delta_m = \delta \quad (4:76)$$

Dividing equation (4:74) by (4:75),

$$\frac{f_s}{f_m} \quad (4:77)$$

or

$$f_m E_s - \overline{\Delta \delta_m} \quad (4:78)$$

Solving for $\Delta \delta_s$ and substituting in equation (4:76),

$$\begin{aligned} f_s E_m \Delta \delta_s - \Delta \delta_m \\ t(C_m - C_s) \end{aligned} \quad (4:79)$$

However, $\Sigma F = 0$. Thus

$$f_s A_s = f_m A_m \quad \text{or} \quad f_m = f_s \frac{A_s}{A_m} \quad (4:80)$$

Substituting equation (4:80) in (4:79),

$$\left(\frac{E_m A_m}{E_s A_s} \right) \quad (4:81)$$

Thus

$$\Delta \delta_m =$$

Thus, from equation (4:75),

$$f_m = \quad - C_s) \quad (4:82)$$

Similarly,

$$(4:83)$$

Thus, if $A_s =$

$$f_s = f_m = \frac{E_m E_s}{E_m + E} \quad (4:84)$$

If, for example, $t = 120^\circ$,

$$\begin{aligned} &= \frac{6,500,000 \times 30,000,000}{6,500,000 + 30,000,000} \times 120(0.000016 - 0.0) \\ &= \frac{195,000,000,000,000}{36,500,000} \times 120(0.0000094) = \frac{19,500}{365} \times 120 \\ &\quad \times 0.94 = 6,040 \text{ lb. per square inch} \end{aligned}$$

In the extreme case of $t = 240^\circ\text{F.}$ change, the stress would not be excessive at 12,080 lb. per square inch. In the case of plastics used with steel, the stress will be about one-third of the above figure, depending on the characteristic of the plastic. For plastics and aluminum alloys, the stress will be less.

The conclusions in regard to the temperature stress are that the problem is one of simple design and that the temperature stresses in general will not be prohibitive.

4:26. General Analysis of Wing Structures.—On the basis of the principles discussed above and the mathematical analysis, a number of studies have been made on wing structures that show promise of being suitable for high-speed airplane wings of minimum thickness, increased wing loading, satisfactory vibration and wing-flutter characteristics, and surface smoothness under load, that is, for wings that are as light as it is possible to make them, consistent with the following requirements:

1. Adequate strength in bending.
2. Adequate rigidity in bending.
3. Adequate strength in torsion.
4. Adequate rigidity in torsion.
5. Maximum natural frequency in bending.
6. Maximum natural frequency in torsion.
7. Elastic axis near the center of pressure.
8. Mass axis near the center of pressure and coinciding with the elastic axis, if possible. (NOTE: See Art. 15:3 for definition of elastic axis.)
9. Stability of the skin under all flight conditions.

4:27. Theoretically Ideal Wing Structure.—Figure 4:3 illustrates a theoretical construction satisfying all nine of the require-

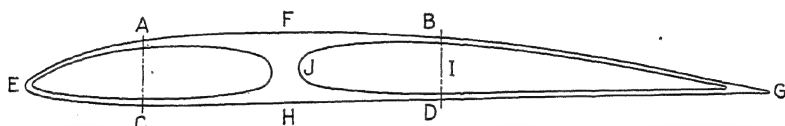


FIG. 4:3.—A theoretically ideal section for (a) strength in bending and torsion, (b) rigidity in bending and torsion, (c) surface smoothness at all loads, (d) stability characteristics.

ments specified in the last article, as follows (bear in mind that wing loadings much greater than for present designs, and thickness-chord ratios much less than for present designs are under consideration):

1. Disposition of the material for *maximum strength-to-weight ratio in bending*. This is due mostly to the I-beam section $ABCD$ and the particular shape of this I-beam section for the best form factor. If the ultimate strength of the material in the I-beam can be developed, the form factor is unity. The principle of design for this maximum form factor dictates the design shape of the I-beam.

The nose and the tail sections assist in resisting bending, to some extent.

2. Disposition of material for *maximum rigidity-weight ratio in bending*. Again the I-beam section is the most ideal for this requirement.

3. Disposition of the material for *maximum frequency of vibration in bending*. Minimum weight and maximum rigidity produce maximum frequency.

4. Skin thick enough at points of high stress to *preclude wrinkling*. If the skin does not wrinkle, the stress in the skin will be approximately the same as for the outer portions of the supporting structure. This condition necessitates a rigid skin.

5. Disposition of the material for *maximum strength-weight ratio in torsion*. For a given stress in the skin the torsional strength is proportional to the area circumscribed by the skin, indicated as $EAFBGDHC$.

6. Disposition of the material for *maximum rigidity-weight ratio in torsion*. The torsional rigidity is approximately proportional to the area circumscribed by the outer shell of the wing.

7. Disposition of the material for *maximum natural frequency in torsion*. This condition requires that the wing section have a maximum rigidity in torsion and a minimum mass moment of inertia about the elastic axis. The latter requirement means that any excess material which does not contribute to the torsional rigidity of the wing must be disposed of in such a way as to make the mass moment of inertia about the torsional axis a minimum. Note that the material at *FJH* used primarily for bending is disposed of in such a way that its mass moment of inertia about the torsional axis is a minimum.

8. The *elastic axis* of the wing in torsion is placed so that it coincides with the *center-of-pressure axis* for the design flight condition.

9. The *elastic axis* and the *mass axis* of the wing are made to coincide as nearly as possible.

10. The skin is made thick enough for the design stress so that *no wrinkles* develop (see Fig. 4:4).

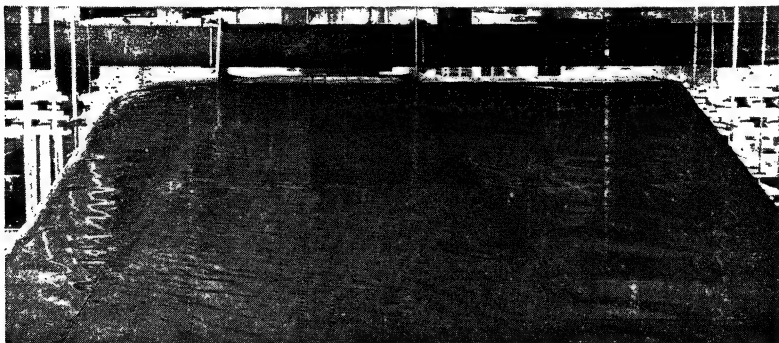


FIG. 4:4.—Development of undesirable wrinkles of wing skin under load.

11. Disposition of structure to leave *interior clear* for gas tanks, guns, etc. (see Fig. 4:5).



FIG. 4:5.—An experimental wing construction in which the upper and lower surfaces are locally reinforced, thus eliminating the conventional ribs. (Courtesy of Curtiss-Wright Corporation.)

This theoretical wing section, of course, as shown, has considerable fabrication difficulties. That, of course, is the problem.

The study, however, gives students of structures and materials, an ideal to serve as a guide. *Note that progress in airplane design of the future will be mostly in structures, as it has been in the last ten years.*

4:28. Possible Trends of Wing-structure Development.—

The engineer of tomorrow is the student of today. Airplane structures of the future will not be the same as present-day airplane structures. It is good for the imagination—with which all aeronautical engineers must be well supplied—to speculate about airplane structures of the future. On the basis of the requirements noted in this chapter, the following possibilities are offered to students for further study and improvement (bear in mind that wing weights of 5 to 15 lb. per square foot, wing loadings of 50 to 100 lb. per square foot, and T/C ratios of about 10 per cent or less are considered):

1. Figure 4:6 illustrates the possibility of casting or pressing a light material reinforced by high-strength bars. If the light material is metal,

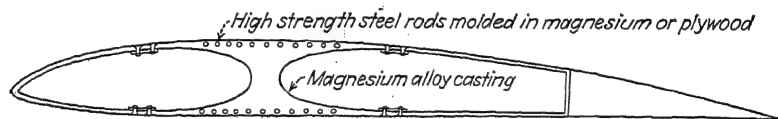


FIG. 4:6.—Cast or pressed light material reinforced by high-strength bars.

the nose and rear sections may be formed of thick flat sheet and welded in place. A program of research would be required to solve the many construction problems and make the construction practical.

2. Figure 4:7 illustrates the possibility of using high-strength steel for a single wing beam and a plastic plywood, quite thick, for the skin. The

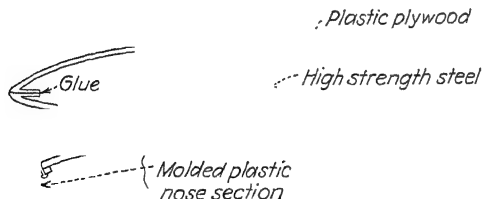


FIG. 4:7.—Wing construction: high-strength steel spar and plastic plywood shell.

plastic could be made to carry its part of the load in proportion to its weight. The steel spar, of course, must be designed for the particular job, the wing in the figure being used merely for illustration.

Figure 4:8 shows multiple spars of steel or aluminum alloys with a skin of plastic plywood or thick magnesium alloy. A program of research would be

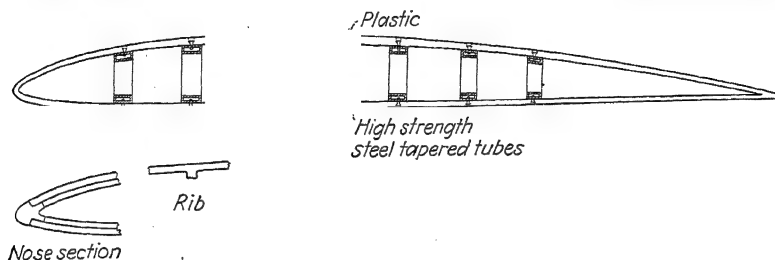


FIG. 4:8.—A study for a combination steel and plastic wing.

required to solve the many construction problems and make the construction practical.

Figure 4:9 shows a conventional corrugated wing construction of present design covered by a thick skin of plastic plywood or magnesium alloy. The internal structure may be of steel or aluminum alloy.

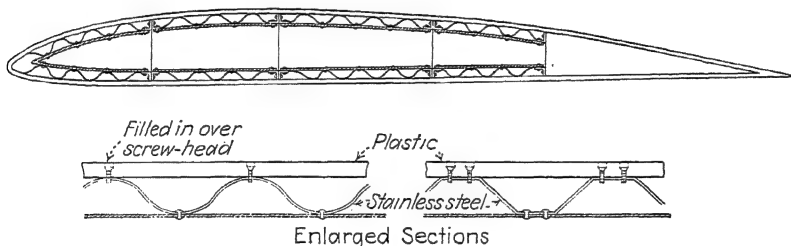


FIG. 4:9.—A combination of plastic material and steel for very thin, high-speed wings.

3. Figure 4:10 illustrates a possible construction of high-strength bars or wires molded into a lightweight material. As previously noted, each mate-

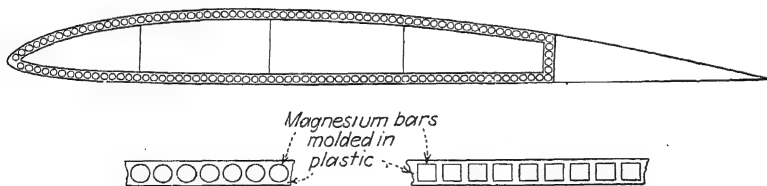


FIG. 4:10.—A study of a possible magnesium-plastic wing.

rial will carry a stress approximately in proportion to its weight. The light material will stabilize the bars or wires, and the bars or wires will add strength to the structure.

4. Figure 4:11 illustrates a possible steel structure modeled after the corrugated-cardboard-box construction. And just as the cardboard is

bought from the manufacturer and then fabricated into boxes, it is assumed that the steel corrugated construction plates will be purchased from a manufacturer and fabricated into airplane structures by welding.

A program of research would be required to solve the many construction problems and make the construction practical.

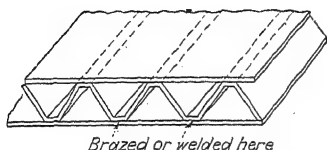


Fig. 4:11.—Special case of the honeycombed section of steel.

When the low-density core of the structure is wood or plastic plywood and the outer structure is metal such as aluminum alloy or steel, this type of structure has been referred to as *Plymetal*.

Two of the problems with respect to this construction are as follows:

(1) Bondage between the metal and the wood or plastic would be difficult.

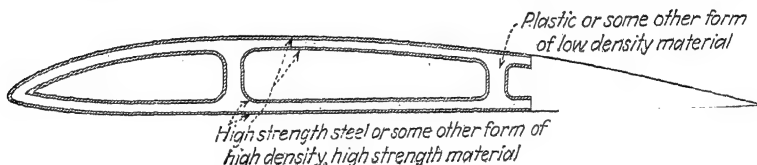


Fig. 4:12.—A wing section based upon the theory that a low-density material supported by a high-density, high-strength material is ideal for wing construction.

This problem has been solved by at least one company by constructing flat plates of a limited size; considerable pressure and heat were required. (2) The forming of the metal sections and their combination with the light material would be difficult.

We have engineers in high positions in our large aircraft factories who have emphasized the desirability of a program of research for this type of construction. If this construction could be made practical, it would be ideal from the standpoint of strength-weight ratio, rigidity, and vibration for almost any part of the structure of an airplane.

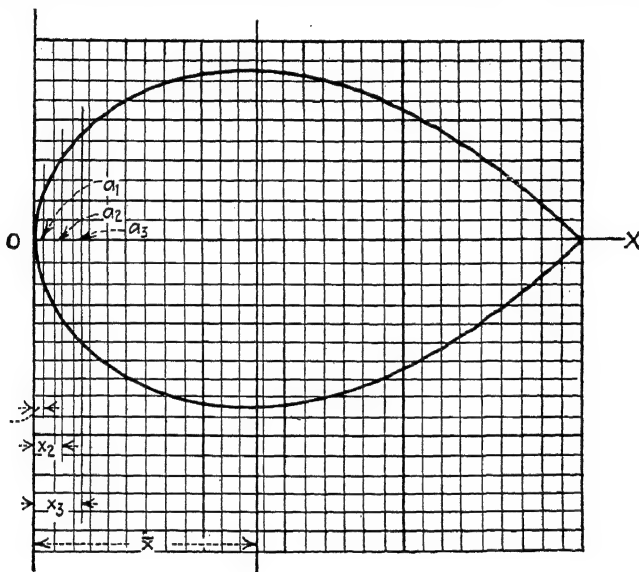
The problem of *shear lag* (Chap. XVII) would be important in the design of this type of wing section. However, a stubby wing closed at the ends by the same stress construction would not be affected very greatly by shear lag.

Our present type of stringer thin-sheet combination, developed to a much higher degree of perfection for steel as well as for aluminum alloys, will undoubtedly occupy the leading position in aircraft construction for a long time before it is finally displaced.

CHAPTER V

PROPERTIES OF STRUCTURAL SECTIONS

5:1. Approximate Methods.—In aircraft stress analyses, it is frequently necessary to compute the *areas*, *centroids*, and *moments of inertia* of irregular cross sections and cross sections of unconventional shapes such as the streamlined section. Probably the



Area of each square = $0.1 \times 0.1 = 0.01$ sq. in.
 FIG. 5:1.—Neutral axis and moment of inertia by approximate method.

simplest course to follow in computing these quantities for irregular sections not subject to mathematical analyses is that indicated by the definition of the quantities. For example,

$$A = (a_1 + a_2 + a_3 + a_4 + \cdots + a_n) \quad (5:1)$$

where A = total areas.

a_1, a_2 , etc. = areas of the parts taken as the basis of calculations.
 For example, in Fig. 5:1, which illustrates the cross section of

a strut, the total area is as indicated in equation (5:1), the value of each term of which may be computed.

If the section is too irregular for the calculation of the increments of area, the work of calculation may be facilitated by plotting the section on coordinate paper, laid off in squares of 0.1-in. sides. These unit squares then will be 0.1 in. by 0.1 in., or 0.01 sq. in. in area. For example, in Fig. 5:1 we have a stream-

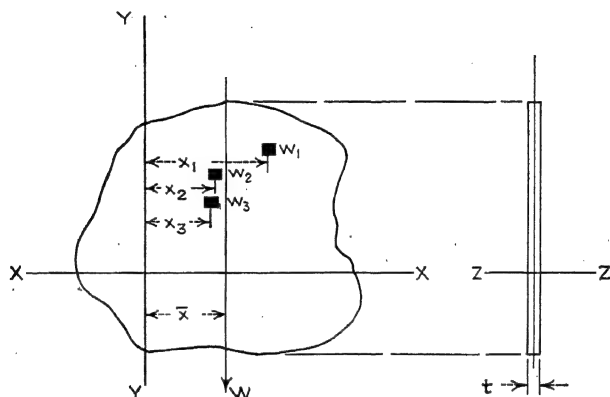


FIG. 5:2.—Location of center of gravity and centroid.

lined section plotted on 0.1-in. cross-section paper. The area, by counting the squares, is in square inches,

$$A = (a_1 + a_2 + a_3 + \dots) \\ = (0.04 + 0.08 + 0.10 + 0.12 + \dots) \quad (5:2)$$

5:2. The Centroidal Axis.—In determining the centroid of the area, use is made of the principle of moments. For example, in Fig. 5:2,

$$W\bar{x} = x_1w_1 + x_2w_2 + x_3w_3 = \Sigma xw \quad (5:3)$$

or since

$$W = \dots w_2 \quad (5:4)$$

we have

$$\bar{x} = \frac{x_1w_1 + x_2w_2}{W} \quad (5:5)$$

Now if the weights w_1, w_2, w_3 , etc., are the weights of a section of a thin plate of thickness t and density ρ per unit volume, then

$$w_1 = \rho t a_1, \quad w_2 = \rho t a_2 \quad (5:6)$$

$$\bar{x} = \frac{w_1 \bar{x}_1 + w_2 \bar{x}_2}{w_1 + w_2} = \frac{\rho t a_1 \bar{x}_1 + \rho t a_2 \bar{x}_2}{\rho t a_1 + \rho t a_2} \quad (5:7)$$

or, for the areas,

$$\bar{x} = \frac{\sum x a}{\sum a} \quad (5:8)$$

which, written in integral form, is

$$\bar{x} = \frac{\int x dA}{A} \quad (5:9)$$

The use of 0.1-in. coordinate paper is also very convenient for the evaluation of equation (5:8) for an irregular section as illustrated in Fig. 5:1. Applying equation (5:8), we tabulate the calculation as in Table 5:1.

TABLE 5:1.—TABULATION OF CALCULATION FOR CENTROID

Area	Area, a , sq. in.	x , in.	xa
a_1			
a_2			
a_n			
	Σa		Σxa

5:3. Centroidal Axes of Small Areas.—For small areas, which are usual in aircraft structures, it appears to be inadvisable to use graphical methods for finding either the centroid or the moment of inertia.

A very practical and accurate method of finding a centroidal axis of an area is as follows: Plot the area on stiff cardboard or a sheet of metal. Cut the section out. Now

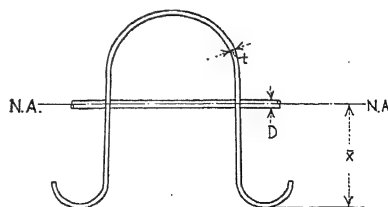


FIG. 5:3.—Neutral axis of thin metal spar by experiment.

balance the cutout section as nearly as possible over a wire of small diameter. The line of contact with the wire will be the centroidal

axis. In finding the centroid of a cross section of a beam of very thin sheet metal, for example, as in Fig. 5:3, a wire of small diameter may be bent to the proper shape for use in place of the cardboard section. The bent wire

may then be balanced across another small straight wire to find \bar{x} .

5:4. Centroid by Integration.—As an example of the determination of a centroidal axis of a section of thin sheet material, consider the section shown in Fig. 5:4. We are to find \bar{y} .

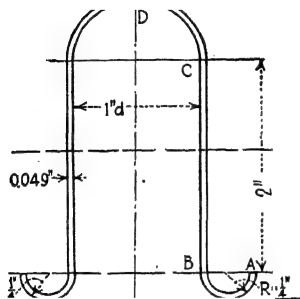


FIG. 5:4.—Centroid and moment of inertia of thin metal spar section by integration.

$$\bar{y} = \frac{\int y \rho t ds}{\int \rho t ds} = \frac{\int y ds}{\int ds} \quad (5:10)$$

where ρ = density of the material.

s = distance along the neutral line of the thin sheet.

Supplying the limits in equation (5:10), we have

$$\bar{y} = \frac{2 \int_A^B y ds + 2 \int_B^C y ds + 2 \int_C^D y ds}{2 \int_A^B ds + 2 \int_B^C ds + 2 \int_C^D ds} \quad (5:11)$$

$$\bar{y} = \frac{2 \left(\int_A^B y ds + \int_B^C y ds + \int_C^D y ds \right)}{2 \left(\frac{1}{4}\pi + 2 + \frac{1}{4}\pi \right)} \quad (5:12)$$

since for a semicircle, as in Fig. 5:11,

$$\begin{aligned} \bar{y}_0 &= \frac{\int y dw}{\int dw} = \frac{2\rho 0.049r^2 \int_0^{\pi/2} \sin \theta d\theta}{2\rho 0.049r \int_0^{\pi/2} d\theta} \\ &= \frac{r \left[\sin \theta \right]_0^{\pi/2}}{\left[\theta \right]_0^{\pi/2}} = \frac{2r}{\pi} \end{aligned} \quad (5:13)$$

We find, for equation (5:12),

$$\bar{y} =$$

$$= \frac{2(0.785)(0.250 - 0.159) + 2(2)(1.25) + (2.57)(1.57)}{2(0.785) + 4 + 1.57}$$

or

$$= 1.285 \text{ in.} \quad (5:14)$$

5:5. Moment of Inertia.—The definition of the moment of inertia of an area about an axis is

$$I_y = \int dA \quad (5:15)$$

It will be recalled that this integral is important because of its appearance in the modulus-of-rupture formula.

The integral may be determined approximately by the formula

$$I_y = x_3^2 a_3 \quad (5:15a)$$

For example, in Fig. 5:1, the moment of inertia of the streamlined section about the *oy*-axis is given by the equation (5:15a). The tabulation will be as in Table 5:2.

TABLE 5:2.—TABULATION OF CALCULATIONS FOR MOMENT OF INERTIA

Area, designation	Area, <i>a</i> , sq. in.	<i>x</i> , in.	<i>x</i> ² <i>a</i>
<i>a</i> ₁			
<i>a</i> ₂			
<i>a</i> ₃			
	Σ <i>a</i>		Σ <i>x</i> ² <i>a</i>

In most cases, the moment of inertia about the centroidal axis is required. If the area of the cross section and the location of the centroidal axis are known, it is a very simple matter to find the moment of inertia about any axis by the use of the parallel-axis theorem.

5:6. Parallel-axis Theorem.—Quite often the parallel-axis theorem is used erroneously. Let us note the assumptions in its derivation.

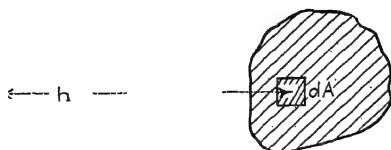


FIG. 5:5.—Parallel axis theorem.

Let us assume in Fig. 5:5 that I_y is known. We are to find $I_{y'}$. We have, by definition,

$$I_{y'} = \int (h + x)^2 dA \quad (5:16)$$

Or, upon expansion,

$$= \int h^2 dA + 2 \int hx dA + \int x^2 dA \quad (5:17)$$

Since

$$\int h^2 dA = h^2 \int dA = h^2 A \quad (5:18)$$

and

$$\int x^2 dA = I_y \quad (5:19)$$

we have

$$I_{y'} = I_y + h^2 A + 2 \int hx dA \quad (5:20)$$

which is the general form of the parallel-axis theorem.

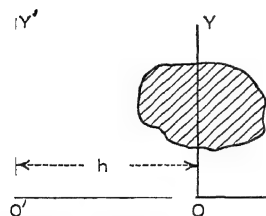


FIG. 5:6.—Moment of inertia about parallel axis through center of gravity.

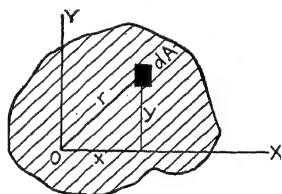


FIG. 5:7.—Polar moment of inertia.

Now, if the oy -axis were the centroidal axis as in Fig. 5:6, the integral $\int x dA$ would become zero. Hence, using a bar above the symbols to refer to the centroidal or gravity axis, we have the special case of the parallel-axis theorem. Writing the general symbol I for $I_{y'}$, we have

$$I = \bar{I} + h^2 A \quad (5:21)$$

It should be specially noted that equation (5:21) refers to the gravity axis of the section.

5:7. Polar Moment of Inertia.—In problems in torsion it is necessary to know the polar moment of inertia of a section. Letting J be the symbol for the polar moment of inertia, we have

$$J = \int r^2 dA \quad (5:22)$$

We note in Fig. 5:7 that

$$r^2 = x^2 + y^2 \quad (5:23)$$

Hence

$$J = \int (x^2 + y^2) dA = \int x^2 dA + \int y^2 dA \quad (5:24)$$

or

$$J = I_y + I_x \quad (5:25)$$

In certain symmetrical areas, such as that of a cylinder, I_y and I_x are equal, so that

$$J = 2I \quad \text{or} \quad I = \frac{J}{2} \quad (5:26)$$

This relation is sometimes useful in the simplification of the calculation of I . For example, for the circular cylinder,

$$J = \int r^2 dA = \int_0^{2\pi} \int_0^a r^2 (r d\theta) dr \quad (5:27)$$

Evaluating the integral,

$$J = \frac{2\pi a^4}{4} = \frac{\pi a^4}{2} \quad (5:28)$$

Since

then

$$I = \frac{\pi a^4}{4} \quad (5:29)$$

5:8. Moment of Inertia of the Cross-sectional Area of a Streamlined Surface.—For the purpose of this illustration, let us assume the streamlined section is composed of an elliptical nose and a parabolic tail, as illustrated in Fig. 5:8. We are to find the moment of inertia about the x - x axis. (The example is for illustration of the *method*.) If we let I_e be the moment of inertia of the elliptical nose and I_p the moment of inertia of one side of the parabolic tail, we have, letting $2a$ and $2b$ be the x - and y -a respectively, of the ellipse,

$$\begin{aligned}
 I_e &= \int y^2 dA = 2 \int_0^{\frac{a}{b} \sqrt{b^2 - y^2}} \int_0^b y^2 dx dy \quad (5:30) \\
 &= \frac{2a}{b} \int_0^b y^2 (\sqrt{b^2 - y^2}) dy
 \end{aligned}$$

If we let

$$y = b \sin \theta,$$

then

$$dy = b \cos \theta d\theta$$

and

$$\sqrt{b^2 - y^2} = b \cos \theta$$

Thus

$$I_e = 2ab^3 \int \sin^2 \theta \cos^2 \theta d\theta = \frac{ab^3}{2} \int \sin^2 2\theta d\theta$$

or

$$I_e = \frac{ab^3}{4} \int_0^{\frac{\pi}{2}} (1 - \cos 4\theta) d\theta = \frac{ab^3}{4} \left[\theta - \frac{\sin 4\theta}{4} \right]_0^{\frac{\pi}{2}}$$

so that

$$I_e = \frac{\pi ab^3}{4} \quad (5:31)$$

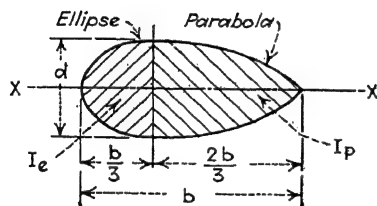


FIG. 5:8.—Streamlined section of elliptic nose and parabolic tail.

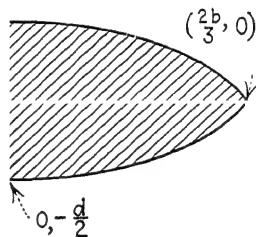


FIG. 5:9.—Parabolic tail of streamlined section.

We note for future reference that the moment of inertia of the complete ellipse is

$$\frac{\pi ab^3}{4} \quad (5:32)$$

The equation of a parabola symmetrical with respect to the y -axis is

$$x^2 = 4p(y - k) \quad (5:33)$$

We note from Fig. 5:9 that, when $y = 0$, $x = 2b/3$ and, when $x = 0$, $y = -d/2$. Substituting these limits in turn in equation

(5:33), we have

$$0 = 4p \left(-\frac{d}{2} - k \right)$$

from which

$$k = -\frac{d}{2}$$

and

$$\frac{4}{3} b^2 = 4p(-k)$$

From this,

$$p = +\frac{2}{9} \frac{b^2}{d} \quad (5:34)$$

from which

$$x = \frac{2b}{3} \sqrt{\frac{2}{d} \left(y + \frac{d}{2} \right)} \quad (5:35)$$

We therefore have

$$I_p = 2 \int_0^{-\frac{d}{2}} \int_0^x y^2 dx dy \quad (5:36)$$

or, integrating with respect to x ,

$$I_p = \frac{4b}{3} \sqrt{\frac{2}{d}} \int_d^0 y^2 \left(\sqrt{y + \frac{d}{2}} \right) dy \quad (5:37)$$

To integrate, let

$$y + \frac{d}{2} = z^2, \quad y = z^2 - \frac{d}{2}$$

and

$$dy = 2z dz$$

Thus

$$\begin{aligned} \int y^2 \left(\sqrt{y + \frac{d}{2}} \right) dy &= 2 \int \left(z^2 - \frac{d}{2} \right)^2 z^2 dz \\ &= 2 \int \left(z^6 - dz^4 + \frac{d^2 z^2}{4} \right) dz = 2 \left(\frac{z^7}{7} - \frac{dz^5}{5} + \frac{d^2 z^3}{12} \right) \\ &= 2 \left[\frac{\left(y + \frac{d}{2} \right)^{\frac{7}{2}}}{7} - \frac{d \left(y + \frac{d}{2} \right)^{\frac{5}{2}}}{5} + \frac{d^2 \left(y + \frac{d}{2} \right)^{\frac{3}{2}}}{12} \right]_0^{\frac{d}{2}} \\ &= 2 \left(\frac{d^{\frac{7}{2}}}{7 \times 8 \sqrt{2}} - \frac{d^{\frac{5}{2}}}{5 \times 4 \sqrt{2}} + \frac{d^{\frac{3}{2}}}{24 \sqrt{2}} \right) \\ &= \frac{2d^3 \sqrt{d}}{4 \sqrt{2}} \left(\frac{1}{14} - \frac{1}{5} + \frac{1}{6} \right) \quad (5:38) \end{aligned}$$

$$I_p = \frac{2 \times 4bd^3}{315} = \frac{bd^3}{39.4} \quad (5:39)$$

Since

$$I_e = \frac{\pi ab^3}{8}, \quad a = \frac{1}{3}b, \quad \text{and} \quad b = \frac{d}{2},$$

then

$$I_e = \frac{\pi b d^3}{3 \times 8 \times 8} = \frac{b d^3}{61.1} \quad (5:40)$$

Thus

$$I = \frac{b d^3}{61.1} + \frac{b d^3}{39.4} \quad 24 \quad (5:41)$$

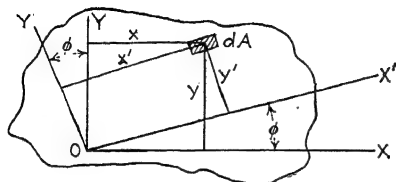


FIG. 5:10.—Moment of inertia about inclined axis.

5:9. Ellipse of Inertia.—It sometimes is desirable to find the moment of inertia about an inclined axis. For this purpose, the ellipse of inertia is useful. Let us determine such an ellipse and note its application. We write, for Fig. 5:10,

$$I_{x'} = \int (y')^2 dA = \int (y \cos \phi - x \sin \phi)^2 dA \quad (5:42)$$

$$= \cos^2 \phi \int y^2 dA + \sin^2 \phi \int x^2 dA - 2 \sin \phi \cos \phi \int xy dA \quad (5:43)$$

$$I_{x'} = I_x \cos^2 \phi + I_y \sin^2 \phi - 2k \cos \phi \sin \phi \quad (5:44)$$

where k is the product of inertia defined by $\int xy dA$.

Likewise we find

$$I_{y'} = I_x \sin^2 \phi + I_y \cos^2 \phi + 2k \cos \phi \sin \phi \quad (5:45)$$

We note in passing, by adding equations (5:44) and (5:46), that

$$I_{x'} + I_{y'} = I_x + I_y \quad (5:46)$$

This is apparent, also, because each side of the equation, as previously noted, is the polar moment of inertia of the section.

Now in order to represent equation (5:44) as an ellipse of inertia, let us assume

$$Me^4 = I_x x^2 + I_y y^2 - 2kxy \quad (5:47)$$

which is the equation of an ellipse in which M is a mass and e is any linear length. This choice is necessary if we are to keep the dimension of the two sides of the equation homogeneous with respect to the units. Let ρ be the polar radius to any point on the curve of the ellipse. Then if ϕ is the angle between this radius and the x -axis, we have

$$y = \rho \sin \phi \quad \text{and} \quad x = \rho \cos \phi \quad (5:48)$$

Thus equation (5:47) becomes

$$Me^4 = I_x \cos^2 \phi + I_y \sin^2 \phi - 2k \cos \phi \sin \phi \quad (5:49)$$

Thus we have

$$\frac{Me^4}{\rho^2} = \quad (5:50)$$

From equation (5:50) it may be concluded that the moment of inertia about any axis is inversely proportional to the square of the polar radius of the ellipse. Thus, if we draw the ellipse

$$\frac{x^2}{a^2} + \frac{y^2}{b^2} = 1 \quad (5:51)$$

so that

$$a = \frac{1}{\sqrt{I_x}} \quad \text{and} \quad b = \sqrt{I_y} \quad (5:52)$$

then

$$\rho = \frac{1}{a^2} \quad (5:53)$$

We thus have

$$\frac{a}{\rho} = a^2 \quad (5:54)$$

or

$$(5:55)$$

The principal axes are, it may be recalled, perpendicular to each other. One is a maximum with respect to ϕ , and the other is a minimum. Let us find ϕ for the location of the principal axes. Thus,

$$dI_{x'} = \sin \phi (-I_x) - 2k \cos 2\phi = 0 \quad (5:56)$$

from which

$$\tan 2\phi = \frac{2k}{I_y - I_x} \quad (5:57)$$

5:10. Moment of Inertia of a Cross Section of Thin Metal.—

In structures of thin sheet metal, full monocoque, or semi-mono-

coque, it becomes necessary at times to compute the moments of inertia of cross-sectional areas.

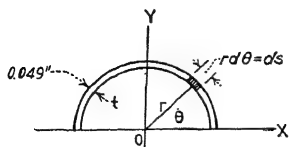


FIG. 5:11.—Moment of inertia of thin-walled tube by integration.

For example, let us compute the moment of inertia of the cross-sectional area of the tube shown in Fig. 5:11. Let us assume that the ratio of radius to thickness is very large so that the radius may be taken as of the neutral line of the

surface. We have, therefore,

$$= \frac{1}{2} r^3 t (2\pi) = \pi r^3 t \quad (5:58)$$

Let us, in order to illustrate a general method, which we shall use to advantage later, find I_x by another method. We have, for a solid cylinder,

$$I = \frac{\pi r^4}{4} \quad (5:59)$$

From this

$$\frac{dI}{dr} = \pi r^3 \quad \text{and} \quad dI = \pi r^3 dr \quad (5:60)$$

If we write I_x for dI and t for dr , we have

$$I_x = \quad (5:61)$$

as before.

Let us apply this method to an elliptical section, such as a monocoque fuselage. We have for the solid section, as indicated in equation (5:32),

$$I = \frac{\pi a^3 b}{4} \quad (5:62)$$

$$dI = I_y = \frac{3\pi a^2 b}{4} da + \frac{\pi a^3}{4} db \quad (5:63)$$

Write t for da and db , and we have

$$I_y = \frac{3\pi a^2 b}{4} t + \frac{a^3}{4} t \quad (5:64)$$

$$= \frac{1}{4} \pi a^2 (3b + a) t \quad (5:65)$$

Let us now apply this method to the formula for the solid streamlined section and obtain a formula for the streamlined

tube. We have

$$I = \frac{bd^3}{24} \text{ [see equation (5:41)]} \quad (5:66)$$

$$(5:67)$$

or, since d and b are taken as the full width and length of the section, $db = 2t$, and $dd = 2t$; hence,

$$\frac{2dt}{24}, \frac{3bd^2t}{24}, \frac{2}{24} \quad (5:68)$$

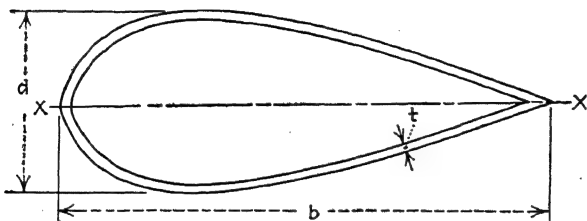


FIG. 5:12.—Approximate moment of inertia of a streamlined tube.

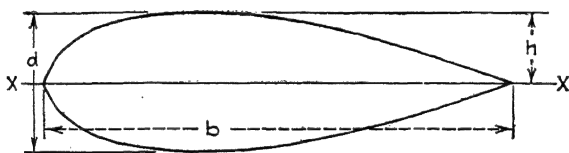


FIG. 5:13.—Solid streamlined section.

where d and b have dimensions as indicated in Fig. 5:12. The area of the streamlined section of Fig. 5:13, as the student may easily verify, is

$$A = 0.785bd \quad (5:69)$$

Let us apply the derivative method to the area formula and derive a formula for computing the area of the cross section of a streamlined tube. Thus,

$$dA = (0.78d) db + (0.785b) dd \quad (5:70)$$

or

$$A_t = 0.785(b + d)t \quad (5:71)$$

so that

$$A_t = 1.57(b + d)t \quad (5:72)$$

5:11. Moment of Inertia of an Airfoil Section.—We note in Fig. 5:13 that, if the symmetrical streamlined section be split

along the line $x-x$, two airfoil sections will be formed. We have, for the entire section,

$$I = \frac{bd^3}{24} = \frac{b(2h)^3}{24} = \frac{bh^3}{3} \quad (5:73)$$

The moment of inertia of the upper half of this section about the $x-x$ axis is

$$I_a = \frac{1}{2} \left(\frac{bh^3}{3} \right) = \frac{bh^3}{6} \quad (5:74)$$

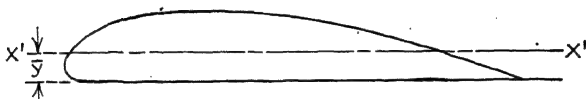


FIG. 5:14.—Section of propeller blade.

The moment of inertia about the centroidal axis $x'-x'$ (Fig. 5:14) is, by the parallel-axis theorem,

$$\bar{I} = I_a - (\bar{y})^2 A \quad (5:75)$$

where A is slightly less than one-half the area of the symmetrical section, that is,

$$A = \frac{0.785}{2} bd = 0.78bh \text{ (approx.)} \quad (5:76)$$

In general, \bar{y} is approximately 40 per cent of the maximum ordinate, which may be verified in each case by an experiment previously described. Thus,

$$\begin{aligned} (\bar{y})^2 A &= (0.4h)^2 (0.78bh) \\ &= \frac{1}{8} bh^3 \text{ (approx.)} \end{aligned} \quad (5:77)$$

Hence,

$$\bar{I} =$$

or

$$\bar{I} = \frac{bh^3}{24} \quad (5:78)$$

5:12. Area of Cross Section of Wing Shell.—The shell, in this case, is a tube in the form of an airfoil section. As noted in equation (5:76), the area of the solid cross section is

$$A = 0.78bh \quad (5:79)$$

from which

$$dA = (0.78h) db + (0.78b) dh \quad (5:80)$$

so that, for the shell,

$$\begin{aligned} A &= 0.78(h + b)(2t) \\ &= 1.56(h + b)t \end{aligned} \quad (5:81)$$

Equation (5:81) holds only for a thick airfoil up to a circular tube in which case $A = 1.56 (D + D)t$ which is πDt (approx.) where D is the diameter. For small values of h the equation does not hold. For example, if $h = 0$, $A = 1.56bt$, which is not correct. The value should be $A = 2bt$. The student should learn to deal practically with such conditions as this. For example, it is easy to introduce a factor in the equation such that when $h = b = D$ the factor reduces to 1.56 but when $h = 0$ the factor reduces to 2, making $A = 2bt$. Such a factor is

$$K = \left(2 - 0.44 \frac{b}{h} \right) \quad (5:82)$$

Thus, when $b = 0$, $K = 2$ and, when $b = h$, $K = 1.56$. Therefore, a more exact equation is

$$A = K(h + b)t = \left(2 - 0.44 \frac{b}{h} \right) (h + b)t \quad (5:83)$$

5:13. The Length of the Periphery of an Airfoil.—We note in passing that the area of the cross section of the shell wing is the length of the periphery times the thickness; that is,

$$A = ct \quad (5:84)$$

where c is the length of the periphery. Equating equation (5:84) to (5:83), we find

$$c = \left(2 - 0.44 \frac{b}{h} \right) (h + b) \quad (5:85)$$

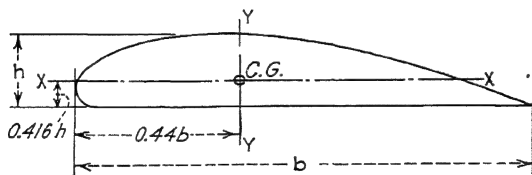


Fig. 5:15.—Moment of inertia and neutral axis of solid airfoil section.

5:14. Other Formulas.—*Air Corps Information Circular 597* gives the following data on airfoil sections suitable for propeller blades (see Fig. 5:15):

$$A = 0.724bh \quad (5:86)$$

$$I_{xx} = 0.0454bh^3 \quad (5:87)$$

$$I_{yy} = 0.0418b^3h \quad (5:88)$$

TABLE 5.3.—PROPERTIES OF ROUND TUBE SECTIONS

Diameter, in.	Thickness, in.	Gage, B. and W.	Area, sq. in.	Round		
				I , in. ⁴	ρ , in.	$\frac{I}{y}$, in. ³
$\frac{1}{8}$	0.022	24	0.01578	0.000103	0.08098	0.000827
	0.028	22	0.01953	0.0001222	0.07911	0.000978
	0.035	20	0.02364	0.001402	0.07701	0.001122
$\frac{3}{16}$	0.022	24	0.02440	0.000381	0.1251	0.002035
	0.028	22	0.03053	0.0004600	0.1231	0.002463
	0.035	20	0.03739	0.0005459	0.1208	0.002912
$\frac{1}{4}$	0.049	18	0.05018	0.0006817	0.1166	0.003636
	0.058	17	0.06776	0.0007498	0.1139	0.003999
	0.035	20	0.05113	0.0013898	0.1649	0.005559
$\frac{5}{16}$	0.049	18	0.06943	0.0017860	0.1604	0.007144
	0.058	17	0.08054	0.002001	0.1576	0.008003
	0.035	20	0.06487	0.002833	0.2090	0.009065
$\frac{3}{8}$	0.049	18	0.08867	0.003704	0.2044	0.01185
	0.058	17	0.10331	0.004195	0.2015	0.01342
	0.035	20	0.07862	0.005036	0.2531	0.01343
$\frac{7}{16}$	0.049	18	0.10791	0.006661	0.2484	0.01776
	0.058	17	0.12609	0.007601	0.2455	0.02027
	0.035	20	0.09236	0.008161	0.2972	0.01865
1	0.049	18	0.12715	0.010882	0.2926	0.02487
	0.058	17	0.14887	0.012484	0.2896	0.02853
	0.035	20	0.10611	0.012368	0.3414	0.02474
$1\frac{1}{8}$	0.049	18	0.14640	0.016594	0.3367	0.03319
	0.058	17	0.17164	0.019111	0.3337	0.03822
	0.065	16	0.19093	0.02097	0.3314	0.04193
$1\frac{1}{4}$	0.035	20	0.11985	0.01782	0.3856	0.03168
	0.049	18	0.16564	0.02402	0.3808	0.04270
	0.058	17	0.19442	0.02775	0.3778	0.04933
$1\frac{3}{8}$	0.065	16	0.2165	0.03052	0.3755	0.05425
	0.035	20	0.13360	0.02467	0.4298	0.03948
	0.049	18	0.18488	0.03339	0.4250	0.05342
$1\frac{1}{2}$	0.058	17	0.2172	0.03867	0.4219	0.06187
	0.065	16	0.2420	0.04260	0.4196	0.06816
	0.035	20	0.14734	0.03309	0.4739	0.04814
$1\frac{3}{4}$	0.049	18	0.2041	0.04492	0.4691	0.06534
	0.058	17	0.2400	0.05213	0.4661	0.07583
	0.065	16	0.2675	0.05753	0.4637	0.08367
2	0.083	14	0.3369	0.07059	0.4577	0.1027
	0.035	20	0.16109	0.04324	0.5181	0.05765
	0.049	18	0.2234	0.05885	0.5133	0.07847
$2\frac{1}{8}$	0.058	17	0.2628	0.06841	0.5102	0.09121
	0.065	16	0.2930	0.07558	0.5079	0.1008
	0.083	14	0.3695	0.09305	0.5018	0.1241
$2\frac{1}{4}$	0.095	13	0.4193	0.10394	0.4979	0.1386
	0.120	11	0.5202	0.12478	0.4898	0.1664
	0.035	20	0.1748	0.05528	0.5623	0.06803
$2\frac{3}{8}$	0.049	18	0.2426	0.07540	0.5575	0.09279
	0.058	17	0.2855	0.08776	0.5544	0.1080
	0.065	16	0.3186	0.09707	0.5520	0.1195
3	0.083	14	0.4021	0.11985	0.5459	0.1475
	0.095	13	0.4566	0.13413	0.5420	0.1651
	0.120	11	0.5674	0.16166	0.5338	0.1990

TABLE 5:3.—PROPERTIES OF ROUND TUBE SECTIONS.—(Continued)

Diameter, in.	Thickness, in.	Gage, B. and W.	Area, sq. in.	Round		
				I , in. ⁴	ρ , in.	$\frac{I}{\rho}$, in. ³
1½	0.035	20	0.1886	0.06936	0.6064	0.07927
	0.049	18	0.2618	0.09478	0.6016	0.1083
	0.058	17	0.3083	0.11046	0.5986	0.1262
	0.065	16	0.3441	0.12230	0.5962	0.1398
	0.083	14	0.4347	0.15136	0.5901	0.1730
	0.095	13	0.4939	0.16967	0.5861	0.1939
1¾	0.120	11	0.6145	0.2052	0.5779	0.2345
	0.035	20	0.2023	0.08565	0.6507	0.09138
	0.049	18	0.2811	0.1194	0.6527	0.1274
	0.058	17	0.3311	0.13677	0.6427	0.1459
	0.065	16	0.3696	0.15156	0.6403	0.1617
	0.083	14	0.4673	0.18797	0.6342	0.2005
2	0.095	13	0.5312	0.2110	0.6302	0.2251
	0.120	11	0.6616	0.2559	0.6219	0.2727
	0.035	20	0.2161	0.1043	0.6948	0.1043
	0.049	18	0.3003	0.1430	0.6901	0.1430
	0.058	17	0.3539	0.16696	0.6869	0.1670
	0.065	16	0.3951	0.18514	0.6845	0.1851
2¼	0.083	14	0.4999	0.2300	0.6784	0.2301
	0.095	13	0.5685	0.2586	0.6744	0.2586
	0.120	11	0.7087	0.3144	0.6660	0.3144
	0.035	20	0.2436	0.1494	0.7831	0.1328
	0.049	18	0.3388	0.2052	0.7782	0.1825
	0.058	17	0.3994	0.2401	0.7753	0.2134
2½	0.065	16	0.4462	0.2665	0.7729	0.2369
	0.083	14	0.5651	0.3322	0.7667	0.2953
	0.095	13*	0.6432	0.3741	0.7627	0.3325
	0.120	11	0.8030	0.4568	0.7543	0.4060
	0.035	20	0.2710	0.2059	0.8716	0.1647
	0.049	18	0.3773	0.2834	0.8667	0.2267
2¾	0.058	17	0.4450	0.3318	0.8636	0.2655
	0.065	16	0.4972	0.3688	0.8612	0.2950
	0.083	14	0.6302	0.4607	0.8550	0.3686
	0.095	13	0.7178	0.5197	0.8510	0.4158
	0.120	11	0.8972	0.6369	0.8425	0.5095
	0.035	20	0.2985	0.2751	0.9600	0.2001
3	0.049	18	0.4158	0.3793	0.9551	0.2759
	0.058	17	0.4905	0.4446	0.9520	0.3233
	0.065	16	0.5483	0.4944	0.9496	0.3596
	0.083	14	0.6954	0.6189	0.9434	0.4501
	0.095	13	0.7924	0.6991	0.9393	0.5084
	0.120	11	0.9915	0.8590	0.9308	0.6248
3½	0.035	20	0.3260	0.3583	1.0484	0.2389
	0.049	18	0.4543	0.4946	1.0435	0.3298
	0.058	17	0.5361	0.5802	1.0404	0.3868
	0.065	16	0.5993	0.6457	1.0379	0.4305
	0.083	14	0.7606	0.8097	1.0317	0.5398
	0.095	13	0.8670	0.9156	1.0276	0.6104
4	0.120	11	1.0857	1.1276	1.0191	0.7518
	0.035	20	0.4360	0.8568	1.4018	0.4284
	0.049	18	0.6082	1.1870	1.3970	0.5935
	0.058	17	0.7183	1.3955	1.3939	0.6978
	0.065	16	0.8035	1.5557	1.3914	0.7779
	0.083	14	1.0214	1.9597	1.3852	0.9799
	0.095	13	1.1655	2.2228	1.3810	1.1114
	0.120	11	1.4627	2.7552	1.3724	1.3726

TABLE 5:4.—PROPERTIES OF SECTIONS. ALUMINUM-ALLOY STREAMLINE TUBES¹
(Standard fineness ratio = 2.36)

T.M. Sk. No.	Major axis, in.	Minor axis, in.	Wall thickness, in.	Area, sq. in.	Least moment of inertia, in. ⁴	Least radius of gyration, in.
61	6.474	2.760	0.134	1.984	1.967	0.996
59	5.428	2.300	0.109	1.332	0.934	0.837
60	5.428	2.300	0.148	1.784	1.215	0.825
164	5.057	2.143	0.109	1.255	0.749	0.773
46	4.720	2.000	0.095	1.023	0.535	0.723
41	4.389	1.860	0.083	0.823	0.379	0.678
73	4.389	1.860	0.095	0.934	0.427	0.676
162	4.050	1.716	0.042	0.407	0.158	0.623
161	4.050	1.716	0.065	0.065	0.237	0.626
42	4.050	1.716	0.083	0.731	0.295	0.635
294	3.977	1.694	0.138	1.244	0.431	0.589
43	3.710	1.572	0.065	0.533	0.181	0.582
72	3.710	1.572	0.072	0.612	0.198	0.569
159	3.710	1.572	0.083	0.729	0.224	0.554
214	3.375	1.430	0.049	0.380	0.104	0.523
215	3.375	1.430	0.057	0.436	0.120	0.525
44	3.375	1.430	0.065	0.477	0.135	0.531
160	3.375	1.430	0.072	0.552	0.147	0.516
105	2.700	1.144	0.042	0.254	0.046	0.423
45	2.700	1.144	0.058	0.360	0.061	0.410
171	2.703	1.140	0.065	0.398	0.066	0.407
163	2.528	1.071	0.065	0.382	0.054	0.376
106	2.360	1.000	0.049	0.294	0.034	0.340
263	2.191	0.928	1.049	0.251	0.027	0.328
170	2.063	0.876	0.049	0.231	0.023	0.316
93	1.874	0.781	0.035	0.163	0.012	0.271
246	1.874	0.781	0.049	0.214	0.016	0.273

¹ Data taken from Aluminum Company of America, blueprint data Jan. 13, 1932.

From these data, we determine the area and moments of inertia for a tubular section (Fig. 5:16) as follows: From equation (5:86),

$$dA = 0.724b \, dh + 0.724h \, db \quad (5:89)$$

From this, writing dh and db as $2t$,

$$\begin{aligned} A &= 0.724(b + h)(2t) \\ &= 1.448(b + h)t \end{aligned} \quad (5:90)$$

Likewise

$$I_{xx} = 0.0908h^2(h + 3b)t \quad (5:91)$$

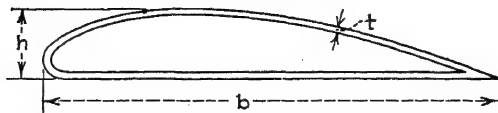


FIG. 5:16.—Shell section of b -chord and h -ordinate.

From equation (5:78) we obtain a similar formula,

$$I_{xx} = \frac{1}{12}h^2(h + 3b)t = 0.084h^2(h + 3b)t \quad (5:92)$$

It will be noted that the two equations differ by only 6 per cent.

CHAPTER VI

FUNDAMENTALS OF STRUCTURAL ANALYSES

6:1. Equations of Static Equilibrium.—It is possible by the method of statics to solve for a maximum of six unknown values of loads in a structure. Let us consider the fundamental principle involved in the solution of problems by statics. Fundamentally, the method of statics is an analytical one. Our graphical methods are applicable only to special cases of statics. Let us first consider the fundamental equations of static equilibrium. With reference to a rectangular coordinate-axis system of notation, the equations specify that the components of the forces parallel to the axes must be in equilibrium and the components of couples about the axes must be in equilibrium. Thus, we write

$$\sum F_x = 0 \quad (6:1)$$

$$\sum F_y = 0 \quad (6:2)$$

$$\sum F_z = 0 \quad (6:3)$$

$$\sum M_x = 0 \quad (6:4)$$

$$\sum M_y = 0 \quad (6:5)$$

$$\sum M_z = 0 \quad (6:6)$$

In these equations, x , y , and z refer to coordinate axes that are perpendicular to each other. Any other set of axes with the same characteristics would serve as well. The moment equations may be varied to suit the problem; that is, the axes x , y , and z , in so far as moments are concerned, may not necessarily be the same as the axes x , y , and z for the forces.

6:2. Application of Equations of Equilibrium.—To solve any problem by statics we proceed as follows:

1. Draw a "free-body" diagram of the complete structure as a unit and then a free-body diagram of each one of the members of the structure as a unit. A *free-body diagram* is the diagram of a structure or a member of a structure in which the outside members that react on the structure or the member in question are removed and vectors representing the forces transmitted by those members are substituted in their places.

2. The next step is to write the equations of equilibrium for the free-body diagram of the complete structure and for each member of the structure. The components of forces parallel to the axes are used.

3. The next step is to incorporate the geometrical and trigonometrical relations and other relations in these equations of equilibrium.

4. We then solve the equations of equilibrium for the unknown quantities.

6:3. Free-body Diagram.—If one is proficient in drawing free-body diagrams of a structure or the members of a structure, one will usually find very little difficulty in the remainder of the solution of a problem. Some of the essential features with respect to the free-body diagram are as follows:

1. Extreme care should be used in drawing the vectors for the *outside* reactions. The vectors must indicate the forces *applied by the outside members* and not the forces applied by the member itself.

2. In case the weights of the members of the structure must be considered, the manner in which this may be done so as to cause the least confusion is always to assume the weight of a member as an outside force. This means that we must consider all our members as weightless, then apply the weight of the member as a vector of an outside force either at the center of gravity or in components, so that the resultant of the components of weight passes through the center of gravity.

3. One mistake that is commonly made in drawing a free-body diagram is as follows: After the convention of *direction* and *sense* has been assumed on the outside of the structure or on some particular member, the definition of the convention is violated on some other member. For example, if member *A* reacts on the member *B* with a force of 10 lb. to the left, then, obviously, we assume the member *B* reacts on the member *A* with a force of 10 lb. to the right. The selection of the sense of the vector is entirely arbitrary for the first member considered. However, the selection of the sense thereafter, in connection with any of the other members, must conform to the selections already made.

4. If a load is applied at the intersection of two or more members, it is sometimes confusing to determine just how we are to apply this load. Quite often, students apply the load to each one of the members. Obviously, this is erroneous because the load really is impressed upon the structure only once. If we apply it to all the members at the particular joint, this is equivalent to applying just that many more loads. The desirable procedure to follow in this case is to assume that the load is applied to one member infinitely near the pin at the joint.

5. In *determining the sign of the forces or of the moments* in methods of statics, probably the least difficulty in guarding against errors is incurred by following the convention of signs adopted for the free-body diagram rather than by following the mathematical convention of signs for the direction cosines. This means that one should constantly bear in mind the physical problem as pictured by the free-body diagram and should constantly observe that the conventions of signs of the free-body diagram are

adhered to in the equations. This will save considerable difficulty in the final equations. It implies that all direction cosines are considered positive. This system is adhered to in this text.

6:4. Example of Equations of Equilibrium. *Example 1.*—In analyzing a fuselage structure for stresses in the low-angle-of-attack conditions, it is necessary to find the down load P on the horizontal stabilizer. The wings are generally analyzed in terms of the actual weight W of the airplane, rather than in terms of the

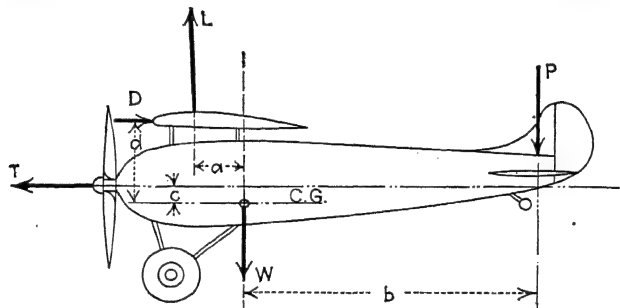


FIG. 6:1.—Equilibrium of airplane in low angles of attack. Dimensions a , c , and d may be negative or positive. Dimension a , in general, is toward the rear from C.G.

lift L , which is the sum of P and W . Assume a monoplane (Fig. 6:1), for which we have determined the spar reactions on the fuselage in terms of the weight of the airplane. Assume the center of drag of all parts other than that of the wings to be on the line of the propeller thrust. Derive equations for determining a correction factor for the spar reactions with a wing load of L and for determining P in terms of the wing drag D , the weight W , and the necessary dimensions.

Neglecting drag of all parts other than that of the wings, we may write the following equations of equilibrium:

$$\Sigma F_x = 0, \quad T = D \quad (6:7)$$

$$\Sigma F_y = 0, \quad L = P + W = KW \quad (6:8)$$

$$\Sigma M_0 = 0, \quad aL + bP + dD - cT = 0 \quad (6:9)$$

We have, combining (6:8) and (6:9),

$$a(P + W) + bP + dD - cT = 0 \quad (6:10)$$

or

$$(a + b)P = cT - aW - dD \quad (6:11)$$

From (6:7),

$$T = D$$

Thus, (6:11) becomes

$$(a + b)P = cD - aW - dD = (c - d)D -$$

Hence,

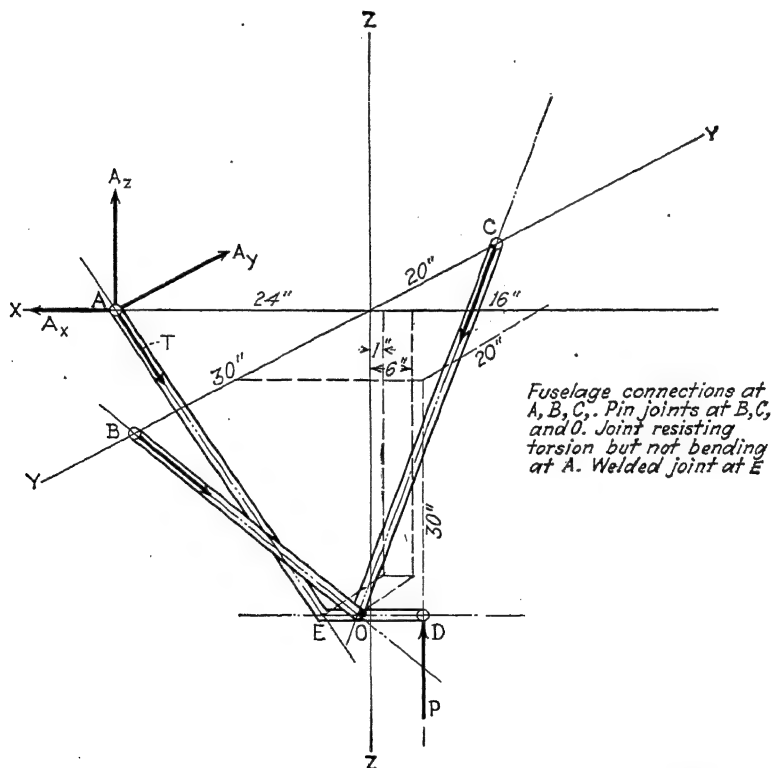
$$(6:12)$$

Substituting (6:12) in (6:8),

$$K = \frac{(c - d)D - aW + aW + bW}{(a + b)W}$$

Therefore,

$$K = \frac{(c - d)D + bW}{(a + b)W}$$



6:2.—Free-body diagram of landing gear. Three-dimension problem in statics.

Example 2.—The following example involves all six of the equations of equilibrium. In Fig. 6:2, which is a diagrammatic sketch of a tripod landing gear, members BO and CO are pin-jointed at both ends. Member AOD is pin-jointed at O to member OB and OC but is restrained at A by a joint designed to take torsion but no bending. B and C are pin joints. Find the reactions at A , B , and C due to the load P . (If any additional restraint is assumed, such as a fixed joint at A , B , C , or O , the structure will be statically indeterminate.) See Table 6:1 for direction cosines.

The components are

$$\begin{aligned} T_x &= 0.570T & B_x &= 0.186B & C_x &= 0.119C \\ T_y &= 0.456T & B_y &= 0.312B & C_y &= 0.795C \\ T_z &= 0.684T & B_z &= 0.932B & C_z &= 0.596C \end{aligned}$$

Let $P = 1$ lb.

The equations of equilibrium are

$$\Sigma F_x = -A_x + 0.186B + 0.119C = 0 \quad (6:13)$$

$$\Sigma F_y = -A_y - 0.312B + 0.795C = 0 \quad (6:14)$$

$$\Sigma F_z = A_z - 0.932B - 0.596C + 1 = 0 \quad (6:15)$$

TABLE 6:1.—CALCULATION OF DIRECTION COSINES

Point	Coordinates			Member	L	Direction cosines		
	X	Y	Z			α	β	γ
A	-24	0	0	AE	43.9	0.570	0.456	0.684
B	0	30	0	BO	32.2	0.186	0.312	0.932
C	0	-20	0	CO	50.3	0.119	0.795	0.596
D	16	20	-30	DO	10.0	1.000	0	0
E	1	20	-30	EO	5.0	1.000	0	0
O	6	20	-30					

$$= 0.570T - 30(0.932)B + 20(0.596)C + 20 = 0 \quad (6:16)$$

$$= 24A_z - 16 + 0.456T = 0 \quad (6:17)$$

$$= 24A_y - 30(0.186)B + 20(0.119)C - 0.684T = 0 \quad (6:18)$$

We solve as follows:

$$\begin{array}{rcl} -24 \times (6:15) & -24A_z + 22.4B + 14.3C & = 24 \\ (6:17) & 24A_z + 0.456T & = 16 \\ \text{Add} & \hline 0.456T + 22.4B + 14.3C & = 40 \end{array} \quad (6:19)$$

$$\begin{array}{rcl} 0.8 \times (6:16) & 0.456T - 22.4B + 9.5C & = -16 \\ \text{Add} & \hline 0.912T & + 23.8C & = 24 \end{array} \quad (6:20)$$

$$(6:18) \quad 24A_y - 5.6B + 2.4C - 0.684T = 0 \quad (6:21)$$

$$\begin{array}{rcl} 24 \times (6:14) & -24A_y - 7.5B + 19.1C & = 0 \\ \text{Add} & \hline -13.1B + 21.5C - 0.684T & = 0 \end{array} \quad (6:22)$$

$$\begin{array}{rcl} 1.71 \times (6:22) & -1.17T - 22.4B + 36.8C & = 0 \\ (6:19) & \hline 0.456T + 22.4B + 14.3C & = 40 \end{array} \quad (6:23)$$

$$\begin{array}{rcl} \text{Add} & \hline -0.714T & + 51.1C & = 40.0 \end{array} \quad (6:24)$$

$$\begin{array}{rcl} 0.783 \times (6:20) & 0.714T & + 18.6C = 18.8 \\ \text{Add} & \hline 69.7C & = 58.8 \end{array} \quad (6:25)$$

$$C = 0.845 \text{ lb.}$$

$$(6:24) \quad 0.714T = 51.1 \times 0.845 - 40 = 3.1 \quad (6:26)$$

$$T = 4.34 \text{ lb.-in.}$$

$$(6:23) \quad 22.4B = 40 - 14.3 \times 0.845 - 0.456 \times 4.34 \quad (6:27)$$

$$B = 1.155 \text{ lb.}$$

$$\begin{array}{rcl} (6:13) & A_z = 0.186 \times 1.155 + 0.119 \times 0.845 \\ & = 0.215 + 0.101 = 0.316 \text{ lb.} \end{array} \quad (6:28)$$

$$\begin{array}{rcl} (6:14) & A_y = 0.795 \times 0.845 - 0.312 \times 1.155 \\ & = 0.672 - 0.361 = 0.311 \text{ lb.} \end{array} \quad (6:29)$$

$$\begin{array}{rcl} (6:15) & A_z = 0.932 \times 1.155 + 0.596 \times 0.845 - 1 \\ & = 1.076 + 0.504 - 1 = 0.580 \text{ lb.} \end{array} \quad (6:30)$$

$$\begin{aligned} A &= \sqrt{A_z^2 + A_y^2 + A_x^2} \\ &= \sqrt{0.3365 + 0.0937 + 0.0968} \\ &= \sqrt{0.5270} = 0.726 \text{ lb.} \end{aligned}$$

6:5. Statically Indeterminate Structures.—A *statically indeterminate structure* is a structure in which the stresses cannot be determined by the methods of statics alone. The outstanding characteristics of the two types of structure, statically determinate and statically indeterminate, are listed in Table 6:2.

The number of restraints to be removed in a statically indeterminate structure to make it statically determinate is the *degree of redundancy*. The restraining members removed are the *redundant members*. For example, consider the structure in Fig. 6:3a. The structure will collapse under any system of loading. How-

ever, if we insert another member, as BD in Fig. 6:3*b*, the structure is then rigid and will not collapse under an assigned load.

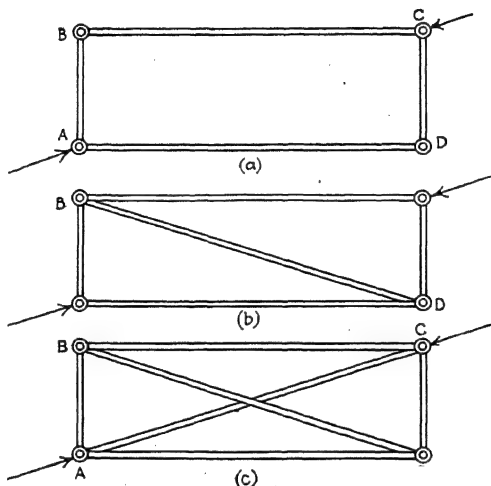


FIG. 6.3.—(a) Unstable; (b) statically determinate; (c) statically indeterminate structures.

If we insert yet another member, as AC in Fig. 6:3*c*, we then have more than enough members in the structure to prevent it from collapsing. The additional member in this case is a *redundant member*. The *degree of redundancy* is 1.

TABLE 6.2.—CHARACTERISTICS OF STRUCTURES

Statically Determinate	Statically Indeterminate
1. Assumed rigid structure	1. Elastic structure
2. Has enough members, and only enough, to prevent the structure from collapsing	2. Has more than enough members to prevent the structure from collapsing
3. Contains no initial stresses	3. If one member is too long or too short, initial stresses will be introduced
Stresses in structure not affected by temperature	4. Stresses affected by temperature
Loads in members not a function of the characteristics of the members	5. Loads in the members are functions of the characteristics of members, such as length, cross-sectional area, modulus of elasticity

6:6. Proportionality of Stress and Strain.—Methods of analyzing statically indeterminate structures are based, in all

cases, on the law of proportionality between stress and strain, that is, on Hooke's law. This law applies as well to a structure of elastic material as to a slender rod. For example, suppose that we consider any structure such as the engine mount in Fig. 6:4. The deflection of point A in the direction of the load W is proportional to the load W regardless of the configuration of the members of the structure. Also, the effect of the load W is independent of the load P applied at the joint B ; that is, whether or not P is applied to the structure, the deflection of

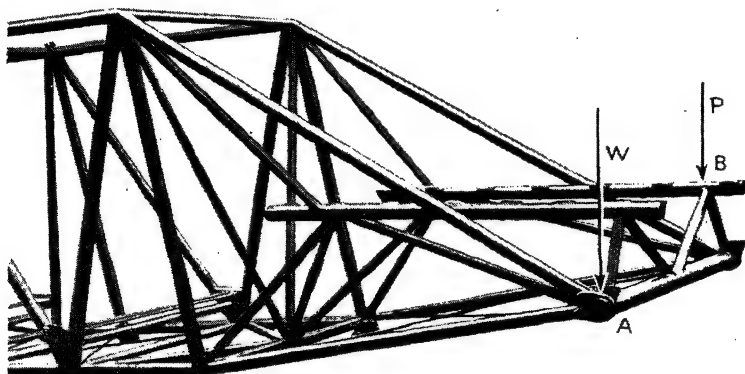


FIG. 6:4.—Effect of one load on structure independent of effect of another.

A caused by W is of the same magnitude. Also, the stress due to the load W in any member of the statically indeterminate structure, as in a statically determinate structure, is independent of the stress due to the load P . The stress in any member of the structure due to both load P and load W is the algebraic sum of the stresses induced by each load separately. We should note, however, that this is true only in so far as the structure does not change its characteristics, as, for instance, by the elimination of a member. For example, suppose one of the members is a wire under an initial stress. If this wire becomes slack, the characteristic of the structure is then changed, and our law no longer holds at this point. The law holds for the new structure and for the structure unchanged; yet it does not hold *through* the change between the two. These laws hold regardless of whether the joints are pinned or fixed rigidly.

It should be noted that, inasmuch as the law of proportionality of stress and strain is the basis for the theoretical determination of stresses in a statically indeterminate structure, *methods of such analyses do not apply above the proportional limit of a material.*

6:7. Initial Stresses.—We have noted that, in the case of a statically indeterminate structure, the insertion of a redundant

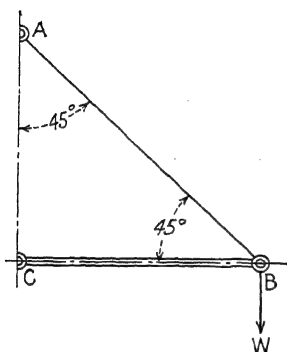


FIG. 6:5.

member, as shown in Fig. 6:3c, introduces initial stress unless the member is exactly the correct length, which is rarely the case. We should note, also, that if the member is of the correct length and is inserted properly the change in temperature may induce a temperature stress due to the difference in the expansion of the members.

Methods of determining the stresses in a statically indeterminate structure are based on the assumption that *the initial stresses in the members are all zero. The total stress is the algebraic*

sum of the initial stress and the stress in the member due to the applied load.

In some cases, this initial stress affects the ultimate strength of the structure. In other cases, it does not. The question is often asked: Why should we analyze the airplane structure for stress when a mechanic may tighten one of the bolts too much, putting extra stresses in the structure that are not considered in our analysis? This problem requires investigation to find out under what conditions the initial stresses are influential in the ultimate strength and under what conditions they are not. Let us consider the structure in Fig. 6:5. Assume pin joints at A, B, and C, 45-degree angles at A and B, and a 90-degree angle at C. Apply the load W at point B. Let W equal 100 lb. The load in the member AB will be $100\sqrt{2}$. The load in the member CB will be 100 lb. Under the load of 100 lb., B will be deflected downward a small distance depending upon the size, the modulus of elasticity, and other characteristics of the members of the structure. Now suppose that to this deformed condition we add another member A'B (see Fig. 6:6), similar in every way to the member AB. We add this member with the initial load of zero.

Now, suppose we remove the 100-lb. weight and allow a redistribution of stress between the members. We note that since $A'B$ and AB are similar in every way, neglecting the small change in shape of the structure due to the deflection, the load will be distributed equally between these two members. That is, the stress in AB will be $50\sqrt{2}$ and the stress in $A'B$ will also be $50\sqrt{2}$. We now have a statically indeterminate structure with known initial stresses.

Apply successively increasing loads to the point B , such as 25 lb., then 100 lb.; then plot the deflection of B for each case, the load being the ordinate and the deflection being the abscissa (see Fig. 6:7). The deflection will be proportional to the strain up to the point A where W is 100 lb. At this point A the member $A'B$ becomes slack again and the characteristic of our structure is changed. Our load-deflection curve will eventually lose its proportionality and drop to the point C where rupture occurs. It is quite obvious in this case that failure in the structure

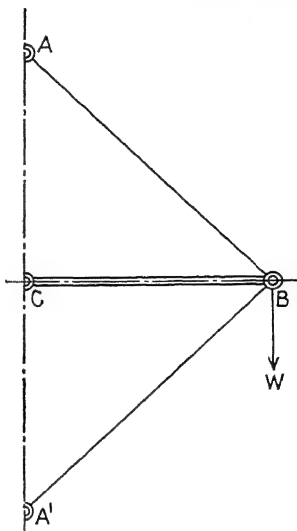


FIG. 6:6.

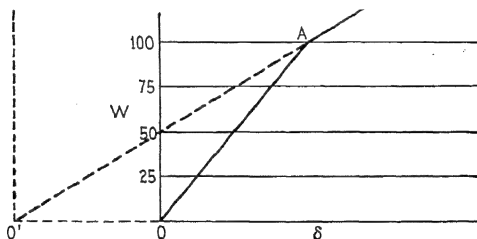


FIG. 6:7.—Load-deflection curve.

is independent of the member $A'B$; consequently, it is independent of the initial stress in the members. We should note, however, that, if the initial stress in the member $A'B$ is great enough so that the point A occurs between B and C , then the initial stress does affect the ultimate strength. This rarely occurs in a structure.

A general rule to follow in this case is that the initial stress of a wire member should not be over one-half the elastic limit of the material.

To continue the illustration, suppose that at the point B on the load-deflection curve $OABC$ we begin to relieve the load. Assume that while the member $A'B$ is still slack we remove the member from the structure. We then continue to relieve the load. Our load-deflection curve will be BAO' . $O'O$ then is the initial deflection of B due to the initial stress in the members of the structure. It will be noticed from this diagram that the *statically indeterminate structure is more rigid than the statically*

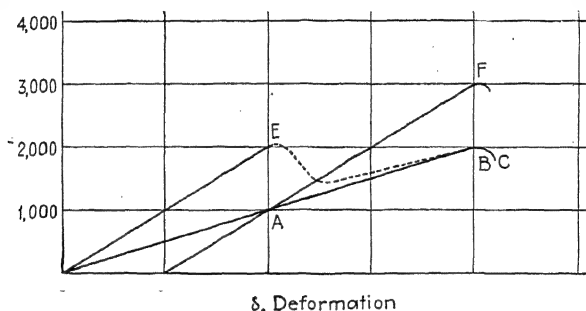


FIG. 6:8.—Effect of initial stresses.

determinate structure, since, with the member $A'B$ removed, the deformation is greater per unit of applied load. We may notice here, too, that *some structures under initial stress are more rigid than the same structures under no stress*. This principle is often made use of where a rigid structure of a light weight is required.

Let us consider another case similar in nature but different in results. Suppose that the members in this structure (Fig. 6:6) are all steel tubes. We note, therefore, that when the load in the member $A'B$ is relieved the member $A'B$ does not drop out from the structure—that is, it still contributes to the strength of the structure. Let us draw a load-deflection curve for this condition (see Fig. 6:8). The curve continues in a straight line until the elastic limit of one member is reached or until the limit of *elastic stability* of $A'B$, as a strut, is attained. Now, the stress in the member AB continually increases. The stress in the member $A'B$ decreases until the load of 100 lb. is reached. It then increases in magnitude but with opposite sign. If the two

members are similar, then the stress in the member AB will always be higher than the stress in the member $A'B$. We should note in this case, however, that the member AB would fail in tension and that the member $A'B$ would fail in compression from the standpoint of elastic instability; that is, it would fail as a strut.

6:8. Strength Increased by Initial Stress.—In certain cases the initial stress may be used to increase the ultimate strength of a structure. For example, considering Fig. 6:6 again, let us assume that the members AB and $A'B$ are steel tubes. Assume that the strength in tension of AB is $2,000\sqrt{2}$ lb. and the strength in compression (as a strut) of $A'B$ is $1,000\sqrt{2}$ lb. With reference to Fig. 6:8, we note that, with the member $A'B$ removed, the W - δ curve will be $O'ABC$, the maximum W occurring at B . Now with $A'B$ in place, and with no initial stress, the W - δ curve will be $O'EBC$. Buckling in $A'B$ occurs at E when the load on this member becomes $1,000\sqrt{2}$ lb.; this occurs when W is $2,000$ lb. If an initial stress of $500\sqrt{2}$ lb. is placed in each of the diagonal members, when the stress in member $A'B$ is reduced to zero, that in the member AB is $1,000\sqrt{2}$ lb. tension, the load W in this case being $1,000$ lb. If W is increased to $3,000$ lb., an addition of $2,000$ lb., the load in AB becomes $2,000\sqrt{2}$ lb. and the load in $A'B$ becomes $1,000\sqrt{2}$ lb., the maximum in both cases. This condition is represented by the W - δ curve OAF . *The initial stress has therefore increased the strength of the structure 50 per cent.*

This example is an elementary case, which may not be found in an airplane structure; yet it illustrates a principle which is fundamental in the design of composite structures such as that of an airplane. *Care should be exercised in this respect that the deflection of the major members of a structure do not cause undue stresses in minor members, thereby causing premature failures in the structure.*

6:9. Elastic Deformation.—We have noted that the method of analysis of a statically indeterminate structure involves the physical characteristics of the members of the structure. These physical characteristics pertain particularly to the *elasticity of the material*, the *cross-sectional area*, and the *length of the members*. We should note here in passing that there are four main elastic constants of a material, namely: the *modulus of elasticity*,

the *modulus of elasticity in shear*, the *bulk modulus*, and *Poisson's ratio*. The analysis of a very general type of structure would involve at least two or three of these elastic constants. However, if a structure consists of small rods, only the modulus of elasticity is involved. We shall consider first this elementary type of structure.

The definition of the modulus of elasticity, Young's modulus, is

$$E = \frac{\text{unit stress}}{\text{unit strain}} = \frac{P/A}{y/L} = \frac{PL}{Ay} \quad (6.31)$$

Young's modulus of elasticity is the ratio of unit stress to unit strain. *Unit stress* is the total reaction in a member divided by the area of cross section of the member. *Unit strain* is the total strain of the member divided by its length. We use P here to indicate the total load in a member, A to indicate the cross section, y to indicate deformation of the member, and L to indicate the length of the member. The units are pounds and inches. We note that

$$y = \frac{PL}{AE} \quad (6.32)$$

Some methods of analyses of indeterminate structures involve the energy in the members of the structure. The energy stored in any member subjected to tension or compression is the average force times the deformation. The average force in this case is expressed by

$$\frac{P}{2} = F \quad (6.33)$$

The deformation is y . (6.34)

We have, therefore, energy stored,

$$u = Py \quad (6.35)$$

Substituting the value of y from (6.32) in (6.35), we have

$$u = \frac{P^2L}{2AE} \quad (6.36)$$

We note that the total energy stored in any structure built of slender struts is the summation of terms similar to equation (6.36).

6:10. Methods of Analysis.—The determination of stresses in statically indeterminate structures belongs to the general subject

of the *mathematical theory of elasticity*. Structures of slender rods and tubes constitute a special study of the general subject. While a great many methods of analyses have been devised, the basis is the *comparison of deformations* of the members of the structure. The *energy* method, while, as noted in equation (6:35), based on the deformation of members, has proved useful in simplifying the problem. The so-called *theory of least work*, or, as it is sometimes called, *theory of minimum energy*, is probably the most generally used and has the most widespread application to all types of structures. Since it is not practical to present several methods in the limited space available, we shall limit the presentation to the fundamental method of comparison of deformations and to the theory of least work.

6:11. Method of Comparison of Deformations.—For the purpose of an elementary example, let us consider a weight W suspended from a rod of length L . Suppose that the area of the cross section of the rod is 4 sq. in. and the weight W is 4,000 lb. It is apparent in this case that, regardless of the material of the rod, the stress will be 1,000 lb. per square inch. Now let us assume that we can split the rod into two parts so that we have two rods of equal area of cross section. It is apparent, in this case, that, if the rods are of the same material, each rod will carry one-half the load, or 2,000 lb. Now, continuing the illustration, suppose that we divide these rods so that one rod has 3 sq. in. and the other 1 sq. in. cross-sectional area. The first will then carry 3,000 lb., and the second will carry 1,000 lb. In other words, *the load that each rod will carry is proportional to the area of the cross section*.

Now, in the case of the two rods of equal cross section, suppose that one is made of steel and the other is made of duralumin. For purposes of illustration, let us assume that the modulus of elasticity of the steel is 30,000,000 lb. per square inch. The modulus of elasticity of duralumin is 10,000,000 lb. per square inch. Now we note that the duralumin is three times as flexible as the steel. This means that for any given deformation the duralumin will carry just one-third as much as the steel. The condition of the structure is such that the deformation in both metals is the same. We compare the deformations and find them equal. This means, then, that the duralumin will carry one-third as much as the steel will carry. They both together

carry 4,000 lb. It is quite apparent that the steel rod will carry 3,000 lb. and the duralumin rod of the same area will carry 1,000 lb. *In general, the load carried is proportional to the modulus of elasticity.* The solution was by means of the comparison of the deformations.

Let us take note of a more general case. Suppose we assume a steel rod and a duralumin rod supporting a weight W . The steel rod has a length L_s , the duralumin rod a length of L_d . The area of cross section and the modulus of elasticity of each we shall indicate by the subscripts s and d . In the solution of this problem we note that the summation of the forces in the y -direction gives us

$$W = P_s = P_d \quad (6:37)$$

W equals the load carried by the steel rod plus the load carried by the duralumin rod. This equation represents the *limit of the method of statics for this problem*. It is quite obvious that we cannot solve the problem from this equation of statics alone. Since there are two unknown quantities, at least another equation is required. We obtain this by the *comparison of the deformation* of the two rods. Let this deformation be y under the applied load W . We find then, for the steel rod, that

$$y = \frac{P_s L_s}{A_s E_s} \quad (6:38)$$

and, for the duralumin rod, that

$$y = \frac{P_d L_d}{A_d E_d} \quad (6:39)$$

Thus

$$\frac{P_s L_s}{A_s E_s} = \frac{P_d L_d}{A_d E_d} \quad (6:40)$$

We note that we have two equations, (6:37) and (6:40), and two unknown terms, P_s and P_d , which enable us to solve for the unknown quantities. Solving, we have

$$P_s = \frac{A_s E_s L_d}{A_d E_s L_s} W \quad (6:41)$$

and from the symmetry of the equation we have

$$P_d = \left(\frac{A_d E_d L_s}{A_s E_d L_d} \right) W \quad (6:42)$$

In words, P_s and P_d are proportionate parts of W , depending upon the physical characteristics of the rods.

6:12. Example of Comparison of Deformations.—Let us consider another example. As illustrated in Fig. 6:9, we have a

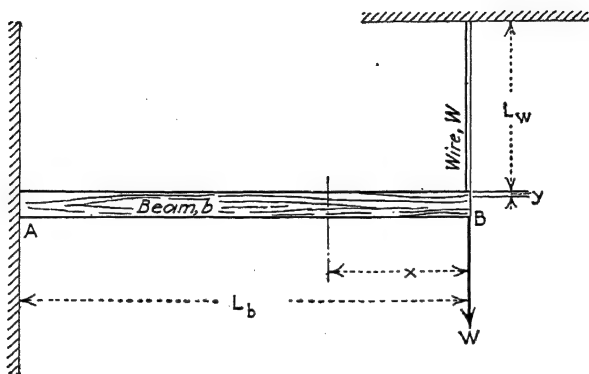


FIG. 6:9.—Combination of beam and wire; statically indeterminate structure, weight W being supported by a combination of cantilever beam AB and a wire GB . From statics, we have the equation

$$W = P_b + P_w \quad (6:43)$$

where P_b is the portion of the load carried by the beam and P_w the portion carried by the wire. We designate the deflection in the direction of the load W as y . We have then the deflection y in terms of the load in the wire,

$$y = \frac{P_w L_w}{A_w E_w} \quad (6:44)$$

and in terms of the deflection of the beam,

$$y = \quad (6:45)$$

where I indicates the moment of inertia of the cross-sectional area of the beam about its neutral axis. Equating (6:44) and (6:45), we have

$$\frac{P_w L_w}{A_w E_w} = \frac{P_b L_b^3}{3 E_b I_b} \quad (6:46)$$

We now have two equations, (6:43) and (6:46), and two unknown terms, P_w and P_b , from which we may find the unknown

quantities in terms of the physical characteristics of the members and the weight W .

It should be noted here that in each one of these examples the direction of the deflection is obvious. Now in general types of

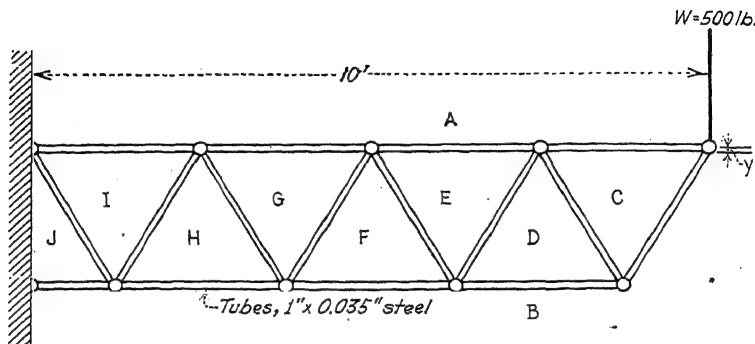


FIG. 6:10.—Deflection of truss by theory of least work.

structures the direction of the deflection of any particular joint may not be known. Thus *the method of deformations is applicable to cases in which the direction of the deflection is known.*

6:13. First Theorem of Least Work.—Consider the energy stored in a structure due to some applied load (for example, see Fig. 6:10).

Let us plot the curve of y as a function of W (see Fig. 6:11). Let us now consider the energy stored in the structure

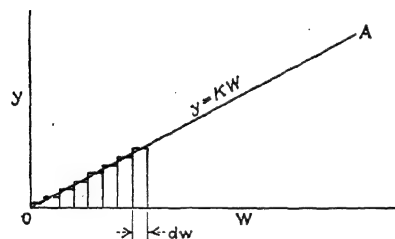


FIG. 6:11.—Energy stored in an elastic structure.

due to the added weight P and the resulting deformation y . We have

$$u = \int y \, dP \quad (6:47)$$

from which

$$\frac{du}{y} \quad (6:48)$$

Expressed in words, *the first derivative of the energy stored in the structure with respect to the applied load is equal to the deformation of the point of application of the load in the direction of the applied*

load. This is Castigliano's first theorem of least work. We note in this case that the energy is the summation of the deposits of energy stored in each member of the structure. As a general rule, we are not concerned with the deflection of the member except as that deflection will enable us to determine the stress. It would not be difficult to find the deflection in a structure under any applied load by the application of this theorem. For example, in a structure of rods,

where P is proportional to the load W causing the deflection. Thus

$$P = KW \quad (6:50)$$

The deflection of the point of application of W is

$$y = \frac{du}{dW} = \frac{d}{2AE} \quad (6:51)$$

or

$$y = \frac{K^2WL}{AE} \quad (6:52)$$

We note also that the internal energy is equal to the work of deformation; hence

$$\sum \frac{P^2L}{2AE} = \frac{1}{2} Wy \quad (6:53)$$

from which y may be found. The substitution of KW for P in equation (6:53) and the proper cancellation produce an equation identical with (6:52). The student may find y in Fig. 6:10 as an exercise.

6:14. Torsional Deformation.—In the consideration of a structure consisting of rods, such as an airplane fuselage or engine mount subjected to a torsional moment T , the angle of twist θ , in radians, may be computed from the equation of internal and external work of deformation by

$$P^2L \quad (6:54)$$

where the units used are inches, pounds, and radians.

6:15. Deformation under Several Loads.—If a structure is subjected to more than one load, then the deformation at the

point of action of the load P in the direction of the line of action of P is the *partial* derivative of the internal energy with respect to the load P ; that is,

$$\frac{\partial u}{\partial P} = y \quad (6:55)$$

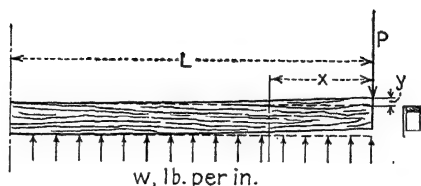


FIG. 6:12.

For example, in Fig. 6:12, the deflection y may be computed as follows:

$$u = \int_0^L \frac{wx^2}{2EI} dx \quad (6:56)$$

But

$$M = \frac{wx^2}{2} - Px \quad (6:57)$$

so that

$$\int_0^L \frac{M}{EI} dx = -y \quad (6:58)$$

Thus

$$\frac{\partial u}{\partial P} = -y \quad (6:59)$$

from which

$$y = \frac{\partial u}{\partial P} \quad (6:60)$$

6:16. Second Theorem of Least Work.—Castigliano's second theorem is generally referred to as the *theory of least work*. This theorem is a simplification and a standardization of the method of comparison of deformations in the determination of stresses in a statically indeterminate structure. For example, with reference to Fig. 6:9 and Art. 6:15,

$$y = \frac{\partial u}{\partial P_b} \quad (6:61)$$

$$= \int_0^L \frac{P_w^2 L_w}{EI} dx \quad (6:62)$$

Since, by statics, $P_b = W - P_w$, (6:63)

$$\frac{\partial u}{\partial W} = \frac{WL_b^3}{3E_bI_b} - \frac{P_wL_b^3}{3E_bI_b} = \frac{P_bL_b^3}{3E_bI_b} \quad (6:64)$$

Or, since, by statics, $P_w = W - P_b$, (6:65)

$$\frac{\partial u}{\partial W} = \frac{(W - P_b)L_w}{A_wE_w} = \frac{P_wL_w}{A_wE_w} \quad (6:66)$$

From equations (6:64) and (6:66), we get

$$\frac{P_bL_b^3}{3E_bI_b} = \frac{P_wL_w}{A_wE_w} \quad (6:67)$$

which with equation (6:63) permits of a solution as noted in equations (6:43) and (6:46).

Now this process may be much simplified if we consider the wire removed and P_w as an outside force. In this case,

$$u = \int_0^L dx \quad (6:68)$$

Noting that

$$= W - P_w \quad (6:69)$$

we obtain

$$(6:70)$$

And since it is obvious that the deformation of the wire in the direction of P_w is P_wL_w/A_wE_w , equation (6:67) may be written.

A further simplification may be made by the following process: Note that

from which

Since u is the energy in the beam and $P_w^2L_w/2A_wE_w$ is the energy in the wire, the sum of the two is the total energy in the structure, which we may designate as U in the equation

$$\frac{\partial U}{\partial P_w} = 0 \quad (6:73)$$

This gives us an equation identical with equation (6:67) which, with the equations of statics, is sufficient to solve for the unknown

values. Equation (6:73) is the basic equation of the theory of least work.

Equation (6:72) is applicable to a general type of structure; for example, u is the energy in all members of the structure except the member w under consideration. Now the deformation of the structure due to P_w , considered as an outside force, is

$$\frac{\partial u}{\partial P_w} \quad (6:74)$$

or, as noted in equation (6:72), $\partial U / \partial P_w = 0$.

6:17. Steps in the Application of the Theory of Least Work as Applied to Structures of Pin-ended Rods.—The *first step* is the examination of the structure and determination of how many members must be removed in order that the structure may be left statically determinate. Also, it should be determined which members should be considered redundant in order to simplify the methods of statics as much as possible.

The *second step* is to compute the loads in the members of the statically determinate structure, preferably by the analytical method of statics. It is assumed that the redundant members have been removed. The graphical method in this connection is not so desirable because of the unknown loads in the removed redundant members, for example, P_1 , P_2 , etc. In determining the loads in the statically determinate structural members, the loads in the redundant members P_1 , P_2 , etc., are considered as outside applied loads. It therefore is obvious that the load in any member will be expressed in terms of the outside loads W_1 , W_2 , etc., and the loads P_1 , P_2 , etc., in the redundant members.

The *third step* is to write the equation of energy for all the members of the structure including the redundant members. Since the loads in the members are expressed in terms of the loads in the redundant members, the energy equation then will involve only the unknown loads P_1 , P_2 , etc., of the redundant members.

The *fourth step* is to take the partial derivative of this energy equation with respect to each of the forces P_1 , P_2 , etc., in the redundant members and to equate each of these resulting equations to zero. This will produce as many additional equations as there are unknown loads P_1 , P_2 , etc.

The *fifth step* is to solve these additional equations simultaneously for the unknown values P_1 , P_2 , etc.

6:18. Example of Second Theorem of Least Work.—Consider an example of torsion in a fuselage structure of the conventional tube-and-wire type. For simplicity, we assume one bay only. In Fig. 6:13 we have one bay of the fuselage. We assume the torque Q applied to bulkhead B . We assume that these bulkheads are absolutely rigid. (You will note that the problem will be considerably more complicated if we assume the bulkhead elastic.)

Let us assume that the wires which do not carry a part of the load are removed. Therefore, we have wires a , b , c , and d as resisting the applied torque. Now we note that the wires a and c may be removed without impairing the stability of the structure. However, upon removal of these wires, of course, a side load cannot be resisted, that is, a side load that normally would be taken by these two wires. We also note that either pair of wires may be removed and still the structure is rigid. However, if the wire a is removed, c carries no load, since the summation of the forces in the x - and y -directions must be zero.

Let us divide the torque Q into couples such as P_1d and P_2b . We note that

$$Q = P_1d + P_2b \quad (6:75)$$

Our equation of energy is

$$U = \frac{P_1^2 L_b}{2A_a E_a} + \frac{P_2^2 L_b}{2A_b E_b} + \frac{P_1^2 L_d}{2A_c E_c} + \frac{P_2^2 L_d}{2A_d E_d} \quad (6:76)$$

If the fuselage is assumed to be symmetrical with respect to the axis, we have

$$P_b = P_d, \quad L_b = L_d, \quad A_b = A_d$$

and if we assume

$$E_a = E_b = E_c = E_d = E \quad (6:77)$$

our energy equation reduces to the following form:

$$U =$$

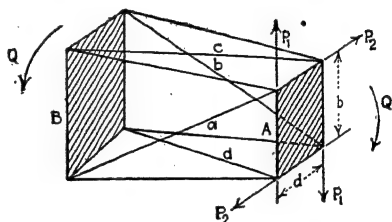


FIG. 6:13.—Torsion in a fuselage bay.

If we let K_1 , K_2 , etc., be constants that may be determined analytically or graphically, we have

$$P_a = K_1 P_1, \quad \text{and} \quad P_b = \quad (6:79)$$

If we substitute these values of P_a and P_b in equation (6:78), we have

$$U = \frac{V^2 D^2 T}{A_a E} + \frac{V^2 D^2 T}{A_b E} \quad (6:80)$$

Now substituting the value of P_1 from equation (6:75) in equation (6:80), we have

$$U = \frac{d}{A_a E} + \frac{d}{A_b E} \quad (6:81)$$

Taking the partial derivative of U with respect to P_2 and equating to zero, we have

$$\frac{\partial U}{\partial P_2} = \frac{-P_2 b) L_a}{d^2 A_a E} = 0$$

and from this equation we can find P_2 .

Now we note that if we consider a number of the bays in the fuselage, together with the cross wires in the bulkhead, we find that there is a redistribution of stress at each bay so that the load carried by each wire and produced by the applied torque Q is a function of the physical characteristics of every member in the fuselage structure.

6:19. General Equation for Statically Indeterminate Structure Composed of Pin-ended Rods.—The work involved in the application of the various methods to the evaluation of forces in redundant members of a statically indeterminate structure, where the degree is greater than the first or second, involves considerable detailed mathematics. Now, if we develop a general method whereby the results may be tabulated in a convenient form, considerable work and energy may be saved. For this purpose, let us consider the structure in Fig. 6:14. This structure has three redundant members, which we may consider to be 1, 2, and 3. Now for all practical purposes we may assume this to be a general type of structure. To simplify, in general, the designation of members, let us designate the assumed redun-

dant member by numerals and the assumed statically determinate members by letters of the alphabet. Let us remove the redundant members and insert in the place of each of them a force of 1 lb. Now, let us proceed to apply the methods of statics to

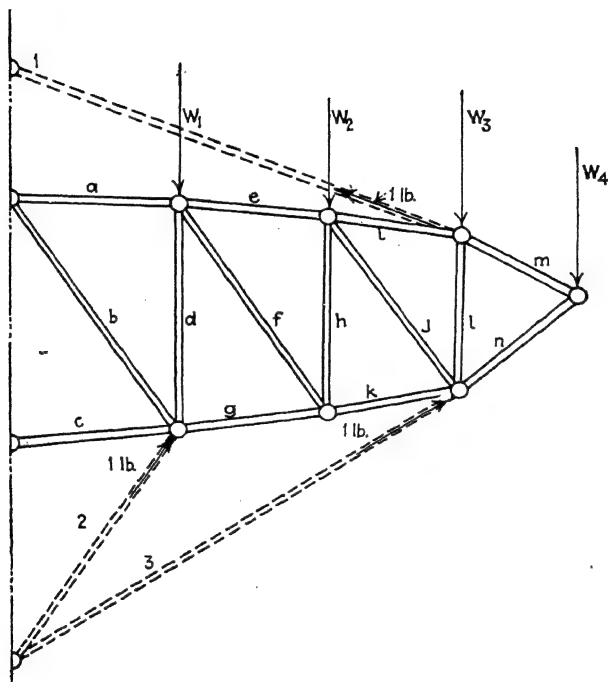


FIG. 6:14.—Statically indeterminate structure.

determine the loads in the statically determinate members *a*, *b*, and *c* as follows:

For example, taking the member *a*, we write the following equation:

$$P_a = P_{0a} + P_1K_{1a} + P_2K_{2a} + P_3K_{3a} + \dots \quad (6:82)$$

where P_a = total load in the member *a*.

P_{0a} = load in the member *a* in the statically determinate structure induced by the weights w_1 , w_2 , w_3 , and w_4 .

K_{1a} = load induced in the member *a* of the statically determinate structure by a 1-lb. force substituted for the member 1.

P_1 = total load in member 1, which is to be determined.

K_{2a} = load in the member a due to the 1-lb. load substituted for member 1.

P_2 = total load in the member 2.

Thus, we may add terms for each redundant member. It will be noted that constants K_{1a} , K_{2a} , and K_{3a} are coefficients which may be determined by methods of statics.

We write a similar equation for the statically determinate member b ,

$$P_b = P_{0b} + P_1 K_{1b} + P_2 K_{2b} + P_3 K_{3b} + \dots \quad (6:83)$$

We note in this equation that we have the same terms as in equation (6:82) but that these terms refer to member b rather than to member a . Likewise, we have the same condition for member c ,

$$P_c = P_{0c} + P_1 K_{1c} + P_2 K_{2c} + P_3 K_{3c} + \dots \quad (6:84)$$

As, in general, we have many possible equations of statics, these three equations will not be the limit of the alphabetically subscripted terms. It will also be noted that we may have any number of redundant members. Now, let us write the equation of energy as follows (in this equation, let us write the energy in the redundant members first):

$$U = \frac{P_1^2 L_1}{2A_1 E_1} + \frac{P_2^2 L_2}{2A_2 E_2} + \frac{P_3^2 L_3}{2A_3 E_3} + \frac{P_a^2 L_a}{2A_a E_a} + \frac{P_b^2 L_b}{2A_b E_b} + \frac{P_c^2 L_c}{2A_c E_c} \quad (6:85)$$

Now, substituting in this equation the values of P_a , P_b , and P_c and $P_1 K_1$, $P_2 K_2$, and $P_3 K_3$ for P_1 , P_2 , and P_3 , respectively ($K_1 = K_2 = K_3 = 1$), we have

$$U = \frac{1}{2A_1 E_1} (P_{0a} + P_1 K_{1a} + P_2 K_{2a} + P_3 K_{3a})^2 L_a + \frac{1}{2A_b E_b} (P_{0b} + P_1 K_{1b} + P_2 K_{2b} + P_3 K_{3b})^2 L_b + \dots \quad (6:86)$$

(similar terms for c , d , e , etc.)

Applying the theory of least work, we take the partial derivative of U with respect to each redundant member and equate each

of these to zero. In these equations, let us designate the physical constants of the members by an appropriate letter; for example, let

$$\frac{L}{AE} = B, \quad \frac{L_1}{A_1 E_1} = B_1 \quad (6:87)$$

Taking the partial derivative, we have

$$\begin{aligned} \frac{\partial U}{\partial P_1} = & P_1 K_1^2 B_1 + K_{1a}(P_{0a} + P_1 K_{1a} + P_2 K_{2a} + P_3 K_{3a} + \cdots) B_a \\ & + K_{1b}(P_{0b} + P_1 K_{1b} + P_2 K_{2b} + P_3 K_{3b} + \cdots) B_b + \\ & + K_{1c}(P_{0c} + P_1 K_{1c} + P_2 K_{2c} + P_3 K_{3c} + \cdots) B_c \\ & + \cdots = 0 \quad (6:88) \end{aligned}$$

Subdividing this equation, we have

$$\begin{aligned} \frac{\partial U}{\partial P_1} = & P_1 K_1^2 B_1 + (P_{0a} K_{1a} B_a - P_{0b} K_{1b} B_b + P_{0c} K_{1c} B_c) \\ & + (P_1 K_{1a}^2 B_a + P_1 K_{1b}^2 B_b + P_1 K_{1c}^2 B_c) + (P_2 K_{1a} K_{2a} B_a \\ & + P_2 K_{1b} K_{2b} B_b + P_2 K_{1c} K_{2c} B_c) \\ & + (P_3 K_{1a} K_{3a} B_a + P_3 K_{1b} K_{3b} B_b + P_3 K_{1c} K_{3c} B_c) \\ & + \cdots = 0 \quad (6:89) \end{aligned}$$

This may be written

$$\begin{aligned} \frac{\partial U}{\partial P_1} = & P_1 K_1^2 B_1 + \sum_a^n P_0 K_1 B + P_1 \sum_a^n K_1^2 B + P_2 \sum_a^n K_1 K_2 B \\ & + P_3 \sum_a^n K_1 K_3 B = 0 \quad (6:90) \end{aligned}$$

Writing a similar equation for the partial derivative with respect to P_2 , we have

$$\begin{aligned} \frac{\partial U}{\partial P_2} = & P_2 K_2^2 B_2 + \sum_a^n P_0 K_2 B + P_2 \sum_a^n K_2^2 B + P_1 \sum_a^n K_1 K_2 B \\ & + P_3 \sum_a^n K_2 K_3 B = 0 \quad (6:91) \end{aligned}$$

and for P_3 we have

$$\begin{aligned} \frac{\partial U}{\partial P_3} = & P_3 K_3^2 B_3 + \sum_a^n P_0 K_3 B + P_3 \sum_a^n K_3^2 B + P_2 \sum_a^n K_3 K_2 B \\ & + P_1 \sum_a^n K_1 K_3 B + \cdots = 0 \quad (6:92) \end{aligned}$$

We can now write these equations for any number of redundant members as 1, 2, 3, 4, 5, etc. These equations, (6:92), (6:93), and (6:94), are the equations to be solved for the unknown loads P_1 , P_2 , and P_3 in the redundant members. We note that there is one equation for each redundant member, making it possible for the solution to be obtained. Now let us note how we should tabulate the quantities for these equations. For example, consider Table 6:3.

TABLE 6:3.—TABULATION OF CALCULATIONS

Member	B	K_1	K_2	K_3	P_0	$P_0 K_1 B$	$P_0 K_2 B$	$P_0 K_3 B$	$K_1^2 B$	$K_2^2 B$	$K_3^2 B$	$K_1 K_2 B$	$K_1 K_3 B$	$K_2 K_3 B$

6:20. The Application of the General Method.—The *first step* is to assume the redundant members in the structure, as, for example, members 1, 2, etc. These redundant members are removed and 1-lb. loads are inserted as substitutions for the end reactions of the members.

The *second step* is to determine by the methods of statics the loads due to the outside applied loads in the members of this structure (with the redundant members removed). These loads are designated as P_0 ; for example, if the statically determinate members are a , b , c , these loads will be P_{0a} , P_{0b} , and P_{0c} .

The *third step* is to determine, by methods of statics, the loads in the members of the statically determinate structure that are due to the 1-lb. load substituted for the member 1. These loads will be, for example, K_{1a} , K_{1b} , and K_{1c} .

The *fourth step* is to determine the loads in the members of the statically determinate structure that are due to the 1-lb. load substituted for the member 2, as, for example, K_{2a} , K_{2b} , and K_{2c} .

The *fifth step* is to compute the constant B for each of the members.

The *sixth step* is to complete Table 6:3.

The *seventh step* is to write the equations as indicated by equations (6:92), (6:93), and (6:94), one equation for each unknown quantity.

The *eighth step* is to solve the resulting equations simultaneously.

6:21. Stresses above Proportional Limit.—In a statically indeterminate structure, as, for example, that shown in Fig. 6:15*a*, in which stresses in the members exceed the proportional limit, there is a tendency for the *unit stresses in all members to approach the same value*, provided the members are of the same material. This can be shown by the theory of least work through successively increasing the load W by increments of 100 lb., using

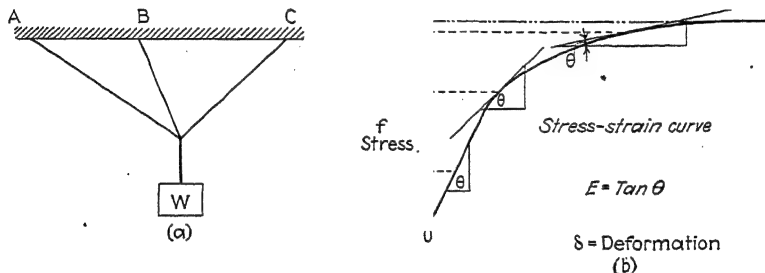


FIG. 6:15.—Stresses above proportional limit.

the modulus of elasticity for each increment as dictated by the total stress in the member as shown by f in Fig. 6:15*b*.

This may also be visualized. For example, suppose the member B becomes stressed beyond the elastic limit before A and C . Its effective modulus of elasticity becomes less, which means that the member stretches more appreciably with smaller increments of load. The stress in the member tends to become constant. In the meantime, however, as the load W is increased, the stresses in A and C are increasing. If one member does not break, it is obvious that they will each reach $f_{(\max)}$ as shown on the curve.

References

1. EVANS, F. G.: The Method of "Least Work" and the Stressing of Aeroplane Structures, *Jour. Roy. Aeronautical Soc.*, Vol. XXXV, No. 247, pp. 642–644, July, 1931.
2. SPOFFORD, C. M.: "Theory of Structures," McGraw-Hill Book Company, Inc., New York, 1928.
3. VAN DEN BROEK, J. A.: "Elastic Energy Theory," John Wiley & Sons, Inc., New York, 1931.

CHAPTER VII

BEAMS, COLUMNS, AND BEAM COLUMNS

7:1. Basic Theory and Formulas.—The student is referred to Chap. III for basic beam theory and formulas.

7:2. Elastic Instability.—The strength of the members of an aircraft structure ordinarily depends not upon the strength of the material but rather upon the magnitude of the modulus of elasticity of the material; that is, the strength of the members of the structure depends upon whether the members, as, for example, a slender strut, a steel fuselage tube, or a thin sheet of metal in monocoque construction, are stable or unstable. This means that for a long strut, where stability is the criterion of strength, it makes very little difference whether we use a high-grade high-strength steel or a low-grade low-strength steel, since the modulus of elasticity of the two is practically the same. Let us give this stability problem more consideration and attempt to visualize just why a member is stable or unstable. Ordinarily this problem is presented purely from a mathematical standpoint involving differential equations of the second order, such as the simple column equation

$$EI \frac{d^2 y}{dx^2} = -Py \quad (7:1)$$

Let us attempt to visualize the physical significance of the instability problem. For this purpose, let us apply our method of

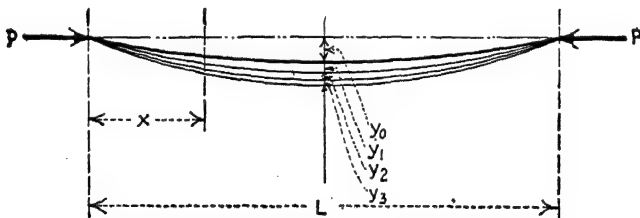


FIG. 7:1.—Successive increments of deflection of an initially bent strut.

graphical integration of the loading on a beam or its equivalent. Let us assume, for example, in Fig. 7:1, that we have a beam

which is slightly bent, we shall say, by a side load. Let us assume that this beam is subjected to an axial load P , which is applied along the neutral axis of the beam in its unstrained position. Let us assume that the deflection is extremely small in comparison with its length, for example, that it has a length of 60 in. and a deflection of $\frac{1}{10}$ in. Now for all practical purposes we may assume that this deflection is proportional to the sine, that is,

$$y = -y_0 \sin \frac{\pi x}{L} \quad (7:2)$$

We note in this equation that, when $x = L/2$, $y = y_0$ and the deflection is at the center; when $x = 0$, $y = 0$; and when $x = L$, $y = 0$. While the true curve may not be exactly this curve, for small deflection such as $\frac{1}{10}$ in. in 60 in., any curve that could be drawn with this maximum deflection could not be distinguished by the eye from any other curve. Now the bending moment at any point x is

$$M_x = Py_0 \sin \frac{\pi x}{L} \quad (7:3)$$

Thus

$$EI \frac{d^2 y}{dx^2} = Py_0 \sin \frac{\pi x}{L} \quad (7:4)$$

Let us now determine the deflection due to this primary bending moment M_x . We note that there will be an additional deflection due to the primary bending moment. Likewise, a second additional deflection will be caused by the additional secondary bending moment. Let us first, however, determine the additional deflection due to this primary bending moment, which we may designate as the *first secondary deflection*. We have

$$EI \frac{dy}{dx} = -\frac{PL}{2} y_0 \cos \frac{\pi x}{L} + C_1 \quad (7:5)$$

In order to evaluate the constant C_1 , we note that when

$$\frac{L}{2}, \quad \frac{dy}{dx} \quad (7:6)$$

We find therefore that

$$C_1 = 0.$$

Integrating again, we have

$$-PL^2 y_0 \sin \frac{\pi x}{L} + C_2 \quad (7:7)$$

Now, to evaluate the constant C_2 , we note that when

$$x = 0, \quad y = 0 \quad (7:8)$$

Therefore

$$C_2 = 0$$

We note now that the primary deflection plus the first secondary deflection gives the first approximate deflection,

$$y \text{ (approx.)} = -y_0 \sin \frac{\pi x}{L} - \frac{PL^2}{\pi^2 EI} y_0 \sin \frac{\pi x}{L} \quad (7:9)$$

which is

$$y \text{ (approx.)} = -y_0 \sin \pi x \quad (7:10)$$

The first secondary bending moment due to this added deflection is

$$\frac{P}{EI} y_0 \sin \frac{\pi x}{L} \quad (7:11)$$

in which we used a positive sign because the moment is positive though the deflection is negative. Now let us determine from this equation the second secondary deflection by successive integrations. We find that

$$dy = L^3 P^2 \pi x \quad (7:12)$$

We notice, as previously, in the evaluation of the constant, that $C_3 = 0$; we have, therefore, the second secondary deflection

$$y = -\frac{L^4}{\pi^4} P^2 \sin \frac{\pi x}{L} \quad (7:13)$$

Thus the total deflection y , including the primary deflection, the first secondary deflection, and the second secondary deflection, etc., is

$$\left(L^2 P - \frac{L^4 P^2}{\pi^2} \right) \quad (7:14)$$

If we let

$$\frac{EI}{L^2} = 2 \quad \text{and} \quad \frac{L^2}{\pi^2} j^2 = g$$

we have

$$y = y_0 \sin \left((1 + g + g^2 + g^3 + \dots) \pi x \right) \quad (7:15)$$

which is a geometric series. We note that the geometric series is convergent when g is less than 1. Therefore, the series for the deflection is convergent when

$$\frac{L^2 EI}{\pi^2 P} <$$

or

$$P < \frac{\pi^2 EI}{L^2} \quad (7:16)$$

We recognize equation (7:16) as Euler's critical loading formula for a column bent in its simplest form. The process which has been performed mathematically would give successive deflections as indicated in Fig. 7:1.

If the series is convergent, this means that each one of the successive double integrations gives a smaller value for the deflection than the preceding double integration. This means then that, if the deflections y_1 , y_2 , y_3 , and y_4 are successively smaller and smaller and if we repeat this integration either mathematically or graphically, we shall reach a limit for the point of stability of the strut. However, if our successive double integrations give us increments that are successively greater than the preceding increment, the process may be continued indefinitely, so that the sum of the series would be infinite; consequently under such a condition the strut is unstable.

If we let

in which P_e is the Eulerian critical load, we have

$$M_x = \quad (7:18)$$

If P in equation (7:18) is less than P_e , the series will be convergent. P in this case is the actual applied axial load on the beam. The maximum bending moment will occur at the center of the beam, since we have assumed the deflection to be a maximum at this point; hence the maximum stress in the beam will occur also at this point. We have at the center

$$M_0 = Py_0 \left[1 + \frac{P}{P_e} + \left(\frac{P}{P_e} \right)^2 + \left(\frac{P}{P_e} \right)^3 + \cdots \right] \quad (7:19)$$

Now we note that the geometrical series may be summed as follows:

$$S = \frac{1}{1 - r} \quad (7:20)$$

which may be verified by dividing as indicated. We thus have

$$M_0 = \frac{Py_0}{r} \quad (7:21)$$

7:3. Strength of a Strut with Bending Load.—As previously pointed out, the theory of elasticity does not account for the strength of the material in any way. Our calculations here will give us only the critical loading on the structure, *on the assumption that the material will not break*. It is quite obvious that there are practical limitations to the calculations in that the material may fail before the elastic instability is reached. This point is the essential difference between the theory of elastic instability and the theory of the rupture in a beam. If the fiber stresses are the criterion of the strength of this beam, before the instability theory will apply, the fiber stresses must be below the proportional limit. Assuming then that the fiber stresses are below the proportional limit, let us determine the relationship between the fiber stresses. For this purpose let us express M_0 in terms of the fiber stress in the outer fiber of the beam. We have, then,

$$M_0 = \frac{f_{bu}I}{c} \quad (7:22)$$

where f_{bu} is the ultimate allowed fiber stress in bending. Now, as an example, let us assume the deflection y_0 in the beam is caused by a concentrated load at the center of the beam. This type of loading will not produce a sine-curve deflection in the beam. However, for small deflections we probably may assume that the curve is a sine curve. The bending moment at the center of the beam is

$$M_b = WL \quad (7:23)$$

and the deflection at the center of the beam due to this bending moment is

$$\frac{WL^3}{48EI} \quad (7:24)$$

Substituting the M_b from equation (7:23) in equation (7:24), we have

We note in equation (7:25) that

$$\frac{L^2}{EI} = \frac{\pi^2}{P_e} \quad (7:26)$$

Substituting these values found in equations (7:22), (7:25), and (7:26) in equation (7:21) and adding M_b , we have

$$(7:27)$$

Now we note that in Euler's formula

$$\frac{P_e}{A} = \frac{\pi^2 EI}{L^2 A} \quad \text{or} \quad \frac{P_e}{A} =$$

where $\rho = \sqrt{I/A}$ = radius of gyration.

The fiber stress is

$$(7:28)$$

where f_{cu} is the ultimate compressive fiber stress of the column.

Now, expressing M_b in terms of the fiber stress, we have

$$M_b = \quad (7:29)$$

where f_{ba} is the allowable bending stress. Now, substituting the value of M_b from equation (7:29) in equation (7:27), we have

$$12c \left(\frac{P_e}{A} - \frac{P}{A} \right) = \frac{f_{ba} I}{c} \quad (7:30)$$

which reduces to

$$f_{bu} = \frac{P}{12} - \frac{P}{A} \quad f_{ba} \quad (7:31)$$

Equation (7:31) gives us the relation between the allowable ultimate bending stress in the beam in terms of the allowable

ultimate compressive stress. In this equation, we set the allowable ultimate bending stress f_{bu} as the proportional limit of the material, and we set the allowable ultimate compressive stress f_{cu} as that which will cause elastic instability, as determined by Euler's critical-load formula or by other appropriate formulas. Now the question arises as to what stress due to the axial load and what stress due to the applied side load will be allowed in the beam.

We note in this case that we have not made any allowance in the stress of the material for the axial load which is impressed upon the material. It is quite apparent that the ultimate allowed bending stress includes the P/A stress. Consequently, to make this formula more applicable, the f_{bu} should be replaced by $f_{bu} - \frac{P}{A}$. Substituting this value in equation (7:31), we have

$$\left(f_{bu} - \frac{P}{A}\right) = \frac{12 \left(f_{cu} - \frac{P}{A}\right)}{D} f_{ba} \quad (7:32)$$

from which, solving for f_{ba} , we find

$$f_{ba} = \frac{12 \left(f_{bu} - \frac{P}{A}\right)}{D} \quad (7:33)$$

Equation (7:33) gives us the allowable bending stress in terms of the applied compressive stress and the ultimate stresses in bend-

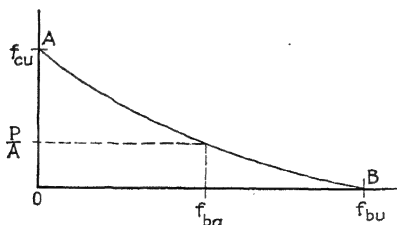


FIG. 7:2.—Elementary chart for combined loading.

ing and compression. The curve of equation (7:33) is of the form shown in Fig. 7:2.

If AB were a straight line as in Fig. 7:3, we might write an equation similar to equation (7:33) as follows: By proportionality of corresponding sides of similar triangles,

$$\left(f_{cu} - \frac{P}{A}\right) : f_{ba} = f_{cu} : f_{bu} \quad (7:34)$$

or

$$= J_{bu} \cdot \left(f_{cu} - \frac{P}{A}\right) \quad (7:35)$$

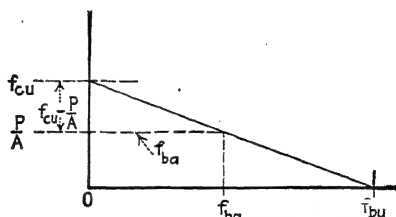


FIG. 7:3.—Quantities entering into an empirical formula for combined loading.

7:4. Ultimate Strength of Simple Struts with Side Load.—

Experiments by the Bureau of Standards showed that the ultimate strength of chrome-molybdenum steel tubes and duralumin tubes, when plotted in the form indicated in Figs. 7:2 and 7:3, produced a chart as shown in Figs. 7:4 and 7:5.¹

¹ Figure 7:4 represents the experimental results obtained in 2-in. chromemolybdenum steel tubes with wall thickness of 0.065 to 0.095 in. in transverse, column, and combined column and transverse tests

In the transverse tests the load was applied at the third points to a freely supported specimen. In the column test the load was applied axially through the ball-and-socket fixtures to approximate "round-end" conditions.

In the combined tests the above two methods of application of load were used simultaneously.

In the figure, the bending stresses produced by the lateral loads are plotted against the axial compressive stresses produced by the axial loads.

The bending stresses were calculated by the simple beam formula $f_b = Md/2I$, in which M = bending moment, produced by the lateral load, d = outside diameter of the tube, and I = moment of inertia of the cross section.

The axial stress is equal to P/A where P is the maximum axial load carried by the tube under the test conditions and A the cross-sectional area. Each point on these experimental curves represents an average of two determinations.

It will be noticed that for all l/r ratios which were used the stresses calculated in this manner for the maximum test loads do not show any significant effect of the thickness of wall. Therefore, the results obtained on different thicknesses of wall were averaged for each particular l/r ratio. These average curves are not shown on the diagram.

The average curves meet the axis of abscissas at points that correspond to the maximum bending stresses in the transverse test of 117,850 to 142,500 lb. per square inch. Although these calculated bending stresses in the

It will be noted in this case, however, that the chart as determined by the Bureau of Standards gives the allowable bending stress or the allowable compressive stress in the strut in terms of the ultimate bending stress, that is, the modulus of rupture, and the ultimate stress as that of a pure column, whether the column be within Euler's range or whether it be a very short column

transverse test (when the axial load is zero) vary with l/r and thickness, the differences are small, being considerably less than the scatter observed in the combined tests.

In order to combine these results on a safe basis, both the axial and the transverse stresses were reduced in the following manner:

The specifications (Navy Department Specification 10231-A, Feb. 7, 1925) call for 95,000 lb. per square inch ultimate and 60,000 lb. per square inch yield point. The average column strength yield of the material was 94,000 lb. per square inch. The average axial stresses calculated from the tests were therefore all reduced in the proportion 60,000/94,000. The transverse stresses were similarly reduced, using the specified value of 95,000 lb. per square inch for the ultimate.

As an illustration of the above procedure, let us consider $l/r = 50$ and the bending stress = 40,000 lb. per square inch. The average experimental curve for $l/r = 50$ intersects the axis of abscissas at 129,900. The abscissa of the given point on the average experimental curve is 40,000, and therefore the abscissa of the corresponding point on the reduced average curve is $40,000 \times 95,000/129,900 = 29,250$. The ordinate of the given point on the average experimental curve is 47,000, and therefore the ordinate of the corresponding point on the reduced average curve is

$$47,000 \times \frac{60,000}{94,100} = 30,000$$

Consequently, the reduced average curve passes through the point 29,250 on the abscissa and 30,000 on the ordinate. These reduced average curves were faired, and the diagram gives these faired curves. The reduced values for $l/r = 30$ lay so close to a straight line that the faired curve was drawn straight.

The average experimental curves and the reduced average curves (not faired) were omitted for the sake of clearness.

It will be seen that these average curves, reduced on the basis of the specification values for yield point and ultimate, lie below all the experimental points. These reduced curves should therefore furnish a safe basis for calculating the stresses that tubes of material meeting these specifications can carry.

Figure 7:5 represents the experimental results obtained on 1½-in. duralumin tubes with wall thicknesses of 0.032 to 0.072 in. in transverse, column, and combined column and transverse tests. The same general procedure as outlined above was used.

involving the strength of the material. Now, although the theory involved in equation (7:33) is applicable with very little error up to the elastic limit, yet it cannot be applied to the chart of the Bureau of Standards. *However, it gives us an indica-*

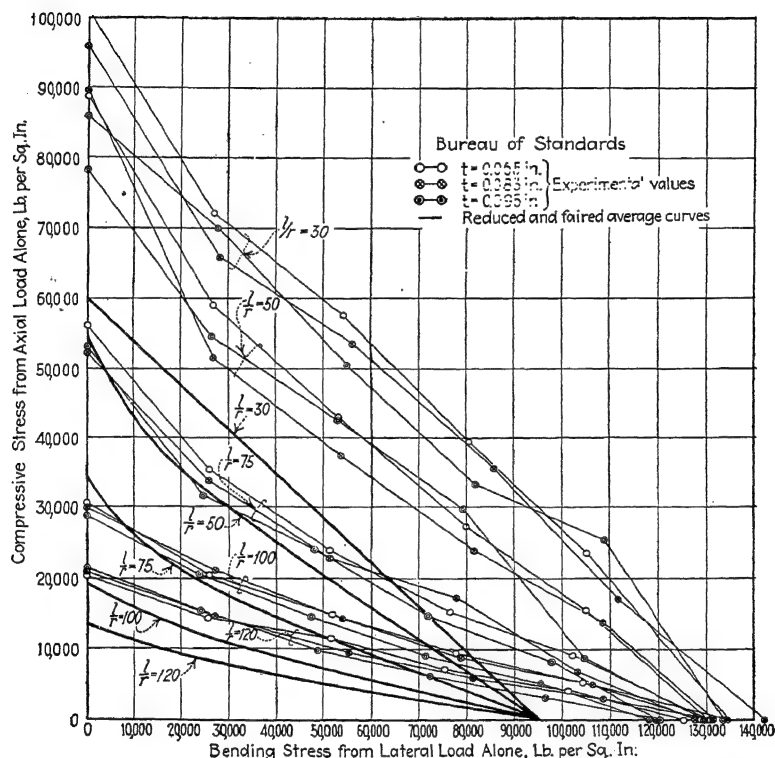


FIG. 7:4.—Experimental values of bending and compressive stresses. Chrome-molybdenum steel tubes; dia. = 2 in.; thickness of wall from 0.065 to 0.095 in.

tion as to the form of the empirical equation that may be derived for expressing the relations in the chart of the Bureau of Standards.

7:5. Combined Allowable Stress.—A chart of the form of Figs. 7:4 and 7:5 does not give us the combined allowable stress in bending and compression. The chart gives us the allowable bending stress, having assumed the compressive stress, or it gives us the allowable compressive stress, having assumed the bending

stress. The more desirable form of representing experimental data on combined loading is as represented in Fig. 7:6. We have represented in this chart the abscissas as the ratio between the bending stress and the total combined bending and compressive stresses. The ordinate is the allowable combined total stress.

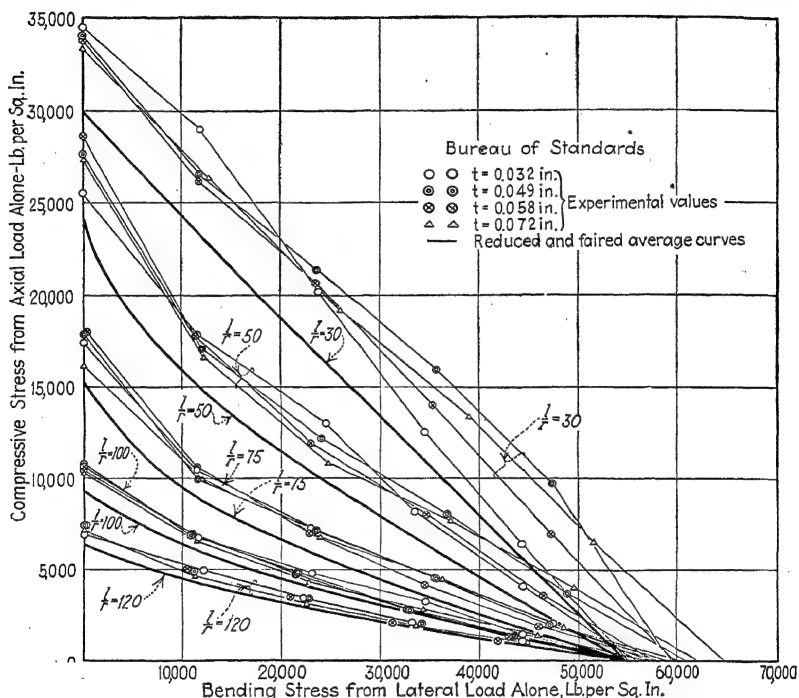


FIG. 7:5.—Experimental values of bending and compressive stresses. Duralumin tubes; dia. = $1\frac{1}{2}$ in.; thickness of wall from 0.032 to 0.072 in.

When the bending stress is zero, the beam is a column without a side load. It is represented by the zero abscissa line as A, A, A . The zero abscissa line, therefore, indicates the strength of the column as computed in the range of a long strut by Euler's formula or in the range of a short strut by an appropriate formula. If no axial load is impressed upon the beam f_{ia} , the combined allowable stress is equal to f_b . The ratio then is 1. Therefore, the ordinate at the point $f_b/f_t = 1$ is an ordinate of ultimate bending stress. This indicates one point B for any particular

material. Thus, for intermediate points, the value of f_{ta} will lie on a curve connecting A and B. Now this type of curve may be determined from Fig. 7:4 or 7:5, and it is found to be

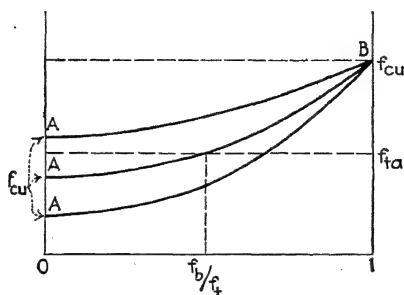


FIG. 7:6.—Application of chart for axially loaded metal beams.

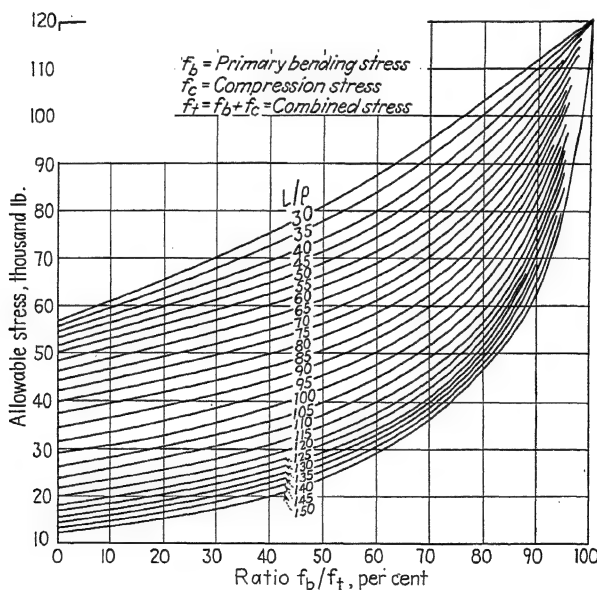
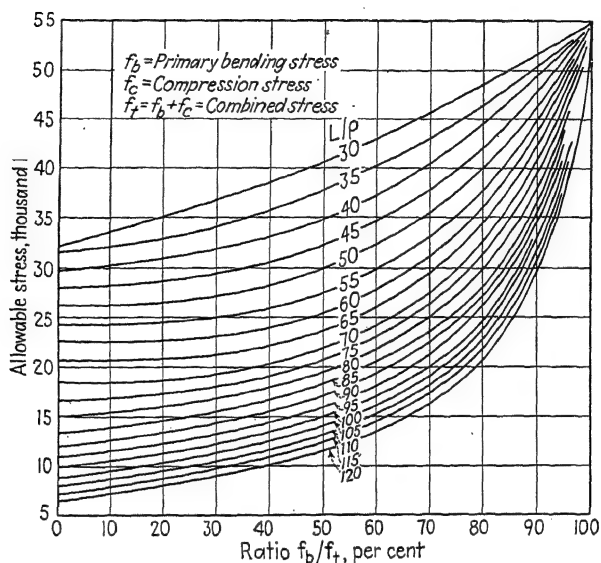


FIG. 7:7.—Allowable stress for aluminum-alloy duralumin tubes subjected to combined bending and compression.

slightly curved as indicated in the figure. Charts similar to Fig. 7:6 for duralumin, chrome-molybdenum steel, and 1025 steel are shown, respectively, in Figs. 7:7, 7:8, and 7:9. These are old curves, but no better data are available.



g. 7:8.—Allowable stress for chrome-molybdenum steel tubes subjected to combined bending and compression.

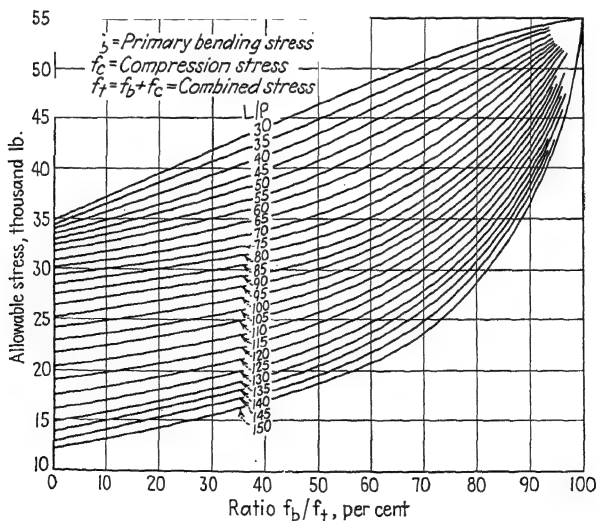


Fig. 7:9.—Allowable stress for specification 1025 steel tubes subjected to combined bending and compression.

7:6. Simple Strut.—It should be emphasized that the majority of the structural members in an airplane structure depend for their strength upon their column action and also that in aircraft work we carry this column action above the theoretical range of calculation, that is, above the proportional limit. Consequently, we are faced with a problem that is very difficult and that has never been solved satisfactorily. Our methods relating to

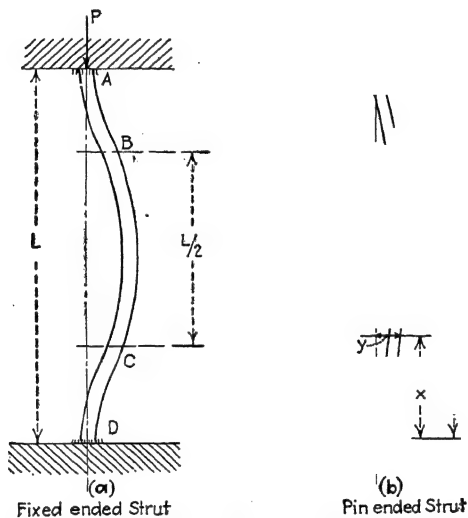


FIG. 7:10.—Simple struts.

these conditions, it should be noted, are mostly makeshift ones, based upon simple experiments. For the purpose of giving this subject more careful study, let us review the calculations pertaining to the simple strut, that is, the simple column. With reference to Fig. 7:10b, we note that the bending moment at any point x is

$$M_x = -Py \quad (7:36)$$

We assume a slight deflection in the column. This assumption is justified inasmuch as it is practically impossible to construct a perfectly homogeneous, uniform, straight column. The equivalent of the deflection may be found in a slight eccentricity or a slight variation in the material. Writing the deflection

equation for the bending moment, we find that

$$EI \frac{d^2y}{dx^2} = -Py \quad (7:37)$$

where we write the negative sign because the deflection is always opposite in sign to the bending moment. We have, from this equation,

$$\frac{d^2y}{dx^2} + \frac{P}{EI} y = 0 \quad (7:38)$$

Letting

$$\frac{P}{EI} = j^2 \quad (7:39)$$

and solving the equation, we have

$$y = A \cos jx + B \sin jx \quad (7:40)$$

In order to evaluate the constants A and B , we note that when

$$x = 0, \quad y = 0 \quad (7:41)$$

from which we find that

$$A = 0 \quad (7:42)$$

We therefore have

$$y = B \sin jx \quad (7:43)$$

It is therefore apparent that the curve is a sine curve. From the nature of the problem we note that the constant B will be the maximum deflection y_0 at the center of the loop. When $x = L/2$, the slope is zero.

The slope is

$$\frac{dy}{dx} = i = Bj \cos jx \quad (7:44)$$

Substituting these values, we have

$$0 = Bj \cos j \frac{L}{2} \quad (7:45)$$

In this case the condition requires that

$$\cos j \frac{L}{2} = 0 \quad (7:46)$$

This condition is satisfied when

$$j \frac{L}{2} = \frac{n\pi}{2} \quad (7:47)$$

where n is an integer. We have, therefore,

$$\sqrt{P} \cdot L = n\pi \quad (7:48)$$

or, letting $n^2 = c$, the coefficient of fixity,

$$P = \frac{c\pi^2 EI}{L^2} \quad (7:49)$$

For the simplest case of bending as represented in the figure, $c = 1$, we have

$$P = \frac{\pi^2 EI}{L^2} \quad (7:50)$$

Now the fiber stress is

$$\frac{P}{A} = \frac{\pi^2 E}{L^2} \quad (7:51)$$

where ρ is the radius of gyration of the cross-sectional area of the strut. Plotting this curve as noted in Fig. 7:11 with P/A , the

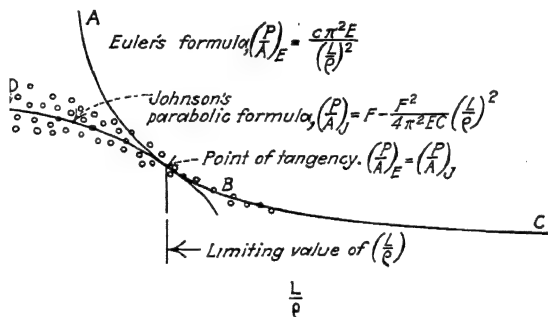


FIG. 7:11.—Tabulation of data for simple strut.

unit fiber stress, as a function of L/ρ of the strut, we find that Euler's formula gives a curve similar to ABC . It is quite apparent that, if the curve be extended in the direction of A for any distance, the fiber stress of the material will be above the elastic limit and may eventually become infinite; therefore this curve will not be available for use except where the compressive stress in the strut is negligible, that is, in the lower range from B to C . In the range of the short strut (low values of L), it is quite apparent that the ultimate strength of the material determines largely the strength of the strut, so that Euler's theory will

not apply. Experiments have shown that there is considerable variation in the experimental results, so that a good general average of these points may be represented by a curve approximately as *BD*. There is no theoretical method of determining this curve *BD*. Empirical formulas have been derived for this, the most important for aircraft use being a parabolic formula (see Art. 3:24). It will be noted in these formulas that, when the

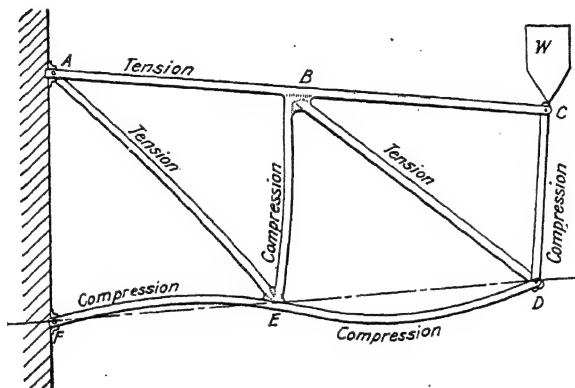


FIG. 7:12.—The unit action of struts in a fuselage.

stress as calculated by Euler's formula reaches the elastic limit, then Johnson's parabolic formula begins to apply.

7:7. Fixity of Joints.—We note that, in Euler's formula,

$$P = \frac{c\pi^2 EI}{L^2} \quad (7:52)$$

where *c* is the coefficient of fixity. For example, if the strut is pin ended as in Fig. 7:10*b*, *c* is 1. On the other hand, if the strut has fixed ends as in Fig. 7:10*a*, the coefficient of fixity is 4, since this condition is equivalent to shortening the strut to half the length; this means that the axial load is raised to four times the initial value. Now in an airplane structure, whereas it appears that some of the struts are fixed, they are in reality not fixed, as will be noted from Fig. 7:12. The struts will take a form somewhat as represented. A joint, as, for example, joint *E*, rotates as a unit, thus eliminating any possibility of complete fixity. In general, it is found for the usual aircraft structure that the coefficient of fixity should not be selected greater than 2 for welded struts and greater than 1 for pin-ended struts. Under certain conditions a

coefficient of fixity of 3 may be allowed; but in general a coefficient of fixity of 4 is never allowed, that is, the structure is never ideal. This fixity of the ends of struts is a problem that is receiving considerable attention from investigators.

7:8. Simple Strut with Uniform Lateral Load.—The strut with a side load presents an intricate problem, as we have noted. Let us consider the problem from the standpoint of the theory of

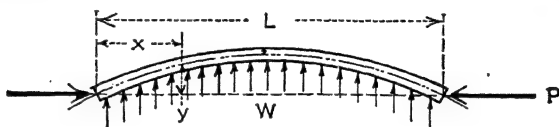


FIG. 7:13.—Symbols for laterally loaded beam.

elasticity. Consider first the beam with a uniform applied load as in Fig. 7:13. We note in this figure that the bending moment is

$$M = EI \frac{d^2 y}{dx^2} = \frac{WLx}{2} + \frac{Wx^2}{2} - Py \quad (7:53)$$

Since we desire to find the bending moment particularly, and not the deflection, let us take the second derivative of this equation as follows (assuming that the moment of inertia is constant):

$$\frac{d^2 M}{dx^2} = \frac{d^2}{dx^2} \left(EI \frac{d^2 y}{dx^2} \right) = w \quad (7:54)$$

We note that in the second term the second derivative of y with respect to x may be written

$$\frac{d^2 y}{dx^2} = \frac{w}{EI} \quad (7:55)$$

so that we have the equation

$$\frac{d^2 M}{dx^2} = P \quad (7:56)$$

Letting

$$\frac{P}{EI}$$

we have the solution of this equation as

$$M = A \cos jx + B \sin jx + \frac{w}{j^2} \quad (7:57)$$

The solution may be verified by substituting in equation (7:56). In this case, when

$$x = 0, \quad M = 0$$

from which we find that

$$0 = A + \frac{w}{j^2} \quad \text{or} \quad A = -\frac{w}{j^2} \quad (7:58)$$

We also note that, when

$$x = l \quad M = 0 \quad (7:59)$$

so that

$$0 = -\frac{w}{j^2} \cos jL + B \sin jL + \frac{w}{j^2} \quad (7:60)$$

from which we find that

$$B = \frac{\frac{w}{j^2} \cos jL - \frac{w}{j^2}}{\sin jL} \quad (7:61)$$

7:9. Lateral Load a Constant Proportion of Axial Load.—Let us now consider another problem in which the lateral load is a fixed proportion of the axial load as, for example, in Fig. 7:14. Writing the equation for this type of load, we find that

$$M_x = EI \frac{w}{dx^2} = \frac{Kx}{2} - Py \quad (7:62a)$$

from which we have

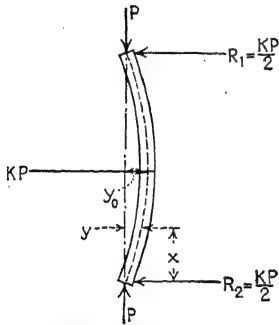


FIG. 7:14.—Beam loaded laterally with concentrated load.

The solution gives

$$y = A \cos jx + B \sin jx + ax + bx^3 \quad (7:62c)$$

where a and b are to be determined by substitution in (7:62b), as

$$\frac{d^2y}{dx^2} = -Aj^2 \cos jx - Bj^2 \sin jx + 6bx \quad (7:63)$$

From (7:62b),

$$-Aj^2 \cos jx - Bj^2 \sin jx + j^2 \cos jx + Bj^2 \sin jx + j^2 ax + j^2 bx^3 = \frac{K}{2} j^2 x \quad (7:64)$$

Equating coefficients of like-powered variables, we have

$$j^2b = 0, \quad b = 0 \quad (7:65)$$

Thus

$$K$$

The complete solution is therefore

$$y = A \cos jx + B \sin jx + \frac{K}{2} x \quad (7:66)$$

We note that when

$$x = 0, \quad y = 0, \quad \text{so that} \quad A = 0 \quad (7:67)$$

Thus

$$K \quad (7:68)$$

We have

$$\frac{dy}{dx} = i = \text{slope} = Bj \cos jx + \frac{K}{2} \quad (7:69)$$

Thus, when $x = L/2$, $i = 0$, if KP is at $x = L/2$,

$$0 = Bj \cos j \frac{L}{2} + \frac{K}{2} \quad (7:70)$$

so that

$$B = - \frac{K/2}{j \cos \frac{jL}{2}} \quad (7:71)$$

Therefore

$$y = \frac{-K/2}{j \cos \frac{jL}{2}} \sin jx + \frac{K}{2} x \quad (7:72)$$

We note

$$(7:73)$$

and

$$x = \frac{L}{2}, \quad = M_0 \quad (7:74)$$

Thus

$$\text{and } \frac{jL}{2} \quad (7:75)$$

or, substituting the value of j , we have

$$M_{(\max.)} = \frac{EIK}{2} \sqrt{\frac{P}{EI}} \tan \sqrt{\frac{P}{EI}} \frac{L}{2} \quad (7:76)$$

Now since

$$f = \frac{P}{A} \pm \frac{Mc}{I} \quad (7:77)$$

then

$$f_{(\max.)} = \quad (7:78)$$

7:10. Stress above the Proportional Limit.—Thus, upon letting f_t be the total stress, the maximum compressive stress is

$$f_{(\max.)} = f_t = \frac{r}{A} + \frac{cN}{\phi} \quad \tan \quad (7:79)$$

From this equation, we can compute the maximum fiber stress. It will be noted in this case that the fiber stress in the beam is proportional to the bending moment and that the deflection is

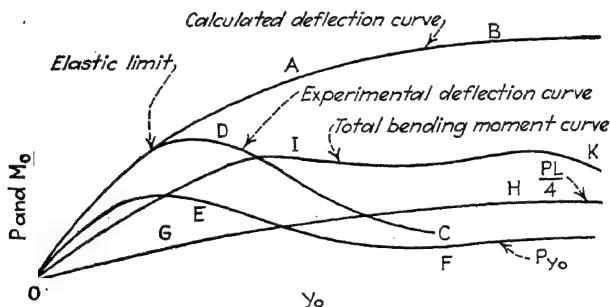


FIG. 7:15.—Approximate variation of quantities for axially loaded beam above elastic limit.

also proportional to the bending moment; therefore, the fiber stress is proportional to the deflection. Now, if an experiment be performed on a strut of this nature in which a set of levers is incorporated so that an applied side load of a given proportion of the axial load may be developed and the deflection, applied load, and all constants may be taken, we find that we obtain a deflection curve similar to the curve ODC in Fig. 7:15. It will be

noted, however, that the theoretical computation of the deflection y_0 will give a curve similar to OAB . Where the curve OAB departs from the curve ODC , we have the elastic limit of the material. It is apparent, therefore, that the use of the theoretical formula for calculation of the stress for deflection above the elastic limit is invalid. Since the fiber stress in the beam is proportional to the deflection, as previously noted, it is apparent that the fiber stress above the elastic limit cannot be determined by this theoretical method. If we extend the chart in Fig. 7:15 to include the bending moment in terms of the deflection, we

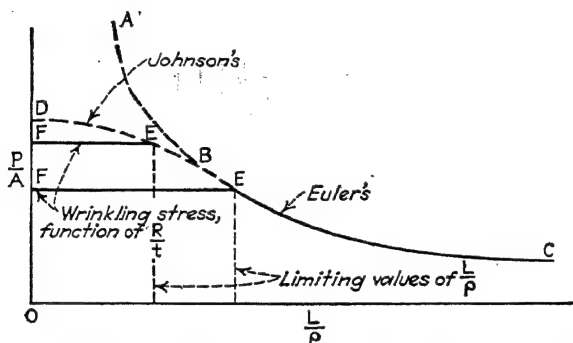


FIG. 7:16.—Tabulation of data for columns with walls of thin sheet metal.

find that the applied bending moment, which is proportional to the axial load, follows a curve of the nature of OGH , the secondary bending moment Py_0 follows a curve similar to OEF , and the total bending moment follows a curve similar to OIK . It is apparent from these experimental curves that the maximum bending moment will ordinarily not occur within the elastic limit but will occur at a stress much higher than the elastic limit; this shows us that special consideration will have to be given to the calculation of the stress, under these combined loading conditions, above the elastic limit.

7:11. Struts of Equal Crumpling and Buckling Strength.—It is quite apparent that if we increase the diameter of a tubular strut, while holding the cross-sectional area of the material a constant and thereby making the walls thinner, the strut may fail by crumpling of the thin walls. In Fig. 7:16 is reproduced the Euler-Johnson curve for a tube. As we decrease the length, the term L/p becomes smaller. Now at some point, as at E , crumpling

occurs. It is obvious that any further decrease in L will not give any increase in the strength of the strut; hence the line EF represents the strength of such short struts.

The crumpling strength of the thin walls is a function of the ratio of radius r to thickness t of the material.

7:12. Eulerian Strut with Variable Cross Section.—Calculated values of the moment of inertia of the cross-sectional area of

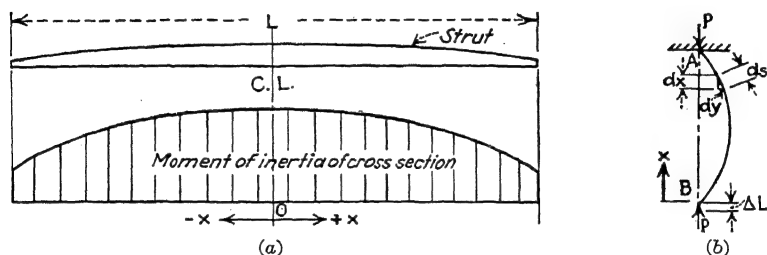


FIG. 7:17.—(a) Strut with variable moment of inertia; (b) elements of a bent strut.

several tapered struts outline a curve similar to that shown in Fig. 7:17a.

This curve is of parabolic form. In the simple strut equation

$$(7:80)$$

I is a variable, varying along an assumed parabolic curve. The parabola is approximately of the form

$$\left(\frac{L}{2}\right)^2 - \frac{4x^2}{L^2} \quad (7:81)$$

Note that the origin is taken at the center line of the strut. When $x = 0$, $I = I_0$, and, when $x = L/2$, $I = 0$. The end conditions, while not exact, affect the buckling strength only slightly. Equation (7:80) becomes

$$-\frac{\pi^2}{L^2} \left(\frac{u}{2} \right) + Py = 0 \quad (7:82)$$

To simplify the symbols, let us replace $2x/L$ by u . We have, therefore,

$$\frac{dy}{dx} = \frac{dy}{du} \frac{du}{dx} = \frac{dy}{du} \frac{2}{L} \quad (7:83)$$

and

$$du^2 \left(\frac{4}{L^2} \right) \quad (7:84)$$

Equation (7:82) becomes

$$(7:85)$$

Letting

$$\frac{PL^2}{4EI_0} \quad (7:86)$$

equation (7:85) becomes

$$(1 - u^2) \frac{d^2y}{du^2} + n^2y = 0 \quad (7:87)$$

Let us now assume the solution to be a power series, as

$$y = a_0 + a_1u + a_2u^2 + a_3u^3 + a_4u^4 + a_5u^5 + \dots \quad (7:88)$$

We now substitute the series (7:88) in equation (7:87) and solve for the coefficients a_0, a_1, a_2 , etc., by means of equating coefficients of like powers of u .

We find

$$\begin{aligned} \frac{d^2y}{du^2} = & 2a_2 + 2 \times 3a_3u + 3 \times 4a_4u^2 + 4 \times 5a_5u^3 + 5 \times \\ & + 6 \times 7a_6u^4 + 7 \times 8a_7u^5 + \dots \quad (7:89) \end{aligned}$$

Substituting (7:89) and (7:88) in equation (7:87), we have

$$\begin{aligned} & 2a_2 + 2 \times 3a_3u + 3 \times 4a_4u^2 + 4 \times 5a_5u^3 + 5 \times 6a_6u^4 \\ & + 6 \times 7a_7u^5 + 7 \times 8a_8u^6 + \dots \\ & - 2a_2u^2 - 2 \times 3a_3u^3 - 3 \times 4a_4u^4 - 4 \times 5a_5u^5 \\ & - 5 \times 6a_6u^6 - 6 \times 7a_7u^7 - 7 \times \\ & + \dots = 0 \quad (7:90) \end{aligned}$$

Assuming a_0 and a_1 are the constant of integration and equating the coefficients of like powers of u , we have

$$\text{Coefficients of } u^0, \quad = -n^2a_0, \quad n^2a_0$$

$$\text{Coefficients of } u^1, \quad 2 \times 3a_3 = -n^2a_1, \quad 2 \times 3$$

$$\begin{aligned} \text{Coefficients of } u^2, \quad & 3 \times 4a_4 - 2a_2 = \\ & a_4 = \frac{a_2(2 - n^2)}{3 \times 4} - \frac{n^2a_0}{2 \times 3 \times 4} (n^2 - 2) \end{aligned}$$

Coefficients of u^3 , $4 \times 5a_5 - 2 \times 3a_3 = -n^2a_3$

$$a_5 = \frac{a_3(2 \times 3 - n^2)}{4 \times 5} = \frac{n^2a_1(n^2 - 2 \times 3)}{2 \times 3 \times 4 \times 5}$$

Coefficient of u^4 , $5 \times 6a_6 - 3 \times 4a_4 = -n^2a_4$

$$a_6 = \frac{\times 4 - n^2}{5 \times 6} = \frac{-a_0(n^2 - 2)(n^2 - 3 \times 4)n^2}{2 \times 3 \times 4 \times 5 \times 6}$$

Thus y is

$$a_0 \left[1 - \frac{n^2}{2} u^2 - 2(n^2 - 3 \times 4)u^6 + \frac{n}{3} u^3 - 2 \times 3 u^5 - \frac{2 \times 3(n^2 - 4 \times 5)u^7}{7} \dots \right] \quad (7:91)$$

Now, when $u = 1$, $y = 0$. Also, when $u = -1$, $y = 0$. Substituting these values of u in turn in equation (7:91) and adding the two equations, we find that the odd-power series drops out. Thus we have

$$y = a_0 \left[1 - \frac{n^2}{2} u^2 - \frac{n^2(n^2 - 2)(n^2 - 3 \times 4)u^6}{2 \times 3 \times 4 \times 5 \times 6} \right] \quad (7:92)$$

If the strut is assumed to fail in the simplest manner, we terminate the series at the third term by letting $n^2 = 2$, in which case

$$y = a_0 \left(1 - \frac{1}{2} u^2 \right) \quad (7:93)$$

Noting that

$$n^2 = \frac{PL^2}{4EI_0} = 2 \quad (7:94)$$

we have

$$P = 8 \frac{EI_0}{L^2} \quad (7:95)$$

This is the load required to cause a deflection of this form, hence

the critical loading. Noting that, for a uniform strut,

$$P_e = \frac{\pi^2 EI}{L^2} \quad (7:96)$$

then the ratio is

$$\frac{P_e}{P} = \frac{9.86}{\pi} = 1.23 \quad (7:97)$$

Thus the nontapered strut is 23 per cent stronger than the tapered strut. The strength-weight ratio is left for the student to calculate.

7:13. Critical Load of Struts with Variable Cross Sections by Energy Method.—If the point B , Fig. 7:17b, moves toward A because of the deflection y of the strut, the work done by P is $P \Delta L$. When this work becomes greater than the elastic energy of bending stored in the strut, the strut will be unstable under the load P .

The energy stored in the strut as a result of the bending moment may be expressed as

$$E = \int_0^L \frac{M^2}{2EI} dx \quad (7:98)$$

Since

$$(7:99)$$

we have

The work done on the strut by the load P is (see Fig. 7:17b)

$$E = P \Delta L \quad (7:101)$$

or since

$$\Delta L = \int_0^L (ds - dx) \quad (7:102)$$

then

$$E = P \int_0^L (ds - dx) \quad (7:103)$$

Since

$$ds = \sqrt{dx^2 + dy^2} = \sqrt{1 + (dy/dx)^2} dx \quad (7:104)$$

and since by expansion in a power series we find the value of ds ,

to infinitesimals of the second order, as

$$ds = \left[1 + \frac{1}{2} \left(\frac{dy}{dx} \right)^2 \right] dx \quad (7:105)$$

we have, from equation (7:103),

$$(7:106)$$

Thus,

$$= \frac{1}{2} P \int_0^L \left(\frac{dy}{dx} \right)^2 dx \quad (7:107)$$

We therefore have for a stable condition

or

$$\int_0^L (dy/dx)^2 dx \quad (7:109)$$

Now let us again consider as an example the tapered strut under the assumption that the curve of deflection is of a parabolic form. Thus

$$(7:110)$$

where $a = L/2$. Assume the deflection curve

$$(7:111)$$

From equation (7:111),

$$\frac{dy}{dx} = \frac{x}{a} \quad (7:112)$$

Substituting equations (7:110) to (7:112) in equation (7:109), we have, since the origin is taken at the center of the strut,

$$P < \frac{1}{\frac{x^2}{a^2}} \quad (7:113)$$

which becomes

$$P < \frac{\left[x - \frac{x^3}{3} \right]_{-\frac{L}{2}}^{+\frac{L}{2}}}{\left[\frac{x^3}{3} \right]_{-\frac{L}{2}}^{+\frac{L}{2}}} \quad (7:114)$$

Since $a = L/2$,

$$P < \frac{L}{\frac{5L^2}{7^2}} \quad (7:115)$$

as previously determined.

It may be noted, by trial, that a considerable error in the assumption of the type of curve will produce very little error in the final result.

7:14. Method of Successive Approximations Applied to Beams.—The general loading-deflection equation of a beam of nonuniform cross section, distributed loads, and axial compression such as may be obtained by differentiating equations (3:60) and (3:73) is

$$\frac{d^2}{dx^2} \left(EI \frac{d^2 y}{dx^2} \right) = dx^2 = f(x, y) \quad (7:116)$$

where I is a function of x . Mathematicians have been able to solve only a very few of the simplest cases of equation (7:16). However, with a thorough understanding of the successive steps of integration of the loading curve, the shear curve, the moment curve, and the slope curve, as illustrated in Art. 3:24, it is a simple matter to obtain approximate answers thoroughly satisfactory for engineering purposes. The author has developed such procedures, on a consulting basis, for the routine solutions of certain cases, mathematically impossible by known methods but easily understandable and usable by junior engineers with only an undergraduate knowledge of mathematics.

7:15. Example of Column of Variable I .—We noted in Art. 7:2 how the critical loading of a constant I column (Euler's) could be obtained by the method of successive approximations. The column could have been investigated for stability under a load P by assuming an initial deflection curve; then, by numerical

step-by-step integration, the y_1 , y_2 , and y_3 curves could have been obtained. If y_2 is less than y_1 where $(y_0 + y_1 + y_2 + y_3 + \dots)$ is the deflection, the column is stable; if not, the column is unstable.

Obviously, the process would have been but a little more difficult if I were variable. In such a case the integration for the slope curve would have been

$$i = \frac{1}{E} \int \frac{M}{I} dx$$

$$= \frac{1}{E} \left(\frac{M_1}{I_1} \Delta x + \frac{M_2}{I_2} \Delta x + \frac{M_3}{I_3} \Delta x + \dots \frac{M_n}{I_n} \right) \quad (7:117)$$

where M_1 = value of M at x_1 .

I_1 = value of I at x_1 , etc.

Thus, if y_0 is the assumed initial curve—a sine or cosine curve would do—we have the first approximation of the additional deflection due to $P y_0$ as y_1 . Thus the slope is

$$i_1 = \frac{P}{E} \int \frac{y_0}{I} dx$$

$$= \frac{P}{E} \left(\frac{y_{01}}{I_1} \Delta x + \frac{y_{02}}{I_2} \Delta x + \frac{y_{03}}{I_3} \Delta x + \dots \right) \quad (7:118)$$

The integration starts at the value of x where i is assumed zero.

$$y_1 = \int i_1 dx$$

$$= (i_{1:1} \Delta x + i_{1:2} \Delta x + i_{1:3} \Delta x + \dots) \quad (7:119)$$

$$= \bar{E} \quad (7:120)$$

Likewise we have

$$i = \frac{P}{E} \int \int \frac{y_1}{I} dx \quad (7:121)$$

and

$$= \frac{P}{E} \int \int \frac{y_2}{I} dx \quad (7:122)$$

If the successive deflections become less than the preceding, the column is stable under the load assumed; otherwise, it is unstable.

A method could be worked out, by this method of successive approximations, for determining the critical load for a particular column.

7:16. Approximate Determination of Shears, Reactions, and Moments.—The shears, reactions, moments, slopes, and deflection may be determined at the supports of a statically indeterminate beam member by the method of *successive approximations*.

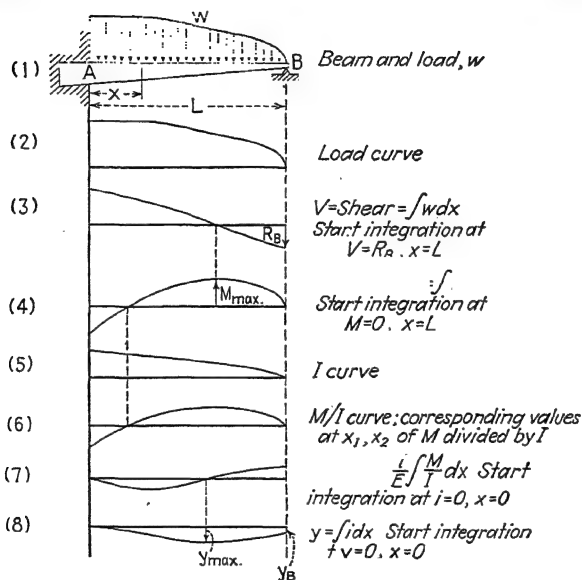


FIG. 7:18.

Consider, for example, the beam of Fig. 7:18. I and w are variables and are functions of x . The differential equation is

$$\frac{d^2}{dx^2} \quad (7:123)$$

where $f_1(x) = I = \text{function of } x$.

$f_2(x) = w = \text{function of } x$.

Assume that these functions cannot be expressed in simple mathematical form.

We are to find the reactions, shears, and moments. The solution of the problem by *orthodox methods* is impossible. However, engineering results may be obtained very easily by *successive approximations*.

7:17. Example.—For example—and this shows only one of many possible ways of solving the problem—consider the steps shown in Fig. 7:18.

We first assume a value of R_B based upon an estimate. To make this estimate, formulas for the uniform beam and uniform load may be used. With R_B assumed, plot the successive curves as shown in Fig. 7:18.

Our calculations finally show a deflection of the support at B of y_B . If no deflection is allowed for B (the support being rigid), we have therefore assumed R_B too small.

We now make an estimate of how much R_B , formerly assumed, must be increased to make $y_B = 0$.

With this new R_B , the integrations must then be repeated. When y_B checks out zero, the solution is correct. The values of moment, shears, reactions, and deflections may then be correctly taken from the curves.

Obviously, for a particular type of problem on beams, methods may be devised for quickly making the successive calculations approach the correct result.

7:18. The Hardy Cross Method of Moment Distribution.—A special and ingenious method of successive approximations for determining the moments at the supports of a beam continuous over several supports, as in the beams found in bridges and large buildings, was originated by Prof. Hardy Cross. It is seldom that beams in airplane structures are continuous over more than three or four supports, and when they are it is simpler to use the three-moment equation.

The method requires considerable explanation and a number of illustrative examples. Therefore, the student is referred to Prof. Cross's book (with Morgan) "Continuous Frames of Reinforced Concrete."

References

1. BOYD, J. E.: "Strength of Materials," McGraw-Hill Book Company, Inc., New York, 1935.
2. ROSS, O. E.: Curves Showing Column Strength of Steel and Duralumin Tubing, *N.A.C.A. Tech. Note* 306, May, 1929.
3. SCHROEDER, A.: Buckling Tests of Light Metal Tubes, *N.A.C.A. Tech. Mem.* 525, 1929.
4. STEINITZ, O.: Buckling and Bending Strength of Struts with Hollow Sections, *Z.F.M.*, Vol. XXI, No. 3, pp. 57-60, 1930.
5. TUCKERMAN, L. B., S. N. PETRENKO, and C. D. JOHNSON: Bureau of Standards, Strength of Tubing under Combined Axial and Transverse Loading, *N.A.C.A. Tech. Note* 307, 1929.

6. WAGNER, HERBERT: Remarks on Airplane Struts and Girders under Compressive and Bending Stresses, Index Values, *N.A.C.A. Tech. Mem.* 500, 1929.
7. YOUNGER, J. E.: Theory of Airplane Structural Members Subjected to Combined Axial and Non-uniform Transverse Loads, *Univ. Calif. Pub. Engineering*, Vol. II, No. 8, pp. 237-275, 1926.
8. YOUNGER, J. E.: Strength of Bent Struts, *Air Corps Information Circ.*, Vol. VI, No. 580, December, 1926.
9. YOUNGER, J. E., and B. M. WOODS: "Dynamics of Airplanes and Airplane Structures," John Wiley & Sons, Inc., New York, 1930.

CHAPTER VIII

CONTINUOUS BEAMS AND CONTINUOUS BEAM COLUMNS

8:1. Three-moment Equation by Least Work.—In Fig. 8:1 is shown a beam continuous over three adjacent supports A , B , and C . Equation (3:73) expresses the moment in the first bay A to B if P in this equation is zero. This equation is expressed in terms of the loading $f(u_1) = w_1$ and in terms of

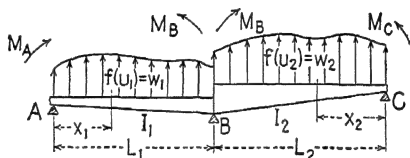


FIG. 8:1.

M_a and M_b . The same equation will apply to the second bay B to C if we place ourselves on the other side of the beam so that C is at our left. In this case, M_c takes the place of M_a , x_2 of x_1 , and L_2 of L_1 . We wish to obtain the relationship among M_a , M_b , and M_c in terms of the beam loading and the physical characteristics of the beam. This is equivalent, for example, to solving for M_b in terms of M_a and M_c . The simplest way of doing this is by the *theory of least work* (see Art. 6:13 to end of chapter for theory of least work). This is a good example of the application of the theory of least work and also gives the equation we require.

The total energy (elastic) in the beam, A to B and B to C , is

$$U = \int_0^{L_1} \frac{M_1^2}{2E_1I_1} dx_1 + \int_0^{L_2} \frac{M_2^2}{2E_2I_2} dx_2 \quad (8:1)$$

Now since $\partial U / \partial M_b = 0$, we have

$$\int_0^{L_1} \frac{\partial M_1}{\partial M_b} E_1 I_1 dx_1 + \int_0^{L_2} \frac{\partial M_2}{\partial M_b} E_2 I_2 dx_2 = 0 \quad (8:2)$$

It is only necessary to perform the operations indicated on the two moment equations, integrate, and arrange. If I_1 and I_2

are constant, we shall obtain

$$\frac{M_a L_1}{E_1 I_1} + \frac{2M_b L_1}{E_1 I_1} + \frac{2M_b L_2}{E_2 I_2} + \frac{M_c L_2}{E_2 I_2} = (\text{loading terms}) \quad (8:3)$$

Thus if $f(u)$ is constant in each span and equal to w_1 and w_2 , respectively, equation (8:16) may easily be obtained. For example, if $f(u) = w$ and $P = 0$ in equation (3:73), we have

$$M_x = M_a \quad (M_b - M_a)x \quad wLx, \quad wx^2 \quad (8:4)$$

Thus,

$$(8:5)$$

As an exercise, the student may complete the solution.

8:2. Effect of Deflection of a Support.—The effect of the deflection of a support of a continuous beam is equivalent to adding a concentrated load at the deflected support.

For example, in Fig. 8:2, the deflection of the simple cantilever beam is

$$y_a = - \frac{P_a x^3}{6EI} \quad (8:6)$$

where y_a takes the sign of P_a —negative in Fig. 8:2.

Thus, since $M_x = P_a x$, we have

$$M_x = + \frac{3EIx}{L^3} y_a \quad (8:7)$$

where M_x takes the sign of y_a —negative in Fig. 8:2.

If AB is one bay of a continuous beam, equation (8:7) will hold for the bay if we assume M_a and M_b are independent moments applied to the bay. Since equation (3:73) is derived on this assumption, we may therefore add equation (8:7), as a term, to equation (3:73).

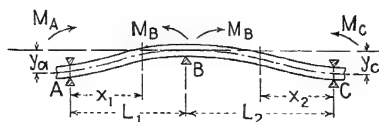


FIG. 8:3.

The moment equation for either of the bays of Fig. 8:3, it being remembered that M_c takes the place of M_a and y_c of y_a

in the second bay, is

$$M_x = M_a + \frac{(M_b - M_a)x}{L} + \frac{3EIx}{L^3} y_a \quad (8:8)$$

where the last term takes the sign of y_a —negative in Fig. 8:2.

Substituting this equation in equation (8:2), we may obtain

$$M_a L_1 + \frac{1}{2} + \frac{1}{2} + M_c L_2 + \frac{3EI y_b}{L^3} \quad (8:9)$$

where right-hand terms take the sign of y_a and y_b .

8:3. Application of Three-moment Equations by Use of

Images.—Many problems of statically indeterminate beams may be simply solved by the use of images. To illustrate, consider the beam of Fig. 8:4— AB , a cantilever beam supported at A .

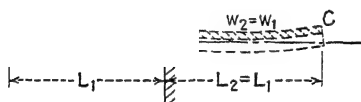


FIG. 8:4.

Problem.—Find M_b .

Solution.—With the wall at B as a mirror, draw the image BC . In this image, $w_2 = w_1$, $L_2 = L_1$, $E_2 = E_1$, $I_2 = I_1$, and

$$M_c = M_a = 0.$$

Thus equation (8:16) becomes (w_1 is negative),

$$2M_b L_1$$

Thus

$$M_b = - \quad (8:10)$$

Problem.—Find the deflection y_a of the cantilever beam of Fig. 8:5 by the use of equation (8:9) and an image.

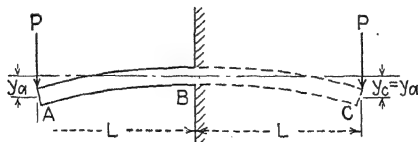


FIG. 8:5.

Solution.—We let $M_a = M_c = 0$, $y_a = y_c$, $E_1 = E_2$, $I_1 = I_2$, and $w_1 = w_2$. Thus, equation (8:9) becomes

$$2M_b L = \frac{6EI y_a}{L} \quad (8:11)$$

Thus

$$M_b =$$

and since

$$M_b = -PL$$

we have

$$y_a = -\frac{PL^3}{3EI} \quad (8:12)$$

Thus we obtain the familiar equation, thereby checking equation (8:9) and illustrating a method.

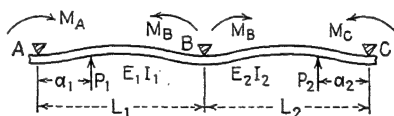


FIG. 8:6.

8:4. Concentrated Load Term for Three-moment Equation.—

With reference to Fig. 8:6, the moment from A to P_1 is

$$M_x = M_a \quad (8:13)$$

and that from P_1 to B is

$$M = M_b - M_a \frac{x_1}{L_1} - \frac{P_1}{2} \left(\frac{L_1}{2} - x_1 \right)^2 \quad (8:14)$$

When these equations, with similar ones for the second bay, are substituted in the least-work equation (8:2), instead of the one integral for each bay there will be two integrals, the first with limits from 0 to a and the second from a to L .

The solution gives the following result:

$$M_a L_1 + 2M_b L_1 + \frac{2M_b L_2}{E_2 I_2} + M_c L_2 = \frac{P_1 a_1}{L_1} (L_1^2 - a_1^2) + \frac{P_2 (L_2^2 - a_2^2)}{L_2} \quad (8:15)$$

The loading terms, of course, may be repeated for each concentrated load.

8:5. Continuous Spar.—The general procedure in analyzing a continuous wing beam is as follows: The beam loading is deter-

mined from the air-loading conditions as specified by the design conditions or by government agencies, and from this the beam and chord loadings are determined. In order to determine the axial load that occurs in the spars, it is necessary to know the reaction at the supports. This implies a knowledge of the reaction in the flying wires or the anti-flying wires as the case may be. The reactions in the outer supports are usually determined by the application of the ordinary three-moment equation.

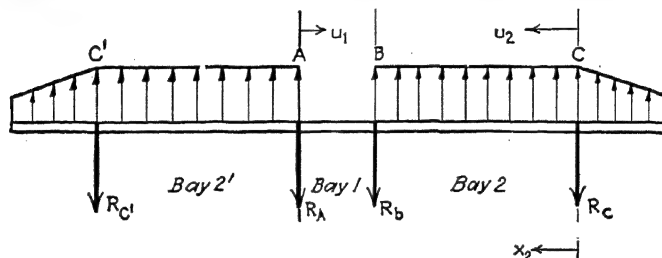


FIG. 8:7.—Continuous wing beam.

The three-moment equation (as may be verified by reference to any standard text on strength of material) is

$$M_a L_1 + \frac{2M_b L_1}{3} + M_c L_2 \quad (8:16)$$

The left-hand side of the three-moment equation is the same, regardless of the type of loading on the bay. The terms on the right-hand side of the equation depend upon the type of loading on the beam. For example, there are terms for concentrated loads, distributed loads, or the combination of the two types of loading (see handbooks on structures). A term is added for each type of loading in each bay. Now, in applying the three-moment equation to the example of Fig. 8:7, we write the equation for the bays A to B and B to C. From conditions of symmetry the moment at A equals the moment at B, and this condition enables us to solve for the values of the moments at A and B with one application of the three-moment equation, since the bending moment C is known from the conditions of the overhang and since all the other quantities necessary are known. By taking the summation of the moments about the point B with reference to the portion of the beam to the right of B, we have

$$M_b = -R_c L_2 + \Sigma f(u_2)(L_2 - u_2) \quad (8:17)$$

from which, since M_b is known, R_c can be found. In most cases the reaction R_c can be determined by ordinary methods of statics, upon assuming that the bending moment at B is zero and taking the summation of the moment about the point B . Neither one of these methods, however, is exact, inasmuch as the moment at B is influenced considerably by the secondary stress in the beam due to the axial load. However, they make very good approximations.

If the reaction at C is determined, the axial component in the spar may then be determined; and the so-called *precise* three-moment equation, which involves the quantities pertaining to the beam as a column, may be applied in so far as Hooke's law applies. See Art. 8:19 and equation (8:46).

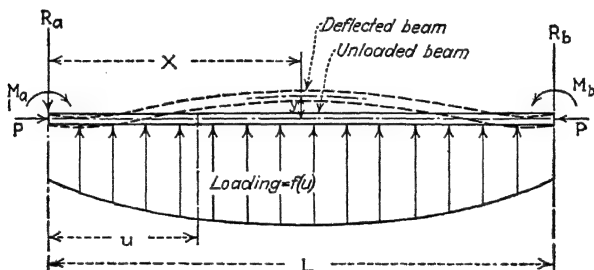


FIG. 8:8.—Nonuniformly loaded beam column.

8:6. Methods of Analysis.—The mathematical analysis of the beam column becomes quite complex if one considers special types of loading and variation in the moment of inertia of the cross-sectional area of the beam. For this reason, special methods of analysis from time to time appear in the literature on the subject. These methods are always limited in their scope and quite often are more difficult to master than the basic theory. For this reason, it seems most expedient to present here as much of the basic theory as appears practical and to leave the special methods for independent study.

Experiments show that the basic theory is fairly accurate for stresses below the proportional limit of the material. Since the theory is based on Young's modulus of elasticity of the material, the result is subject to the variability of this constant, which is approximately 5 to 15 per cent.

8:7. Basic Equation for Distributed Load.—With reference to Fig. 8:8, the bending moment at x for a distributed load $f(u)$ and

an axial load P is [see equation (3:73)]

$$M_x = M_a + \frac{(M_b - M_a)x}{L} - \frac{x}{L} \int_0^L f(u)(L-u) du - \int_0^x f(u)(x-u) du - Py \quad (8:18)$$

It is desired to find M_x in terms of x (y being eliminated). Differentiating equation (8:18) with respect to x , we have the shear,

$$\frac{dM_x}{dx} = M_a - \frac{1}{L} \int_0^L f(u)(L-u) du + \int_0^x f(u) du - P \frac{dy}{dx} \quad (8:19)$$

Differentiating again, we have the loading,

$$\frac{d^2M_x}{dx^2} = f(x) - P \frac{d^2y}{dx^2} \quad (8:20)$$

Since

$$\frac{d^2y}{dx^2} = \frac{M_x}{EI} \quad (8:21)$$

equation (8:21) becomes, upon letting $P/EI =$

$$\frac{d^2M_x}{dx^2} + j^2M_x = f(x) \quad (8:22)$$

8:3. Solution of the Differential Equation.—The solution of this equation is obtained as follows: Multiply the equation by the integrating factor $\cos jx$ and obtain the exact differential equation

$$\cos jx \frac{d^2M_x}{dx^2} + j^2M_x \cos jx = f(x) \cos jx \quad (8:23)$$

the integral of which is

$$\cos jx \frac{dM_x}{dx} + jM_x \sin jx = \int f(x) \cos jx dx + B \quad (8:24)$$

Now multiply equation (8:22) by the integrating factor $\sin jx$, and integrate; thus,

$$\sin jx \frac{dM_x}{dx} - jM_x \cos jx = \int f(x) \sin jx dx - A \quad (8:25)$$

Eliminating dM_x/dx between equations (8:24) and (8:25), we obtain

$$M_x = A \cos jx + B \sin jx + \frac{\sin jx}{j} \int f(x) \cos jx \, dx - \frac{\cos jx}{j} \int f(x) \sin jx \, dx \quad (8:26)$$

The equation may be written, as may be easily verified,

$$M_x = A \cos jx + B \sin jx + \frac{1}{j} \int_0^x f(u) \sin j(x-u) \, du \quad (8:27)$$

8:9. Evaluating the Constants.—The boundary conditions for evaluating the constants are

$$\begin{aligned} \text{When } x = 0, \quad M_x &= M_a \\ \text{When } x = L, \quad M_x &= M_b \end{aligned}$$

from which

$$A = M_a \quad (8:28)$$

and

$$B = \frac{M_b}{\sin jL} - \frac{M_a \cos jL}{\sin jL} - \frac{1}{j \sin jL} \int_0^L f(u) \sin j(L-u) \, du \quad (8:29)$$

We thus obtain the equation for the moment between the supports

$$M_x = M_a \frac{\sin j(L-x)}{\sin jL} + M_b \frac{\sin jx}{\sin jL} - \frac{\sin jx}{j \sin jL} \int_0^L f(u) \sin j(L-u) \, du + \frac{1}{j} \int_0^x f(u) \sin j(x-u) \, du \quad (8:30)$$

8:10. Simple Beam Column with Uniform Load.—If, in equation (8:30), we let $M_a = M_b = 0$ and $f(u) = w$, we obtain

$$-jM_x = \frac{w}{j \sin jL} [\sin jx + \sin j(L-x)] - \frac{w}{j} \quad (8:30a)$$

The moment of instability occurs when $\sin jL = 0$. Thus,

$$jL = m\pi \quad \text{or} \quad \frac{P}{EI} = \frac{m^2\pi^2}{L^2}$$

or

$$P = \frac{m^2\pi^2 EI}{L^2} \quad (8:31)$$

The beam will probably fail from overstrain of fibers before this load is reached.

8:11. Simple Beam Column with Concentrated Loads.—If, in equation (8:30), we let $M_a = M_b = 0$ and $f(u) du = Q$, we obtain

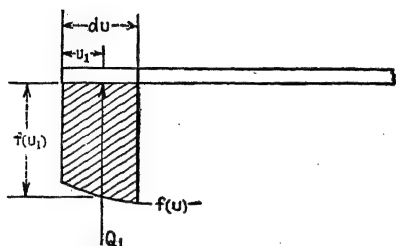


FIG. 8:9.—Equivalent concentrated load.

an equation for concentrated loads Q_1, Q_2 , etc. A study of Fig. 8:9 will show the transformation involved. $f(u)$ is the average magnitude of loading, and du is the distance along the beam under consideration. For example, $f(u)$ may be 10 lb. per inch and du taken as 2 in. Thus $Q = 10$

$\times 2 = 20$ lb., considered as a concentrated load. Thus we may write equation (8:30)

$$M_x = -\frac{\sin jx}{j \sin jL} \left[\sum_0^L Q_1 \sin j(L - u_1) + Q_2 \sin j(L - u_2) + \dots \right] + \frac{1}{j} \left[\sum_0^x Q_1 \sin j(x - u_1) + Q_2 \sin j(x - u_2) + \dots \right] \quad (8:32)$$

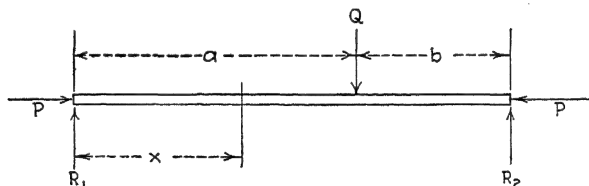


FIG. 8:10.—Beam column with concentrated lateral load.

For example, the equation for the loading shown in Fig. 8:10 is

$$M_x = -\frac{\sin jx}{j \sin jL} (-Q \sin jb) + \frac{1}{j} [-Q \sin j(x - a)] \quad (8:33)$$

If we let $b = x = a = L/2$,

$$M_x = +\frac{\sin j \frac{L}{2}}{j \sin jL} Q \sin j \frac{L}{2} = \frac{Q}{2j} \frac{\sin j \frac{L}{2}}{\cos j \frac{L}{2}} \quad (8:35)$$

(8:30) is valid only from O to x ; hence the validity holds also for the special cases of equations (8:32) and (8:37).

8:14. Other Types of Loading.—If the loading curve can be expressed mathematically, its value may be substituted for $f(u)$ in equation (8:30), and the integrals evaluated. If the loading curve cannot be expressed mathematically, equation (8:32) may be used. In this case, Q is $f(u) \Delta u$, in which $f(u)$ is the mean loading for the interval Δu . Then u is the abscissa of the mean loading.

8:15. Location of Maximum Moment.—To find the location of the maximum moment, we differentiate equation (8:30), equate to zero, and solve for x . Thus

$$\frac{dM_x}{dx} = -\frac{j \cos j(L-x)}{\sin jL} + \frac{jx}{\sin jL} - \frac{\cos jx}{\sin jL} \int_0^L f(u) \sin j(L-u) du + \int_0^x f(u) \cos j(x-u) du = 0 \quad (8:39)$$

This is the equation for the shear.

In general, the evaluation of x in equation (8:39) is not possible. When this is the case, it is necessary to plot the curve to find the maximum moment.

8:16. Maximum Moment for Uniform Loading.—Substituting w for $f(u)$ in equation (8:39), we find

$$\tan jx = \frac{M_b - \frac{w}{j^2} - M_a \cos jL + \frac{w}{j^2} \cos jL}{\left(M_a - \frac{w}{j^2}\right) \sin jL} \quad (8:40)$$

From this, x may be evaluated.

If this value of x be substituted in equation (8:30), we obtain

$$M_{x(\max)} = \frac{M_a - \frac{w}{j^2}}{\cos jx} + \frac{w}{j^2} \quad (8:41)$$

There may not be a maximum between the supports A and B ; and, in this case, x will be a negative value or a value greater than L . Equations (8:40) and (8:41) may be more readily obtained by the indicated operation on the equations in Art. 7:8.

8:17. Variable Moment of Inertia.—If the moment of inertia is a variable, then j in equation (8:22) is a function of x . This

equation has not been solved. If M_a and M_b are known, however, the bending moment, shear, deflection, etc., may be obtained by successive approximate integrations, the principles of which are illustrated in Art. 3:21.

If, however, M_a and M_b are functions of j , as in the case of a beam continuous over more than two supports, this method cannot be used, since M_a and M_b cannot be determined. *If the variation of I is small, the average value of I will probably give results sufficiently accurate.* If the minimum value of I is taken, the results will be conservative. Since there is considerable variation in the modulus of elasticity and since wing beams are the major members of an airplane, it appears that the conservative method should be required.

8:18. Slope and Deflection of Beam Column.—In equation (8:30), by substituting $EI \frac{d^2y}{dx^2}$ for M_x and integrating, we obtain

$$\begin{aligned} \frac{dy}{dx} = & M_a \frac{\cos j(L-x)}{j \sin jL} - M_b \frac{\cos jx}{j \sin jL} + \frac{\cos jx}{j \sin jL} \int_0^L \\ & f(u) \sin j(L-u) du - \frac{1}{j^2} \int_0^x f(u) \cos j(x-u) du \end{aligned} \quad (8:42)$$

The boundary conditions are

When $x = L$, $dy/dx = i_b = \text{slope at } B$

Substituting the boundary conditions in equation (8:42), solving for C_1 , substituting C_1 in equation (8:42), and integrating, we obtain

$$\begin{aligned} EIy = & - \cos jL \\ & + \frac{\sin jx}{j^3 \sin jL} - \int_0^L f(u) \sin j(L-u) du - \frac{x \cos jL}{j^2 \sin jL} \int_0^x \\ & \sin j(L-u) du - \frac{1}{j^3} \int_0^x f(u) \sin j(x-u) du + \frac{x}{j^2} \int_0^L f(u) \cos j(L-u) \\ & - \frac{x}{j^2} \int_0^L f(u) du + \frac{x}{j^2} \int_0^x f(u) du - \frac{1}{j^2} \int_0^x u f(u) du + EIi_b \\ & + C_2 \end{aligned} \quad (8:43)$$

The boundary conditions are:

$$\text{When } x = 0, \quad y =$$

Thus,

$$M_a \quad (8:44)$$

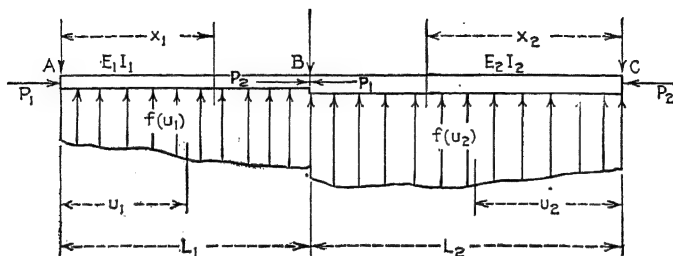


FIG. 8:12.—Continuous beam column with nonuniform lateral load.

8:19. Three-moment Equation for Beam Column.—Solving for i_b in equation (8:43), letting $x = L$, and introducing the subscript 1 for bay 1 of Fig. 8:12, we obtain

$$\begin{aligned} i_b = & \frac{1}{E_1 I_1 L_1} \left[\frac{M_a L_1}{j_1 \sin j_1 L_1} - \frac{M_a}{j_1^2} + \frac{M_b}{j_1^2} - \frac{M_b L_1 \cos j_1 L_1}{j_1^2 \sin j_1 L_1} \right. \\ & - \frac{1}{j_1^3} \int_0^L f(u_1) \sin j_1 (L_1 - u_1) du_1 + \frac{L_1 \cos j_1 L_1}{j_1^2 \sin j_1 L_1} \int_0^L f(u_1) \\ & \quad \sin j_1 (L_1 - u_1) du_1 \\ & + \frac{1}{j_1^3} \int_0^L f(u_1) \sin j_1 (L_1 - u_1) du_1 - \frac{L_1}{j_1^2} \int_0^L f(u_1) \\ & \quad \cos j_1 (L_1 - u_1) du_1 \\ & \left. + \frac{1}{j_1^2} \int_0^L u_1 f(u_1) du_1 - E_1 I_1 y_a \right] \quad (8:45) \end{aligned}$$

An equation similar to equation (8:45) is required for the section of the beam from C to B . The only changes in equation (8:45) necessary are that M_c be substituted for M_a , $-i_b$ for i_b , and y_c for y_a and that subscript 2 be introduced.

Obtaining this equation for bay 2, adding it to equation (8:45), simplifying, multiplying by 6, and substituting the notation x for u , we obtain

$$\begin{aligned} \frac{M_a L_1}{E_1 I_1} \alpha_1 + 2 \frac{M_b L_1}{E_1 I_1} \beta_1 + 2 \frac{M_b L_2}{E_2 I_2} \beta_2 + \frac{M_c L_2}{E_2 I_2} \alpha_2 = & \frac{L_1^2}{E_1 I_1} \psi_1 \\ & + \frac{L_2^2}{E_2 I_2} \psi_2 + \frac{6y_a}{L_1} + \frac{6y_c}{L_2} \quad (8:46) \end{aligned}$$

where

$$= \frac{6(jL \operatorname{cosec} jL - 1)}{\quad} \quad (8:47)$$

$$= \frac{3(1 - jL \cot jL)}{\quad} \quad (8:48)$$

and

$$\psi = \int_0^L \left[\frac{6 \sin jx}{(jL)^2 \sin jL} - \frac{6x}{L(jL)^2} \right] f(x) dx \quad (8:49)$$

8:20. Three-moment Equation for Uniform Load.—When $f(x) = w$, the term L^2 becomes

$$\frac{wL^3}{4EI} \gamma \quad (8:50)$$

where

$$\gamma = \frac{3 \left(\tan \frac{jL}{2} - \frac{jL}{2} \right)}{(jL/2)^3} \quad (8:51)$$

8:21. Functions α , β , and γ .—The functions α , β , and γ have been calculated and tabulated (see Table 8:1). In some tables, j as used in this text must be replaced by $1/j$. After the constants α , β , and γ are obtained, equation (8:46) is used exactly as the ordinary three-moment equation.

8:22. The ψ -function.—In equation (8:49), let $x = KL$, where K is a fraction varying from 0 to 1. We have

$$dx = L dK \quad \text{and} \quad f(x) = f(KL)$$

When $x = L$, $K = 1$, and, when $x = 0$, $K = 0$; thus, equation (8:49) becomes

$$\psi = \int_0^1 \left[\frac{6 \sin KjL}{(jL)^2 \sin jL} - \frac{6K}{(jL)^2} \right] f(KL)L dK \quad (8:52)$$

$L dK$ is an element of length along the span, and $f(KL)$ is the average intensity of loading at this element. Thus $f(KL)L dK$ is the total loading that may be assumed concentrated at the center of the element. Let this be Q_k ; then

$$\psi = \sum_{K=0}^{K=1} \left[\frac{6 \sin KjL}{(jL)^2 \sin jL} - \frac{6K}{(jL)^2} \right] Q_k$$

TABLE 8:1.—CONTINUOUS BEAM COLUMN, THREE-MOMENT EQUATION,
FUNCTIONS α , β , AND γ *
(Abridged for classroom use)

JL , radians	α	β	γ	JL , radians	α	β	γ
1.00	1.1304	1.0737	1.1133	2.70	4.3766	2.7619	3.7863
1.10	1.1617	1.0912	1.1379	2.71	4.4757	2.8121	3.8671
1.20	1.1979	1.1114	1.1686	2.72	4.5795	2.8648	3.9517
1.30	1.2396	1.1345	1.2039	2.73	4.6885	2.9199	4.0405
1.40	1.2878	1.1610	1.2445	2.74	4.8029	2.9778	4.1337
1.50	1.3434	1.1915	1.2914	2.75	4.9233	3.0386	4.2317
1.60	1.4078	1.2266	1.3455	2.76	5.0499	3.1027	4.3349
1.70	1.4830	1.2673	1.4085	2.77	5.1835	3.1702	4.4436
1.80	1.5710	1.3147	1.4821	2.78	5.3245	3.2414	4.5584
1.90	1.6750	1.3704	1.5689	2.79	5.4736	3.3166	4.6797
2.00	1.7993	1.4365	1.6722	2.80	5.6315	3.3963	4.8082
2.10	1.9493	1.5158	1.7967	2.81	5.7990	3.4807	4.9444
2.20	2.1336	1.6124	1.9491	2.82	5.9770	3.5704	5.0892
2.30	2.3640	1.7325	2.1392	2.83	6.1664	3.6659	5.2432
2.40	2.6596	1.8854	2.3822	2.84	6.3685	3.7676	5.4075
2.41	2.6935	1.9031	2.4103	2.85	6.5845	3.8764	5.5832
2.42	2.7287	1.9212	2.4391	2.86	6.8160	3.9928	5.7713
2.43	2.7649	1.9398	2.4687	2.87	7.0646	4.1179	5.9733
2.44	2.8021	1.9589	2.4993	2.88	7.3322	4.2525	6.1907
2.45	2.8403	1.9786	2.5306	2.89	7.6212	4.3977	6.4255
2.46	2.8798	1.9989	2.5630	2.90	7.9343	4.5550	6.6798
2.47	2.9204	2.0198	2.5964	2.91	8.2745	4.7259	6.9561
2.48	2.9624	2.0413	2.6307	2.92	8.6455	4.9121	7.2573
2.49	3.0056	2.0635	2.6662	2.93	9.0516	5.1160	7.5871
2.50	3.0502	2.0864	2.7027	2.94	9.4982	5.3401	7.9496
2.51	3.0963	2.1100	2.7405	2.95	9.9915	5.5875	8.3500
2.52	3.1438	2.1343	2.7794	2.96	10.5393	5.8622	8.7946
2.53	3.1931	2.1595	2.8197	2.97	11.1510	6.1688	9.2910
2.54	3.2437	2.1855	2.8612	2.98	11.8386	6.5134	9.8489
2.55	3.2963	2.2124	2.9043	2.99	12.6171	6.9035	10.4804
2.56	3.3508	2.2402	2.9488	3.00	13.5057	7.3486	11.2013
2.57	3.4072	2.2690	2.9949	3.01	14.5295	7.8813	12.0317
2.58	3.4657	2.2988	3.0427	3.02	15.7219	8.4583	12.9988
2.59	3.5262	2.3297	3.0922	3.03	17.1282	9.1623	14.1393
2.60	3.5890	2.3618	3.1435	3.04	18.8116	10.0049	15.5044
2.61	3.6542	2.3950	3.1968	3.05	20.8620	11.0314	17.1677
2.62	3.7220	2.4295	3.2522	3.06	23.4176	12.3096	19.2388
2.63	3.7925	2.4654	3.3097	3.07	26.6860	13.9446	21.8886
2.64	3.8569	2.5027	3.3696	3.08	31.0160	16.1105	25.3989
2.65	3.9421	2.5415	3.4319	3.09	37.0244	19.1156	30.2701
2.66	4.0218	2.5819	3.4969	3.10	45.9234	23.5659	37.4839
2.67	4.1047	2.6241	3.5646	3.11	60.4566	30.8334	49.2647
2.68	4.1914	2.6680	3.6353	3.12	88.4522	44.8321	71.9577
2.69	4.2820	2.7140	3.7092	3.13	164.7487	82.9812	133.8017

* See equations (8:47), (8:48), and (8:51). From Ref. 4, by permission.

If we let

$$\frac{6 \sin KjL}{\sin jL} \quad \frac{6K}{(jL)^2} \quad (8:54)$$

then

$$Y_k Q_k \quad (8:55)$$

For example,

$$(YQ)_{(k=0.9)} \quad (8:56)$$

The domain of the Y -function is sufficiently limited so that a table of the numerical values may be constructed. Such a table may be found in Reference 6. This table enables one to calculate ψ for any type of loading, so that the function may be incorporated in the three-moment equation.

If the loading curve may be expressed mathematically, that is, if $f(x)$ is a known function of x , ψ may be evaluated by integrating equation (8:49). If the loads are concentrated, ψ may be found from equation (8:53).

References

1. BERRY, ARTHUR: The Calculation of Stresses in Aeroplane Wing Spars, *Trans. Roy. Aeronautical Soc.*, No. 1, London, 1919.
2. HOWARD, H. B.: "The Stresses in Aeroplane Structures," Sir Isaac Pitman & Sons, Ltd., London, 1934.
3. NEWELL, J. S.: The Investigation of Structural Members under Combined Axial and Transverse Loads, *U.S. Air Service Information Circ.* 2400, Secs. 1 and 2, 1925.
4. NILES, A. S., and J. S. NEWELL: "Airplane Structures," John Wiley & Sons, Inc., New York, 1929.
5. WARNER, E. P., and S. P. JOHNSTON: "Aviation Handbook," McGraw-Hill Book Company, Inc., New York, 1931.
6. YOUNGER, J. E.: Theory of Airplane Structural Members Subjected to Combined Axial and Non-uniform Transverse Loads, *Univ. Calif. Pub. Eng.*, Vol. II, No. 8, pp. 237-275, 1926.
7. YOUNGER, J. E.: Critical Loading of Structural Members Subjected to Combined Axial and Transverse Loads, *Air Corps Information Circ.*, Vol. VI, 581, 1926.

CHAPTER IX

ANALYSIS OF TORSION MEMBERS

9:1. Basic Theory of Torsion.—Three phases of the torsion problem are evident, namely:

1. Torsion involving stresses below the elastic limit.
2. Torsion involving stresses above the elastic limit.
3. Torsion involving the elastic stability of the structure.

The first phase has for its basic theory the mathematical theory of elasticity. The second phase is not subject, at the present state of knowledge, to calculations based on pure theory. Experimental curves, empirical formulas, and approximations

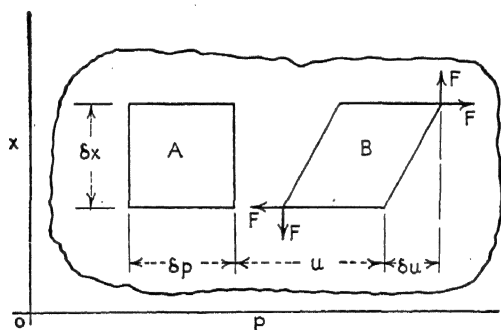


FIG. 9:1.—Elements of shear in a plate.

based on the theory of elasticity form the basis of practical calculations. The third phase is within the field of the theory of elasticity; but, in general, the mathematics involved is too difficult for practical use, unless simplifying assumptions are made which limit the accuracy of the method. Structures of thin sheet metal, in general, are considered in the third classification.

9:2. Shear Modulus of Elasticity.—With reference to Fig. 9:1, an elementary block of volume $(\delta x)(\delta p)t$ in an elastic structure subjected to shear is moved from A to B and distorted, as noted,

by the shear force. Letting E_s represent the shear modulus, we have

$$\nu_s = \frac{\text{unit shear}}{\text{unit strain}} \quad (9:1)$$

$$\text{Unit shear } s = \frac{F}{t(\delta p)} \quad \text{and} \quad \text{unit strain} = \frac{\delta u}{\delta x} \quad (9:2)$$

But

$$\delta u = \frac{\partial u}{\partial x} \delta x$$

so that

$$E_s = \frac{\partial u / \partial x}{\partial u / \partial x} = \frac{\partial x}{\partial u} \quad (9:3)$$

The relationship between E_s , the modulus of elasticity E , and Poisson's ratio μ is

$$E_s = \frac{E}{2(1 + \mu)} \quad (9:4)$$

In general, μ for aircraft materials is approximately 0.25. Hence E_s may be assumed about $\frac{2}{5}E$.

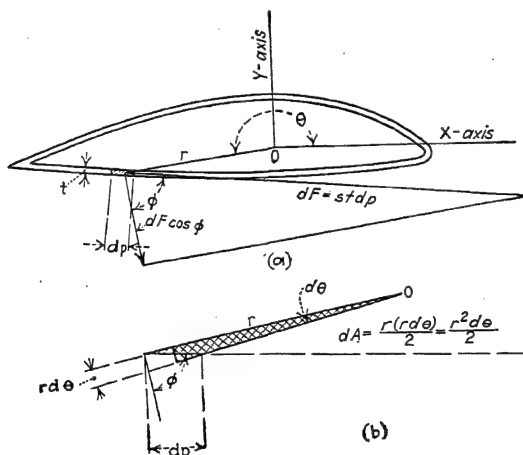


FIG. 9:2.—Stresses in the walls of a tube.

9:3. Torsional Stress in a Thin-walled Tube.—Referring to Fig. 9:2, we have a tubular section with thickness of wall t . We let F represent the total shear force per unit length at any point. This total shear force also exists perpendicular to F as represented in the figure, that is parallel to the z -axis of the airfoil. F must be constant around the contour of the airfoil to satisfy

the requirements of equilibrium; thus

$$F = ts = \text{constant} \quad (9:5)$$

where t = thickness, in.

s = unit shear stress, lb. per square inch

Taking the summation of moments about an assumed axis O , we have the torque

$$dM = r (dF) \cos \phi = (rst \cos \phi) dp \quad (9:6)$$

We note from Fig. 9:2b that

$$dp = \frac{r(d\theta)}{\cos \phi} \quad (9:7)$$

so that

$$dM = r^2 st (d\theta) \quad (9:8)$$

We also note from this figure that

$$r^2 (d\theta) = 2(dA) \quad (9:9)$$

so that, since st is constant,

$$M = 2st \int dA = 2stA \quad (9:10)$$

where A is the mean enclosed area bounded by the inner and outer curves.

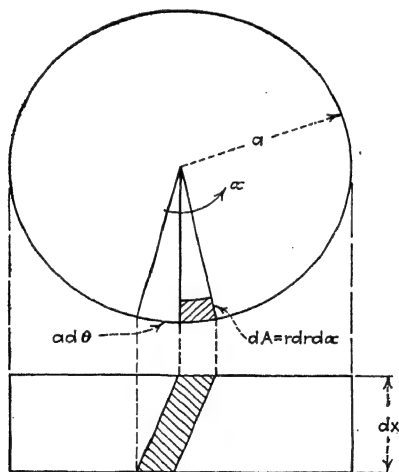


FIG. 9:3.—Shear in a solid cylinder.

9:4. Torsional Stress in a Solid Round Rod.—With reference to Fig. 9:3, the torsional moment M is expressed thus:

$$M = \int sr \, dA \quad (9:11)$$

Since

$$\tau:r = \quad (9:12)$$

therefore

$$M = \frac{s_{(\max.)}}{a} \int r^2 dA \quad (9:13)$$

Let $\int r^2 dA = J$, the polar moment of inertia of the area; then

$$s_{(\max.)} = \frac{Ma}{J} \quad (9:14)$$

The units are inches and pounds.

9:5. Angle of Twist of a Solid Round Rod.—With reference to Fig. 9:3, by definition,

$$\begin{aligned} \text{from which} \quad \tau_s &= \frac{a(d\theta)/dx}{a} \quad a \quad d\theta \\ &= \frac{s_{(\max.)}}{aE_s} \int_0^L dz \quad \frac{1}{aE_s} \end{aligned} \quad (9:16)$$

Substituting (9:14) in (9:16),

$$\frac{M}{E_s J} \quad (9:17)$$

The units are radians, inches, and pounds.

9:6. Other Compact Solid Rods.—Except for a few simple cross sections of torsion members, such as the circle, the ellipse, and the square, precise torsion formulas have not been derived. The mathematics involved in the theory of elasticity in torsion becomes too complicated for the scope of this text. The student is referred to texts on the mathematical theory of elasticity.

For an elliptical cross section we have

$$L$$


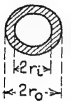
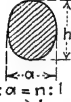

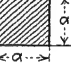
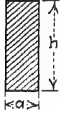

where A is the area of the cross section in square inches.

For other compact sections, approximately,

$$\theta = \frac{40JM}{E_s J} L \quad (9:19)$$

9:7. Torsional Stress in Various Cross Sections.—The student should note especially that the stress formulas in the preceding paragraph and in the following table give the stress which is developed *below the elastic limit of the material or below the buckling strength of the thin-walled tubes*. They do not give the allowable strength—that is, the breaking strength.

TABLE 9:1.—EQUATIONS OF TORSION¹

No. Cross section	Moment (torsion)	Shear stress
1 	$M = \frac{\pi}{2} r^4 E_s \theta$ $M = \frac{\pi}{2} r^3 s$ $= \frac{J s}{r}$	$s(\max.) = r E_s \theta$ $= \frac{M r}{J}$
2 	$M = \frac{\pi}{2} (r_o^4 - r_i^4) E_s \theta$	$s(\max.) = r_o E_s \theta$ $= \frac{M r_o}{J}$
3  h:a=n:1 n>1	$M = \frac{\pi}{16} \left(\frac{n^3}{n^2 + 1} \right) a^4 E_s \theta$ $= \frac{\pi}{16} n a^3 s(\max.)$ $M^* = \frac{1}{4\pi^2} \frac{E_s \theta A^4}{J}, A = \text{area}$	At end of small axis: $s(\max.) = \frac{n^2}{n^2 + 1} a E_s \theta$ $= \frac{16 M}{\pi n a^3}$ At end of large axis: $s = \frac{1}{n} s(\max.)$
4  h:a=h_i:a_i=n:1 n>1	$M = \frac{\pi}{16} \left[\frac{n^3}{n^2 + 1} \right] (a^4 - a_i^4) E_s \theta$ $= \frac{\pi}{16} \frac{(a^4 - a_i^4)}{a} s(\max.)$	At end of small axis: $s(\max.) = \left[\frac{n^2}{n^2 + 1} \right] a E_s \theta$ $= \frac{16 M a}{\pi n (a^4 - a_i^4)}$ At end of large axis: $s = \frac{1}{n} s(\max.)$
5 	$M = 0.1404 a^4 E_s \theta$ $= 0.208 a^3 s(\max.)$ $M^* = 0.0234 \frac{E_s \theta A^4}{J}$	At the middle of the side: $s(\max.) = 0.6753 a E_s \theta$ $= \frac{M}{0.208 a^3}$ At corners, $s = 0$
6  h:a=n:1 4>n>1	$M = n \psi a^4 E_s \theta$ in which $n \psi = \frac{1}{3} \left(n - 0.630 + \frac{0.052}{n^4} \right)$ For a section between a square and a flat sheet $M^* = K \frac{E_s \theta A^4}{J}$ K varies from 0.0234 for square to 0.0278 for flat sheet.	At the middle of the long side: $s(\max.) = \psi_1 a E_s \theta$ in which $\psi_1 = 1 - \frac{0.65}{1 + n^3}$ At corners, $s = 0$
7 	$M = \frac{h^4}{15 \sqrt{3}} E_s \theta$ $= \frac{b^4}{46.188} E_s \theta$ $M^* = 0.0222 \frac{E_s \theta A^4}{J}$	In the middle of the side: $s(\max.) = \frac{h}{2} E_s \theta = \frac{b}{2.309} E_s \theta$ At corners, $s = 0$
8 For any compact section without re-entrant-angles	Approximately $M^* = K \frac{E_s \theta A^4}{J}$	$s = \frac{M \vartheta}{J}$ where ϑ is the distance from the axis of twist to the fiber. At corners and sharp edges, $s = 0$.

¹ Die Lehre der Drehungsfestigkeit von Dipl.-Ing. Constantin Weber, Forschungsarbeiten auf den gebiete Ingenieurwesens, 1921.

* See Ref. 1, p. 177.

E_s = modulus of elasticity in shear.

θ = angle of twist per unit length, radians.

M = torsional moment, in.-lb.

s = shear stress, lb. per square inch.

J = polar moment of inertia.

A = area of cross section, sq. in.

9:8. Torsional Rigidity of a Shell-type Monoplane Wing.—In the designing of cantilever monoplane wings to preclude torsional wing flutter, as has been demonstrated experimentally, torsional rigidity is an important factor. The torsional rigidity of a wing is also important with respect to the maintenance of a constant relative angle of attack throughout the span of the wing; we must also know its magnitude in order to compute the torsional period of the wing.

In general, the contribution of the spars, in a shell type of wing, to the torsional rigidity is of secondary importance; hence we omit their effects from our calculations. The most uncertain quantities in the calculations are the modulus of elasticity in shear of the stressed-cover material and the degree of buckling in the cover. However, a few experiments on wings of the type under discussion should afford a basis for determining coefficients that will account for discrepancies between theory and practice.

9:9. Angle of Twist of a Shell Wing.—We assume that the entire rigidity in torsion of the shell wing is due to the shell and that the bending stresses are negligible.

In the development of the formula for the angle of twist in terms of the applied torque and the physical characteristics of the material, we resort to the method of energy. With reference to Fig. 9:4, the applied torque varies along the semi-span L of the wing and is thus a function of x . The total torque at x is M , and

$$M = \int_x^L q \, dx \quad (9:20)$$

The integral can be readily evaluated by approximate methods. We shall represent the angle of twist at x by θ . θ is thus a function of x . Now the external energy *per unit length* expended in the twisting of the wing is $\frac{q}{2} \theta$, and the energy expended per length dx is

$$du = \frac{q}{2} \theta \, dx \quad (9:20a)$$

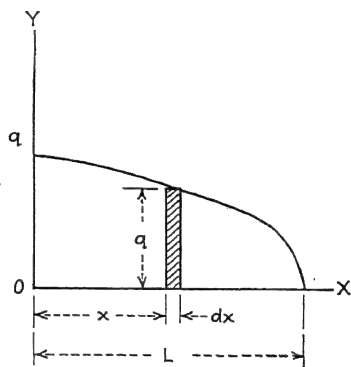


FIG. 9:4.—Integration of torsion curve.

from which the total energy expended from x to the end of the wing is

$$u = \int_x^L \frac{q}{2} \theta \, dx \quad (9:20b)$$

If M is a concentrated torque applied at the end of the wing and θ_0 is the angle of twist at the end in radians, the total expended energy in the twisting of the wing is

$$u = \frac{M}{2} \theta_0 \quad (9:20c)$$

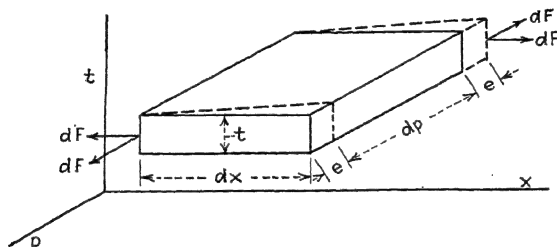


FIG. 9:5.—Shear in elementary surface area of wing'skin.

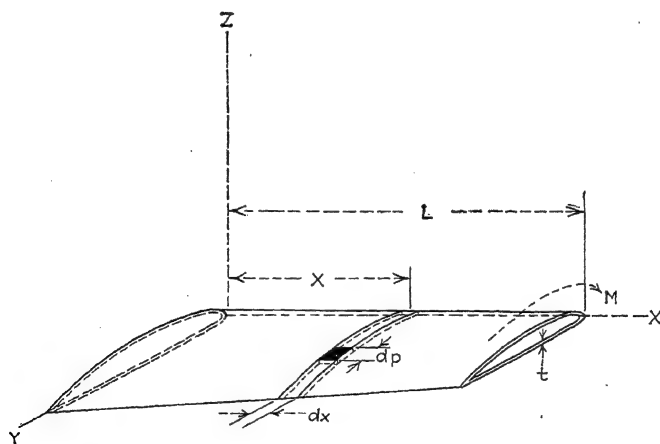


FIG. 9:6.—Elements of a shell wing.

9:10. Elastic Potential Energy.—We shall now set up an equation of the potential energy stored in the shell of the wing in the twisted position; this we shall equate to equation (9:20b) and solve for θ .

In Fig. 9:5 is sketched a differential block taken from the shell of the wing as shown in Fig. 9:6. To this block, a shear force dF

is applied. The magnitude of dF is stated thus:

$$dF = st(dp) \quad (9:21)$$

where s = unit shear stress.

t = thickness of the shell.

$t(dp)$ = area on which dF acts.

The energy stored in the differential block because of the motion of dF through a distance e is

$$d(du) = \frac{dF}{2} e \quad (9:22)$$

We note that the shear modulus of elasticity E_s is expressed by

$$\tau = \frac{s}{(e/dx)} = s \frac{dx}{e} \quad (9:23)$$

from which

$$e = \frac{s \, dx}{E_s} \quad (9:24)$$

Substituting (9:24) and (9:21) in (9:22), we obtain

$$d(du) = \frac{s^2 t (dx)}{2} \quad (9:25)$$

from which

$$u = \int_x^L \int_0^c \frac{s^2 t}{2E_s} dx \, dp \quad (9:26)$$

where the limit c is the periphery of the wing section at x . The thickness t and the shear stress s may be a function of both x and s . Equating (9:26) and (9:20b), we obtain

$$= \frac{1}{2E_s} \int_x^L \int_0^c s^2 t \, dx \, dp \quad (9:27)$$

From equation (9:10), we have

$$\frac{M}{2A} \quad (9:28)$$

where A is the area enclosed by the shell at section x . Substituting (9:28) in (9:27), we obtain

$$(9:29)$$

Substituting the value of M from equation (9:20) in equation (9:29), we obtain

$$\int_x^L q\theta \, dx = \frac{1}{4E_s} \int_x^L \left(\int_x^L \frac{q \, dx}{A^2 t} \right)^2 dx \, dp \quad (9:30)$$

9:11. Approximate Solution of the Energy Equations.—Equation (9:30) appears to be formidable, but an approximate solution can be readily obtained. If we take ΔL for L and make x zero, we can assume the variables to be constant for this delta-length and equal to the average value. We can also assume that t is constant around the periphery of the wing, since this will undoubtedly be the case in the practical type of construction. Equation (9:30) thus becomes

$$q \, \Delta\theta \int_0^{\Delta L} dx = \int_0^{\Delta L} \int_0^c dx \, dp \quad (9:31)$$

Integrating, we obtain

$$q(\Delta\theta)(\Delta L) = \frac{q^2(\Delta L)^2(\Delta L)c}{4A^2tE_s} \quad (9:32)$$

from which

$$= \frac{q(\Delta L)(\Delta L)c}{A^2tE_s} \quad (9:33)$$

The application of equation (9:33) is as follows: Suppose, for instance, the semi-span of a cantilever stressed-skin tapered wing is 20 ft. We shall take ΔL as 1 ft. (12 in.) and compute $\Delta\theta$ for each increment. The total angle of twist at the tip is

$$\Delta\theta_0 = \Delta\theta_1 + \Delta\theta_2 + \Delta\theta_3 + \cdots + \Delta\theta_{20} \quad (9:34)$$

The quantities for the determination of $\Delta\theta_1$ will be computed from a section of the wing 6 in. from the tip, for $\Delta\theta_2$ from a section 18 in. from the tip, etc.; for $\Delta\theta_{20}$, they will be computed from a section 6 in. from the root section. Note that $Q_1 = q_1 \Delta L$, $Q_2 = Q_1 + q_2 \Delta L$, etc.

9:12. Torsion in Box Beams of Rectangular Cross Sections.—In the case of a box beam of rectangular cross section with sides of thickness t_1 and height b and top and bottom of thickness t_2 and

width d , equation (9:30) may be written,

$$\int_x^L q \theta \, dx = \frac{1}{4E_s} \int_x^L \left[2 \int_0^b + 2 \int_0^d \left(\frac{\int_0^L q \, d}{A^2 t_2} \right) \cdot dp \, dx \right] \quad (9:35)$$

From equation (9:35) we determine an equation corresponding to equation (9:33) as follows:

$$\left[\sum_x^L (\Delta L) d \right]$$

For the torsion angle produced at the end of a uniform beam by a torque M applied at the end of the beam, we write M for $\sum_x^L q \, \Delta L$ and L for ΔL in equation (9:36). Thus,

$$MLb + MLd = \frac{M}{2A^2 E_s} \left(\frac{b}{t_1} + \frac{d}{t_2} \right) \quad (9:37)$$

We note that $A = bd$.

An equation similar to (9:37) and derived from (9:33) is

$$\theta = \frac{Mc}{J} L \quad (9:38)$$

9:13. Angle of Twist of a Round Tube.—The calculation of the torsion angle of a round tube is a special case of the above process. We note that for a round tube,

$$\theta = \frac{M}{J} L \quad (9:39)$$

Let us see if equation (9:39) is a special case of equation (9:38) and thus check our theory for a round tube.

$$\frac{\pi r_1^4}{2} = \frac{\pi}{2} \quad (9:40)$$

where r_1 and r_2 are the inner and outer radii, respectively. Expanding equation (9:40),

$$J = \frac{\pi}{2} (r_2^4 - r_1^4) \quad (9:41)$$

Now $\frac{\pi}{2} (r_2^2 + r_1^2)$ is the average enclosed area A is the average radius r , and $r_2 - r_1$ is the thickness t . Thus

$$J = \quad (9:42)$$

and

$$\tau = \frac{M}{2A E_s r t} \quad 2\pi r M \cdot L = M c \cdot L \quad (9:43)$$

which checks equation (9:38).

9:14. Torsion of Multiconnected Thin-walled Cylinders.—Prof. F. M. Baron (Ref. 6) has proposed the following method of *successive approximations* for solving this problem. In Fig. 9:7 is shown a monocoque wing section composed of three parallel tubes A, B, and C. The section is subjected to a torsional couple M . We are to find the

shear stresses in the thin walls in terms of the physical characteristics of the material and the structure and of the torque M .

We note [equation (9:10)] that

$$M = 2stA, \quad st = \frac{M}{2A} \quad (9:44)$$

where M = torsional couple, lb.-in.

A = circumscribed area, sq. in.

s = shear stress, lb. per square inch.

t = inches thickness of the wall.

Note that st is constant.

9:15. Angle of Twist.—We note also [equation (9:29)] that

$$\frac{1}{2} \int_x^L \theta \, dx = \frac{1}{s} \int_x^L \tau \, dx$$

where θ = angle of twist, radians.

E_s = shear modulus.

q = torque per unit length.

The remaining symbols are the same as in equation (9:44). If we assume θ , x , and M constant and note that

$$\int_x^L q \, dx = M \quad (9:46)$$

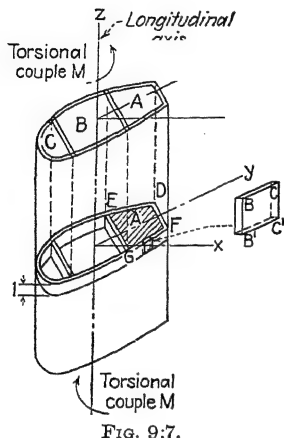


FIG. 9:7.

we have

$$\frac{1}{2} \quad (9:47)$$

or

Note that c is the circumference and dp is an infinitesimal length on the periphery.

Substituting the value of M from equation (9:44), in equation (9:48), taking ΔL as a unit of length along the z -axis, and noting that st is constant (Art. 9:3),

$$\int_0^c s (dp) = 2E_s \theta A \quad (9:49)$$

If we let $F = st$, a constant (see Art. 9:3), we have

$$\int_0^c \frac{F}{t} dp = 2E_s \theta A \quad (9:50)$$

9:16. Assumptions of the Method.—The following assumptions are made (see Fig. 9:7):

1. The wing section is straight, of constant cross section, and of homogeneous, elastic, isotropic material. (NOTE: If the wing is tapered, the method may be applied with fair accuracy to successive lengths of ΔL .)
2. All the elements of cross section rotate through the same angle. The angle is proportional to the longitudinal coordinate of the cross section and the constant θ measuring the angle of twist per unit of length.
3. The displacement of any element of any cross section in the direction of the longitudinal axis is a function of the transverse coordinates only.
4. The structure is hollow with walls so thin in proportion to the important transverse dimension that the shearing stresses may be assumed uniformly distributed across the thicknesses of the walls.

9:17. Basic Theory of the Method of Successive Approximations.—In Fig. 9:7, consider a horizontal slice through the wing as shown. Let the height of the slice be one unit, this unit being assumed small. Let the total force F be transferred across the thickness t of the wall at section B . The unit shear s at section B is the force F divided by the thickness t . The equilibrium conditions of the element $BB'CC'$ requires a total force F to be transferred across the thickness of the wall at section C .

Then at any junction of the walls, the condition of static equilibrium requires that the quantity of force F "flowing" into a junction must equal the quantity of force F "flowing" away from the junction.

Continuity of the deformations along a closed path such as $GEDF$ requires that the algebraic sum along the closed path of the relative displacements in the direction of the longitudinal axis must be zero. This requirement plus assumptions 1, 2, and 3 lead to equation (9:50) as previously noted. Writing equation (9:50) for $GEDF$ of Fig. 9:7, we have

$$\int_F^G \frac{F}{t} dp + \int_G^E \frac{F}{t} dp + \int_E^D \frac{F}{t} dp + \int_D^F \frac{F}{t} dp = 0$$

Since each integral is a length of the periphery of A_c , we may write equation (9:51),

$$\frac{Fc}{t} = 2E_s \theta A_c \quad (9:52)$$

where c is a portion of the periphery, such as F to G or G to E .

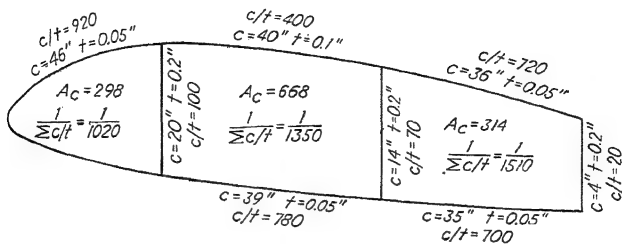
If we can distribute the stress so as to satisfy equation (9:52), we have the stress problem solved. This is done as follows:

9:18. Detailed Procedure and Example.—The method of analysis (see Ref. 6) is a method of successive approximations. The solution to the problem is guessed at and approximately corrected. The revised answer is treated as a new guess and successively corrected until a reasonable degree of precision is obtained. The convergence is reasonably rapid, and the method is useful. With some experience and judicious guessing, the convergence may be speeded up.

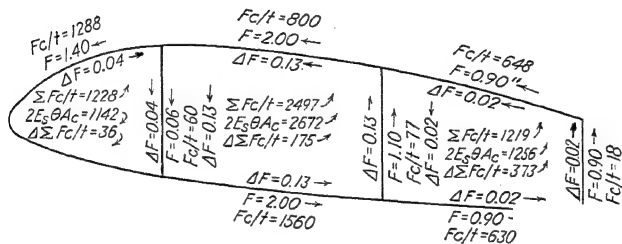
The method of analysis proposed always satisfies the condition of statics and successively corrects the errors in continuity of deformation until the condition of continuity is also satisfied. Other orders of procedure have been tried by Baron (see Ref. 6), but the foregoing is recommended for its simplicity.

The order of computations made in the method of successive approximations is as follows (see Fig. 9:8):

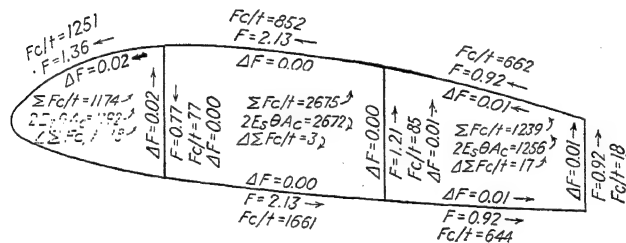
1. Assume a distribution of forces F along the walls satisfying the condition of statics.
2. Compute the following:
 - a. The area A_c within each elementary closed circuit.



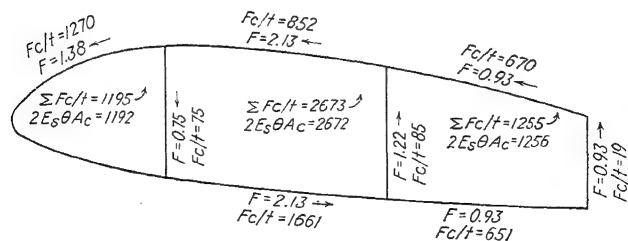
(a) - Dimensions



(b) - First approximation



(c) - Second approximation



(d) - Third approximation

FIG. 9:8.—Computations for successive approximations.

b. The quantity length c /thickness t for each wall.

c. The quantity $\frac{1}{\sum c}$ for each elementary closed circuit.

3. Compute the algebraic sum $\sum F \frac{c}{t}$ for each closed circuit, with due attention to the circulation right or left of the forces in the circuit.

4. Choose a constant $2E_s\theta$ for the section making the product of $2E_s\theta$ and the area A_c within each elementary closed circuit approximately equal to the quantity $\sum F \frac{c}{t}$ of the circuit.

5. For each closed circuit, compute the correction $\Delta \sum F \frac{c}{t}$ needed to make the resultant quantity $\sum F \frac{c}{t}$ equal to $2E_s\theta A_c$.

6. For each wall of each closed circuit, compute the corrections $\Delta \sum F \frac{c}{t}$ by the corresponding factors $\frac{1}{\sum \frac{c}{t}}$ of the circuits. Write the result ΔF by the wall, with the attention to the circulation of the correcting forces.

7. Compute the revised forces.

8. Treat the revised forces as new guesses and repeat steps 3, 5, 6, and 7 to any desired precision.

9:19. Arrangement of Computations.—The arrangements of computations suggested for the procedures outlined are illustrated in Fig. 9:8. Along each wall, write the quantity c/t , the assumed force F with its direction, and the value Fc/t with its direction. Write the quantity $\sum c/t$ inside each elementary closed circuit and the quantities $\frac{c/t}{\sum c/t}$ of each wall along the wall and inside the circuit considered. Write in each elementary circuit the value of the area A_c , the value $\sum Fc/t$ with its circulation right or left, and the selected value of $2E_s\theta A_c$. Put a curved arrow pointing to the smaller of the last two values. The arrow will show the circulation of the first correction $\Delta \sum Fc/t$. The difference between the values of $\sum Fc/t$ and $2E_s\theta A_c$ is the magnitude of the first correction $\Delta \sum Fc/t$. For the procedure of successive corrections, with due attention to the circulation of the corrections, write in columns perpendicular to each wall and inside each circuit the products of the corrections $\Delta \sum Fc/t$ and the factor $\frac{c/t}{\sum c/t}$ of the wall.

9:20. Angle of Twist.—After F is found by the method of successive approximations, the angle of twist per unit length may

be found from equation (9:50).

Angle of twist per unit length and the integral will apply to any of the tubes *A*, *B*, or *C* (Fig. 9:7). For tube *A* and a length *L*, letting subscript 1 refer to side *GE*, 2 to *ED*, 3 to *DF*, and 4 to *FG*, we have

$$\left(\frac{F_1}{t_1} c_1 + \frac{F_2}{t_2} c_2 + \frac{F_3}{t_3} c_3 + \frac{F_4}{t_4} c_4 \right) \quad (9:54)$$

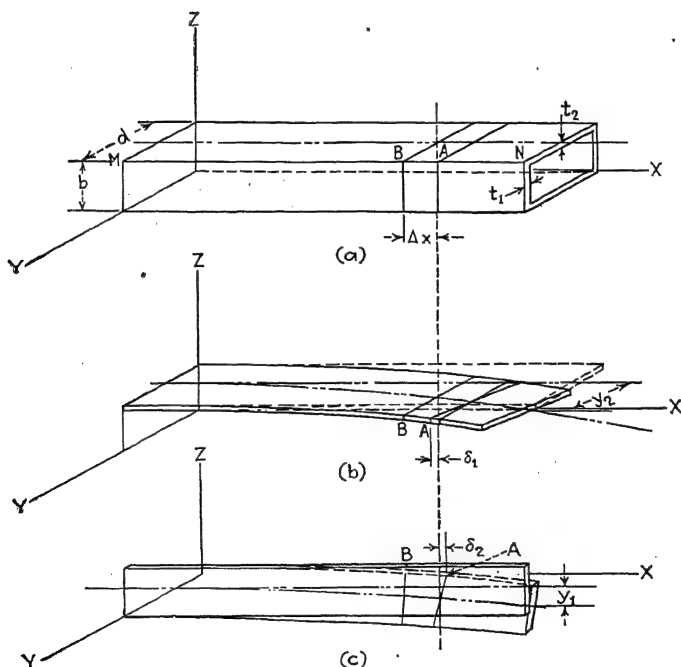


FIG. 9:9.—Bending in sides of box beam.

9:21. Torsion in a Box-wing Beam.—A stressed-skin wing usually has for its supporting member a box beam. This box is usually the central section of the wing with the leading and trailing edges of the wing removable. An approximation of such a wing is shown in Fig. 14:1*a*. When a wing of this construction is twisted by a torsional couple through an angle, the couple is

resisted by a shearing force as calculated from equation (9:10) and by the bending forces induced in the four sides by the deflections y_1 and y_2 . Figure 9:9 shows the resulting interaction between the narrow and broad sides of the beam caused by this bending action in torsion. In *a* consider a Δx length BA . In *b*, with the broad side unrestrained by the action of the narrow side, the Δx length is compressed a distance δ_1 by the bending action. In *c*, with the narrow side unrestrained by the broad side, the Δx length is extended a distance δ_2 by the bending action. This implies that the point *A*, considered as a part of the broad side, has moved to the left a distance of δ_1 and, considered as a part of the narrow side, has moved to the right a distance δ_2 . In the first case a compressive stress in the fiber results, and in the second case a tensile stress results. It is apparent, therefore, that in the box beam *a* the shear restraint at the edge, preventing the point *A* from moving freely to the left or right, tends to neutralize the tensile and compressive deformation and hence to neutralize the tensile and compressive bending stresses.

As a simple example of such neutralization of tensile and compressive stresses, consider the torsion of a square box beam $b = d$ with $t_1 = t_2$. From the symmetry of the structure it is obvious that the point *A* will move neither to the left nor to the right; hence no tensile or compressive stress is developed at that point. This condition results, according to the theoretical analysis (see Chap. XIV), when $t_1b = t_2d$.

When t_1b is greater than t_2d , the point *A* moves to the right, and hence a tensile stress is developed.

In stressed-skin wings, t_2d (of the top and bottom flanges) is greater than t_1b (of the webs); therefore a twist of the wing decreases the bending stresses in the webs (considered as spars).

In general, it appears that in stressed-skin wings the torsion in the wing does not increase the bending stresses (of tension and compression).

The shears induced by torsion and bending, however, are added to obtain the design shear.

References

1. PRESCOTT, JOHN: "Applied Elasticity," Longmans, Green and Company, New York, 1924.
2. TIMOSHENKO, S.: "Theory of Elasticity," McGraw-Hill Book Company, Inc., New York, 1934.

3. YOUNGER, J. E., and B. M. WOODS: "Dynamics of Airplane Structures," John Wiley & Sons, Inc., New York, 1931.
4. YOUNGER, J. E.: Miscellaneous Collected Airplane Design Data, Formulas, and Methods, *Air Corps Information Circ.*, 644, 1930.
5. TRAYER, G. W., and H. W. MARCH: The Torsion of Members Having Sections Common in Aircraft Construction, *N.A.C.A. Tech. Rept.* 334, 1929.
6. BARON, F. M.: Torsion in Multiconnected Thin-walled Cylinders, paper presented at National Meeting of the American Society of Mechanical Engineers (A.S.M.E.), 1941 (to be published in 1942 in *Jour. Applied Mechanics*).

CHAPTER X

ELEMENTARY PRINCIPLES OF DESIGN OF SHEET-METAL CONSTRUCTION

10:1. Fundamental Concepts.—The study of thin sheet-metal structures is a study of the strength of tubes with thin walls, in tension, compression, shear, and bending. We note that the strength of a tube in *compression* (as a column) and in *bending* is proportional to the moment of inertia of the cross-sectional area about a transverse neutral axis. The strength in torsion is proportional to the polar moment of inertia of the cross-sectional area about the longitudinal axis. Both these moments of inertia, for the same weight per unit length of tube, are increased by increasing the diameter D for constant cross-sectional area. For example, with reference to Figs. 10:1*a* and 10:1*b*, make $r_1 = 2r_0$; then t is obtained for the constant area A from the equation

$$A = 2\pi r_0 t_0 = 2\pi r_1 t_1 \quad (10:1)$$

Thus

$$\frac{r_0 t_0}{2r_0} = \frac{t_0}{2}$$

Since

$$J_0 = 2\pi r_0^3 t_0 \quad \text{and} \quad J_1 = 2\pi r_1^3 t_1 \quad (10:2)$$

then

Thus the moment of inertia is increased four times.

10:2. Types of Thin Sheet-metal Structures.—If the tube of Fig. 10:1 be increased to such size and made such shape that the resulting shell is an airplane fuselage or an airplane wing, the structure is referred to as a *monocoque*, *stressed-skin*, or *shell* type of construction. However, strictly as defined, no such airplane structure has ever existed. Since the thin sheets of such large size would be quite unstable, it is necessary that supporting structures be added in the form of bulkheads or diaphragms and

compression ribs or stringers (see Fig. 10:2). This type of structure is called *semi-monocoque* or *semi-stressed skin*.

The application of the principles of thin sheet-metal design to the construction of beams and struts of corrugated strips of stainless steel is generally referred to as *corrugated-strip-steel construction* (see Fig. 10:3). The same principle, of course, is also applicable to duralumin and other metals.

10:3. Compressive Strength of Thin Curved Sheets.—If a thin-walled tube is subjected to an axial load, it may fail in one or both of two ways: (1) by buckling as a column; (2) by local buckling or wrinkling of the thin walls. An example of wrinkling is shown in Fig. 10:4.

If we assume that the fiber stress which will cause wrinkling is a function of the modulus of elasticity E , the radius of curvature R , and the thickness t , we write¹

$$f = f(E, R, t) \quad (10:3)$$

Applying the principle of dimensions, we write

$$f = KE^a R^b t^c \quad (10:4)$$

The absolute dimensions of these quantities are as follows: of f , a force per unit area, M/T^2L ; of E , a force per unit area, M/T^2L ; of R , a length L ; and of t , a length L . We therefore write equation (10:4) as

$$= KE^a R^b t^c = \frac{M}{T^2L} = \frac{M^a}{T^{2a}L^a} L^b L^c \quad (10:5)$$

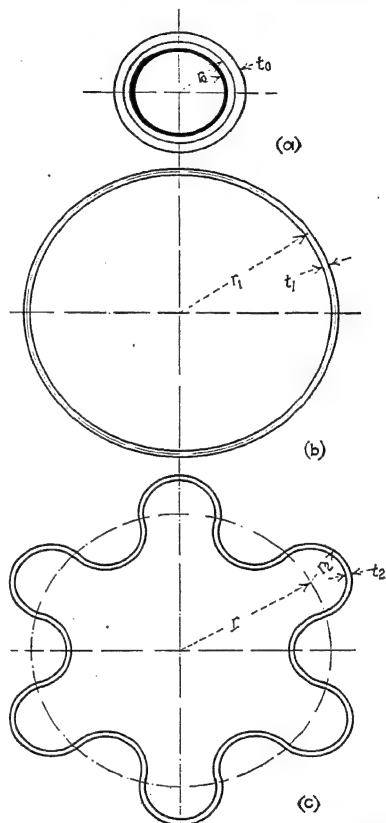


FIG. 10:1.—Tubes of equal cross-sectional area as structural members.

¹ For an elementary treatment of the method of dimensions (dimensional analysis), see J. E. Younger, "Mechanics for Engineering Students," Chaps. 44-47, International Textbook Company, Scranton, Pa.

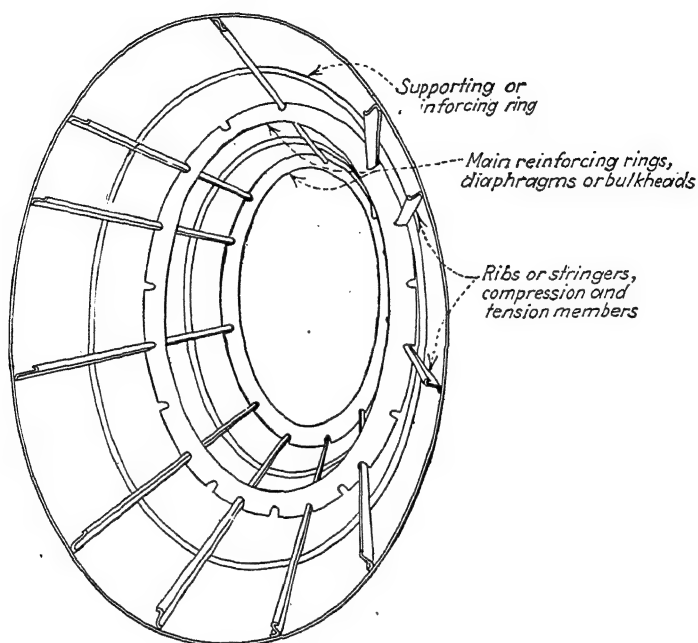


FIG. 10:2.—Semi-monocoque fuselage.

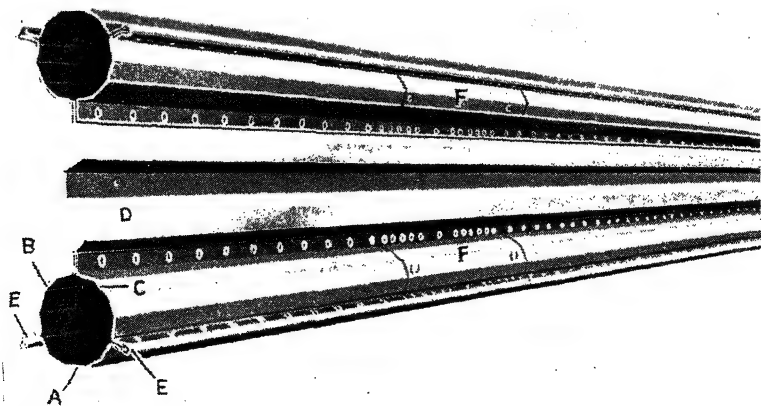


FIG. 10:3.—Showing a type of single-web spar, developed and extensively used by Armstrong Whitworth Aircraft, Ltd.

Equating exponents, we have for M ,

$$1 = a, \quad a = 1$$

for T ,

$$-2 = -2a, \quad a = 1$$

and, for L ,

$$-1 = -a + b + c$$

or

$$b + c = 0, \quad b = -c$$

Thus, equation (10:4) may be written

$$(10:6)$$

Experimental data and a mathematical analysis of the problem show that c is approximately 1. When f/E is plotted as a function of R/t for available experimental data, K is found to vary, in the same laboratory, 100 per cent or more for the same value of R/t . This is due to the difficulty of obtaining ideal test conditions. It is reasonable to suppose, therefore, that worse variations will occur in practical structures. What appears to be a conservative design value is $K = 0.12$. $K = 0.24$ represents about the average data. We write as our preliminary design formula for axial compression

$$f = 0.12E \frac{c}{\bar{\rho}} \quad (10:7)$$

10:4. Equal Strength in Buckling and Wrinkling.—If we consider a Euler strut of thin walls, we have

$$\frac{P}{A} = c\pi^2 E \quad (10:8)$$

where L = length of the strut.

ρ = radius of gyration.

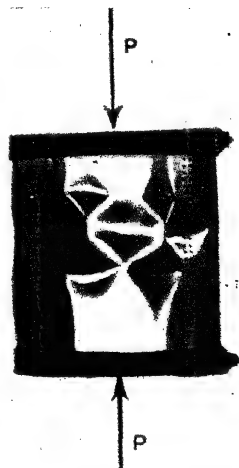


FIG. 10:4.—Wrinkling of thin curved sheets.

a pin-ended strut, $c = 1$. Solving for L/ρ in terms of t/R , we have, approximately,

$$\frac{L}{\rho} = 9 \sqrt{\frac{R}{t}} \quad (10:9)$$

For example, if a tube of 4 in. diameter has a wall thickness of 0.020 in., L/ρ at which wrinkling occurs is 90. For lengths of tube less than this, failure will be by wrinkling, and, for lengths greater, by buckling.

Equation (10:9) is confirmed by the chart for *buckling* and *wrinkling* strength of corrugated sheets (Fig. 10:8). For the curve $c = 1$, wrinkling occurs at $L/\rho = 90+$ for a value of $R/t = 100$ and at $L/\rho = 45-$ for a value of $R/t = 25$.

For $c = 2$,

$$\frac{L}{\rho} = 9 \sqrt{2 \frac{R}{t}} \quad (10:10)$$

For $c = 3$,

$$\frac{L}{\rho} = 9 \sqrt{\frac{R}{t}} \quad (10:11)$$

10:5. Use of Corrugations.—Equation (10:7) tells us that, for a constant thickness t , f is increased by decreasing R . We may

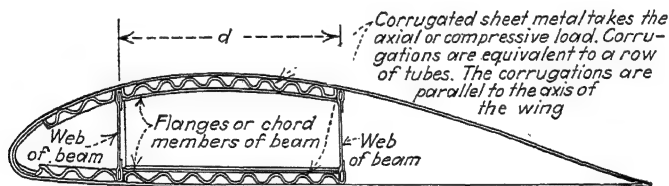


FIG. 10:5.—Modern stressed-skin wing.

therefore, with reference to Fig. 10:1c, improve the strength-to-weight ratio of a tube by longitudinal corrugations. The design of the box beam shown in Fig. 10:5 is based on this principle.

10:6. Strength of Corrugations.—The classical report of C. G. Brown (Ref. 14 to Chap. XIII) is the basis for our present knowledge of the properties of aluminum-alloy corrugated sheet. The report is based on 260 column tests. The following is reproduced from that report:

CORRUGATED ALUMINUM-ALLOY SHEET

1. *Shape.*—The dimensions of standard corrugated aluminum-alloy sheet are shown in Fig. 10:6.

2. *Properties.*—The geometrical properties of the standard corrugations are:

$$\begin{aligned}\rho &= 0.359D \\ W_e &= 1.228W \\ R &= 0.282P\end{aligned}$$

where I = moment of inertia, in.⁴ per inch width.

ρ = radius of gyration.

D = depth of corrugation.

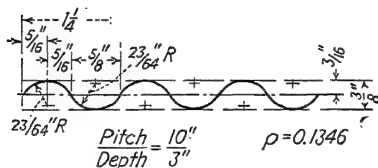
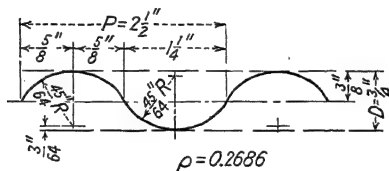
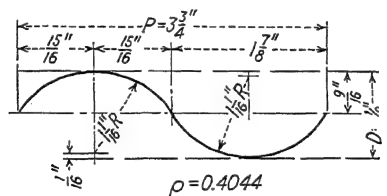
P = pitch of corrugation.

W = width of corrugated sheet.

W_e = width of equivalent flat sheet.

R = radius of curvature of corrugation.

t = thickness of sheet.



$$\text{Radius of gyration} = 0.719 \times \frac{D}{2}$$

$$\text{Curvilinear length of one corrugation} = 1.228 \times \text{pitch}$$

$$\frac{R}{P} = 0.282$$

FIG. 10:6.—Standard corrugations in aluminum-alloy sheet.

The section properties of other corrugations, in terms of their pitch-to-depth ratio, are shown in Fig. 10:7.

3. *Column strength.*—Heat-treated corrugated aluminum-alloy sheet in column action may be designed by the Euler straight-line-column formula for duralumin, provided that the unit stress as determined by the column formula does not exceed the buckling stress for the corrugated sheet.

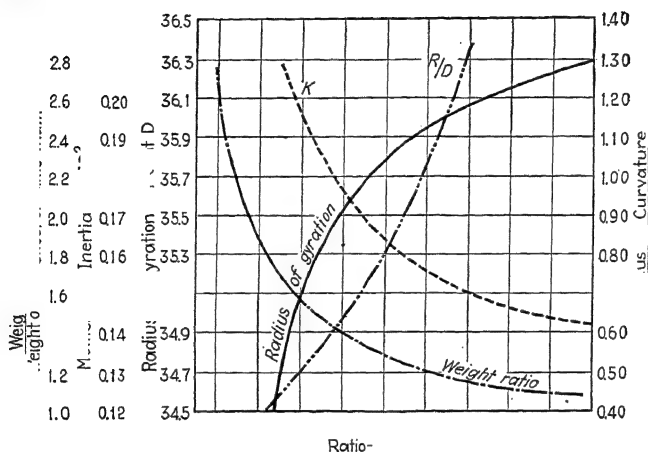


Fig. 10:7.—Section properties of corrugated sheet.

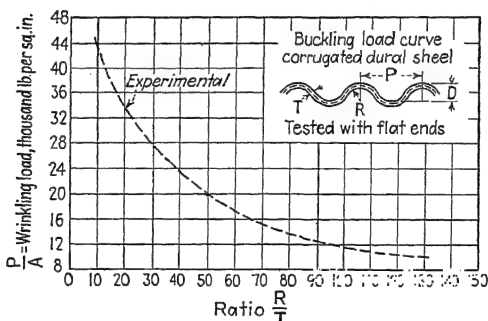


Fig. 10:8.—Buckling stresses in corrugated aluminum-alloy sheet.

Figure 10:8 gives the wrinkling stress as a function of R/t , the ratio of the radius of the curvature of the corrugation to the thickness of the sheet. It should be kept in mind that the wrinkling stress is independent of L/ρ and of the restraint coefficient c .

Figure 10:9 expresses the properties of corrugated aluminum-alloy sheet as a function of both L/ρ and R/t . Its use can best be made clear by an example.

Consider a sheet having an R/t of 50 and $c = 1$.

If L/ρ is 80, the allowable P/A is 15,000 lb. per square inch.

If L/ρ is 40, the allowable P/A is 20,000 lb. per square inch.

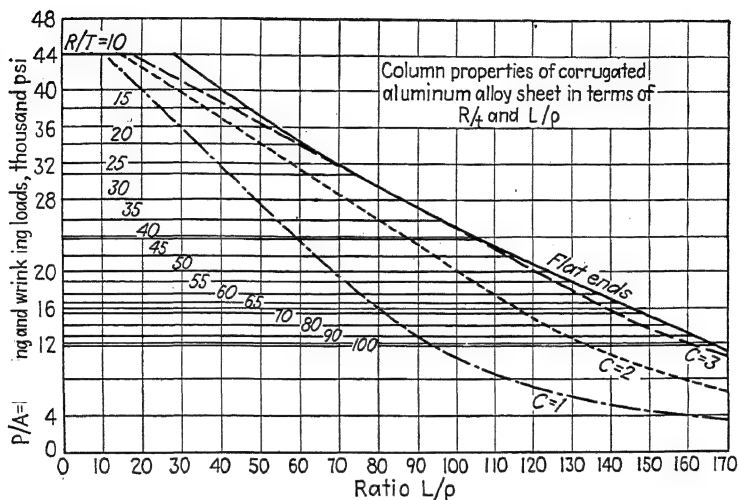


FIG. 10:9.—Column properties of corrugated aluminum-alloy sheet.

10:7. Strength of Thin-walled Tubes in Bending.—Since the stresses in general are below the elastic limit of the material, the bending stress (tension or compression) may be computed by the modulus-of-rupture formula. This stress f , however, must be below the allowable stress f_a . The stress f_a is the critical stress that causes wrinkling. In a manner similar to that of Art. 10:3, it can be shown that

$$(10:12)$$

where $c = 1$.

Failure will occur, of course, in compression.

If we let M_a be the allowable bending moment, then

$$M_a R = K E t^3 \quad (10:13)$$

Since $I = \pi t R^3$, we find that

$$M_a = \quad (10:14)$$

10:8. Longitudinal Shear in Bending.—The maximum longitudinal shear occurs in the plane of the neutral axis (see Fig.

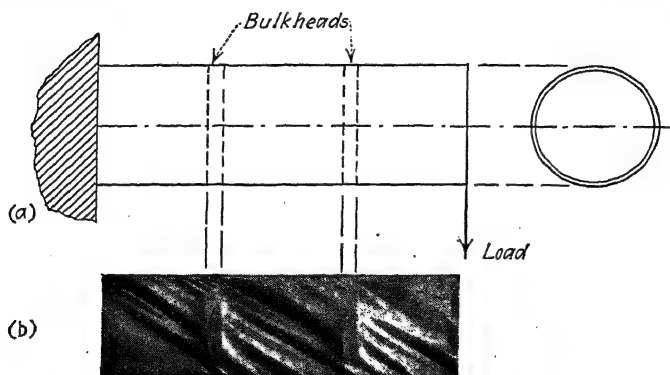


FIG. 10:10.—Shear in bending of thin-walled tube. (a) "Free-body" diagram; (b) wrinkling of sides of tube.

10:10). Its value may be computed, below the elastic limit of the material, by the equation

$$s = \frac{VQ}{Ib} \quad (10:15)$$

Since V is the vertical shear on the beam, b is $2t$, Q is $2R^2t$, and I is πR^3t , we have

$$s = \frac{2VR^2t}{\pi R^3t} = \frac{V}{\pi Rt} \quad (10:16)$$

10:9. Fittings in Monocoque Structures.—The function of a fitting is to transmit stresses from one member of a structure to another member or to other members. The proper design of fittings requires that this transmission of stress be accomplished efficiently. The characteristics of this efficiency we may list as follows:

1. Minimum weight for the accomplishment of the function of the fitting.
2. Transmission of stress without inducing fitting stresses, such as may cause local failures or eccentric loadings.

In the design of a fitting, careful consideration should be given to the following features:

1. Ultimate strength of component parts of the fittings with reference to tension, compression, shear, and elastic stability.

2. Method of attachment to members to develop the design strength of the fitting and members, such as riveting, bolting, and welding.
3. The rigidity of the fitting.

In framed structures, the rigidity of a fitting receives little consideration since, in general, if a fitting has the ultimate

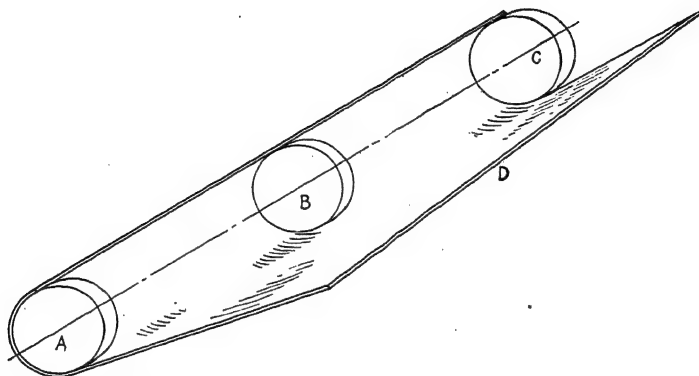


FIG. 10:11.—The fundamental principle of transmission of loads in monocoque structures. The thin sheet *D* is rolled about the bulkheads *A*, *B*, and *C*.

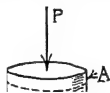


FIG. 10:12.—Transmission of concentrated axial load to distributed load through rigid bulkhead fitting *A*.

strength necessary, it also has the rigidity necessary. In monocoque structures, however, this condition in general does not exist; a fitting that has only the ultimate strength that is necessary would not in general have the rigidity that is necessary. As a matter of fact, the problem of rigidity is of such importance in

fitting design for monocoque structures that it may be said that *rigidity is the criterion of design*.

10.10. Distribution of Stress.—In a framed structure we are concerned solely with the transmission of concentrated loads, while in monocoque structures we have the additional requirement that the fitting must transmit stresses received into the fitting as a concentrated load but discharged as a distributed load. The fitting, in this case, has the double duty of *transmission* and *distribution*. It is this distribution of stress which makes the rigidity requirement necessary.

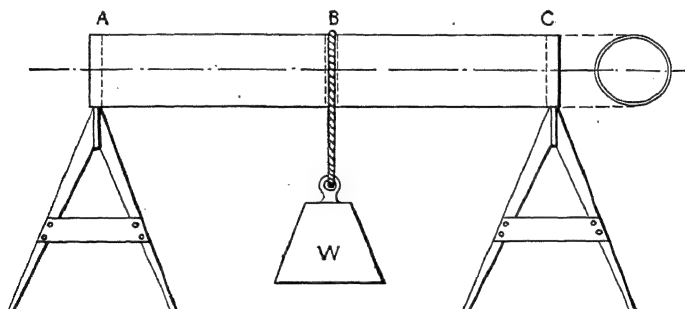


FIG. 10:13.—Concentrated loads applied to fittings or bulkheads A, B, and C, develop full strength of monocoque tube.

Let us now consider a few illustrations of these fundamental requirements in design, beginning with the most elementary cases. We note that monocoque structures are in general tubular in form, as, for example, the monocoque fuselage, the stressed-skin wing, the monocoque engine nacelle, and control torque tubes. It is apparent, therefore, that a study of transmission of stresses as tension, compression, shear, and bending to a thin-walled tube embodies all the elements of monocoque fitting design. Consider, therefore, the thin-walled tube shown in Fig. 10:11.

In this figure we have a tube constructed by rolling a thin sheet of metal around three solid bulkheads of great rigidity A, B, and C. When the tube is completed by riveting or welding the longitudinal seam, concentrated loads may be applied as noted in Figs. 10:12, 10:13, and 10:14.

We have thus provided for compression, tension, bending, torsion, and shear in our fittings A, B, and C. In so far as the

transmission of stress, concentrated to distributed, is concerned, these fittings are perfect, inasmuch as stresses may be developed in the thin metal equal to or greater than the allowable stresses for an infinite length of the tube. In other words, the fittings are perfect in so far as they do not introduce *local stresses*, that is, stresses that cause the thin sheet to fail because of improper distribution of the concentrated load.

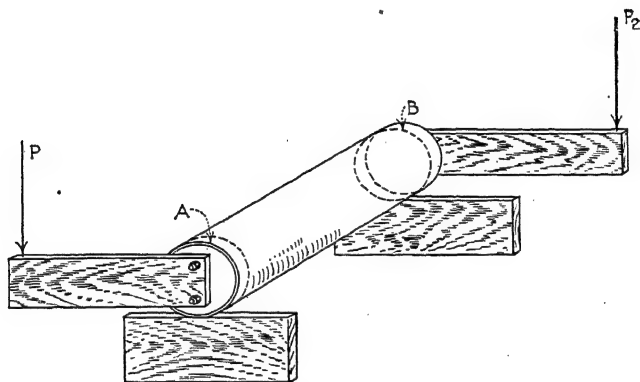


FIG. 10:14.—Torque and concentrated loads, transmitted to monocoque tube through rigid bulkhead fittings, A and B.

We note, however, that, while the fittings transmit stresses perfectly, they are not in general satisfactory because of excessive weight. Our problem now becomes one of reducing the weight without seriously affecting the transmission and distribution qualities of the fittings. The most efficient fitting will represent a compromise of the problem.

10:11. Application in Design.—Before, however, we consider the problem of weight, let us note the application of the bulkhead fitting to airplane structures. *It may be concluded that a rigid bulkhead in a monocoque structure is a perfect fitting for the transmission and distribution of stress.* We accordingly arrive at the following design features in regard to metal monocoque aircraft construction: Wings, tail surfaces, chassis, engine mounts, etc., may be attached to a monocoque fuselage through the medium of rigid bulkheads built into the fuselage for this specific purpose. Likewise, we may attach engine nacelles to stressed-skin wings, engine mounts to monocoque nacelles, etc., through rigid bulkheads.

10:12. Weight Reduction.—We have noted that an efficient fitting represents a compromise between the reduction of weight and the transmission and distribution of stress. Let us now consider the problem of weight reduction, which is the most difficult in design. The question constantly before us is: *How light can we make these bulkheads and yet meet the strength and rigidity requirements?* A mathematical analysis is difficult,

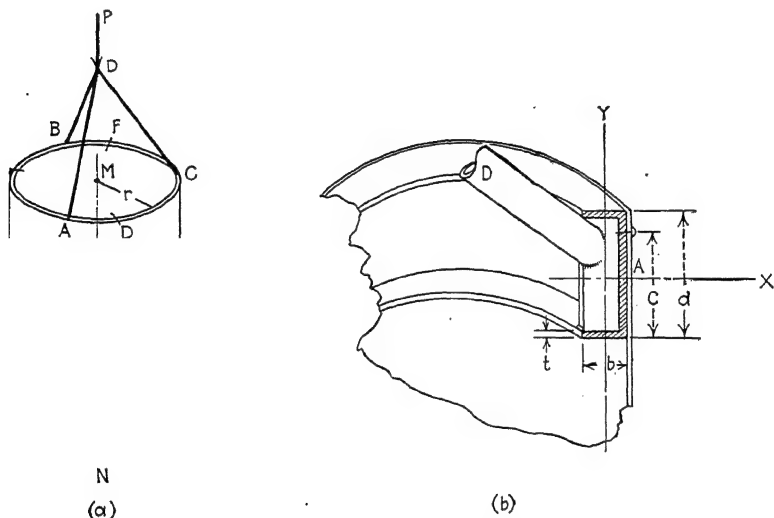


FIG. 10:15.—Transmission and distribution of concentrated load.

inasmuch as the ultimate strength is involved in conjunction with the elasticity of the material.

10:13. Axial Compressive Load.—Let us now, to fix ideas, consider a problem of weight saving in design. Let us assume that we are to design a fitting for a simple axial compressive load (see Fig. 10:15).

The load P is to be transmitted to the tube MN so that the load per unit of circumference is $KP/2\pi r$. Assume that the allowable stress, that is, the crumpling stress in the walls of the tube, is $0.9P/2\pi r$. The uneven distribution of stress will of course be caused by the nonperfect rigidity of the fitting. The maximum stresses in the thin walls of the cylinder will occur at A , B , and C , and the minimum stresses at points D , E , and F , halfway between

the points *A*, *B*, and *C*. A bulkhead in the form of a ring, designed to resist bending about the *x-x* axis, as shown in Fig. 10:15*b*, would be desirable. Bending about the *y-y* axis could be prevented, if necessary, by tie rods *A* to *B*, *B* to *C*, and *C* to *A*. The hoop of Fig. 10:15*b* must be designed so that the deflection of the circular beam at any point is greater than 90 per cent of the deflection of the points of application of the loads at *A*, *B*, and *C*. The problem is within the province of the theory of elas-

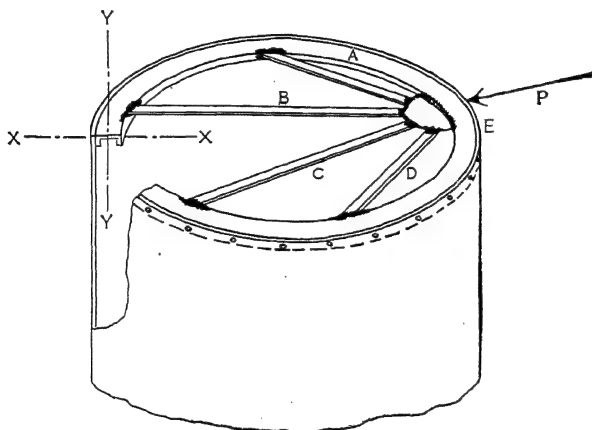


FIG. 10:16.—Possibility in reduction of weight of a fitting to transmit and distribute a concentrated load.

ticity, since the stresses will, in general, be well within the proportional limit, so that Hooke's law applies.

It is rarely, if ever, that this same condition, in its simple form, occurs in aircraft construction. The thin walls of the tube will undoubtedly be braced by vertical and horizontal supports, so complicating the problem that a model test appears to be the only solution.

An application of this fundamental principle occurs in the design of an engine-mount fitting.

We may note in passing that the attachment of thin metal to the bulkhead is a problem of importance. If the riveting process is used, the stress may be more evenly distributed by riveting at the top, as shown in Fig. 10:15*b*, allowing the space designated as *c* as a support for the thin sheet to prevent local wrinkling because of high local rivet stresses.

A concentrated load applied perpendicularly to the axis of the tube, as shown in Fig. 10:16, may be provided for by a fitting of the general type shown in the figure.

In this case, stiffness in bending about the y - y axis is desirable. This stiffness is improved by supports A , B , C , and D , which at the same time provide against local failure in the fitting at E .

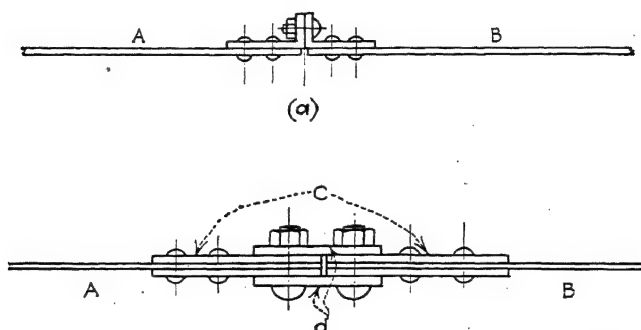


FIG. 10:17.—Fitting for axial connection of two tubes such as stressed-skin wings. Unless the fitting is very rigid, a bending stress is induced in the thin metal.

10:14. Fuselage and Wing Joints.—An interesting and important problem is the design of a fitting to connect two similar tubes, the tube to be subjected to bending. Such a fitting may be the connection between the outer panel and the center section of a stressed-skin cantilever wing or the connection between sections of a monocoque fuselage. It is obviously impossible to acquire a smooth enough fit in the ends of the thin skin to eliminate local failures in compression. Actual contact of the skins, therefore, seems undesirable. Figure 10:17 shows two commonly used joints, (1) a tension joint, and (2) a shear joint. The rivets and bolts should be designed to carry a load greater than the design loads in the thin sheets A and B , since there is considerable uncertainty in the analysis of a fitting. The flanges to be riveted to the thin sheet should be wide enough to afford the proper rigidity to the fitting and to provide ample riveting space. A wide flange would also afford support to the thin sheet against local wrinkling caused by concentrated loads at the rivets.

In the fitting of Fig. 10:17b the thin sheets A and B are reinforced against local wrinkling by heavier sheets C . These reinforcing sheets may be of about 0.064-in. material for 0.30-in. walled tube with a width of about 3 to 6 in.

High-strength steels such as stainless and nickel steels, if properly protected from corrosive action by bitumastic paint, would be advantageous because of their rigidity (high modulus of elasticity). Figure 10:18 shows a stressed-skin wing with a fitting similar to the tension type (see Fig. 10:17a).

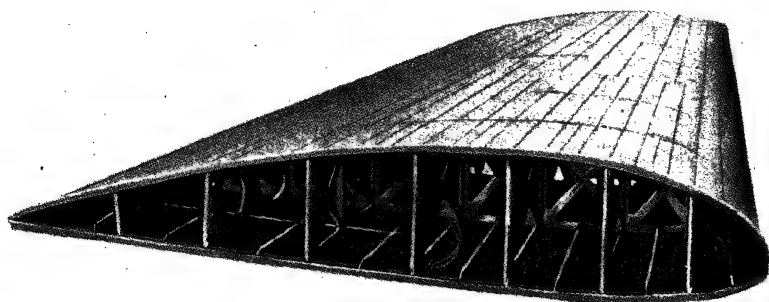


FIG. 10:18.—Joint in stressed-skin wing. (Courtesy of Northrop.)

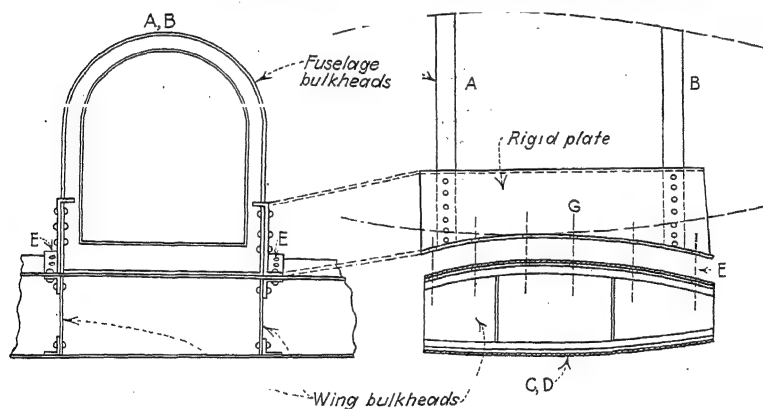


FIG. 10:19.—Fuselage-wing connection in stressed-skin structure.

10:15. Fuselage-wing Connection.—The connection of two tubes set at right angles to each other presents an interesting design problem; this is the problem to be solved in the connection of a monocoque fuselage to a monocoque wing. It is, of course, obvious that the connection may be made through bulkhead rings in the fuselage and bulkheads or heavy ribs in the wing. Figure 10:19 shows the major portion of such a joint. A and B

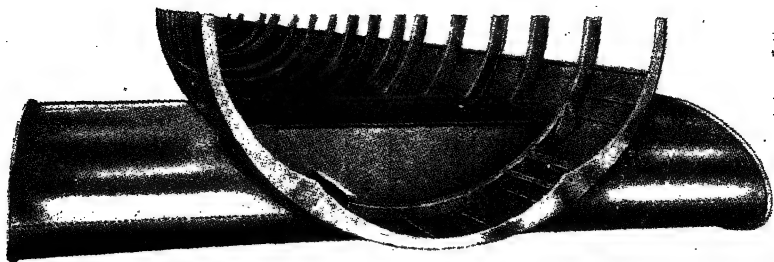


FIG. 10:20.—Principle of fuselage-wing connection in stressed-skin structures.
(Courtesy of Northrop.)

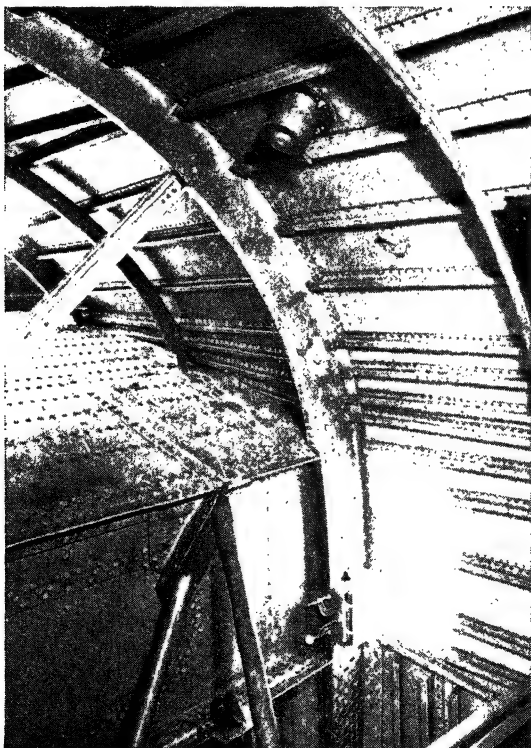


FIG. 10:21.—Wing box beam to fuselage attachment, B-24. (Courtesy of Consolidated Aircraft Corporation.)

are the fuselage bulkhead rings to which is attached a rigid member G .

The member G is formed to fit the contour of the wing and by a row of bolts at E may be made an integral part of a wing bulkhead C or D . The fuselage bulkheads, in this connection, must be designed to withstand the stresses in an unbalanced

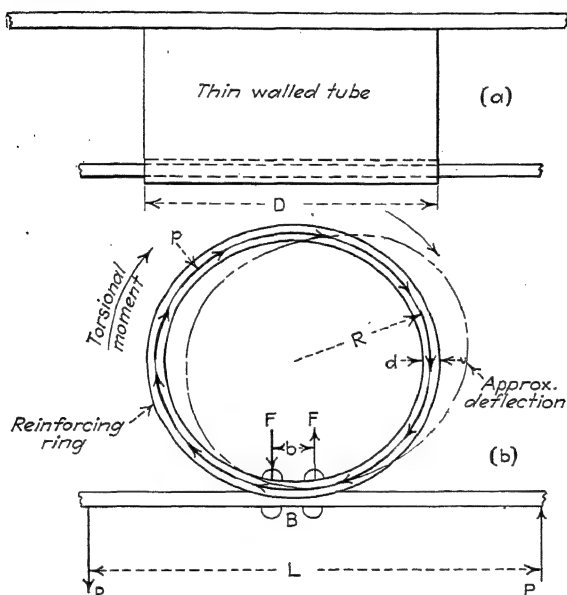


FIG. 10:22.—Resistance of reinforcing ring.

wing-loading condition. Figure 10:20 shows a slightly different application of the same principle.

Figure 10:21 shows this principle applied to a semi-monocoque fuselage for attaching a box-spar wing.

10:16. Strength and Rigidity of a Bulkhead Ring.—Consider first the case of torsion in the fuselage as from an uneven loading on the right and left span of the wing. The ideal case is that shown in Fig. 10:22. The moment PL is calculated from the wing loading. F is therefore determined from

$$Pl = Fb \quad (10:17)$$

from which F , the design loads for the bolts, for this case, may be found. The free-body diagram of the ring is shown in Fig.

10:22*b*, together with the approximate form of the deflection curve. The torsional moment is [see equation (9:10)]

$$2sAt = Fb \quad (10:18)$$

If t , the thickness of the skin, is constant around the ring, the force per unit length is st , which is

$$M \quad (10:19)$$

The maximum bending moment will occur at B , its value being given by equation (10:17). If strength were the only requirement, it would not be difficult to design the beam to carry

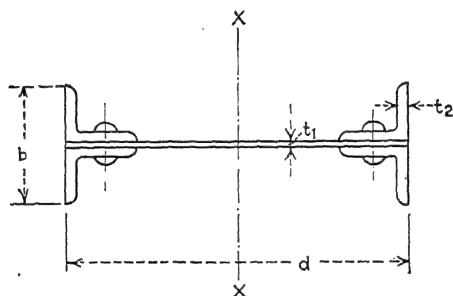


FIG. 10:23.—Cross section of built-up fuselage reinforcing ring.

the moment at this point. Since, however, *rigidity is of primary importance*, the problem is not so simple.

Since the rigidity is proportional to the width d of the ring, it is desirable to make d as great as possible. A large d , however, is not desirable from the standpoint of space in the passenger cabin, so that a compromise must be arrived at. A reasonable value for d would be about 2 to 4 in. for a fuselage of approximately 5 to 7 ft. in diameter.

The material of the ring should be so arranged that the moment of inertia of the cross-sectional area of the ring will be as great as possible. This requirement dictates an I-beam with a thin web as in Fig. 10:23. (The I-beam may not be selected because of other features, such as ease of production, etc.) For $d = 3$ in., the dimensions for duralumin would be approximately:

$$t_1 = 0.040 \text{ to } 0.064 \text{ in.}$$

$$t_2 = \frac{1}{16} \text{ to } \frac{1}{8} \text{ in.}$$

where K is a constant, the value of which is not required in this analysis, and since

$$dF = dp \sin \theta$$

we have

$$dF = Kry \sin^2 \theta d\theta \quad (10:21)$$

Then

$$W = \int dF = Kry \int_0^{2\pi} \sin^2 \theta d\theta \quad (10:22)$$

The loading on the circular ring would be therefore of the form shown in Fig. 10:26, in which dF is given by the equation

$$dF = A \sin^2 \theta d\theta \quad (10:23)$$

Now it would be possible to extend the analysis to the calculation of the numerical value of the load curve in terms of W , assuming ideal conditions, especially no wrinkling, being assumed, and to compute the stresses in the ring as well as the deformation. However, it is doubtful whether this is justifiable in the absence of data on the *required rigidity to preclude wrinkling in the skin*. It is probable that a ring possessing the required rigidity will be many times too strong; hence it appears that for strength calculations conservative approximations of the loading of Fig. 10:26 and of bending conditions in the ring are sufficient to prove ample strength. A ring built up and loaded with the approximate design load would be desirable for rigidity tests.

10:18. Attaching Motor Mounts to Monocoque Structures.—

The principle discussed in Art. 10:13 is applied in the design of an engine-mount fuselage- or engine-mount nacelle fitting. It appears not to be practical to extend a monocoque structure to the mounting ring of the engine, because access to the engine auxiliaries requires many openings through the stressed skin; and *openings in stressed skin destroy its efficient use*. Figure 10:27 shows the bulkheads and bracing framework of a semi-monocoque engine nacelle. The welded-steel tubular engine-mount ring is to be bolted to ring A through vibration-absorption material. Figure 10:28 shows an engine mount attached to a monocoque fuselage using the basic principle of design.

10:19. Design of Empennage Connections.—The principle involved in the design of monocoque fuselage connections for vertical fins and horizontal stabilizers is the same as that involved in the design of a bulkhead for a large thin-walled tube to trans-

mit torsion, bending, and shear to the walls of the tube. Figure 10:29 illustrates the case. In this figure, *B* is a bulkhead of the

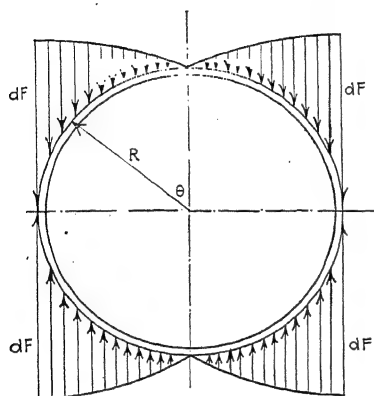


FIG. 10:26.—Distribution of shear load on a reinforcing ring.

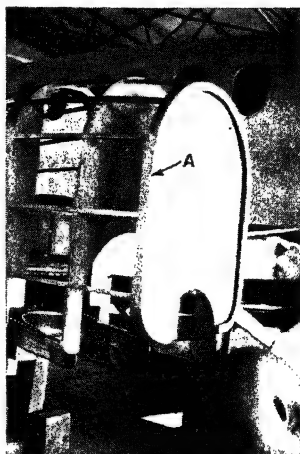


FIG. 10:27.—Combination fire-wall and bulkhead fitting for stressed-skin nacelle. (The skin has not been applied.)

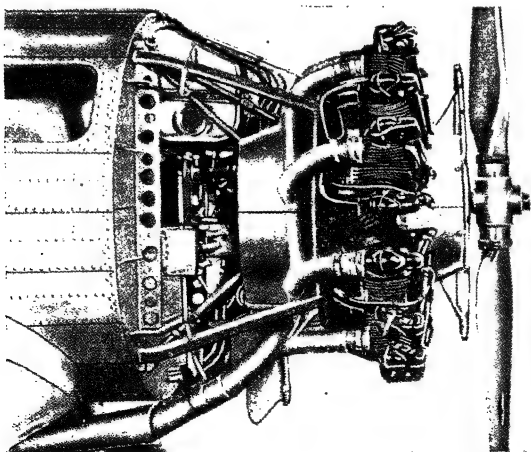


FIG. 10:28.—Attachment of motor mount to monocoque fuselage. (Courtesy of Northrop.)

fuselage. *A* is a fin spar—a built-up *I*-beam or channel section. The web of the spar and the web of the bulkhead are one con-

tinuous sheet of metal. The spar is anchored to the bulkhead ring at *C* and *D* so as to carry the design side load on the beam. In covering this connection with the skin of the fuselage, care must be used that no free edges of the skin remain at *D*, where the spar protrudes from the fuselage. The student must bear in

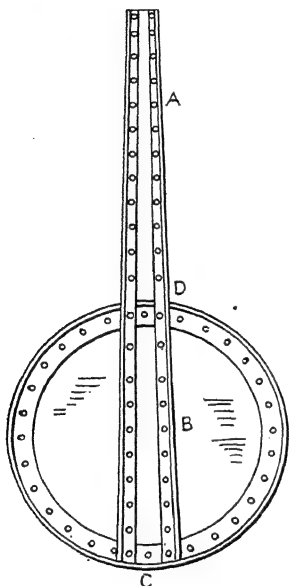


FIG. 10:29.—Principle of connection of fins and stabilizers to stressed-skin fuselage. The bulkhead *B* and the spar *A* are integral.

mind that the *skin must be homogeneous in every respect to develop its strength.*

A variable thickness of skin on the fuselage, as noted from equation (9:10), is another point to be considered. The strength in shear is proportional to the area of the cross section of the fuselage; hence, since the fuselage approaches a small diameter at the empennage end, the skin must be made thicker to provide for the strength and rigidity.

These same principles, of course, are also used in the design of stabilizer connections.

10:20. Design of Chassis-mono-coque-wing Connections.—The principle involved in this design problem is the same as that involved in the design of a fitting to transmit and distribute a concentrated load applied perpendicularly to the axis of the tube. In this case, two wing bulk-

heads will be required to provide for the side-load condition.

10:21. Application of Stringers.—To increase the axial compressive strength of large thin-walled tubes, reinforcing *stringers* parallel to the axis of the tube are used (see Figs. 10:2 and 10:30). In calculating the strength, in compression, of the combination of stringers and tube walls, it should be borne in mind that *a failure of the weaker of the two may cause a premature failure in the stronger.* In general, the combined strength is the product of the unit stress at failure of the weakest element and the area of the total cross section bearing the compressive load. Failure may occur in any one or more of the following ways:

1. Wrinkling of the sheet-metal skin.
2. Buckling of the stringer as a column in the direction of the radius of curvature of the sheet.
3. Buckling of the stringer in the direction perpendicular to the radius of curvature (twisting of the stringer).
4. Local wrinkling of the stringer.

10:22. Types of Stringers.—Let us consider the advantages and disadvantages of the stringers in Fig. 10:30 with reference to the types of failure listed in the last paragraph. The Z-section *c* and the channel section *d*, while they may be attached readily to the skin, have free edges which readily wrinkle, permitting the stringer to fail sideways. The bulb-angle section *e*, while containing no free edges and while quite stiff against buckling normal to the sheet, may buckle in torsion unless well braced. The hat section *a*, while easy to attach and possessing great resistance in buckling in planes both normal and parallel to the plate, contains considerable flat-surface area, which for thin material will wrinkle readily. Section *b* has the same characteristics, but on account of the curvature of the section is resistant to wrinkling. Section *f* is quite generally used for stainless steel, since it is easily fabricated. The *v*-notches in the sides strengthen the flat sides against wrinkling. There are free edges, but these are limited in width. If the skin is thin in comparison with the thickness of the plate of which the stringer is made, the stringer should be made complete by the addition of strip *A* between the stringer and the skin.

Section *g* contains the same amount of material as section *f* but its radius of gyration is greater, the section being thus improved from a strength standpoint. *Section h from a strength-weight-ratio standpoint with respect to wrinkling, buckling, and twisting is the best of the sections.*

10:23. Buckling of Stringers as Columns.—Closed tubes, such as in Fig. 10:30*a*, *b*, *g*, *f*, and *h*, used as columns are subject to calculations by the column formulas of Euler and Johnson. However, sections such as the channel section with free edges will fail because of the instability of the free edges, and hence they are not subject to these calculations. Special curves and methods are required for each such type of section.

When a closed section is used as a stringer, the stringer is restrained from buckling in three directions by the skin—parallel,

each way, to the sheet, and outward from the center of the tube. The stringer however may buckle inward, carrying the skin with it. It is thus apparent that *a small eccentricity in the loading on the stringer to give it a tendency to fail outward is desirable*.

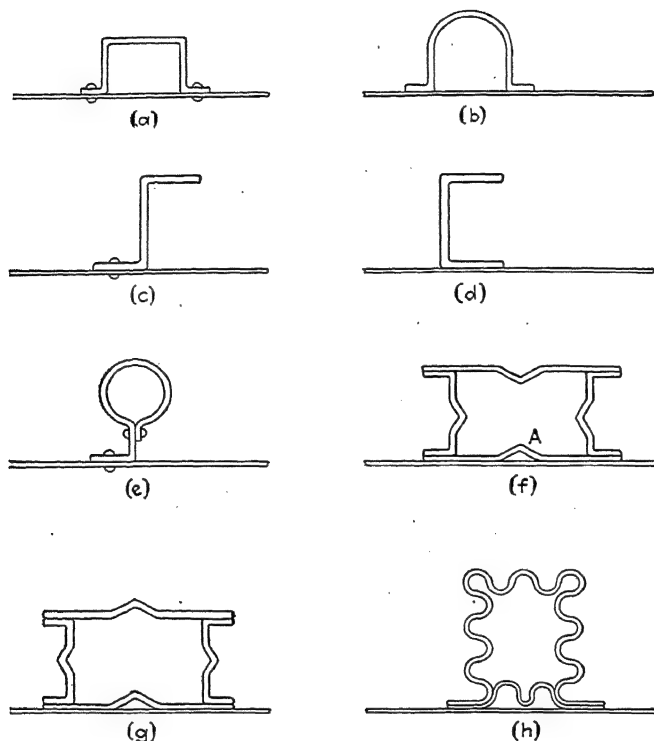


FIG. 10:30.—Longitudinal stiffeners or stringers.

able. This may be done at the bulkhead rings by allowing the ring the right of way next to the skin at the crossing of the stringer and ring and/or supplying gusset plates.

10:24. Mutual Support of Stringers and Sheet.—In a stringer-sheet combination, the stringers support the sheet metal against wrinkling and the sheet metal supports the stringers against buckling. Three methods are obvious in the analysis of the strength of such a combination.

1. Assumption of independent action of stringer and sheet.

2. Assumption that the load carried is the sum of the load carried by the stringer when tested alone plus the load carried by an effective width of the sheet adjacent to the stringer. The stress in the effective width is assumed to be the same as the stress in the stringer.

3. Assumption that a combination of an effective width of sheet and the stringer behaves as a column. The radius of gyration and area of the column are calculated for the combination.

10:25. Stringers for Large Tubes.—As the size of a tube, such as a fuselage or wing section, is increased, the advantages of mono-coque construction seem to decrease. Above this limit a semi-monocoque structure with stringers and bulkhead rings seems to be desirable, with the load being carried in unison by the stringers and skin. However, a further increase in size seems to lessen the advantage of the skin in carrying stress, so that, of necessity, we revert to the frame type of structure with the skin being used to carry tension and shear only (with no compression), to support the stringers, and to cover the frame.

For such large tubes, it seems desirable to use as thin skin as possible for covering and shear and to require the stringers, exclusively, to carry the compressive load. The stringers then may be designed approximately and conservatively (for closed sections) by column formulas.

10:26. Flat Sheet under Edge Compression.—Data are available (see Ref. 8 to Chap. XI) on the compressive strength of flat sheets of stainless iron, duralumin, monel metal, and nickel. The average physical properties of the materials are shown in Table 10:1.

TABLE 10:1.—PHYSICAL PROPERTIES OF MATERIALS
(For Figs. 10:31, 10:32, 10:33, and 10:34)

Material	Tensile strength, lb./sq. in.	Yield point, lb./sq. in.	Modulus of elasticity, lb./sq. in.
Stainless iron.....	80,000	45,000	29,000,000
Duralumin.....	60,000	40,000	10,000,000
Monel metal.....	80,000	30,000	24,000,000
Nickel.....	70,000	35,000	28,000,000

Figures 10:31, 10:32, 10:33, and 10:34 show curves for the strength of the plates under edge compression, with the vertical edges of the plate held from lateral motion by *v*-notch grooves.

A study of the curves will show that the load curves rise rather rapidly, almost in proportion to the width for a few inches of width. It appears that the width at which the curve deviates appreciably from a straight line should be the optimum spacing of the stringers for flat sheets or for curved sheets with very small curvature. If stringers are spaced farther apart than the optimum, then the central portion of the sheet between the stringers carries very little of the load as indicated by the tests. If we take

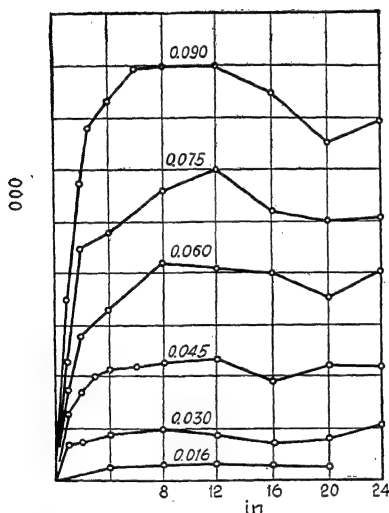


FIG. 10:31.—Maximum load for duralumin plates 24 in. long in direction of loading. (Courtesy of N. A. C. A.)

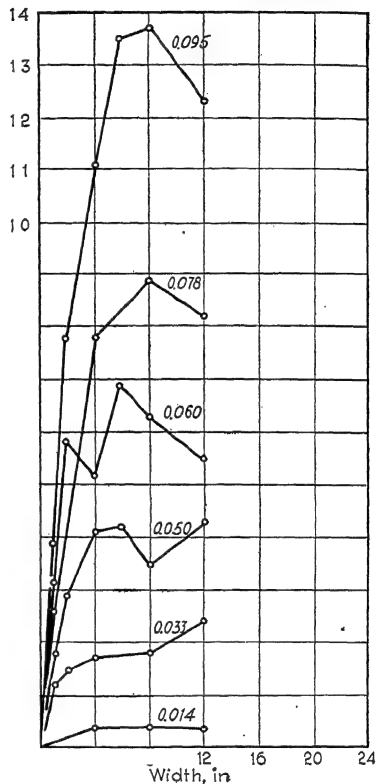


FIG. 10:32.—Maximum load for stainless iron plates 24 in. long in direction of loading. (Courtesy of N. A. C. A.)

the optimum width as b , then for spacing wider than b we may assume that for a width b , bisected by the stringer, the load as indicated by the curves for width b is carried by the flat sheet. We may call the width b the *effective width*, which may be assumed to be acting with the stringer considered as a strut. This effective width would then apply to points 2 and 3 of the analysis in Art. 10:24. It must be borne in mind that the design stress

must not be higher than the stress (pounds per square inch) computed for width b from the figures.

10:27. Stringer-stressed-skin Combination.—If the data of the last paragraph are used for computing the strength of a stringer-stressed-skin combination for a slightly curved surface,

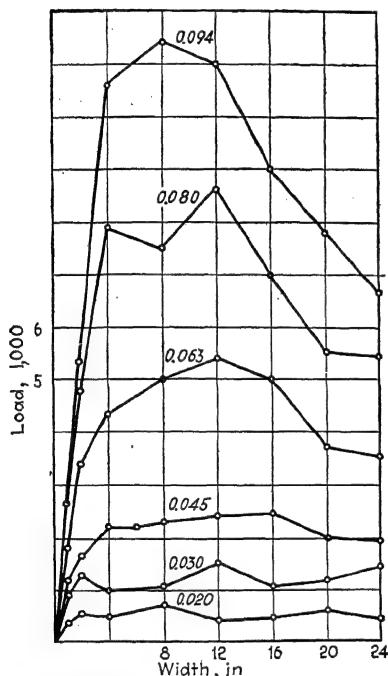


FIG. 10:33.—Maximum load for monel metal plates 24 in. long in direction of loading. (Courtesy of N. A. C. A.)

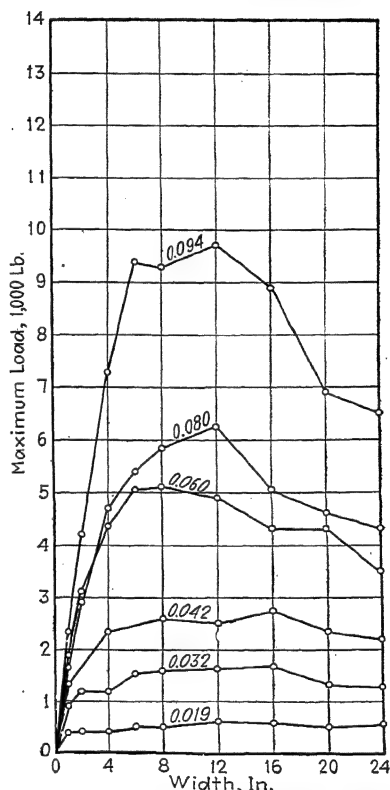


FIG. 10:34.—Maximum load for nickel plates 24 in. long in direction of loading. (Courtesy of N. A. C. A.)

on the assumption that the curved sheet will be only a little stronger than the flat sheet, care must be used in computing the moment of inertia of the cross-sectional area of the combination. The moment of inertia of the combination for the curved sheet will be less than for the flat sheet. This is apparent from Fig. 10:35. While the difference in strength experimentally

and theoretically is small and may be neglected, the student must bear in mind that the condition exists.

10:28. Windows and Doors for Stressed-skin Fuselage.—

The principle to be used in the design of window and door openings in a stressed-skin fuselage is as follows: *The bracing and reinforcement about the windows and doors must be such that the distortion of the ring about the opening will not be greater than the distortion of a similarly placed ring on the sheet metal if the opening did not exist.* This would indicate that openings should be placed where the stress is the lowest, if a choice is allowed.

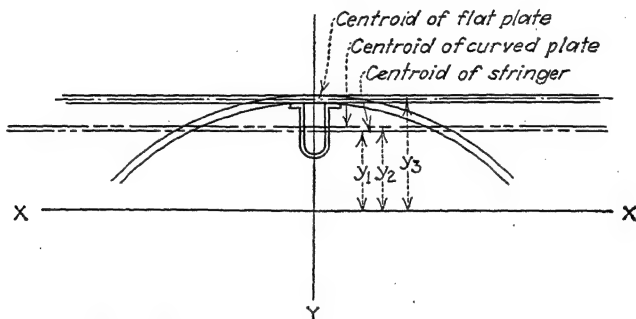


FIG. 10:35.—Combination of stringer and plate.

This specified condition, of course, is the theoretical ideal which may never be attained. The student should bear this principle in mind and approach the problem from the standpoint of rigidity first and strength second.

In general, a door in a semi-monocoque fuselage requires several stringers to be cut. The loads in the stringers, obviously, must be transmitted around the door without undue distortion of the fuselage at the door section. If undue distortion is permitted, high stresses will be introduced at other points of the structure. The design then becomes the design of a ring beam around the door subjected to parallel compressive forces, with the special requirement that the ring should not be distorted more than would be the case if the door were not cut out of the surface.

10:29. Design of a Stressed-skin Wing Structure.—The major phases of such a design are:

1. Determination of the applied loads.
2. Determination of the elastic axis.
3. Design of flanges.

4. Design of webs.
5. Design of bulkheads (ribs).

Let us now consider these last three items in detail.

10:30. Calculation of Axial Load in Flanges.—For a stressed-skin wing in which the center portion of the wing, *A* to *B* (Fig. 10:36), is the supporting spar, it is probably sufficiently accurate

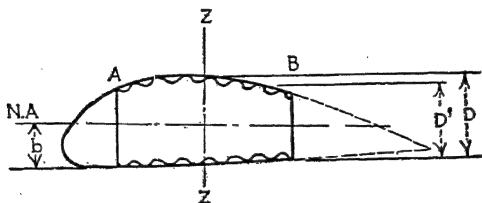


FIG. 10:36.—Elements of a stressed-skin wing.

to calculate the load in the flanges for the preliminary design as follows:

Let

M_x = bending moment to which the wing is subjected at station x .

P = total axial load on a flange.

D' = average depth of spar.

Then

$$P = \frac{M_x}{D'} \quad (10:24)$$

A more accurate method for final design, which will apply to a stressed-skin wing with any number of spars, is as follows: First, find the neutral axis by the formula

$$b = \frac{+}{\text{area of supporting material}} + \frac{+}{\text{area of supporting material}} + \frac{+}{\text{area of supporting material}} \quad (10:25)$$

where a_1, a_2 , etc. = small increments of area.

y_1, y_2 , etc. = distances from the reference line to the increment of area.

Second, compute the moment of inertia of the area of the supporting material about this axis by the formula

$$I = \Sigma a_1 v_1^2 + a_2 v_2^2 + a_3 v_3^2 + \dots \quad (10:26)$$

where v is the distance of the small increment of area from the neutral axis.

Then, third, if M_x is the bending moment at the section x , the fiber stress f in pounds per square inch is computed from

$$M_x v \quad (10:27)$$

To find the approximate load on the flange of a spar, take v the average for the flange and compute

$$P = fA = \frac{M_x \bar{v}}{I} A \quad (10:28)$$

where P = total axial load on the flange being considered.

A = area of the cross section of the flange.

This method may be used to find the loading due to the chord component of air load by finding the neutral axis Z - Z .

No twisting of the wing, of course, is assumed in these methods. This is a reasonable assumption if the shell cover is continuous around the periphery of the cross section.

The *allowable load* in the flanges is important. This is a function of the structural characteristics of the wing. In general, the allowable load in column action is the design allowable load.

If data are not available on the particular design, only a very approximate prediction of strength can be made unless experiments are resorted to.

References

See References following Chaps. XI, XII, and XIII.

CHAPTER XI

DESIGN OF FLAT REINFORCED PLATE STRUCTURES

11:1. Flat Sheet, Edge Compression.—Figure 11:1 shows a flat sheet of width b and length a subjected to an edge compressive load P parallel to the edge a . If the width b is quite small in comparison with the thickness t , then Euler's formula expresses the value of P quite accurately in the long-column range. However, if the sheet is many times wider than the thickness, the stress and deformations in the outer fibers as expressed by

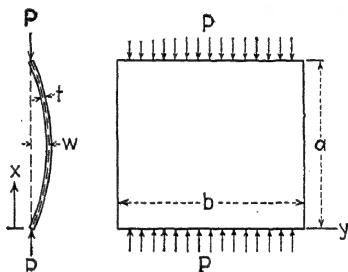


FIG. 11:1

are influenced by Poisson's ratio μ . In (11:1), ϵ_x is the unit strain in the outer fiber.

The unit strain ϵ_x is affected by Poisson's ratio as follows:

$$\epsilon_x = \frac{f_x}{E} \quad (11:2)$$

We note, however, that

$$(11:3)$$

Substituting (11:3), in (11:2), we have

$$\epsilon_x = \frac{f_x}{E} - \mu^2 \frac{f_x}{E} = \frac{f_x(1 - \mu^2)}{E} \quad (11:4)$$

In terms of the radius of curvature d^2w/dx^2 , we have

$$\epsilon_x = \frac{c}{\rho} = c \frac{d^2w}{dx^2} \quad (11:5)$$

Thus, equating (11:4) and (11:5),

$$\frac{f_x(1 - \mu^2)}{E} = c \frac{d^2w}{dx^2} \quad (11:6)$$

Or since $f_z = M_z c / I$,

$$EI \frac{d^2 w}{dx^2} = M_z c \quad (11:7)$$

Thus in the moment equation for a long column,

$$EI \frac{d^2 w}{dx^2} = -P w \quad (11:8)$$

the term $\frac{E}{1 - \mu^2}$ takes the place of E in the equation for the slender column. Thus, solving equation (11:8), we obtain Euler's equation for a flat sheet used as a column,

$$P = \frac{c \pi^2 EI}{a^2 / (1 - \mu^2)} \quad (11:9)$$

where c is the fixity coefficient. In equation (11:9),

$$I = \frac{bt^3}{12} \quad \text{and} \quad A = bt \quad (11:10)$$

Thus equation (11:9) becomes

$$P = \frac{c \pi^2 E A}{12 a^2 (1 - \mu^2)} \quad (11:11)$$

If the edges are free along the sides of dimension b , then $c = 1$; if these edges are fixed, $c = 4$.

11:2. Short-column Range.—Equation (11:11) is, of course, applicable only for the elastic range of the material and not for the plastic range of small values of a/t . In this lower range the following empirical curve applies:

$$(11:12)$$

A curve could also be obtained for this range by using equation (11:11) with the *tangent modulus* instead of E .

There is, of course, only one satisfactory method of finding the curve for the short-column range, and that is to resort to column tests for the material under consideration.

A temporary solution of the problem would be to use the same F_{cu} and n as used for short tubes of the same material. This undoubtedly would be conservative.

11:3. Flat Panels, Edge Compression, and Shear.—Equation (11:11) may be written in the following form:

$$F_{cu} = K \frac{\pi^2 E t^2}{12(1 - \mu^2)} \quad (11:13)$$

where K is a function of the ratio a/b and the number of waves.

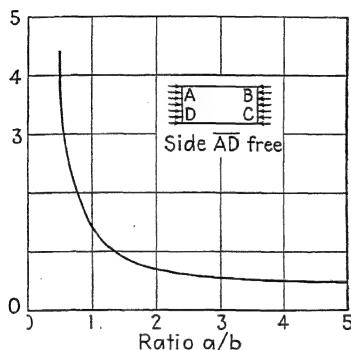


FIG. 11:2.—Graph of constant K for calculating critical compressive stress for a rectangular plate with three simply supported and one free edges.

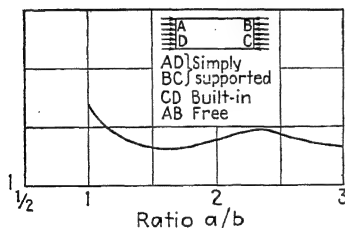


FIG. 11:4.—Graph of constant K for calculating critical compressive stress for a rectangular plate with two opposite sides simply supported, the third built in, and the fourth free.

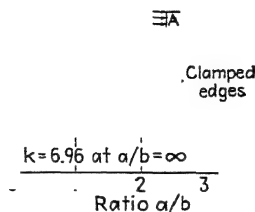


FIG. 11:3.—Graph of constant K for calculating critical compressive stress for a rectangular plate with two edges loaded and all four edges clamped.

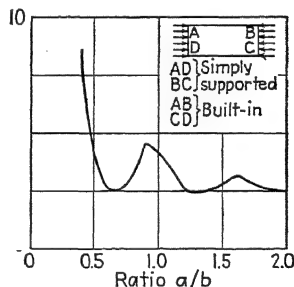


FIG. 11:5.—Graph of constant K for calculating critical compressive stress for a rectangular plate, two opposite sides simply supported, and two others built in.

in the buckled sheet. This equation is usually referred to as the *Bryan formula* and F_{cu} as the *Bryan load*.

If the flat plate of Fig. 11:1 is supported in various ways along the edges a as well as the edges b , the value of K is still a function of the number of waves and the ratio of length to width.

The values of K for a number of conditions have been determined and published (see Refs. 1, 7, and 12).

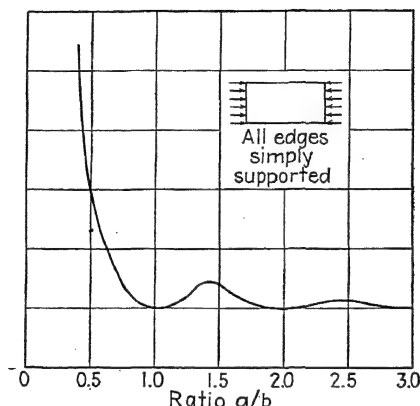


FIG. 11:6.—Graph of constant K for calculating critical compressive stress for a simply supported rectangular plate.

Charts of these values of K are given in Figs. 11:2, 11:3, 11:4, 11:5, 11:6, and 11:7. See Fig. 11:1 for a and b .

It should be particularly noted that equation (11:13) and the values of K from the tables apply only *before* the plate buckles ever so slightly. A *very slight* buckle of the plate radically changes the assumed loading conditions on which the analyses were based.

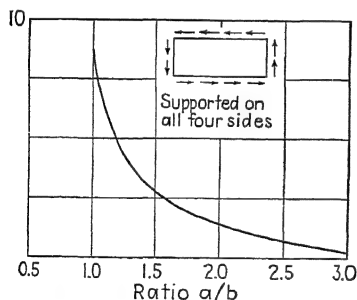


FIG. 11:7.—Graph of constant K for calculating critical shear stress for a rectangular plate supported on four sides and submitted to the action of a uniform shear. a is the length.

(11:13). At this stress and below (provided that the stress is below the proportional limit), F_c is uniform along the edge of the flat sheet. The same stress is also induced in the vertical stiffener (stringer). Thus, the total load for a width b is

11:4. Flat-panel-stiffener Combination.—Figure 11:8 shows a flat sheet of thickness t supported by horizontal and vertical stiffeners. Between the stiffeners, flat panels of width b and length a are formed. The buckling stress of these panels is given by equation

$$P = F_c t b + F_c A_s \quad (11:14)$$

where A_s is the area of cross section of the vertical stiffener.

11:5. Stiffener Spacing.—In equation (11:13), if we let $F_{cu} = F_{cy}$, the compressive yield stress of the material of the flat sheet, and solve for b , we have

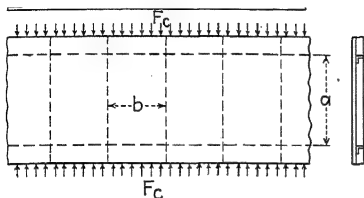


FIG. 11:8.

A panel of this width buckle at the yield point and will take on a permanent set.

The buckling load, however, is not the maximum load of the flat-sheet-stiffener combination, by any means.

If we take $K = 4$ (free edges, and $b = a$),

$$b = \sqrt{\frac{E t^3}{F_c}} \quad (11:16)$$

In this equation, for steel or aluminum alloy, $\mu = 0.30$.

A design width of b for thickness of sheet in present use is in general impractical. For example, a thickness of 0.030 aluminum-alloy sheet would give a stringer pitch of about 1 in.

If we take $K = 6.97$ (for all four edges clamped), the b becomes

$$b = 2.52t \sqrt{\frac{E}{F_c}} \quad (11:17)$$

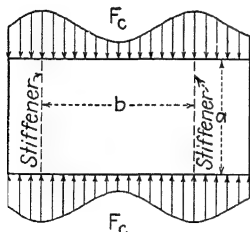


FIG. 11:9.

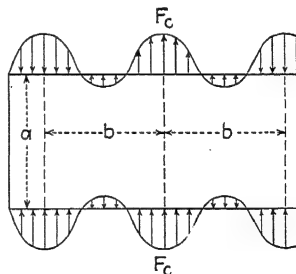


FIG. 11:10.

11:6. Stresses above Buckling Stress.—After the sheet has buckled, the stress distribution is uneven as shown in Fig. 11:9, and equation (11:13) no longer applies. If F_c is further increased

to near the maximum strength of the structure and the panel is a part of a continuous strip of which a is only one bay, tension may even be developed at the center of the width b as shown in Fig. 11:10.

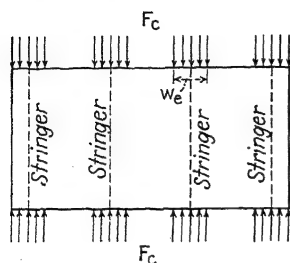


FIG. 11:11.

The following facts stand out:

1. The Bryan formula does not apply after the sheet is buckled.
2. The distribution of the stress is a function of the magnitude of the edge load.
3. The magnitude of the stress in the flat sheet at the stringer is approximately the same as the stress in the stringer.
4. The stringer and flat sheet are mutually supporting.

11:7. Effective Width.—Undoubtedly, more mental and experimental efforts have been spent on the problem of the strength of the thin-sheet-stringer combination than on any other one subject in aircraft structures. It is more than likely that any of the methods developed (see Refs. 2, 3, 4, 5, 9, and 12) will give results as accurate as the variation in materials and structural accuracy will justify.

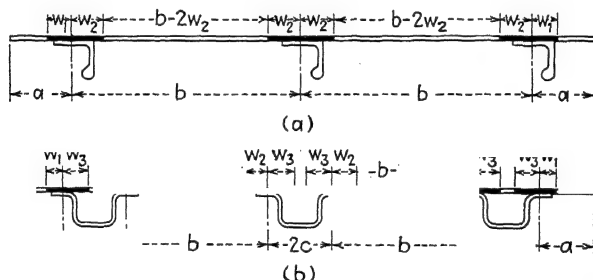


FIG. 11:12.—Effective widths of sheet for sheet-stiffener combinations. (a) Panel with stiffeners having a single line of connection to the sheet. (b) Panel with stiffeners having a double line of connection to the sheet.

All methods are based upon the idea of effective width w_e (see Fig. 11:11), which carries a stress F_c equal to that of the stringer. The basic equation for calculation of the effective width is taken as

$$\frac{\bar{E}}{f_c} \quad (11:18)$$

This equation, as may be noted, is an adaptation of equations (11:16) and (11:17).

The coefficient c is usually assumed to be constant. The ANC-5 Handbook gives the value of c a maximum of 1.70, as shown in Table 11:1 and Fig. 11:12.

In this table (to quote from ANC-5) it should be noted that these values apply when the sheet remains unbuckled between the points of connection to the stringer and when the quantity

$$\frac{t}{c \cdot b} \text{ (see Ref. 4) does not exceed 0.4.}$$

TABLE 11:1.—EFFECTIVE-WIDTH CONSTANTS FOR ALUMINUM-ALLOY SHEET

Type of stiffener	Stiffener	w	c for equation (11:18)	$w_{(max.)}$ (refer to Fig. 11:12)
Stiffeners having single line of connection	Edge	w_1	0.60	a
	Edge	w_2	0.85	$\frac{b}{2}$
	Intermediate	w_2	0.85	$\frac{b}{2}$
Stiffeners having double line of connection	Edge	w_1	0.60	a
	Edge	w_2	0.85	$\frac{b}{2}$
	Edge	w_3	0.85	c
	Intermediate	w_2	0.85	$\frac{b}{2}$
	Intermediate	w_3	0.85	c

NOTE: The above constants apply when the sheet remains unbuckled between rivets and when $\sqrt{\frac{E}{f_c}} \frac{t}{b}$ does not exceed 0.4.

Plate-stiffener combinations may fail by instability in bending or, if the stiffener sections are open, by twisting instability. Local instability failures can occur at free edges or between widely spaced rivets. The support afforded by the sheet will tend to stabilize the stiffeners and may have an appreciable effect on the type of failure involved. For these reasons, it generally is necessary to establish allowable stresses for sheet-stiffener combinations by reference to test data for specimens closely simulating those used in the actual structure (see Refs. 13, 14, and 15).

It should be noted that the radius of gyration of a composite column consisting of a stiffener and its effective width of sheet may be less than that for the stiffener alone. The extent to

which this effect should be considered is a matter for the designer to decide on the basis of his own experience.

11:8. Load Carried by Stiffened Panel.—On the basis of the effective width w_e , noting that the area of cross section of the sheet is $w_e t$ and letting A_s equal the area of one stringer and n equal the number of stringers, we find that the total load carried is

$$P = n f_c (A_s + w_e t) \quad (11:19)$$

The stress f_c is the allowable stringer stress.

11:9. Allowable Stringer Stress.—The stringer, of course, is a column, and the allowable stress is determined accordingly. Note that the effective width of the flat sheet should be assumed as a part of the column in the stress calculation.

If a stringer is continuous so that its length is na , in which a is the distance between cross stringers and the length of the flat panel, the pin-ended column length is a . (Coefficient of fixity = 1.) If the cross stringers are heavy enough to support the length stringers, the coefficient-of-end fixity may be greater than 1.

11:10. Fischel's Method.—The following method of attacking the flat-sheet-stringer problem is presented as an illustration of a practical analysis from which the airplane structural-engineering student may learn much.

Starting with the Bryan formula, it is assumed that all edges of the panel are clamped. A value of K of 6.97 is assumed. Solving,

$$= 2.5t \sqrt{\frac{E}{f_{st}}} \quad (11:20)$$

This corresponds to equation (11:17). In this equation, b_e is the effective width, and f_{st} is the stringer stress. Other symbols to be used are b , stiffener spacing, and f_{sh} , sheet stress. All units are pounds and inches.

Equation (11:20) represents the effective width of flat sheet acting at any particular stiffener stress at or above the initial buckling stress.

11:11. Effect of Variation in Modulus of Elasticity.—The above formula is on the assumption that the same material is used in both the stiffener and the sheet and that the compressive stress of the material does not exceed the proportional limit.

However, such conditions are not always met in aircraft design; hence, it is necessary to consider these variables.

The modulus of elasticity of the aluminum alloys begins to decrease from a value of about 10^7 after the proportional limit is reached. Howland (Ref. 8) has shown this variation of the modulus with stress as the ratio de/df_{sh} , known as the *tangent modulus*, and has plotted average curves of E against tensile stress for several materials. This tangent modulus should be used in the effective-width equation, rather than the constant modulus. Sufficient proof of the tangent modulus is

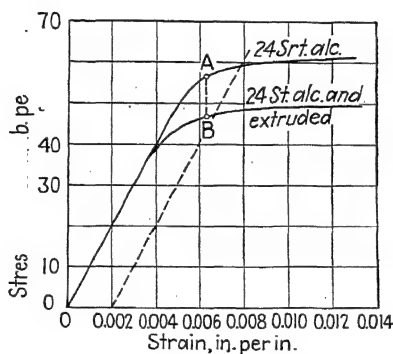


FIG. 11:13.—Typical stress-strain curves for 24ST Alclad, 24ST extruded duralumin, and 24SRT Alclad.

still lacking, but it is undoubtedly a fair approximation of actual conditions. It should be noted that since stiffener stress is used in the formula the modulus of the stiffener at the particular stress and not the modulus of the sheet should be used in determining the effective width.

Differences between the strength of the sheet material and that of the stiffener material must be compensated for in the formula. Since stiffener stress is of primary concern, it is necessary to express the effective-width formula in terms of stiffener stress and correct for the different strength of the sheet.

Sechler (Ref. 4) has shown by strain measurements on a panel that at the higher stresses most of the load in the sheet is carried by that portion adjacent to the stiffener. By assuming that all the stress is carried by a rectangular sheet adjacent to the stiffener equal in width to b_{e1} and acting at the stiffener stress, the load in the sheet will be $b_{e1}tf_{sh}$ where f_{sh} is the sheet stress corresponding

to the stiffener stress at the same unit strain. (points *A* and *B* in Fig. 11:13) and b_{e1} is the uncorrected effective width corresponding to the stiffener stress. Expressing this load in terms of stiffener stress and the correct effective width (b_e) acting at the stiffener stress, the following equation is obtained:

$$P = f_{sh} t b_{e1} = \quad (11:21)$$

or

$$b_e = \frac{f_{sh}}{f_{st}} b_{e1} = 2.52t \frac{f_{sh}}{f_{st}} \quad (11:22)$$

It may be seen that when the stress-strain curves of the two materials coincide the value of f_{sh}/f_{st} will be unity and the original equation will be obtained. The above equation may be used for a combination of *SRT* stiffeners and *ST* sheet or any other combination of materials whose stress-strain curves are known.

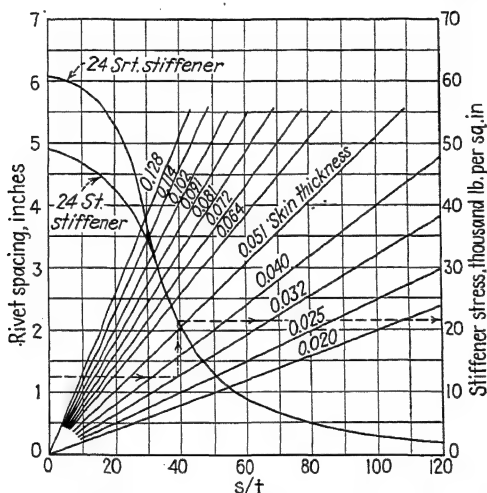
11:12. Effect of Inter-rivet Buckling.—The strength of the sheet after inter-rivet buckling occurs may be treated in a manner similar to that for dissimilar materials, and the same assumptions may be used. Inter-rivet buckling is a column failure of the sheet between rivets; and since the total load in the sheet is assumed to be carried by an effective width at the stiffener, this effective width may be regarded as representing the column between rivets. When a column of any type is loaded axially in compression, it will sustain its maximum stress over a relatively large deflection before any large decrease is detected. Thus, it may safely be assumed that after inter-rivet buckling occurs the sheet stress at which it occurs will remain practically constant till the failure stress of the stiffener is reached. Then, proceeding as before, the effective width of the sheet at stiffener stresses above the inter-rivet buckling stress will be represented by

$$b_e = 2.52t \frac{f_e}{f_{st}} \sqrt{\frac{E}{f_{st}}} \quad (11:23)$$

Combining this equation with the equation for dissimilar materials,

$$\frac{f_e}{f_{st}} \quad (11:24)$$

The inter-rivet buckling stress f_e was originally determined by Howland (Ref. 8) and corrected by Newell (Ref. 9). However, the corrected curves given by Newell do not cover the range of stresses above 44,000 lb. per square inch; hence, in Fig. 11:14, curves for inter-rivet buckling stress are given to cover the entire range of stresses covered by the curves in Fig. 11:13. The curves in Fig. 11:13 were selected as representing typical stress-strain curves for 24ST Alclad and 24SRT extruded



11:13. Application of Theory to Design.—In Fig. 11:15 are plotted curves of effective width of sheet against stiffener stress for various standard gages of 24ST Alclad sheet commonly used in aircraft design. The curves are plotted for *rivet pitch* = 0, or continuous attachment of sheet to stiffener, and for two

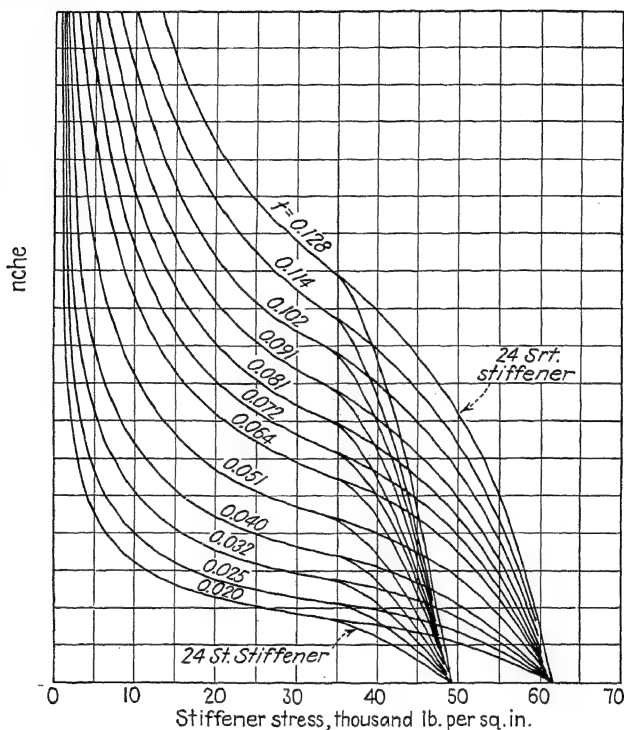


Fig. 11:15.—Curves of effective width of skin vs. stiffener stress for various standard sheet gages of 24ST Alclad.

stiffener materials, 24ST Alclad and 24SRT Alclad, whose stress-strain curves are shown in Fig. 11:13. It may also be assumed without serious error that extruded 24ST duralumin has the same properties as 24ST Alclad; hence, the 24ST Alclad curves may be used for this material. It should be obvious that the limiting value of b_e in the curves of Fig. 11:15 is the stiffener spacing.

To use the curves for any rivet spacing above *pitch* = 0, determine the inter-rivet buckling stress f_e from Fig. 11:14 for

the proper stiffener material. If this is below the design stiffener stress f_{st} , determine the ratio f_c/f_{st} and multiply this by the effective-width determined from Fig. 11:15 for pitch = 0. For any other combination of sheet and stiffener materials, the effective width must be determined from equation (11:24).

The agreement of test data with the general theory is shown in Fig. 11:16. The test points given in Table 2 of Reference 10 are compared with the theoretical curve for 0.032 sheet. The rivet spacing on the test panel was 1 in. for which, from Fig. 11:14, the inter-rivet buckling stress is 34,000 lb. per square inch. The theoretical curve is corrected for inter-rivet buckling and shows good agreement with the test data, especially at the high stresses where the experimental method of determining the effective width was most accurate. Points taken from Fig. 4 of Reference 11 for 0.023 sheet attached to corrugations are also compared with the theoretical curve, and again good agreement is obtained.

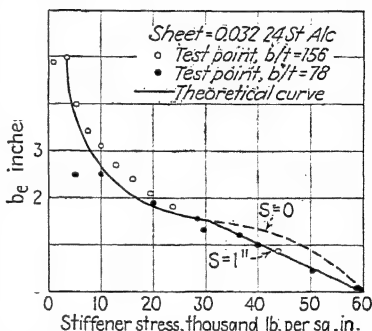


FIG. 11:16.—Comparison of test data with general theory.

As previously mentioned, there are exceptions to the general theory. It has been found from an examination of available test data on stiffened test panels that for values of b/t less than 75 the moments induced into the stiffeners by the sheet become of sufficient magnitude to alter the boundary conditions. This variation of effective width with b/t is mentioned in Reference 10 and is due to a decreasing stiffener spacing or an increasing sheet gage, causing an increase in the moments induced into the stiffener. A reduction factor of 0.76 for sheet-stiffener combinations with a b/t below 75 gives a more nearly correct effective width; that is, the effective width determined by equation (11:24) or from Fig. 11:15 should be reduced 24 per cent. This reduction corresponds to an effective width for a simply supported edge.

References

1. BRYAN, G. H.: On the Stability of a Plane under Thrusts in Its Own Plane with Application to the Buckling of Sides of a Ship, *Proc. London Math. Soc.*, Vol. XXII, 1891.

2. FISCHEL, J. ROBERT: Effective Widths in Stiffened Panels under Compression, *Jour. Aeronautical Sciences*, Vol. VII, No. 5, pp. 213-216, March, 1940.
3. VON KARMAN, TH., E. E. SECHLER, and L. H. DONNELL: The Strength of Thin Flat Plates in Compression, *A.S.M.E. Jour. Applied Mechanics*, Vol. LIV, No. 2, p. 53, 1932.
4. SECHLER, E. E.: Stress Distribution in Stiffened Panels under Edge Compression, *Jour. Aeronautical Sciences*, Vol. IV, No. 8, p. 320, 1937.
5. MARGUERRE, KARL: The Apparent Width of the Flat Plate in Compression, *N.A.C.A. Tech. Mem.* 833, July, 1937.
6. TIMOSHENKO, S.: "Theory of Elastic Stability," p. 339, McGraw-Hill Book Company, Inc., New York, 1936.
7. TIMOSHENKO, S.: "Strength of Materials," Vol. XI, pp. 604-609, D. Van Nostrand Company, Inc., New York, 1930.
8. HOWLAND, W. L.: Effect of Rivet Spacing on Stiffened Thin Sheet under Compression, *Jour. Aeronautical Sciences*, Vol. III, No. 12, p. 434, 1936.
9. NEWELL, J. S.: Letter to the Editor, *Jour. Aeronautical Sciences*, Vol. IV, No. 6, p. 263, 1937.
10. DICKINSON, H. B., and J. R. FISCHEL: Measurement of Stiffener Stresses and Effective Widths in Stiffened Panels, *Jour. Aeronautical Sciences*, Vol. VI, No. 6, p. 249, 1939.
11. SANDERSON, P. A., and J. R. FISCHEL: Corrugated Panels under Combined Compression and Shear Load, *Jour. Aeronautical Sciences*, Vol. VII, No. 4, pp. 148-154, February, 1940.
12. "Strength of Aircraft Elements," A.N.C.-5 Handbook, Government Printing Office, Washington, D.C., 1940.
13. LUNDQUIST, E. E.: Local Instability of Centrally Loaded Columns of Channel Section and Z-Section, *N.A.C.A. Tech. Note* 722, 1939.
14. STOWELL, E. Z., and E. E. LUNDQUIST: Local Instability of Columns with I-, Z-, Channel, and Rectangular Tube Sections, *N.A.C.A. Tech. Note* 743, 1939.
15. DUNN, L. G.: An Investigation of Sheet Stiffener Panels Subjected to Compression Loads with Particular Reference to Torsionally Weak Stiffeners, *N.A.C.A. Tech. Note* 752, 1940.
16. LUNDQUIST, E. E., and CLAUDE M. FLIGG: A Theory for Primary Failure of Straight Centrally Loaded Columns, *N.A.C.A. Tech. Rept.* 582, Washington, 1937.
17. WAGNER, HERBERT: Torsion and Buckling of Open Sections, *N.A.C.A. Tech. Note* 807, 1936.
18. LUNDQUIST, E. E.: The Compressive Strength of Duralumin Columns of Equal Angle Section, *N.A.C.A. Tech. Note* 413, 1932.
19. RAMBERG, McPHERSON, and LEVY: Experimental Study of Deformation and of Effective Width in Axially Loaded Sheet-stringer Panels, *N.A.C.A. Tech. Note* 684, 1939.
20. COX, H. L.: The Buckling of Thin Plates in Compression, *R. & M. No.* 1554, *British Aeronautics Research Committee*, 1933.

CHAPTER XII

DESIGN OF CURVED REINFORCED PLATE STRUCTURES

12:1. Factors Influencing Strength.—The factors influencing the strength of curved sheet subjected to edge loads are

1. The elasticity of the material, as expressed by the modulus E or E_s .
2. The radius of the curved sheet, r .
3. The thickness of the sheet, t .
4. The proportional and elastic limits of the material.
5. The ultimate strength of the material.
6. The length of the curved sheet (cylinder), and the fixity of the ends.
7. The type of failure of the curved sheet.

By analogy to the column curves, Fig. 12:1 shows the typical curved-sheet strength curves. In this figure, r/t takes the place of L/ρ (ratio of length to radius of gyration) of the column

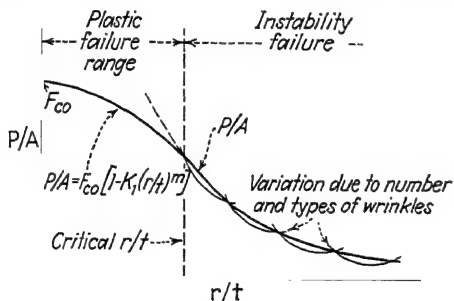


FIG. 12:1.—Failure of walls of a tube by wrinkling.

curve. It was shown (Art. 10:3) by the dimensional analysis that P/A is a function of r/t . This type of analysis does not reveal the exact nature of this function. However, the variation of P/A for apparently similar conditions and materials is so great that the mathematically complicated solution by orthodox methods of the theory of elasticity is not justified. It is therefore desirable to resort to approximations and empirical formulas.

12:2. Types of Failure.—Figure 12:2b, c, and d, and Fig. 19:4 illustrate types of failure of thin curved sheets subjected to edge loads. In the instability range, for large values of r/t , the

failure is more apt to be in the form of Figs. 10:4 and 12:2*b* and *d*. In the plastic range, Fig. 12:2*c* represents the type—an accordion effect, an element forming a sine curve.

In any case, however, there is a resistance to wrinkling as shown in Fig. 12:2*a*. In this figure an elementary strip of width $r d\theta$ is assumed cut from the cylinder wall. The length L of

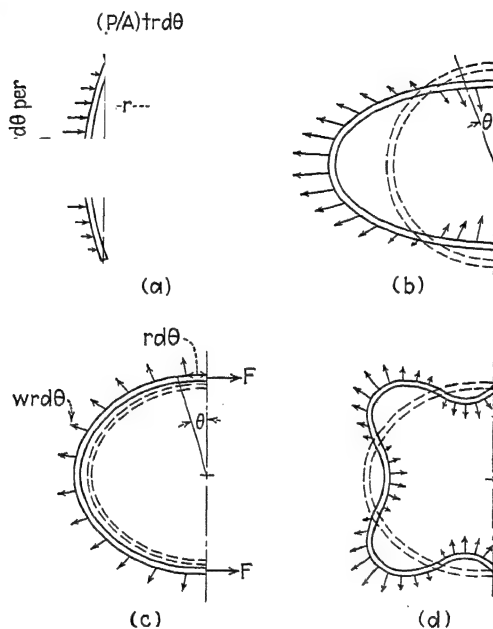


FIG. 12:2.

this strip, it is important to note, is the length of the wrinkle at its first appearance.

12:3. Equation of Equilibrium of Curved Sheet.—In Fig. 12:2*a*, considering the element AB as a column, we note particularly that y is considered extremely small and L is the length of the initial wrinkle. The theory holds only for an infinitesimal value of y , and then only with fair accuracy. (NOTE: The purpose of presenting this elementary form of analysis is to enable the student more clearly to tie up the curved-plate theory with the column theory and to obtain a clearer insight into the problem of wrinkling.)

Starting with the equation of a column of flat sheet [equation (11:8)], we write (substituting y for w)

$$E'I \frac{d^2 y}{dx^2} = -Py \text{ (moment equation)} \quad (12:1)$$

where

$$E' = \frac{E}{1 - \mu^2}$$

Differentiating twice to obtain the loading equation, we have

$$E'I \frac{d^4 y}{dx^4} = -P \frac{d^2 y}{dx^2} \text{ (loading equation)} \quad (12:2)$$

The right-hand side of the equation is the component of the axial load tending to bend the element to form the wrinkle. However, this load is opposed by (Fig. 12:2a) the load $f(x)$. Thus, adding this supporting term to equation (12:2), we have

$$E'I \frac{d^4 y}{dx^4} + P \frac{d^2 y}{dx^2} = f(x) = -wr \, d\theta \quad (12:3)$$

12:4. Forces Opposing Wrinkling.—A wrinkle, inward or outward, causes a *hoop-tension* effect which acts to pull the wrinkle out of the shell. The hoop tension, as the student can find in any elementary book on mechanics, is expressed by

$$F = wr \quad (12:4)$$

where F = hoop tension per inch along an element.

w = radial load per square inch = $f(x)$.

However, in terms of the deformation and the physical characteristics of the material (from the equation E = ratio of unit stress to unit strain),

$$F = \frac{E't}{r} (\delta c) \quad (12:5)$$

where c is the circumference. In terms of the radius r , where $\delta r = y$,

$$F = \frac{E't(2\pi \delta r)}{r} = E' \frac{t}{r} y \quad (12:6)$$

Since, for the elementary strip, (Fig. 12:2a),

$$r = \frac{(r \, d\theta) t}{12} \quad \text{and} \quad P, \text{ for the strip, becomes } \frac{t}{A} (tr \, d\theta)$$

we have, after equating (12:4) and (12:6),

$$\frac{t}{r^2} \quad (12:7)$$

Thus equation (12:3) becomes

$$(12:8)$$

Cancel $d\theta$ and let

$$J^2 = \left(\frac{t}{A} + \frac{12}{E't^3} \right) = \frac{12}{E't^2} \left(\frac{P}{A} \right) \quad (12:9)$$

and

$$\frac{12}{A} \quad (12:10)$$

Thus,

$$(12:11)$$

12:5. Solution and Stability Criterion.—The solution of equation (12:11), as the student may verify by trial or by reference to any elementary text on differential equations, is

$$y = A \cosh px + B \sinh px + C \cos qx + D \sin qx \quad (12:12)$$

in which

and

$$\frac{2}{2} \quad (12:13)$$

To evaluate the constants, we choose x such that when (1) $x = 0$, the bending moment is zero, so that $y'' = 0$; (2) $x = L$, $d^2y/dx^2 = 0$; (3) $x = 0$, $y = 0$; (4) $x = L$, $y = 0$. Solving, we have, letting $m = 1, 2, 3$, etc.,

$$(12:14)$$

From this, we find

$$\frac{P}{A} = \frac{E'L^2}{12L^2} \quad (12:15)$$

When r becomes infinite, we have a flat sheet, the last term of (12:15) becomes zero, and (12:15) becomes Euler's formula for a flat sheet. Thus the P/A of a curved sheet is the Euler load for a flat sheet plus an additional load due to curvature.

12:6. Minimum Edge Load.—Since P/A is a function of L , the wrinkle length, to find the length L for a minimum P/A we write

$$\frac{d(P/A)}{dL} = \frac{2\pi^2 E' t^2}{12L^3} - \frac{2E'L}{12L^3} = 0 \quad (12:16)$$

from which

$$L^2 = \sqrt{12} \quad (12:17)$$

Substituting in (12:15), we have

$$\frac{P}{A} = \frac{\sqrt{12}}{6} \quad \frac{t}{r} = 0.58E' \quad \frac{t}{r} = 0.58 \frac{E}{r} \frac{t}{r}$$

In view of the inaccuracies of construction and the variation of characteristics of materials, it should not be expected that the constant of equation (12:18) can be used in design. However, it is felt that the analysis is worth the few paragraphs devoted to it to enable the student to study the phenomenon of wrinkling. Note that the final equation is of the same form as that given by the dimensional analysis (Art. 10:3).

12:7. Design Data, Axial Compression, Duralumin. Instability Range.—Figure 12:3 (see Ref. 2, p. 11) shows f_c/E as a function of r/t plotted on log-log coordinate paper. All the data are undoubtedly in the instability range of Fig. 12:1. The curve C is given in Reference 2 as the lower limit of test data for the most perfect test specimens. The author of the present volume has added curve D as a safe design curve. The equation for the design curve is, in the nearest simple form,

$$f_c = \frac{P}{A} = \quad (12:19)$$

The upper limit is assumed to be $f_c =$ about 16,000 at $r/t = 200$ [see equation (12:20) for f_c from r/t of 0 up to 200].

Inasmuch as equation (12:19) applies to the instability range, it undoubtedly will apply to all aluminum alloys.

Plastic Range.—Figure 12:4 (Ref. 9, p. 8) shows f_{cr} as a function of r/t from 0 to 60. The author of Reference 8 gives curve A as a design curve. Curve B , proposed by the author of the present volume, has the merit of being simple—a straight line, which is generally used in the plastic range of aluminum-alloy

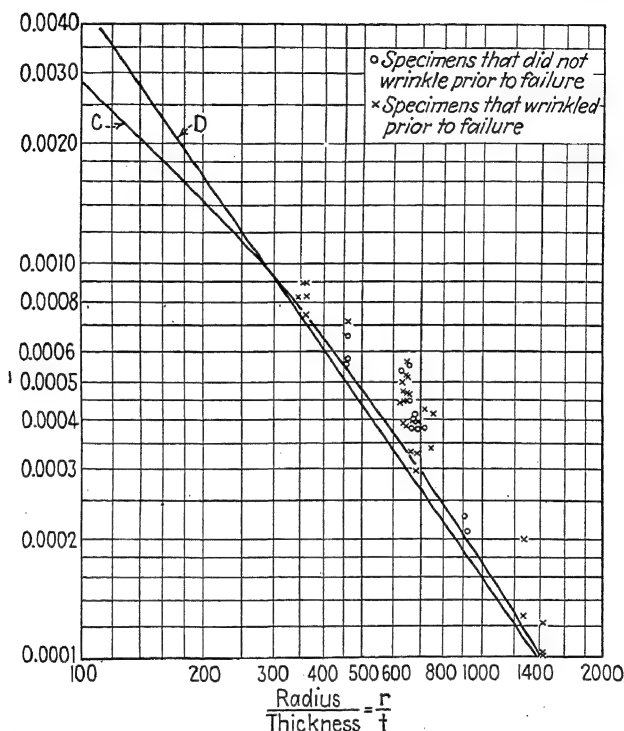


FIG. 12:3.—Effect of wrinkling prior to failure on the strength of thin-walled duralumin cylinders in compression. Tests by N.A.C.A. Curve C, lower limit of test data given by N.A.C.A.

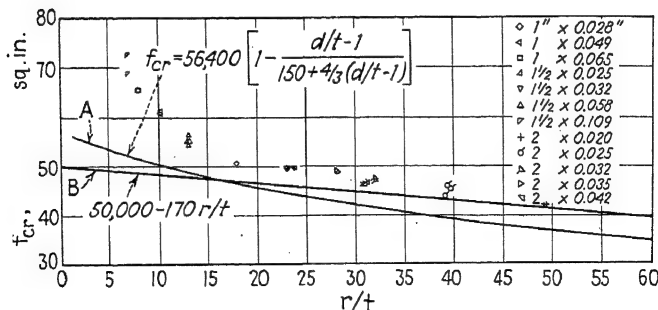


FIG. 12:4.—Diagram of f_{cr} , r/t for duralumin (axial loading).

columns. The equation of curve *B* is

$$\frac{P}{A} = f_c = 50,000 - 170 \frac{r}{t} \quad (12:20)$$

This curve intersects the curve of equation (12:19) at about $f_c = 16,000$ and $r/t = 200$, this being the approximate limit of the curve.

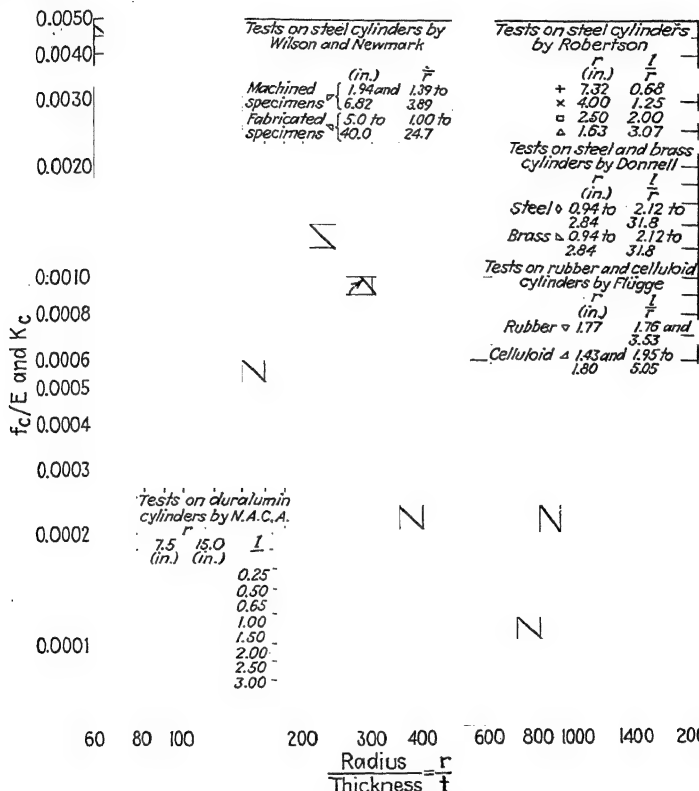


FIG. 12:5.—Logarithmic plot of f_c/E and K , against r/t for several materials. Curve *C* is the lower limit of test data for the most perfect test specimens.

The student is also referred to Figs. 13:2 and 13:3 for charts of P/A as dictated by the Army-Navy-Civil Committee on Aircraft Requirements.

12:8. Design Data, Axial Compression, Steel. Instability Range.—The chart of Fig. 12:5 (see Ref. 2, p. 9) shows f_c/E plotted as a function of r/t for steel with other materials.

Curve *D* appears to the author to be a conservative design curve for steel for r/t from 60 up. The equation for this curve is

$$\frac{0.084E}{r/t} \quad (12:21)$$

Plastic Range.—In Fig. 12:6 (Ref. 9, p. 7) the author of the present volume has added only the curve *B*, which has the merit

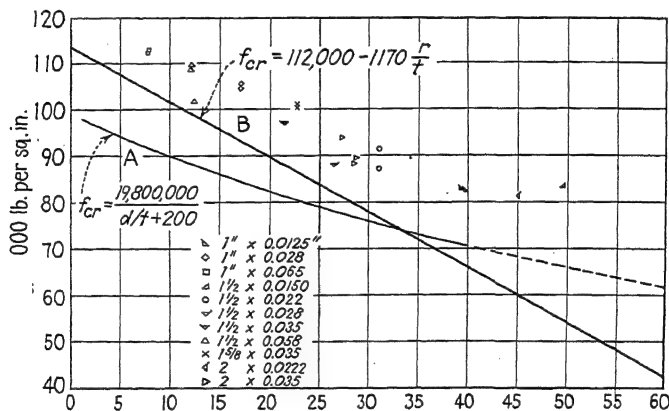


FIG. 12:6.—Diagram of f_{cr} , d/t for chromium-molybdenum steel (axial loading).

of being simple and which intersects the curve of the instability range [equation (12:21) and Fig. 12:5] at approximately $f_c = 42,000$ and $r/t = 60$. The equation for curve *B* is

$$= 112,000 - 1,170 \frac{r}{t} \quad (12:22)$$

12.9. Design Data, Bending, Duralumin.—Up to the point of failure of the thin-walled cylinder in bending, the stress obviously may be expressed by the standard *modulus-of-rupture* equation

$$f_b = \frac{Mr}{I} \quad (12:23)$$

where $I = \pi r^3 t$. The allowable maximum of f_c in this equation is obtained by experiment. The failure, of course, is in compression, though, as in the case of the modulus of rupture, the

allowable stress is greater than for axial compression, because the compression side of the cylinder is supported by the tension side.

Figure 12:7 (Ref. 5, Fig. 5) shows a collection of experimental results on duralumin. Curve *C* was given in the reference as the lower limit of the N.A.C.A. test data. The test data of r/t from 10 to 60 are obviously in the plastic range of the curve of Fig.

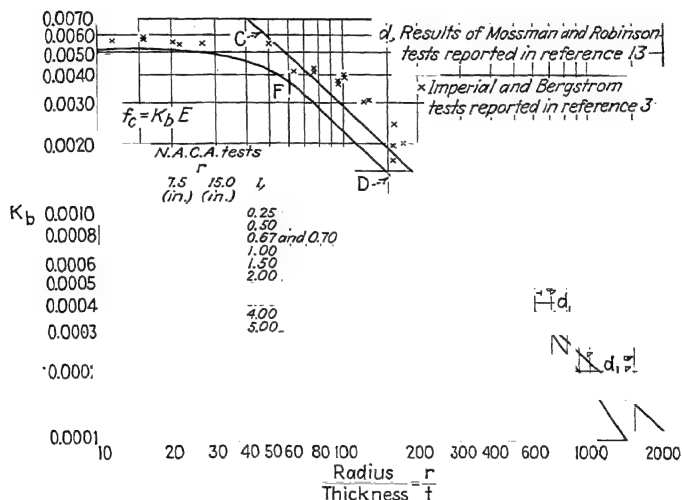


Fig. 12:7.—Logarithmic plot of K_b against radius/thickness ratio (pure bending tests). Curve *C* is obtained from Fig. 12:5.

12:1. The author has drawn in curve *D*—a straight line from *F* to *G*, the instability range. The equation is

$$f_b = \frac{0.225E}{r/t} \quad (12:24)$$

The equation for the plastic range is

$$f_b = 52,000 - 231 \frac{r}{t} \quad (12:25)$$

This formula is a straight line such as is generally used in the plastic range of the duralumin columns.

12:10. ANC-5 Requirements for Bending, Aluminum Alloy.—

Figure 12:8 shows the requirements of the ANC as reproduced from Fig. 5-18 ANC-5 Handbook. Note the straight-line

variation for the range of D/t given (plastic range) as in the case of columns (D = outside diameter; t = wall thickness).

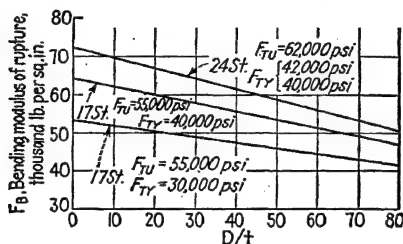


FIG. 12:8.—Bending modulus of rupture, aluminum-alloy round tubing restrained against local buckling at loading points.

12:11. Design Data, Bending, Steel. *Instability Range.*—In the absence of specific data, equation (12:24) may be used for preliminary design.

Plastic Range.—Figure 12:9 (see Ref. 9, p. 10) shows test data on chrome-molybdenum steel tubing. The equation given in Reference 9 is

$$r = \frac{32,500,000}{\frac{2r}{t}} \quad (12:26)$$

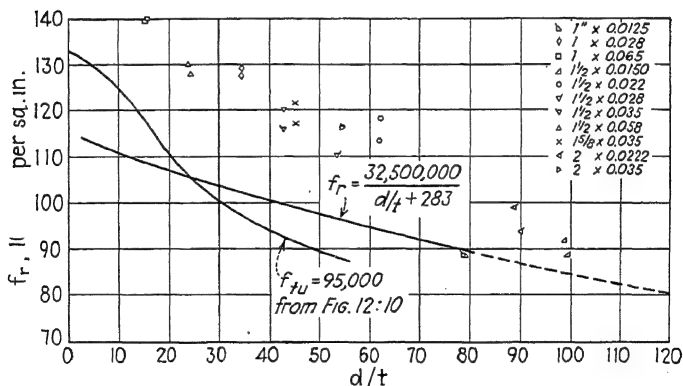


FIG. 12:9.—Diagram of f_r , d/t for chrome-molybdenum steel (transverse loading).

The author of this volume has plotted on this chart the curve for $F_{tu} = 95,000$ from Fig. 4-20 of the ANC-5 Handbook (Fig. 12:10) as the allowable design curve for chrome-molybdenum steel in bending.

12:12. Bending of Chrome-Molybdenum Tubes ANC Specifications.—Figure 12:10 is reproduced from Reference 11, the ANC-5 Handbook, revised October, 1940.

12:13. Experimental Data as Affected by Specifications.—In the manufacture and heat-treatment of thin sheets, especially tubes, considerable variation is to be expected. It is impossible to draw wall thicknesses perfectly uniform and heat-treat to the exact degree specified. In the heat-treatment the specifications are assumed to be a minimum; for example, when 95,000 lb. per square inch is specified as the ultimate tensile strength for chrome molybdenum, the manufacturer makes certain that his heats are such that none of the tubes drops below this in strength. This may mean, however, that many tubes will develop a tensile strength of 120,000 lb. per square inch or more, but none will develop less than 95,000 lb. per square inch.

For these reasons, it is to be expected that experimental data will show considerable scatter in spite of the accuracy of the experimental work. One should remember therefore that a finely drawn set of design curves is nothing more than an estimate, usually conservative.

12:14. Correction of Experimental to a Standard Specification.—If a tube or other beam fails by bending, in the plastic range, it appears that the modulus of rupture may be approximately proportional to the ultimate strength in tension. Thus if a tension test on a tube shows its tensile strength to be 110,000 lb. per square inch for a standard specification of 95,000 lb. per square inch, then an experimental modulus of rupture of 130,000 lb. per square inch should be reduced by the proportion

$$\frac{95,000}{110,000} \times 130,000 = 112,500 \text{ lb. per square inch}$$

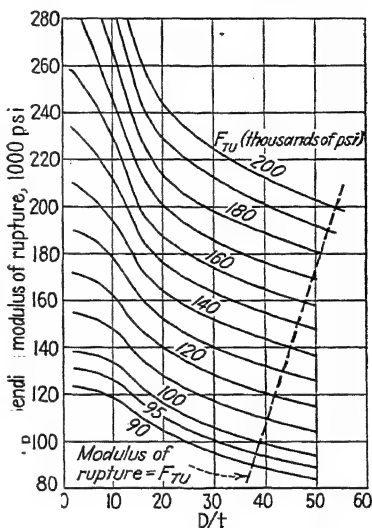


FIG. 12:10.—Bending modulus of rupture, chrome-molybdenum steel tubing.

Reference 11 specifies a method of this sort for the "Reduction of Test Results to Standard" (Civil Aeronautics Administration Method, Art. 1.544, pp. 1-28, revised October, 1940). This method pertains to columns.

Since there may not be a simple proportionality between shear and tension, pure shear tests may be necessary to provide correction data for torsion of tubes.

In the instability range, the modulus of elasticity is the strength factor. This does not vary appreciably with heat-treatment, so that it may, for practical purposes, be assumed constant.

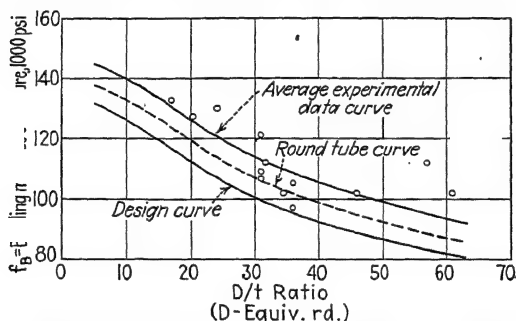


FIG. 12:11.—Bending strength of chrome-molybdenum streamline tubes.

In the region between plastic and instability ranges, there is a gradual transition from one type of failure to another; thus corrections must be made to vary, probably in a direct proportion, from one range to the other.

12:15. Bending of Tubes, Chrome-Molybdenum Streamline.

Figure 12:11 shows the results of tests on 14 streamlined chrome-molybdenum tubes at the University of Maryland to supply needed design data, with D/t of equivalent round varying from 15 to 60. The data are corrected for a guaranteed ultimate of 100,000 lb. per square inch, as described in Art. 12:14. The design curve is drawn below all test points and parallel to the 100,000 lb. per square inch curve of Fig. 12:10 for round tubes. The bending moment was applied in the plane of the minor axis.

Because of wartime conditions it was necessary to take the experimental tubes from miscellaneous stock; hence the wide scatter of points because of the wide variation of physical properties. Since, however, these represent conditions with which the designer is confronted, the design curve should be practical.

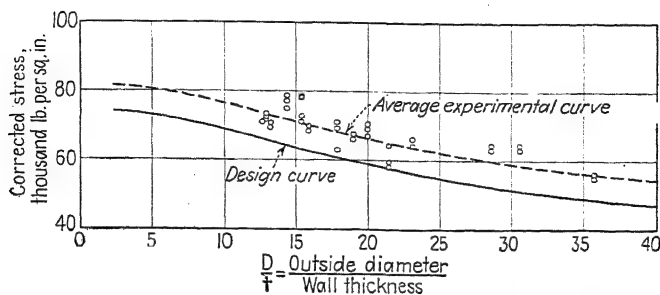


FIG. 12:12.—Modulus of rupture of S.A.E.-1025 round steel tubing. Guaranteed ultimate tensile 55,000 lb. per square inch, length/diameter = 20.

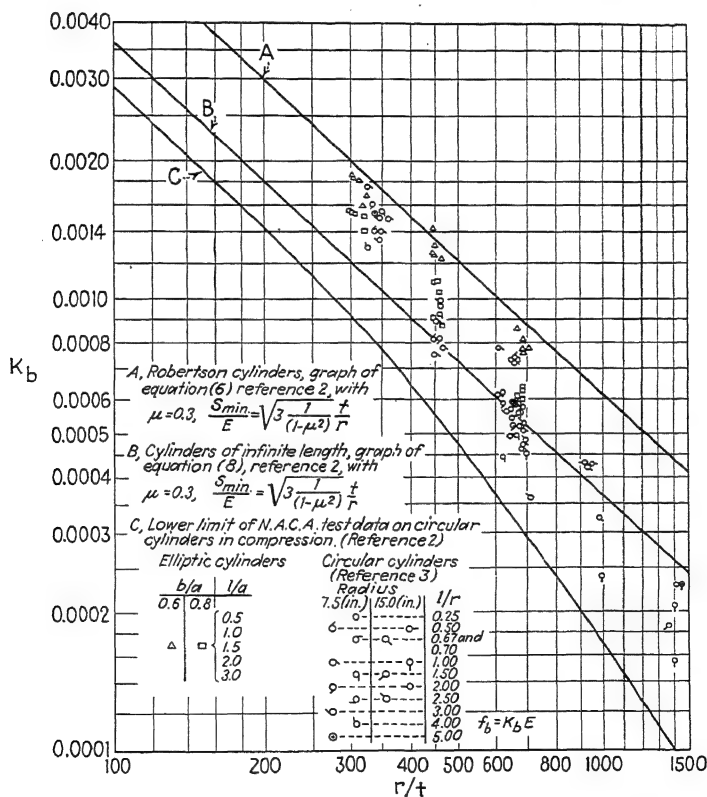


FIG. 12:13.—Logarithmic plot of K_b against radius/thickness ratio (pure bending tests), where, $f_b = K_b E$.

12:16. Bending of Tubes, 1025 Steel.—Figure 12:12 shows the results of experiments carried out at the University of Maryland to obtain design data of 1025 seamless steel tubing. The data are corrected to a tensile ultimate specification strength of 55,000 lb. per square inch, as described in Art. 12:14. The ultimate tensile strength averaged about 50 per cent higher than 55,000 lb. per square inch.

12:17. Bending, Duralumin Elliptical Cylinders.—In Fig. 12:13 (Ref. 15, Fig. 8) the results from bending elliptical cylinders are plotted with the results from bending round cylinders.

The author of Reference 15 states that the bending loads were applied in the plane of the major axis a of the ellipse. In the case of $b/a = 0.8$, wrinkling did not usually occur prior to failure.

Failure is defined as the complete collapse of the compression side of the cylinder with the formation of diamond-shaped wrinkles. In the case of $a/b = 0.6$, preliminary wrinkles are usually formed prior to failure.

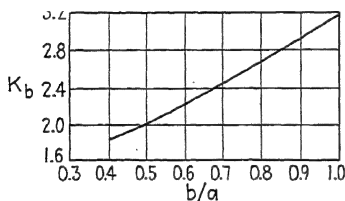


FIG. 12:14.

In the presentation of the results, it has been assumed that the ordinary theory of bending applies and that the stress on the extreme compression fiber at failure is given by the equation

$$Mc = \frac{M}{k_b a^2 t} \quad (12:27)$$

where M = bending moment applied in the plane of the major axis of the ellipse.

a = semi-major axis of the ellipse.

k_b = nondimensional coefficient that varies with the eccentricity of the ellipse (see Fig. 12:14).

The radius r in the ellipse is obviously the radius of curvature at the ends of the major axis.

12:18. Torsional Failure of Thin-walled Cylinders.—The shear stress f_s in the walls of the cylinder due to a torque Q is

$$\frac{Q}{2At} \quad (12:28)$$

where Q = torque, in.-lb.
 t = shear stress.

A = circumscribed area = πr^2 .

t = thickness of skin.

The thin walls of the cylinder fail by instability due to the compressive load (see Fig. 12:15). By the combined stress formula [equation (3:24)], since there are no applied tension or compression stresses,

$$f_c = f_s, \quad \theta = 45 \text{ degrees}$$

If we cut the tube across the 45-degree line, an ellipse is formed with the major axis, $a = \sqrt{2} r$, and the minor axis, $b = r$. Thus we have the equivalent of an elliptic cylinder subjected to compressive load $f_c = f_s$. The buckles are creases inclined to the axis at about 45 degrees.

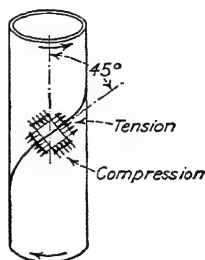


FIG. 12:15.

12:19. Torsion, Round Cylinders, Duralumin.—Figures 12:16 and 12:17 (Ref. 16) show the results of torsion tests on 65 round cylinders of 7.5 and 15.0 in. radius with length varying from 2.25

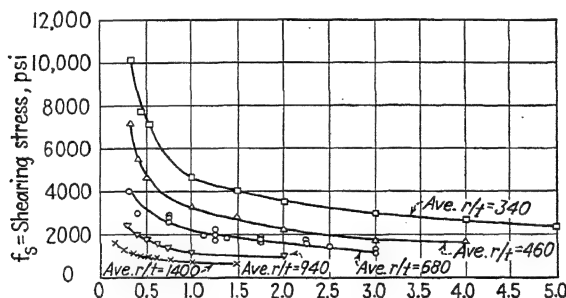


FIG. 12:16.—Shearing stress at failure.

to 45.0 in. The cylinders were constructed of 17ST aluminum-alloy sheet of thicknesses of 0.0105 to 0.0228 in. These figures show the variation of failing shear stress as a function of both the ratios, *radius to thickness* and *length to radius*.

Figures 12:18 and 12:19 show the results of torsion tests by the Aluminum Company of America laboratories (see Ref. 17).

Figure 12:20 shows the ANC specification. It is a reproduction of Fig. 5-7 of Reference 11.

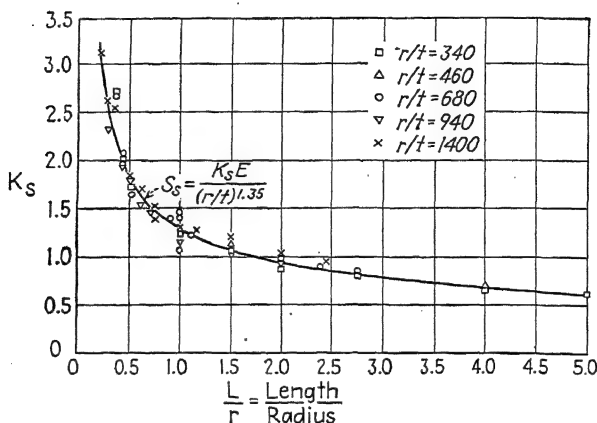


FIG. 12:17.—Variation of K_s with length-radius ratio. $S_s = f_s$.

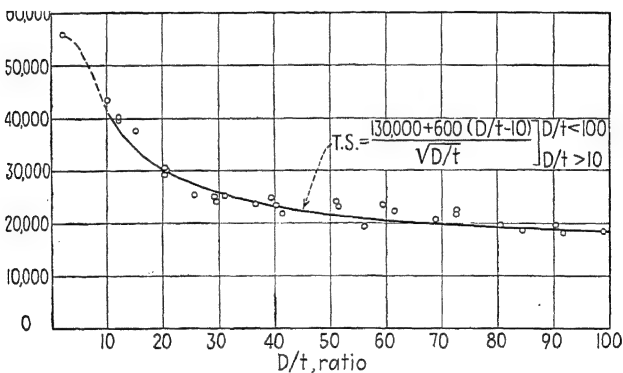


FIG. 12:18.—Curve showing relation between torsional strength and D/t ratio of round 17ST tubing.

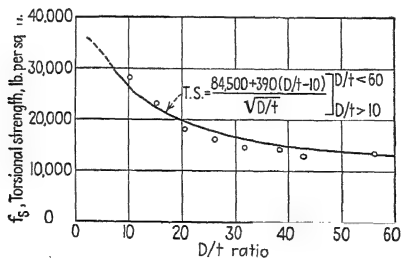


FIG. 12:19.—Curve showing relation between torsional strength and D/t ratio of round tubing. Aluminum alloy 51SW.

12:20. Design Charts for Duralumin Tubes, Torsion.—Figures 12:21 and 12:22 (Ref. 18) show design curves based on tests of 102 tubes of 17ST aluminum alloy. It was found in these tests that the torsional strength of aluminum-alloy tubes may be described by the help of the three variables

$$\frac{M}{D^3}, \quad f_{ult.}, \quad \text{and} \quad \frac{t}{D}$$

where M = torque, in.-lb.

D = diameter, in.

$f_{ult.}$ = tensile strength of the tube material.

t = tube-wall thickness, in.

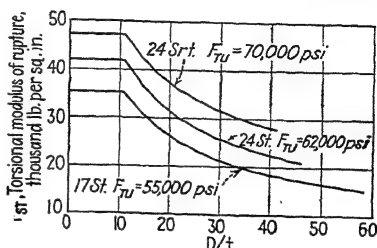


FIG. 12:20.—Torsional modulus of rupture of aluminum-alloy round tubing.

A simple example will illustrate the use of Fig. 12:21.

Find the wall thickness of a 2-in. 17ST aluminum-alloy tube 5 ft. long that will just fail when subjected to a torque of 2,000

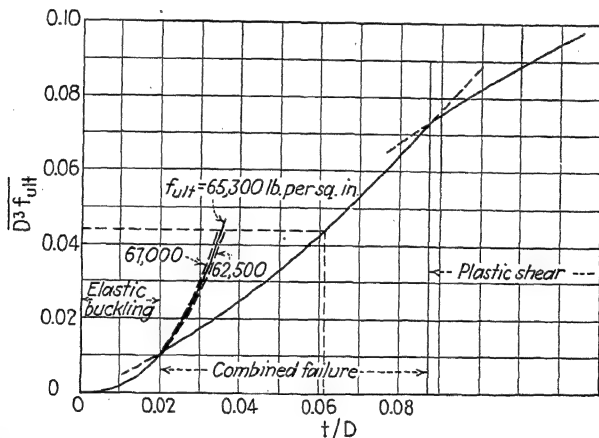


FIG. 12:21.—Design chart for torsional strength of 17ST aluminum-alloy tubes.

lb.-ft. The tensile strength of the tube material is 68,000 lb. per square inch.

We have, in answer,

$$\frac{M}{D^3} = \frac{2,000 \times 12}{\pi \times 68,000} = 0.0441$$

According to Fig. 12:21, this corresponds to

$$\frac{t}{D} = 0.061, \quad t = 0.061 \times 2 = 0.122 \text{ in.}$$

Thus the wall thickness of the tube that may be expected to fail under about 2,000 lb.-ft. torque would be 0.122 in.

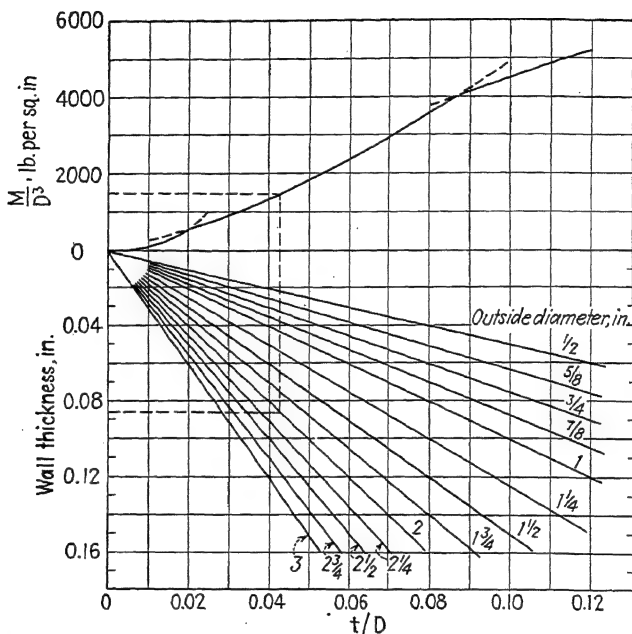


FIG. 12:22.—Design chart for torsional strength of 17ST aluminum-alloy tubes, 19–60 in. long, satisfying Navy Specification 44T21a. ($f_{ult.} = 55,000$ lb. per square inch.)

A design chart may be derived from Fig. 12:21 for aluminum-alloy material required to satisfy certain specifications for minimum tensile strength. Figure 12:22 shows such a chart for 17ST tubing complying with Navy Specification 44T21a. The upper half of the figure was constructed from Fig. 12:21 by substituting 55,000 lb. per square inch for $f_{ult.}$; the lower half is a set of straight lines corresponding to commercially available diameters of 17ST tubing. The following example illustrates the chart:

Find the wall thickness of a 2-in. 17ST aluminum-alloy tube 5 ft. long that will just fail when subjected to a torque of 1,000 lb.-ft.

The material of the tube shall just meet Navy Specification 44T21. We have, in answer,

$$\frac{M}{D^3} = \frac{1,000 \times 2}{2^3} = 1,500$$

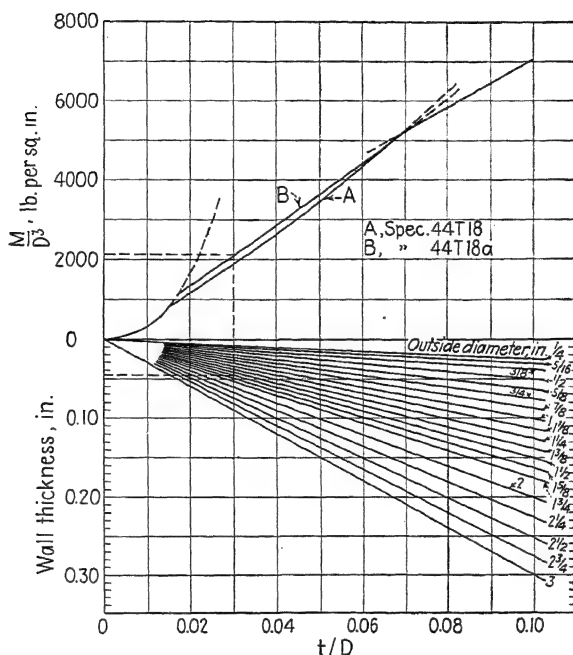


FIG. 12:23.—Design chart for torsional strength of chrome-molybdenum steel tubes, 19–60 in. long, satisfying Navy Specification 44T18a ($f_{ult.} = 60,000$ lb. per square inch) and Navy Specification 44T18a ($f_{ult.} = 95,000$ lb. per square inch, $f_{yield} = 75,000$ lb. per square inch).

It is seen by following the dotted line in Fig. 12:22 that this value corresponds to a wall thickness of $t = 0.086$ in. in a tube 2 in. in diameter.

12:21. Torsion, Round and Streamlined Tubes, Steel.—

Figure 12:23 (from Ref. 18) is a design chart for chrome-molybdenum round tubes in torsion. It is based on the results of tests on 63 tubes and the variables

$$\frac{M}{D^3}, \quad \frac{t}{D}, \quad \text{and} \quad f_{ult.} \quad (\text{see Art. 12:20 for explanation of symbols})$$

An example illustrates the use of the chart.

Find the wall thickness of a $1\frac{1}{2}$ -in. chrome-molybdenum steel tube 5 ft. long that will fail when subjected to a torque of 600 lb.-ft. The tensile yield strength of the tube material is

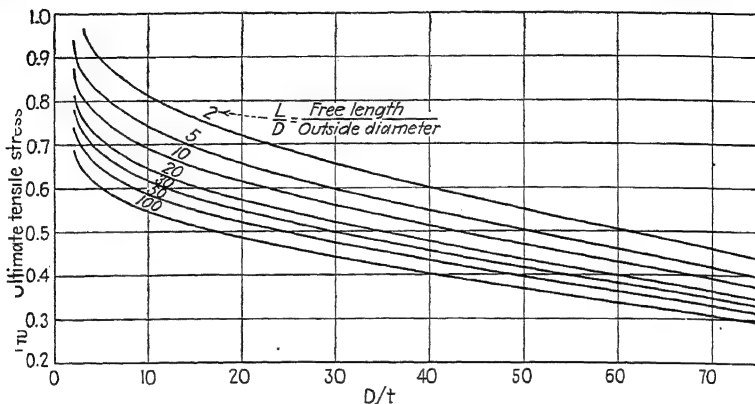


FIG. 12:24a.—Torsional modulus of rupture of round alloy-steel tubing.

75,000 lb. per square inch, and its tensile ultimate strength is 95,000 lb. per square inch.

We have, in answer the following: The material of the tube specified in the problem just meets Navy Specification 44T18a.

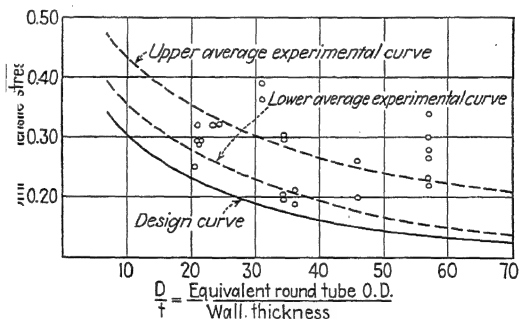


FIG. 12:24b.—Torsion strength of chrome-molybdenum streamline tubes.

The curve of Fig. 12:23 can be applied directly to solve the problem. Thus,

$$M = \frac{600 \times 12}{1.5^3} = \frac{7,200}{3.375} = 2,130 \text{ lb. per square inch}$$

The ordinate $T/D^3 = 2,130$ intersects curve B at $t/D = 0.03$. A vertical through the point of intersection extending into the

lower half of the chart intersects the inclined line $D = 1.5$ in. at a value of $t = 0.045$ in.—the answer.

ANC Specification for Torsion Strength of Chrome-Molybdenum Steel Tube.—See Fig. 12:24a, which is a reproduction of Fig. 4-22 of Reference 11.

ANC Specification for Torsion Strength of S.A.E.-1025 Round Steel Tubing.—See Fig. 12:25 which is a reproduction of Fig. 4-21 of Reference 11.

Figure 12:24b shows a design curve for chrome-molybdenum steel streamlined tubes, based on experiments at the University of Maryland. The design curve is probably low.

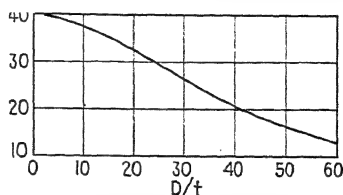


FIG. 12:25.—Torsional modulus of rupture of 1025 round steel tubing.

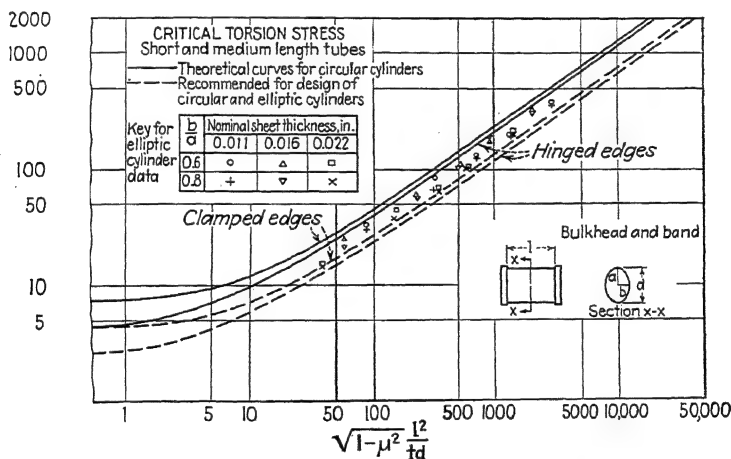


FIG. 12:26.—Shearing stress at failure S for elliptic cylinders in torsion.

12:22. Torsional Strength of Elliptical Duralumin Cylinders.
The shear stress is calculated by the formula

$$f_s = \frac{Q}{2At} \quad (12:29)$$

where Q = applied torque, in.-lb.

f_s = shear stress.

t = thickness, in.

$A = \pi ab$, area of ellipse.

With reference to Fig. 12:26 (Ref. 15), the shearing stress as given by this equation was calculated for each test cylinder at the conditions of first wrinkle and ultimate load. These stresses were used in plotting the experimental points of Fig. 12:26, which is the type of chart used by Donnell in Reference 4 for presenting the results of torsion tests on thin-walled cylinders of circular section. It will be noted that the experimental points for the ultimate-load plot lie between the theoretical curves and those recommended for design. From the data from torsion tests of circular cylinders between these same curves (Ref. 4), it may be concluded that the shearing stress at ultimate load for an elliptic cylinder is the same as for the circumscribed circular cylinder of the same sheet thickness and length.

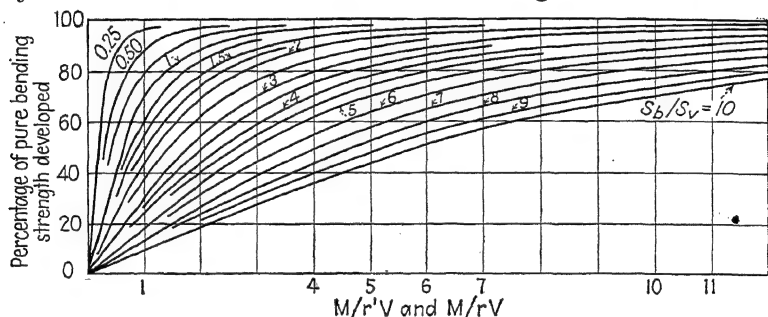


Fig. 12:27.—Chart for bending strength of thin-walled duralumin cylinders subjected to combined transverse shear and bending.

12:23. Combined Bending and Transverse Shear Strength of Duralumin Round and Elliptical Cylinders.—These conditions are shown in Fig. 12:27 (Ref. 15). The abscissa $M/r'V$ applies to the elliptical cylinders, and M/rV refers to the round cylinders. In both cases,

$$\frac{M}{r'V} = \frac{S_b}{S_v} \quad (12:30)$$

where

$$S_b = \frac{M}{k_b a^2 t} \quad (12:31)$$

and

$$S_v = \frac{V}{k_v a t} \quad (12:32)$$

and

$$r' = \frac{k_b}{r} t \quad (12:33)$$

Where a = semimajor axis of the ellipse.

In these equations, k_b and k_v are obtained from Fig. 12:28. In equation (12:32), V is the transverse shear in the plane of the major axis of the ellipse. In equation (12:31), M is the

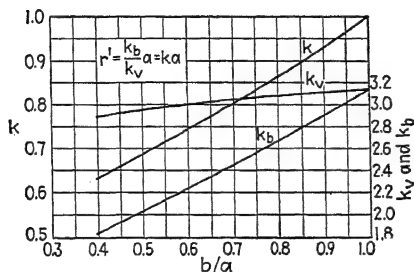


FIG. 12:28.—Stress coefficients.

bending moment applied in the plane of the major axis of the ellipse.

In order to use the curves of Fig. 12:27 in design, it is necessary to know the loading condition $M/r'V$ or M/rV and to be able to predict the values of S_b and S_v .

S_v is defined as the shearing stress on the neutral axis at failure in pure transverse shear. If S is the shearing stress at failure for a cylinder of the same dimension in torsion equation (12:29), approximately,

$$S_v = 1.25S \quad (\text{see Ref. 15}) \quad (12:34)$$

and also

$$S_b = \frac{Mc}{I} - \frac{M}{k_b a^2 t} \quad (12:35)$$

where a is the semi-major axis and k_b is determined from Fig. 12:28.

If the quantities $M/r'V$, S_b , and S_v are known, the maximum allowable moments and/or stress on the extreme fiber can be read from the chart of Fig. 12:27 as a percentage of that for pure bending.

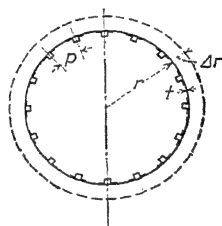


FIG. 12:29.—Cylinder dimensions

In checking the strength of any section between adjacent bulkheads, the largest value of $M/r'V$ in that section should be used to enter on the chart of Fig. 12:27. This procedure tends toward conservatism and is certainly justified by the wide scattering of the test data.

12:24. Stringer-curved-sheet Combination.—If a thin-walled cylinder is reinforced by stringers parallel to an element of a cylinder, the compressive load is resisted by the reinforced cylinder as follows:

1. The stringer as a column acting alone.
2. The support given the stringer by the curved sheet.
3. The curved sheet acting alone.
4. The support given the curved sheet by the stringer.

The method of determining an effective width for a flat-sheet-stringer combination (Chap. XI) is quite generally used for a curved-sheet-stringer combination. To the load calculated on this basis is added a load carried by the remainder of the curved sheet after the effective width is subtracted,

$$f_c = \frac{KE}{r/t} \quad (12:36)$$

A.N.C. specifications give $K = 0.25$.

This method provides for all four items above if item 2 is considered in the determination of the allowable stringer stress. This item is considered in the next article.

12:25. Support of Stringer by Curved Sheet.—The stringer, as a column, is supported elastically by the curved sheet. As in the case of an element of a curved sheet (Fig. 12:2a) the moment equation of the stringer (unsupported column) is equation (12:1), and the loading equation is (12:2), with E replacing E' . Likewise, equation (12:3) is the loading equation for the stringer as a beam column.

The term $f(x)$ is the supporting force exerted by the cylindrical wall on the stringer. A solution of the problem depends upon the determination of the nature of this supporting force.

12:26. Equation of Support of Stringer.—If we assume that the initial movement of the stringers toward their buckling state causes a circumferential tension or compression of the skin of the cylinder, we may obtain a solution. While this solution will not be exact, it will give an indication of the relationship

between the variables involved. This relationship may serve as a guide in correlating the experimental data.

The radial load $f(x)$ causes a hoop tension (or compression) in the skin of F lb. This is explained in Art. 12:4 and is expressed mathematically in equation (12:6). Writing E for E' ,

$$F = E \frac{t}{r} y \quad (12:37)$$

where y = deflection of the stringer.

r = radius.

t = skin thickness.

If we let p be the pitch of the stringers (see Fig. 12:29), c the circumference, and n the number of stringers, we have

$$p = \frac{c}{n} \quad (12:38)$$

The hoop tension F in a pressure vessel is the radial pressure w (pounds per square inch) times the radius r ,

$$F = wr \quad (12:39)$$

The supporting load $f(x)$ on the stringer is the radial pressure w times the pitch p .

Thus

$$F = wr = + \frac{f(x)}{p} r = -E \frac{t}{r} y \quad (12:40)$$

Thus

$$f(x) = -E \frac{tp}{r^2} y \quad (12:41)$$

Thus letting $J^2 = P/EI$ and $n^4 = tp/Ir^2$, we have equation (12:11), the solution of which is (12:12). Using the same limits as in Art. 12:5, we obtain, as in equation (12:15), the solution for the load P per stringer,

$$P = \frac{\pi^2 EI}{L^2} + E \frac{t}{r} \frac{p}{\pi^2} L^2 \quad (12:42)$$

12:27. Support Given Stringer by Curved Sheet.—The first terms on the right-hand side of equation (12:42) is Euler's column formula. As the curved walls approach flatness ($r = \infty$), the second term on the right-hand side vanishes. Thus the support due to the curved sheet is

$$\text{Support} = \text{function of } E, \frac{t}{r}, \frac{p}{r}, L \quad (12:43)$$

While equation (12:42) is for a Euler column (instability range), we assume we may use its form to express the relationship for the complete range of the stringer, plastic and instability.

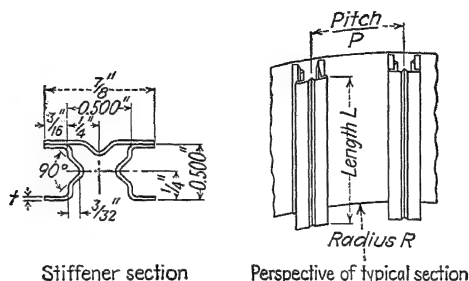


FIG. 12:30.

In equation (12:42) if we let P_t be the total load per stringer and P_c the critical load of the stringer (including a part of the skin to make the stringer complete) as determined by methods applicable to columns, we write (12:42) as

$$(12:44)$$

That is, the added support is a function E , the ratio tp/r^2 , and L . Since E is a constant for the same material, it may be excluded.

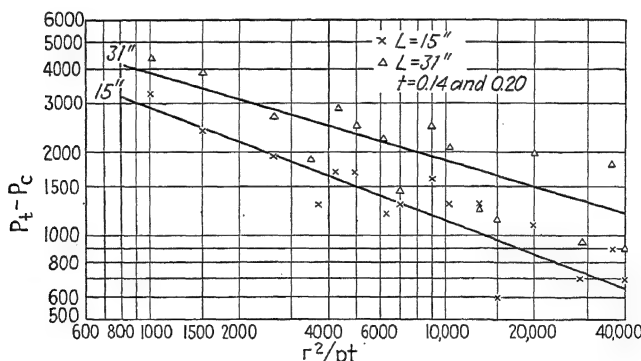


FIG. 12:31.—Stiffener unit load increase due to curvature.

12:28. Experimental Data.—Figure 12:31 (Ref. 7) shows a plot of $(P_t - P_c)$ as a function of r^2/pt . (This term is inverted to obtain whole numbers.) The data for Fig. 12:31 were from tests made on cylindrical shells of hard-drawn 18-8 stainless steel

sheet having an ultimate strength of 175,000 to 185,000 lb. per square inch. The cylinders (see Fig. 12:30) varied from 30 to 60 in. in diameter and had lengths of 11, 15, 22, and 31 in. Stiffeners and sheet were identical in thickness at values of 0.014, 0.020, 0.030, and 0.050 in. Stiffener spacings of 1.24, 2.27, 4.33, and 10.51 were employed. The specimens were spot-welded throughout.

The student will note from a few of the following sample values used in Fig. 12:31 that the added strength is quite large.

Stringer Alone, P_c	$P_t - P_c$
2,900	3,500
4,700	5,030
1,300	4,430

It appears, at least, that, instead of item 2 (Art. 12:24) being negligible, it is the most predominating factor. Additional research is desirable. Perhaps the student may be able to add to the present knowledge.

References

1. YOUNGER, J. E.: Metal Wing Construction, Part II, Mathematical Investigation, A.P.M. 1020, U.S. Army Air Corps, Wright Field, 1927.
2. LUNDQUIST, E. E.: Strength Test of Thin Walled Duralumin Cylinders in Compression, *N.A.C.A. Rept.* 473, 1933.
3. YOUNGER, J. E.: Principle of Similitude as Applied to Research of Thin Sheet Structures, *Trans. A.S.M.E. Aeronautical Engineering*, Vol. V, No. 4, October-December, 1933.
4. DONNELL, L. H.: Stability of Thin Walled Tubes under Torsion, *N.A.C.A. Tech. Rept.* 479, 1933.
5. LUNDQUIST, E. E.: Strength Tests of Thin Walled Duralumin Cylinders in Pure Bending, *N.A.C.A. Tech. Note* 479, 1933.
6. LUNDQUIST, E. E.: Strength Tests of Thin Walled Duralumin Cylinders in Combined Transverse Shear and Bending, *N.A.C.A. Tech. Note* 523, 1935.
7. BROWN, C. G., J. MATULAITIS, and J. E. YOUNGER: The Compressive Strength of Stainless Steel Sheet Stringer Combinations, Part III, *Air Corps Information Circ.* 706, 1936.
8. NEWELL, J. L., and J. H. HARRINGTON: Progress Report on Methods of Analysis Applicable to Monocoque Aircraft Structures, *Air Corps Tech. Rept.* 4313, 1937.
9. OSGOOD, W. R.: The Wrinkling Strength and the Bending Strength of Round Aircraft Tubing, *N.A.C.A. Tech. Rept.* 632, 1938.
10. NILES, A. S., J. C. BUCKWALTER, and W. D. REED: Bending Tests of Circular Cylinders of Corrugated Aluminum Alloy Sheet, *N.A.C.A. Tech. Note* 595, 1937.

11. "Strength of Aircraft Elements," A.N.C.-5 Handbook, U.S. Government Printing Office, Washington, D.C., October, 1940.
12. HOFF, N. J.: Instability of Monocoque Structures in Pure Bending, Reprinted from *Jour. Roy. Aeronautical Soc.*, April, 1938.
13. MOSSMAN, RALPH W., and R. G. ROBINSON: Bending Tests of Metal Monocoque Fuselage Construction, *N.A.C.A. Tech. Note* 357, 1930.
14. FULLER, F. B., The Torsional Strength of Solid and Hollow Cylindrical Sections of Heat-treated Alloy Steel, *Jour. Aeronautical Sciences*, Vol. III, No. 7, May, 1936.
15. LUNDQUIST, E. E.: Strength Tests of Thin Walled Duralumin Cylinders of Elliptic Section, *N.A.C.A. Tech. Note* 527, 1935.
16. LUNDQUIST, E. E.: Strength Tests of Thin Walled Duralumin Cylinders in Torsion, *N.A.C.A. Tech. Note* 427, 1932.
17. MOORE, R. L.: Torsional Test of 17ST and 51SW Round Tubing, Aluminum Company of America, P.T. Nos. 31-40, 1931.
18. STANG, A. H., W. RAMBERG, and G. BACK: Torsion Tests of Tubes, *N.A.C.A. Rept.* 601, 1937.

CHAPTER XIII

DESIGN OF THIN-WALLED COLUMNS AND STRINGERS

13:1. Thin-walled Tubes as Columns.—Thin-walled tubes fail as columns in three principal ways.

1. Euler instability at large values of length-to-radius-of-gyration ratio L'/ρ , in which $L' = L/\sqrt{c}$, c being the coefficient of end fixity.
2. Instability of the walls of the tube, that is, *wrinkling*. Wrinkling is a function of radius- or diameter-to-thickness ratio r/t or D/t .
3. Plastic failure of the material. This type of failure is usually combined with the failure by instability of the walls in the low range of L'/ρ .

For the design L'/ρ , the strength of the tube as a column must be checked for strength, both for Euler *buckling* and for *wrinkling*.

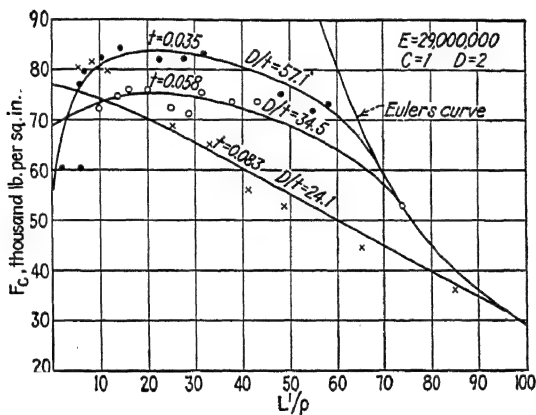


FIG. 13:1.—Typical column curves of thin-walled tubes.

13:2. Characteristics of Column Curves.—Figure 13:1 shows the theoretical and experimental characteristics of thin-walled tube-column curves. Note the following special features:

1. In the Euler range, for the same L'/ρ and for the same diameter of tube, the thinnest tube will carry the greatest unit stress P/A . For example, 2-in. by 0.035-in. steel tube has a cross-sectional area of 0.2161 sq. in. and a radius of gyration of 0.6949 in., while a 2-in. by 0.065-in. steel tube has an area 0.3951 sq. in. and a radius of gyration of 0.6845 in. Thus, while the area of the second tube is nearly double that of the first tube, the radius of

gyration of the two is about the same. Therefore, at the same L/ρ the thinnest walled tube will carry nearly twice the unit stress of the thick-walled tube.

This condition requires that the thin-walled-tube curve leave the Euler curve at a higher value than the thick-walled tube. Thus, for D/t ratios the highest values will be at the top and the lowest values will be at the bottom. Not only is this theoretically true, but the curves of Fig. 13:1, selected from a great number of experiments by the author at the University of Maryland, bear this out.

2. In the very low range of L/ρ , the tube fails by wall wrinkling. In this range the tube with the thinnest wall fails at the lowest unit stress. It is therefore, for different values of D/t , necessary for the column curves to cross each other.

13:3. ANC Column Formulas and Charts for Aluminum-alloy Tubing.—Table 13:1 shows the column formulas for round

TABLE 13:1.—ANC COLUMN FORMULAS FOR ROUND ALUMINUM-ALLOY TUBING
(Revised October, 1940)

Material	F_{ty} , lb./sq. in.	, lb./sq. in.	Short-column formula*	Critical L'/\dagger	Long-column formula*
Aluminum alloy, general.....		$\leq 200,000$			
17ST...	30,000	34,500	$34,500-245 \frac{L'}{\rho}$	94	
17ST...	40,000	42,500	$42,500-334.5 \frac{L'}{\rho}$	84	101.6×10^6
24ST...	40,000 42,000	50,000	$50,000-427 \frac{L'}{\rho}$	78	101.6×10^6
24SRT.	58,000	70,000	$70,000-707 \frac{L'}{\rho}$		101.6×10^6

* $L'/\rho = L/\rho \sqrt{c}$; L'/ρ shall not exceed 150 without specific authority from the procuring or licensing agency.

\dagger Critical L'/ρ is that above which the columns are "long" and below which they are "short."

aluminum-alloy tubing, revised October, 1940 (see Ref. 3). Note that, in the general formulas of Fig. 3:25, $n = 1$, so that a straight line represents the short-column range in each case.

Figure 13:2 shows the graphs for Table 13:1 with an added chart for critical wrinkling stress as a function of D/t . Whichever is the smaller critical value from the chart of D/t or L/ρ is the design stress.

Figure 13:3 shows the ANC design curves for aluminum-alloy streamline tubing (Ref. 3).

13:4. ANC Column Chart for Aluminum-alloy Corrugations.— Figures 13:4 and 13:5 show these column charts as given in Reference 3. See Art. 10:6 for the properties of corrugated sheet, moments of inertia, area of cross section, etc. See also column curves for corrugated sheet, Fig. 10:9. Reference 14

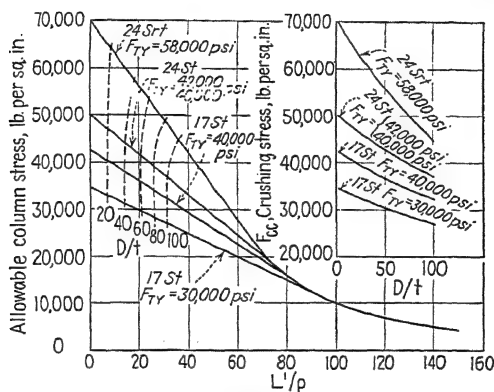


FIG. 13:2.—Allowable column and crushing stresses for aluminum-alloy round tubing.

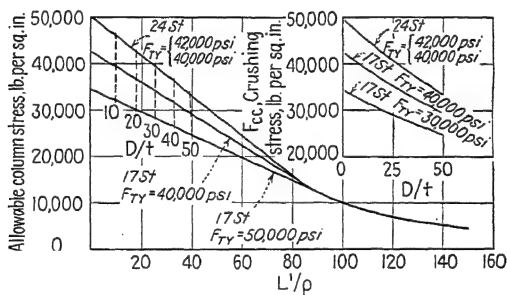


FIG. 13:3.—Allowable column and crushing stresses for aluminum-alloy streamline tubing.

is apparently the basic source of all these charts. The chart of Fig. 10:9 was recommended by Brown in this report, based on 250 to 300 tests.

13:5. ANC Column Formulas and Charts for Steel Tubing.— These formulas are shown in Table 13:2, from Reference 3.

Figure 13:6 shows the ANC curve for 1025 round steel tubing.

Figure 13:7 shows the ANC curve for chrome-molybdenum round steel tubing.

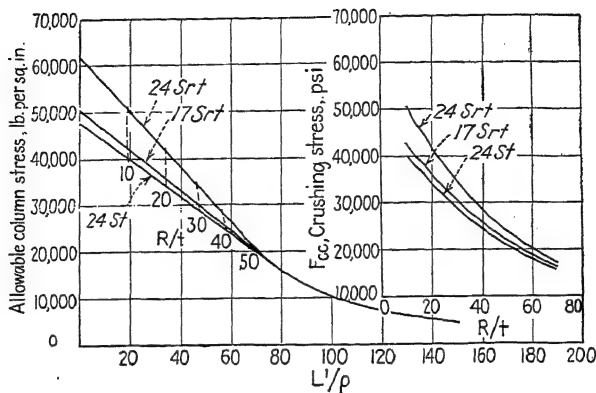


FIG. 13.4.—Allowable column and crushing stresses, corrugated aluminum-alloy sheet (circular corrugations).

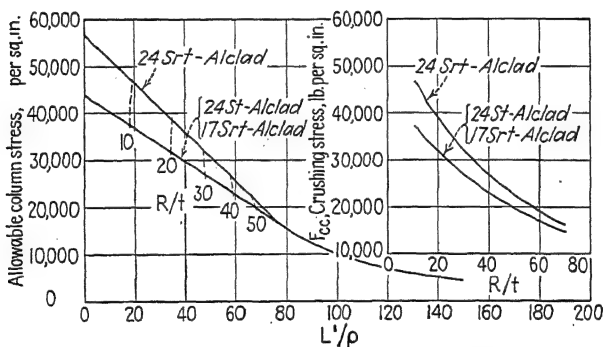


FIG. 13.5.—Allowable column and crushing stresses, corrugated aluminum-alloy sheet (aluminum covered, circular corrugation).

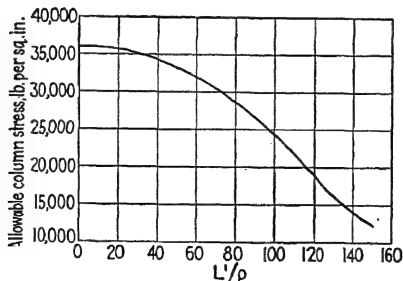


FIG. 13.6.—Allowable column stress for 1025 steel round tubing.

Figure 13:8 shows the ANC chart for chrome-molybdenum streamline tubing. $F_{TY} = 75,000$ lb. per square inch.

(F_{TY} = yield strength, lb. per square inch.)

Figure 13:9 shows the ANC chart for chrome-molybdenum streamling tubing. $F_{TY} = 85,000$ lb. per square inch.

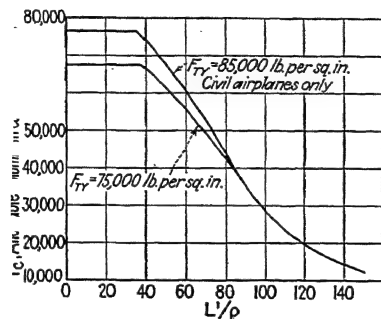


FIG. 13:7.—Allowable column stress, chrome-molybdenum round tubing.

Figure 13:10 shows the ANC column curves for heat-treated alloy steel tubing.

TABLE 13:2.—ANC COLUMN FORMULAS FOR ROUND STEEL TUBES
(Revised October, 1940)

Material	F_{co} , sq. in.	F_{TY} , lb./ sq. in.	Short-column formula*	Critical $L'†$	Long- column formula*
1025.....	36,000	36,000	$36,000 - 1.172 \left(\frac{L'}{\rho}\right)^2$	124	
X-4130.....	75,000	79,500	$79,500 - 51.9 \left(\frac{L'}{\rho}\right)^{1.5}$	91.5	$\frac{286 \times 10^6}{(L'/\rho)^2}$
X-4130.....	85,000	90,100	$90,100 - 64.4 \left(\frac{L'}{\rho}\right)^{1.5}$	86.0	$\frac{286 \times 10^6}{(L'/\rho)^2}$
Heat-treated alloy steel....	100,000	100,000	$100,000 - 8.74 \left(\frac{L'}{\rho}\right)^2$	75.6	$\frac{286 \times 10^6}{(L'/\rho)^2}$
Heat-treated alloy steel....	135,000	135,000	$135,000 - 15.92 \left(\frac{L'}{\rho}\right)^2$	65.0	$\frac{286 \times 10^6}{(L'/\rho)^2}$
Heat-treated alloy steel....	165,000	165,000	$165,000 - 23.78 \left(\frac{L'}{\rho}\right)^2$	58.9	$\frac{286 \times 10^6}{(L'/\rho)^2}$

* $L'/\rho = L/\rho \sqrt{c}$; L'/ρ shall not exceed 150 without specific authority from the procuring or licensing agency.

† Critical L'/ρ is that above which columns are "long" and below which they are "short."

Effects of Welding (ANC Requirement).—The primary failure stress of a column having welded ends can be determined from the formulas of Table 13:2 without regard to the effects of welding. These stresses, however, should not exceed a "cutoff"

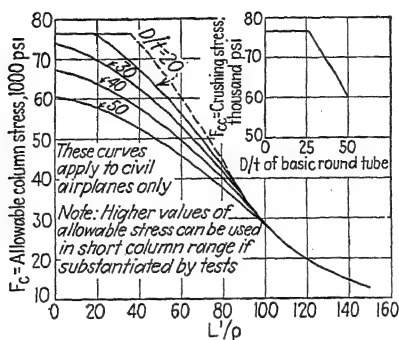


FIG. 13:8.—Allowable column and crushing stresses, chrome-molybdenum streamline tubing $F_{tu} = 75,000$ lb. per square inch.

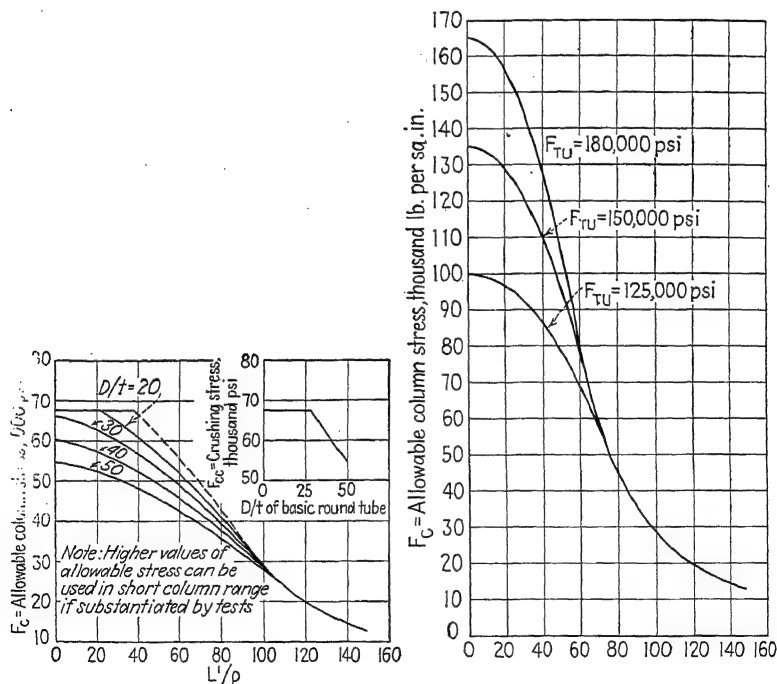


FIG. 13:9.—Allowable column and crushing stresses, chrome-molybdenum streamline tubing $F_{tu} = 85,000$ lb. per square inch.

FIG. 13:10.—Allowable column stress for heat-treated alloy-steel round tubing.

By solving equations (13:4) and (13:5) for τ , we may find τ in terms of L'/ρ or f_{cr} .

This method is used in Reference 4, based upon the formulas

$$f_{cr} = 43,700 \left(1 - 0.00752 \frac{L'}{\rho} \right) \text{ for } 41,200 > f_{cr} \\ > 19,600 \text{ lb. per square inch} \quad (13:6)$$

and

$$f_{cr} = \frac{105}{\pi^2} \quad \text{for } f_{cr} < 19,600 \text{ lb. per square inch.} \quad (13:7)$$

The last two equations are the same as (8) and (9) of Reference 9.

From equations (13:5), (13:6), and (13:7), it was found [Ref. 4, equation (19)] that

$$\frac{f_{cr}}{8,925}$$

13:10. Effective Modulus Applied to Flat Aluminum-alloy Sheet.—We may reason that, if the effective modulus $\bar{E} = \tau E$ can be applied to Euler's formula to obtain values for the plastic range, it can also be applied to the Bryan formula for flat sheet; thus [equation (11:13)],

$$\sqrt{12b(1 - \mu^2)} = \sqrt{12b^2(1 - \mu^2)} \quad (13:9)$$

or

$$\frac{f_{cr}}{12b^2(1 - \mu^2)} = \frac{f_{cr}}{12b^2(1 - \mu^2)} \quad (13:10)$$

However, it is found from tests that, in the plastic range, the flat sheet does not behave exactly as the free column. In Reference 4, it is noted that a careful study of the theory and of such experimental data as are available indicates that a conservative assumption is (for 24ST aluminum alloy)

$$\eta = \quad (13:11)$$

The coefficient η being substituted for τ in (13:9) and (13:10), thus

$$\sqrt{12b^2(1 - \mu^2)} \quad (13:12)$$

13:11. Critical Stringer Stress Based on the Flat-plate Theory.—Reference 4 gives a method and charts for computing

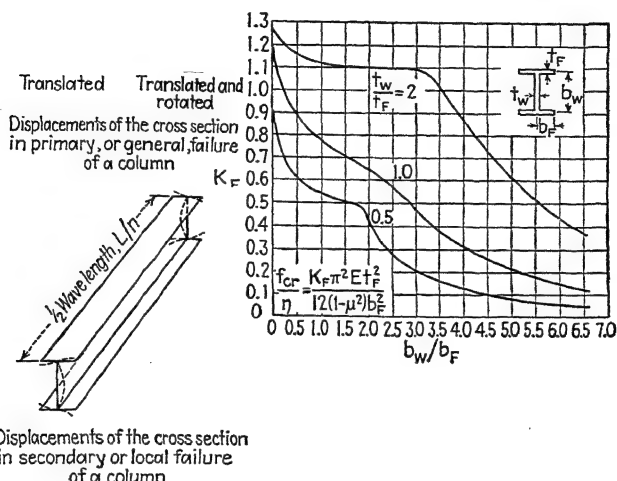


FIG. 13:16.—Minimum values of K_F for centrally loaded columns of I-section ($\mu = 0.3$).

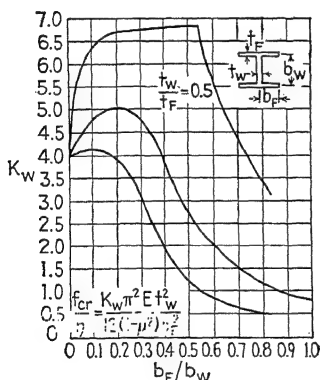


FIG. 13:17.—Minimum values of K_w for centrally loaded columns of I-section ($\mu = 0.3$).

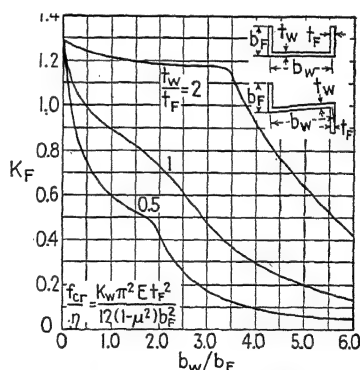


FIG. 13:18.—Minimum values of K_F for centrally loaded columns of channel section and Z-section ($\mu = 0.3$).

the critical stress in certain stringers, based on equations (13:8), (13:11), and (13:12) (see Figs. 13:16, 13:17, 13:18, 13:19, 13:20, and 13:21). An example (Ref. 4) illustrates the use of these charts:

Example.—Consider an I-section of 24ST aluminum alloy (Fig. 13:16). $b_F = 1$ in. $b_W = 2$ in. $t_F = 0.1$ in. $t_W = 0.1$ in.

Solution.—For use in Fig. 13:16, we find $b_W/b_F = 2/1 = 2$, $t_W/t_F = 0.1/0.1 = 1$. Thus, from Fig. 13:16, $K_F = 0.662$.

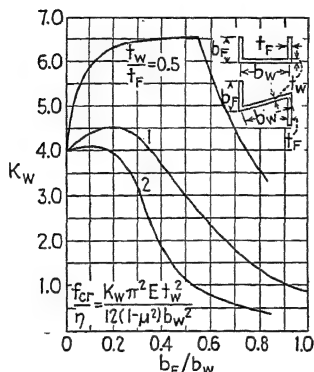


FIG. 13:19.—Minimum values of K_w for centrally loaded columns of channel section and Z-section ($\mu = 0.3$).

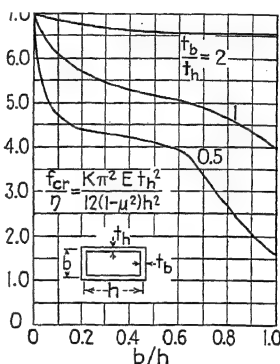


FIG. 13:20.—Minimum values of K for centrally loaded symmetrical rectangular tube ($\mu = 0.3$).

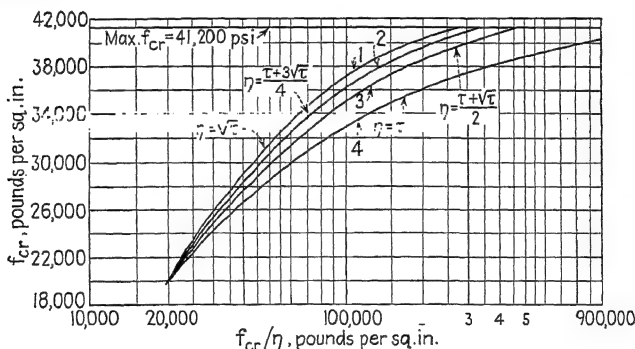


FIG. 13:21.—Variation of f_{cr} with f_{cr}/n for 24ST aluminum alloy. When $f_{cr}/n < 19,600$ lb. per square inch, $N = 1$ and $f_{cr} = f_{cr}/N$.

Taking $E = 10,660,000$ lb. per square inch and $\mu = 0.3$, we have equation (13:12),

$$\frac{f_{cr}}{\eta} = \frac{0.662 \times \pi^2 \times 10,660,000 \times (0.1)^2}{12(1 - 0.3^2) \times (1)^2} = 63,800 \text{ lb. per square inch.}$$

From curve 3 of Fig. 13:21 we find $f_{cr} = 33,000$ lb. per square inch.

13:12. Chrome-Nickel 18-8 Stainless-steel Sheet.—Figure 13:22 shows the column curve for the stainless-steel section shown in Fig. 13:23 (Ref. 12).

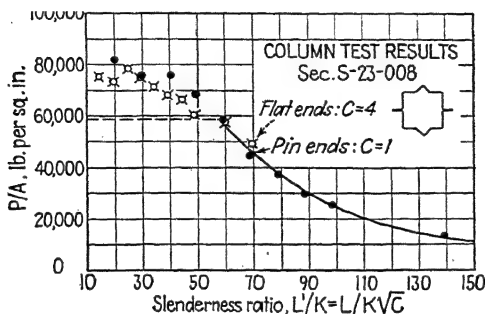


FIG. 13:22.—Stainless-steel column curve.

13:13. Application of Load to Stringers.—It is not always desirable to apply the axial load to the centroid of the cross-sectional area of the cross section of a stringer. For example, tests show that in the case of a channel (Fig. 13:24) the allowable load is greatest when the application is made near the back of the

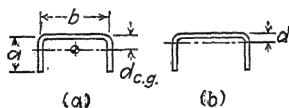


FIG. 13:23.—Section S-23-008.

FIG. 13:24.—Channel section.

channel. This is due to the backplate being supported at each edge and because the corners can be loaded to high stresses without local failure. The free edge of the channel will carry very little load. To locate the axial load so that this free edge will have no loading, see curve *B*, Fig. 13:25. If the member or fitting is riveted to the channel along the sides of the channel at a distance d from the back, the above condition of zero loading in the edge of the leg may be approximated. Note that d is determined so that the bending stresses cancel the compressive stress at the free edge.

13:14. Instability Failure of a Stringer by Twisting.—Figure 13:26a shows a bulb-angle stringer, Fig. 13:26b shows an I-section column, and Fig. 13:26c shows an assumed extruded section, to make clearer to the student the phenomenon of twisting. The

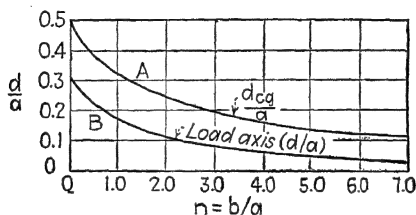


FIG. 13:25.—Properties of channels.

following analysis based on Fig. 13:26a will hold equally well for a and b and for other conditions of twisting.

If AB (Fig. 13:26c) is the cross section of a column, it is assumed, in the Euler theory, that the entire section has the same

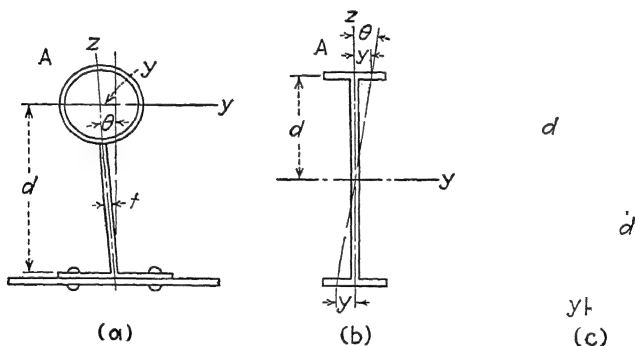


FIG. 13:26.—Failure by twisting.

deflection y . However, if the column is restrained from bending, it will twist as noted. Considering the section A of Fig. 13:26a, b , or c as an independent column subjected to a column load P that causes a deflection $y = \theta d$ and assuming no restraint, we have

$$EI \frac{d^2 y}{dx^2} + Py = 0 \text{ (moment equation)} \quad (13:13)$$

which, of course, is Euler's column equation for section A of length L . Differentiating (13:13) twice with respect to x , we

have the loading equation for the flange A , as a beam,

13:15. General Equation for Elastic Support.—However, the section A is restrained by an elastic load. Let this be w , the unit load (pounds per inch) along x . In Fig. 13:26*a*, the restraining load obviously is proportional to y . In fact, if the web of thickness t is assumed to run to the center of A , using the formula for the deflection of a cantilever beam, we have

$$y = \frac{wd^3}{6EI} \text{ per inch along } x$$

so that

$$(13:15)$$

where I_w per unit length is $1xt^3/12$. In general terms, we assume

$$w = Ky = K\theta d \quad (13:16)$$

where θ is the angle of twist in radians. Thus, adding $(-Ky)$ to the right-hand side of (13:14), we have

$$(13:17)$$

Thus, letting,

$$j^2 = \frac{r}{EI} \quad \text{and} \quad n^4 = \frac{\Lambda}{EI} \quad (13:18)$$

we have the equation

$$(13:19)$$

13:16. Solution of the Equation.—Equation (13:19) is a differential equation quite common in mechanics and elementary mathematics. The solution, which may be found in most texts on differential equations, is

$$y = A \cosh px + B \sinh px + C \cos qx + D \sin qx \quad (13:20)$$

where

$$p = \frac{1}{2} \sqrt{-j^2 + \sqrt{j^4 - \Lambda}} \quad \text{and} \quad q = \frac{1}{2} \sqrt{j^2 + \sqrt{j^4 - \Lambda}} \quad (13:21)$$

If L is the length of the pin-ended column, or the distance between points of inflection of the waves into which member A bends, we have the limits

(a) When $x = 0$, the bending moment is zero, requiring that $\frac{d^2y}{dx^2} = 0$

(b) When $x = L$, $\frac{d^2y}{dx^2} = 0$

(c) When $x = 0$, $y = 0$

(d) When $x = L$, $y = 0$

Thus, substituting the limits (a), (b), (c), and (d), we find the critical buckling load

$$qL = m\pi \quad (13:22)$$

For the minimum, load $m = 1$. Thus, we find

$$j^2 = \frac{\pi^2}{L^2} + \frac{\pi^2}{\pi^2} \quad (13:23)$$

Then, substituting the values of j and n , we have

$$P = \frac{\pi^2 EI}{L^2} + K \frac{L^2}{\pi^2} \quad (13:24)$$

13:17. Euler's Load for Bulb Angle.—We note [equation (13:15)] that, for the bulb angle (Fig. 13:26a),

$$K =$$

Thus,

$$L^2 + \quad (13:25)$$

where L is the distance between points of inflection of the bulb section A . If the stringer is held rigid at the bulkheads and D is the distance between the bulkheads, the distance between the points of inflection is $L = D/2$.

In the plastic range the tangent modulus \bar{E} may be substituted for the E in the Euler term of the equation. The second E refers to the bending of the web sideways and hence is not affected much by the axial load.

13:18. Wave Length of Twist and Critical Load.—To find the wave length, we find L for the minimum value of P . Thus,

$$\frac{dP}{dL} + 2KL \quad (13:26)$$

from which

$$L^2 = \pi^2 \sqrt{\frac{EI}{K}} \quad (13:27)$$

Thus [equation (13:24)],

$$P = - \frac{\pi^2 EI}{L^2} + \frac{K}{\pi^2} \pi^2 \sqrt{\frac{EI}{K}} = 2 \sqrt{KEI} \quad (13:28)$$

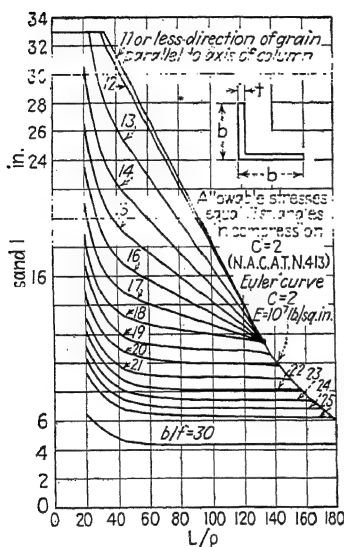


FIG. 13:27.—Allowable stresses equal 17ST angles in compression for $C = 2$.

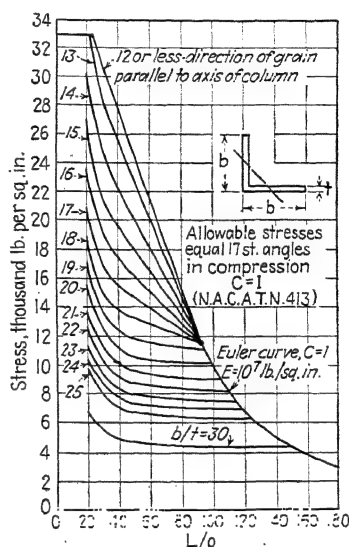


FIG. 13:28.—Allowable stresses equal 17ST angles in compression for $C = 1$.

Therefore, for the bulb angle (Fig. 13:26a), in which the stringers are not attached to the bulkheads, substituting the value of K from $Et^3/4d^3$, we have

$$P = \quad = E \quad (13:29)$$

13:19. Angle Sections under Compression.—Figures 13:27 and 13:28 show the allowable compressive stress for equal-leg-angle sections of 17ST aluminum alloy.

References

1. NEWELL, J. S., and J. H. HARRINGTON: Progress Report on Methods of Analysis Applicable to Monocoque Aircraft Structures, *Air Corps Tech. Rept. 4313*, 1937.

2. YOUNGER, J. E., consulting editor, "Aircraft Tubing Data," Summerill Tubing Company, Bridgeport, Pa., 1941.
3. "Strength of Aircraft Elements," A.N.C.-5 Handbook, Government Printing Office, Washington, D.C., October, 1940.
4. STOWELL, E. Z., and E. E. LUNDQUIST: Local Instability of Columns with I-, Z-, Channel, and Rectangular-tube Sections, *N.A.C.A. Tech. Note* 743, 1939.
5. OSGOOD, W. R.: The Double-modulus Theory of Column Action, *Civil Engineering*, Vol. V, No. 3, pp. 173-175, March, 1935.
6. LUNDQUIST, E. E., and C. M. FLIGG: A Theory for Primary Failure of Straight Centrally Loaded Columns, *N.A.C.A. Tech. Rept.* 582, 1937.
7. LUNDQUIST, E. E.: On the Strength of Columns that Fail by Twisting, *Jour. Aeronautical Sciences*, Vol. IV, No. 6, pp. 249-253, April, 1937.
8. TIMOSHENKO, S.: Theory of Elastic Stability, McGraw-Hill Book Company, Inc., New York, 1936.
9. OSGOOD, WILLIAM R., and M. HOLT: The Column Strength of Two Extruded Aluminum-alloy H-sections, *N.A.C.A. Tech. Rept.* 656, 1939.
10. LUNDQUIST, E. E.: Local Instability of Symmetrical Rectangular Tubes under Axial Compression, *N.A.C.A. Tech. Note* 686, 1939.
11. LUNDQUIST, E. E.: Local Instability of Centrally Loaded Column of Channel Section and Z-section, *N.A.C.A. Tech. Note* 722, 1939.
12. BARLOW, H. W.: The Column Strength of Closed, Thin-walled Sections of 18-8 Stainless Steel, *Jour. Aeronautical Sciences*, Vol. VIII, No. 4, pp. 151-161, February, 1941.
13. GOTTLIEB, R., T. M. THOMPSON, and E. C. WITT: Combined Beam-column Stresses of Aluminum Alloy Channel Sections, *N.A.C.A. Tech. Note* 726, 1939.
14. BROWN, C. G.: The Column Properties of Corrugated Aluminum Alloy Sheet, *Airplane Dept. Mem.* 110, Wright Field, Dayton, Ohio, 1930.
15. SHANLEY, F. R.: Engineering Aspects of Buckling, *Aircraft Engineering (London)*, Vol. XI, No. 119, pp. 13-20, January, 1939.

CHAPTER XIV

TORSIONAL RIGIDITY OF WING BOX BEAMS

14:1. Historical Note.—In 1927, in connection with the aluminum-alloy construction development program, the author wrote as follows (Ref. 3):

The structural success of large cantilever monoplanes depends primarily on the torsional and flexural rigidity of the wings, assuming that the strength requirements have been met. Of these two stiffness characteristics the torsional rigidity is the more important, since it is this characteristic which determines the uniformity of the angle of attack and the tendency to flutter. Adequate torsional rigidity, it appears, is intimately associated with stiff wing covering, that is, covering such as plywood, duralumin, or steel sheet designed integral with the primary trussing of the wing.

Apparently very little attention has been given to the prediction and requirements of torsional rigidity of wings, notwithstanding that some of the outstanding disasters in aviation may be traced to that source. This may be due to the apparent complexity of the problem. It is apparently complex because the problem is relatively new and very little thought the results of which have been made available for general use has been given to the subject. It may be safely predicted, however, that, in time, methods will be developed which will make the analysis of torsional rigidity simpler and more accurate than our present strength calculations. This is probable because rigidity involves low stresses, far below the proportional limit, while strength involves the modulus of rupture of the material, a very uncertain quantity.

14:2. Fundamental Principles.—In approaching the subject of torsional rigidity and strength, we must study first the fundamental principles involved. To do this, we consider the simplest and most conventional case, that of the box beam. With the fundamental principles well established, the limitations of the theory noted and supplemented by experimental data, and the theory simplified as far as possible, consistent with the desired degree of accuracy, the more complicated wing structure may then be attacked logically, consistently, and with confidence.

As in many cases of mathematical analysis, the results are difficult of application. It is not the result that is important to the student, but rather the study of the relationship among the quantities, characteristics, and dimensions of a given structure. In the process of studying the analysis involved, the student must, of necessity, study this relationship, a knowledge of which is of primary importance in design.

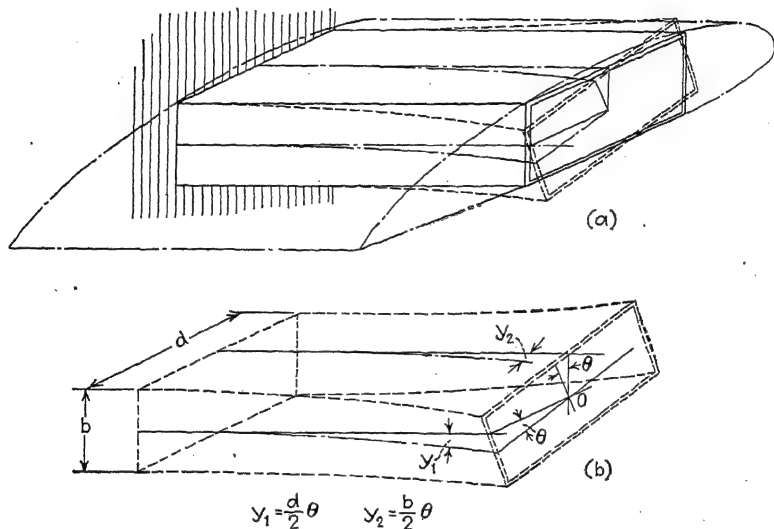


FIG. 14:1.—Twisted box spar.

For the conditions on which the following analyses are based, the final equations, below the elastic limit, undoubtedly express quite accurately the deformations and stresses. In dealing with special cases and structures that are not exactly like those on which the analyses are based, the student must be prepared to formulate his own judgment according both to theory and experiment. This is true for any mathematical analysis.

14:3. Equations of Equilibrium.—With reference to Fig. 14:1, we assume an airplane wing built about a single box spar with uniform cross section, as noted in the figure. We propose to predict the stresses in tension, compression, and shear in the web and flanges of the beam together with the deflection, due to resultant aerodynamic couple and force.

We note in Fig. 14:1 and in Art. 9:21 that, as the beam is twisted through an angle θ , each of the four sides is subjected to two types of stress, namely, pure bending stresses (tension and compression) and pure shear due to the interaction at the corners. We may state, then, that the impressed bending moment (that created by the aerodynamic forces) on any side is balanced by an internal bending moment composed of the sum of the moments resulting (1) from the extension and compression of the fibers and (2) from the resultant shear at the corners. We shall designate this impressed bending moment by M_1 for the narrow side of the beam and M_2 for the broad side. We note that

$$\frac{dM_1}{dx} = V \quad \text{and} \quad \frac{dM_2}{dx} = V \quad (14:1)$$

where V is the shear caused by the aerodynamic load. These shears are the result of an applied torque Q . Thus,

or

$$Q = V_1 d + V_2 b \quad (14:2)$$

where d = distance between the neutral planes of the narrow sides.

b = distance between the neutral planes of the broad sides.

Q , of course, is determined from the airfoil characteristics.

The internal moment resulting from the extension and compression of the fibers we denote by M_b and note that M_b may be expressed in terms of the stress in the outer fiber as

$$M_{1b} = \frac{f I_1}{b/2} = \frac{2f I_1}{b} \quad (14:3)$$

and

$$\frac{f I_2}{d/2} = - \frac{2f I_2}{d} \quad (14:4)$$

where f = tensile or compressive stress per unit area.

I = moment of inertia of the cross section of the side in the plane of bending.

As in preceding and succeeding equations the subscript 1 refers to the narrow side, and the subscript 2 refers to the broad side.

$$\frac{d}{dx} = -\frac{2I_2}{d} \frac{df}{dx} + Fd \quad (14:11)$$

Multiplying (14:10) by d and (14:11) by b and adding to satisfy equation (14:2), we have

Since

$$I_1 = \frac{t_1 d^3}{12} \quad \text{and} \quad \frac{t_2 b^3}{12} \quad (14:14)$$

where t is the thickness of the sides, equation (14:13) becomes

$$(14:15)$$

It will be noted that the sign of f in equation (14:8) is arbitrary. Thus, the term $(t_1 b - t_2 d)$ of equation (14:15) might as well arbitrarily have been written $(t_2 d - t_1 b)$. From the nature of the problem the resultant effect of any tension or compression developed due to the torsion Q must act to oppose Q . It is thus obvious that the sign of $(t_1 b - t_2 d)$ or $(t_2 d - t_1 b)$ must always be positive. In other words, we are concerned only with the absolute value.

14:7. Special Cases of Torsion.—We observe that $t_1 b$ is the area of the cross section of the narrow side and $t_2 d$ is the area of the cross section of the broad side. When the areas of the two sides are equal, the tension and compression term drops out of equation (14:15) and

$$Q = 2b \, dF \quad (14:16)$$

If s is the shear per unit area,

$$F = t \quad (14:17)$$

We note that (bd) is approximately the average area bounded by the outer and inner curve of the box beam. For instance, if we let A_1 represent the area bounded by the outer curve, the magnitude of A_1 is $(b + t_2)(d + t_1)$; and if we let A_2 represent the area bounded by the inner curve, the magnitude of A_2 is $(b - t_2)(d - t_1)$. We have, therefore,

$$A = A_1 = bd + \quad (14:18)$$

and since t_2 and t_1 are very small in comparison with bd , we can neglect $t_2 t_1$ without appreciable error. The formulas

$$Q = 2b \, dF = 2At_1 s_1 = 2At_2 s_2 \quad (14:19)$$

or

$$\tau = \frac{Q}{A} \quad \text{and} \quad (14:20)$$

are standard for computing the shear stress in thin-walled tubes and beams.

14:8. Bending Combined with Torsion.—To evaluate the stresses f and F in equation (14:15), we make use of the following relations:

The resultant of the shearing force at each corner parallel to the axis of the beam is zero; that is,

$$F = \text{constant} \quad (14:21)$$

where F has the values previously assigned.

To obtain other equations for the evaluation of the stresses, we now study the deformation at the edges of the box beam in a length Δx . Referring to Fig. 14:2, we note that, if the narrow side were not restrained by the broad side at the edge, the element of length Δx , noted as (CA) , would be extended a length ϵ_1 . A similar length on the broad side would be compressed a length ϵ_2 , so that the total displacement would be the sum of ϵ_1 and ϵ_2 . This is made clear in Art. 9:21. From similar triangles EOD and ADB , we have

$$\rho_1 : \Delta x = \frac{b}{2} : \epsilon_1 \quad (14:22)$$

where ρ_1 is the radius of curvature. Approximately, and according to the usual assumption in beam theory,

$$\rho_1 = \frac{b}{d^2 y_1 / dx^2} \quad (14:23)$$

We thus obtain, from (14:22),

$$\epsilon_1 = \frac{b}{2} \frac{d^2 y_1}{dx^2} \Delta x \quad (14:24)$$

In a similar manner, we obtain, for the broad side,

$$d \frac{d^2 y_2}{x^2} \Delta \quad (14:25)$$

14:9. Bending in Terms of Angle of Rotation.—For a small angle of rotation, we note from Fig. 14:1 that

$$\text{and} \quad y_2 = \theta \frac{U}{2} \quad (14:26)$$

which substituted in (14:24) gives

$$bd \, d' \quad (14:27)$$

and in (14:25) gives

$$bd \, d^2 \theta \quad (14:28)$$

14:10. Resultant Deformation at Corners.—Now, considering the sides of the beam continuous at the edges, we note that a total deformation in the material must be affected an amount ϵ , as shown in Art. 9:21,

$$\epsilon = \epsilon_1 + \quad (14:29)$$

This deformation induces in the material a tensile or compressive stress by extending or compressing the fibers and a shear stress by sliding the layers parallel to the neutral axis of each side relative to points on the neutral axis. For instance, in Fig. 14:2, in which is assumed no shear at the edge, the tensile stress is

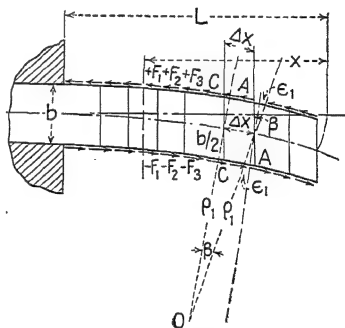


FIG. 14:3.—Bent beam, no extension or compression of fibers.

while, in Fig. 14:3, we have assumed a shear force F of sufficient magnitude to maintain the distance Δx , (CA), constant, so that there is no extension or compression of the fibers. In this case the extended length $\Delta x + \epsilon_1$ has been returned to its original length Δx . This shear deformation, which we shall hereafter designate as ϵ_s , in this special case is equal to ϵ_1 . The shear force F required to create this deformation is found in the following manner: Representing the shear modulus of elasticity by E_s , we have, by definition,

$$E_s = \frac{\text{average shearing stress}}{\text{average shearing strain}} \\ = \left(\frac{\Delta F}{2} \div t_1 \right) \div \left(\frac{\epsilon_s}{2} \div \frac{b}{2} \right) \Delta F$$

Since $\Delta F = \frac{\partial F}{\partial x} \Delta x$,

$$E_s = \frac{b}{2t_1\epsilon_s} \frac{\partial F}{\partial x} \Delta x \quad (14:31)$$

and so

$$\frac{\partial F}{\partial x} = \frac{2E_s t_1 \epsilon_s}{b \Delta x} \quad (14:32)$$

and

$$\frac{b \Delta x}{\partial x} \frac{\partial F}{\partial x} \quad (14:33)$$

14:11. Combined Deformation at Edge.—The combined deformation at the edge is the sum of the deformation ϵ_1 due to bending and ϵ_s due to shearing. Thus,

$$\frac{E}{\Delta x} (\epsilon_1 \quad (14:34)$$

Thus, substituting the values of ϵ_1 and ϵ_s from equations (14:27) and (14:33), we have

$$\frac{E}{\Delta x} \left(\frac{bd}{4} \frac{\partial^2 \theta}{\partial x^2} \Delta x + \frac{b \Delta x}{2E_s t_1} \frac{\partial F}{\partial x} \right) \\ \frac{Ebd}{4} \frac{\partial^2 \theta}{\partial x^2} + \frac{Eb}{2E_s t_1} \frac{\partial F}{\partial x} \quad (14:35)$$

We can now write the equation for the broad side of the beam similar to (14:35) by noting that f will be opposite in sign and b and t_1 will be replaced by d and t_2 , respectively. Thus,

$$\frac{Ed}{4} \frac{\partial^2 \theta}{\partial x^2} - \frac{Ed}{2E_s t_2} \frac{\partial F}{\partial x} \quad (14:36)$$

14:12. Torsional Moment in Terms of Bending and Shear Stresses.—From equation (14:15) we note that

$$Q = \frac{bd}{6} (t_1 b - t_2 d) \frac{\partial f}{\partial x} + 2b \, dF \quad (14:37)$$

from which

$$(14:38)$$

letting $\partial Q/\partial x = q$, constant, the distributed torque,

$$\frac{\partial F}{\partial x} = \frac{q}{2bd} - \frac{1}{12} (t_1 b - t_2 d) \frac{\partial^2 f}{\partial x^2} \quad (14:39)$$

14:13. Bending Stress in Terms of Angle of Twist.—Upon substituting (14:39) in (14:35), there results

$$\begin{aligned} & 2\theta \quad Eb \\ & \frac{Ebd}{4} \frac{\partial^2 \theta}{\partial x^2} \quad qE \quad \frac{\sigma_y}{2\alpha^2} \end{aligned} \quad (14:40)$$

Upon substituting (14:39) in (14:36), there results

$$\begin{aligned} f &= -\frac{Ebd}{4} \frac{\partial^2 \theta}{\partial x^2} - \frac{Ed}{4} \\ &= -\frac{Ebd}{4} \frac{\partial^2 \theta}{\partial x^2} - \frac{qE}{4} - t_2 d \frac{\sigma_y}{2\alpha^2} \end{aligned} \quad (14:41)$$

Multiplying (14:40) by d/t_2 and (14:41) by b/t_1 and adding the resulting equations, we eliminate the term involving $\partial^2 f/\partial x^2$, obtaining

$$= \frac{Ebd}{4} \left(\frac{t_1 d - t_2 b}{t_1 d + t_2 b} \right) \frac{d^2 \theta}{dx^2} = e \frac{d^2 \theta}{dx^2}$$

where $e = \frac{Ebd}{4} \left(\frac{t_1 d - t_2 b}{t_1 d + t_2 b} \right)$

Before proceeding further, it should be noted that the sign of f in equation (14:35) is arbitrarily selected. We assume f to be of opposite sign to the radius of curvature on the narrow side. This requires that $(t_1 d - t_2 b)$ in equation (14:42) always be positive.

14:14. Shear Stress in Terms of Angle of Twist.—Taking the derivative of (14:42) with respect to x and substituting it in equation (14:38), we obtain the value of F .

$$F = \frac{Ebd}{2bd} - \frac{1}{12} \left(\frac{Ebd}{4} \right) \left(\frac{t_1 d - t_2 b}{t_1 d + t_2 b} \right) \frac{d^3 \theta}{dx^3} \quad (14:43)$$

Letting

$$\frac{E(bd)^2(t_1 b - t_2 d)(t_1 d - t_2 b)}{4(t_1 d + t_2 b)} \quad (14:44)$$

we have

$$F = \frac{Q}{2bd} - \frac{1}{2b} \frac{d^3 \theta}{dc \, dx^3} \quad (14:45)$$

We note that the product $(t_1b - t_2d)(t_1d - t_2b)$ must always be written with a positive sign; that is, the designation of the sides must be chosen so as to make this product positive.

To obtain the angle of twist θ , we equate equations (14:40) and (14:41) and substitute the value of $\partial^2 f / \partial x^2$ from (14:42). We thus obtain

$$\frac{d^4 \theta}{dx^4} = cq \quad (14:46)$$

where

$$\frac{48E_s t_1 t_2}{E(t_1 b - t_2 d)(t_1 d - t_2 b)} \quad (14:47)$$

and

$$c = \frac{24(t_1 d + t_2 b)}{t_1 d - t_2 b} \quad (14:48)$$

We note that n^2 and c are always given a positive sign.

14:15. Solution of the General Equation.—In the solution that follows, the following combination of constants occurs:

$$\frac{ce}{n^2} = \frac{E(t_1 d - t_2 b)}{t_1 d} \quad (14:49)$$

$$c = \frac{t_1 d}{t_1 d - t_2 b} \quad (14:50)$$

The solution of (14:46) as can be verified by trial or reference to any text on differential equations is

$$= A \cosh nx + B \sinh nx + \frac{cq}{n^2} \quad (14:51)$$

Equation (14:51) is the general equation of the angle of twist of a box beam of uniform cross section loaded with a uniform torque of q in.-lb. per inch. In the special cases that follow, we shall take the origin at the tip of the cantilever overhang.

14:16. Cantilever Beam, Concentrated Torque, Q , at Tip.—In this case, $dQ/dx = q = 0$; thus, (14:46) becomes

$$\frac{d^4 \theta}{dx^4} - n^2 \frac{d^2 \theta}{dx^2} = 0 \quad (14:52)$$

the solution of which is

$$\frac{d^2 \theta}{dx^2} = A \cosh nx + B \sinh nx \quad (14:53)$$

The boundary limits are as follows:

$$(a) \text{ When } x = 0, \quad f = 0$$

$$(b) \text{ When } x = L, \quad F = 0$$

which require, from equation (14:42), that

$$(a) \text{ When } x = 0, \quad \frac{d^2\theta}{dx^2} = 0$$

and, from (14:45), that

$$(b) \text{ When } x = L, \quad \frac{d^2\theta}{dx^2} = cQ$$

The limit (a) gives

$$\frac{d^2\theta}{dx^2} = B \sinh \quad (14:54)$$

The limit (b) gives $B = \frac{c}{n} \frac{Q}{\cosh nL}$; so

$$\frac{d^2\theta}{dx^2} = \frac{Q}{n \cosh nL} \sinh \quad (14:55)$$

Substitution of this value of $d^2\theta/dx^2$ in (14:42) gives the stress

$$f = Q \frac{ce}{n \cosh nL} \frac{nx}{nL} \quad (14:56)$$

and

$$\frac{\cosh nx}{\cosh nL} \quad (14:57)$$

in equation (14:45) gives

$$F = \frac{Q}{2bd} - \frac{Q}{\cosh nL} \frac{\cosh nx}{\cosh nL} \quad (14:58)$$

$$= \frac{Q}{2bd} \left(1 - \frac{\cosh nx}{\cosh nL} \right) \quad (14:59)$$

14:17. Angle of Twist.—The angle of twist is found as follows: Integrating equation (14:54), we obtain

$$\frac{d\theta}{dx} = \frac{B}{n} \cosh nx + \quad (14:60)$$

$$= \frac{B}{n^2} \sinh nx + Dx + \quad (14:61)$$

The limits are as follows: When $x = L$, $d\theta/dx = 0$; and when $x = L$, $\theta = 0$. The value of B is given by equation (14:55). Thus,

$$Q \left(\frac{\sinh}{\cosh nL} \right) = \frac{c}{n^2} Q(L - x) \quad (14:62).$$

14:18. Cantilever Beam, Uniformly Distributed Load.—Equation (14:51) is the solution of this case. The limits are as follows: (a) When $x = 0$, $f = 0$; (b) when $x = L$, $F = 0$. These require (a) [equation (14:42)] that when $x = 0$,

and (b) [equation (14:45)] that when $x = L$, $d^2\theta/dx^2 = cQ$. The limits (a) and (b) give, respectively,

$$\nu = \frac{1}{n \cosh nL} + \frac{1}{n^2 \cosh nL}$$

Thus,

$$\frac{d^2\theta}{dx^2} = \frac{cq}{n^2} \left[1 - \frac{\cosh n(L-x)}{\cosh nL} + \frac{nL \sinh nx}{\cosh nL} \right]$$

14:19. Bending Stress.—Substituting equation (14:64) in (14:42) gives

$$\frac{-t_2b}{t_1t_2bd} \left[1 - \frac{\cosh n(L-x)}{\cosh nL} + \frac{nL \sinh nx}{\cosh nL} \right] \quad (14:65)$$

14:20. Shear Stress.—Differentiating (14:64), we have

$$cq \left[\frac{n \sinh n(L-x)}{\cosh nL} + \frac{n^2L \cosh nx}{\cosh nL} \right] \quad (14:66)$$

Substituting in equation (14:45),

$$F = \frac{qx}{\cosh nL} - \frac{q}{\cosh nL} \left[\frac{\sinh n(L-x)}{\cosh nL} + \frac{nL \cosh nx}{\cosh nL} \right] \quad (14:67)$$

14:21. Angle of Twist, Uniform Torque.—Integrating equation (14:64), we obtain

$$\theta = \frac{cq}{n^2} \left[\frac{x^2}{2} - \frac{\cosh n(L-x)}{n^2 \cosh nL} + \frac{nL \sinh nx}{n^2 \cosh nL} \right]$$

The limits are (a) when $x = L$, $d\theta/dx = 0$; (b) when $x = 0$, $\theta = 0$. Thus,

$$= \frac{cq}{\cosh} \frac{\cosh n(L-x)}{\cosh} \frac{nL \sinh nx}{\cosh nL} \quad (14:69)$$

14:22. Other Types of Loading.—If the torque on the cantilever wing is distributed, $q = f(x)$, thus,

$$Q = \int f(x) dx \quad (14:70)$$

If this value of Q is used in the derivation of the general equation (14:46) and in the subsequent analyses, equations may be derived for various types of loading.

14:23. Applications.—The foregoing analysis of a box beam was completed by the author in 1928 in connection with the early development of shell construction at Wright Field, 1926 to 1930. The report was not published but appeared in blueprint form as Airplane Branch, Airplane Department Memorandum 1023. The analysis does not apply very well to our present, very thin, wrinkling structures. It appears, however, that the heavy structures of the future, completely welded, may be subject, with fair accuracy, to an analysis of this nature.

References

1. REISSNER, H.: Neuere Probleme aus der Flugzeugstatik, *Z.F.M.*, Vol. XVII, No. 18, pp. 384–393, Sept. 28, 1926; Vol. XVIII, No. 7, pp. 153–158, Apr. 14, 1927.
2. GREENE, C. F., and J. E. YOUNGER: Metal Wing Construction, Part I, Experimental Studies and Discussion, *A.C.T.R. Ser. 3361, Material Div., U.S. Army Air Corps*, 1929.
3. YOUNGER, J. E.: Metal Wing Construction, Part II, Mathematical Investigations, *A.C.T.R. Ser. 3288, Material Div., U.S. Army Air Corps*, 1930.
4. ATKIN, E. H.: Stresses in Metal-covered Planes, *Aircraft Engineering*, Vol. V, No. 53, pp. 162–164, July, 1933.
5. EBNER, HANS: Torsional Stresses in Box Beams with Cross Sections Partially Restrained against Warping, *N.A.C.A. Tech. Note 744*, 1934.
6. KUHN, PAUL: Analysis of 2-spar Cantilever Wings with Special Reference to Torsion and Load Transference, *N.A.C.A. Tech. Note 508*, 1935.

CHAPTER XV

INTRODUCTION TO CANTILEVER-WING ANALYSIS

15. 1. Applied Loads.—The determination of the distribution of air loading on a cantilever wing for the various assumed or required design conditions is a problem in aerodynamics. If the engineer is confident that government requirements, in this respect, are sufficiently accurate for design purposes, he may proceed with load calculation as specified in the requirements.

In using required loading conditions for design purpose, the student should consider carefully the following problems:

1. *The distribution of the air load on a twisted wing.*—In such a wing, the angle of attack varies with the semi-span. Wings are sometimes designed twisted so that all sections experience a maximum ratio of lift to drag at the same time or so that all sections experience a maximum lift at the same time. It is apparent, in this case, that the air-load distribution with respect to the semi-span is a function of the angle of attack at the section under consideration.

2. *The distribution of air load on a wing the cross section of which varies with the semi-span.*—Such a wing is one that varies in chord and ordinate-chord ratio. The wing will have a thick cross section at the root and a thin cross section at the tip.

3. *The redistribution of the air load on the wing because of twisting in the wing.*—It has been the usual practice to assume wings to twist, in calculating the distribution of loads on wing spars, without taking into consideration the aerodynamic effect of such twisting. It is suggested that, where the twist of a wing is appreciable, a careful investigation concerning its flutter tendencies should be carried out.

15.2. Resolution of Wing Loading into a Force and a Couple.—It appears more logical and simple to analyze a cantilever wing from the standpoint of pure bending and pure torsion, and then to add the resulting stresses algebraically, than to analyze it from the standpoint of spar-distribution loading based on spar rigidity in bending. The old method is based on the assumption that the

rigidity of the wing in torsion depends solely on the spar rigidity in bending. As a matter of fact the *spars of modern airplane wings of the cantilever type contribute, in general, only a very small percentage of the torsional rigidity of the wing.*

The principle involved in the proposed method of analysis is that of the resolution of a force into a force and a couple. For example, as noted in Fig. 15:1, the load W of a , applied x -distance in front of O , may be resolved into a load W through O and a couple Wx about O . Now, if, when the load W is applied at O , no twisting in the wing results, the wing may be analyzed for stresses in pure bending caused by the load W and for stresses in pure torsion caused by the couple Wx . The algebraic sum of the stresses for the two conditions will then be the net design stresses.

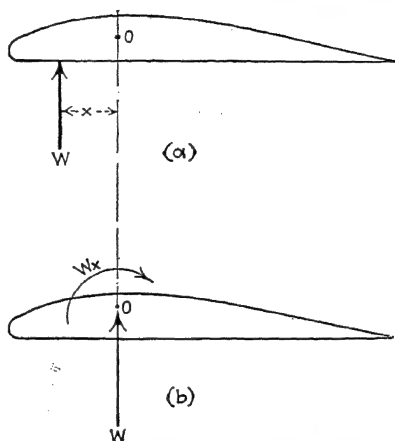


FIG. 15:1.—Resolution of wing loading into load through, and torque about, elastic axis.

15:3. Elastic Axis.—*The elastic axis of a cantilever wing is a line approximately parallel to the spars, along which a load may be applied without inducing a twist in the wing. Also, we may define it as the axis about which the wing rotates when subjected to a couple. This axis, the student will note, is that indicated by O in Fig. 15:1.*

The elastic axis of a wing may be determined quite readily by experimental methods. In simple cases, the axis may be determined by theoretical methods for stresses below the elastic limit of the material. If, however, the wing is quite rigid in torsion, as, for example, a "stressed-skin wing,"—one that carries the flying load in the skin—very little error will be involved in determining the elastic axis approximately. The student may note that, for a two-spar wing, the location of the elastic axis is not necessary, except for computing the couple, since, when such a wing is subjected to a couple, the spar loads form a couple. The spar loadings induced by the couple will therefore be equal and

opposite. It follows, of course, from this statement that the bending moments are equal and opposite.

15:4. Location of Elastic Axis.—To fix ideas and to illustrate a method of analysis, let us consider the simple case shown in Fig. 15:2.

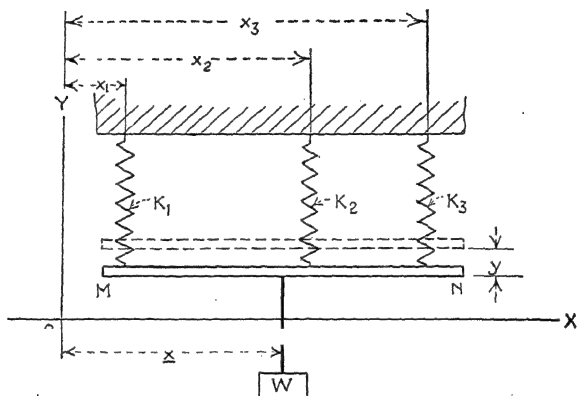


FIG. 15:2.—Elements of elastic axis.

The weight W is being carried by three elastic springs of spring constants k_1, k_2, k_3 . We are to find x so that

$$y_1 = y_2 = y_3 \quad (15:1)$$

Letting w_1, w_2 , and w_3 represent the loads carried respectively by each spring, we have

$$\Sigma F_y = 0$$

or

$$W = w_1 + w_2 + w_3 \quad (15:2)$$

Also,

$$\Sigma M_o = 0$$

or

$$W\bar{x} = w_1x_1 + w_2x_2 + \quad (15:3)$$

From equation (15:1) we find

$$(15:4)$$

Now three equations of the type represented by equations (15:2), (15:3), and (15:4) are sufficient and necessary to solve for \bar{x} ,

locating the elastic axis. From equation (15:4) we have

$$w_2 = \frac{k_2}{k_1} w_1 \quad \text{and} \quad w_3 = \frac{k_3 w_1}{k_1} \quad (15:5)$$

Substituting equations (15:5) and (15:2) in (15:3), we have

$$\bar{x} = \frac{w_1 x_1 + \frac{k_2}{k_1} w_1 x_2 + \frac{k_3}{k_1} w_1 x_3}{w_1 + \frac{k_2}{k_1} w_1 + \frac{k_3}{k_1} w_1}$$

Simplifying,

$$\bar{x} = \frac{k_1 x_1 + k_2 x_2 + k_3 x_3}{k_1 + k_2 + k_3} \quad (15:6)$$

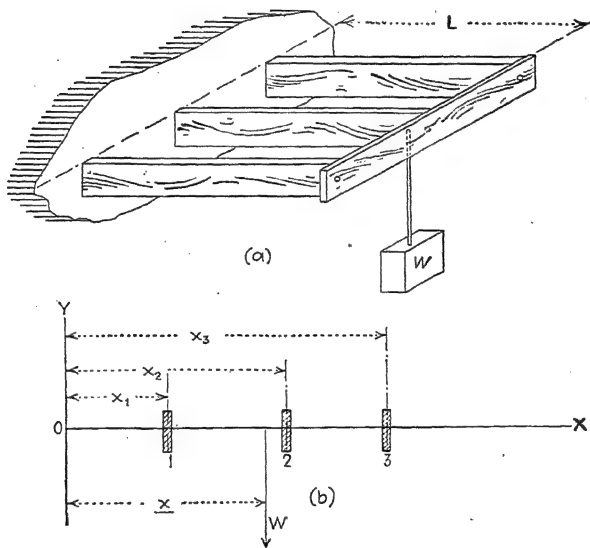


FIG. 15:3.—Elastic axis of three uniform spars.

Let us now consider the case of three spars, as illustrated in Fig. 15:3. Writing equations similar to (15:2), (15:3), and (15:4), we have

$$\Sigma F_y = 0$$

or

$$W = w_1 + w_2 + w_3 \quad (15:7)$$

Also,

$$\Sigma M_0 = 0$$

or

$$W\bar{x} = w_1x_1 + w_2x_2 + w_3x_3 \quad (15:8)$$

and

$$y_1 = \frac{w_1L^3}{3EI_1} = y_2 = \frac{w_2L^3}{3EI_2} = y_3 = \frac{w_3L^3}{3EI_3} \quad (15:9)$$

Solving these equations, we find

$$\bar{x} = \frac{I_1x_1 + I_2x_2 + I_3x_3}{I_1 + I_2 + I_3} \quad (15:10)$$

For any number of spars we may write

$$\bar{x} = \frac{I_1x_1 + I_2x_2 + \dots + I_nx_n}{I_1 + I_2 + \dots + I_n}$$

We note here that this equation locates the elastic axis at the end of the beams only and for a concentrated load only. If the elastic curves of deflection of the beams are the same, the elastic

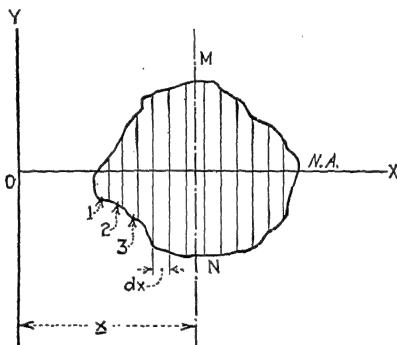


FIG. 15:4.—Location of elastic axis.

axis is a straight line. This implies that there exists a constant ratio at any section of the wing between I_1 , I_2 , and I_3 . While the elastic axis of a cantilever wing, in most cases, is not a straight line, it appears that little error will be introduced by drawing a straight line as a mean curve through points obtained by successive application of equation (15:10). Further investigation is left for the student.

15:5. Elastic Axis, More General Equation.—It may be found desirable to use a more general equation than equation (15:11). Let us consider the subject further.

In Fig. 15:4, let MN represent the cross section of a beam of length L . We divide the beam into strips as 1, 2, 3, etc., of

width dx . Thus, as equation (15:11), we have

We note that I is a function of x , as, for example, in Fig. 15:5,

$$I = \frac{y^3 dx}{12} \quad (15:13)$$

and, since $y = kx$, we have

$$I = \frac{k^3 x^3}{12} dx \quad (15:14)$$

Equation (15:12) becomes, therefore,

$$\Delta = \int I x dx$$

where I must be expressed in terms of x . If we take as a special case the value of I in equation (15:14),

$$\int_0^d \frac{k^3 x^3}{12} dx = \frac{k^3}{12} \frac{x^4}{4} = \frac{k^3}{48} d^4 \quad (15:16)$$

15:6. Elastic Axis and Shear.—The determination of the elastic axis in the few preceding paragraphs has been from the standpoint of bending only. While, in general, such determination is sufficient, it may be found that the shear in a particular type of wing is great enough to render such results too inaccurate. Let us consider the shear. With reference to Fig. 15:6, the modulus of elasticity in shear is

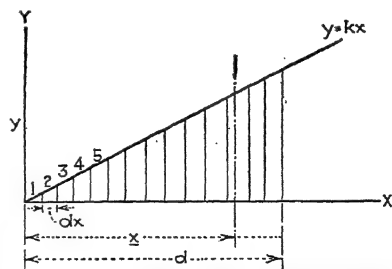


FIG. 15:5.—Elastic axis of a solid beam.

$$V dx \quad (15:17)$$

or

$$\frac{V}{AE_s} dx \quad (15:18)$$

where V is the shear at the section. For a concentrated load w at the end of the beam, V equals w so that

$$wL \quad (15:19)$$

We note therefore that, in order to include the shear deflection, equation (15:9) would be written

$$w_2L \quad \frac{1}{3EI_3} + \frac{1}{E_s A_s} \quad (15:20)$$

It is now necessary only to solve equations (15:20), (15:7), and (15:8) for the value of x .

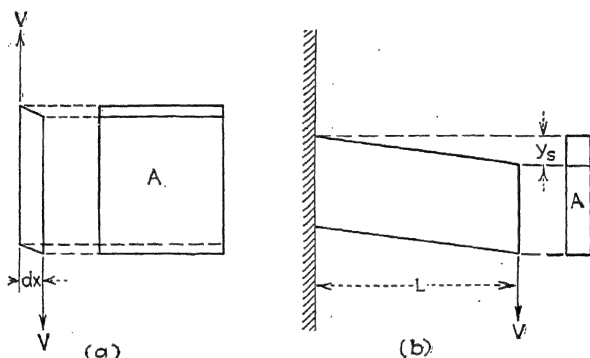


FIG. 15:6.—Elements of shear in a beam.

15:7. Trussed Spars.—The location of the elastic axis in a cantilever wing supported by trussed spars may be determined approximately by equation (15:11). However, as a large portion of the deflection is due to the deformation in vertical and diagonal bracing members and since it is assumed in the development of equation (15:11) that the deflection is due solely to the extension and compression of outer fibers, as in the flange members of the spars, the result may not be sufficiently accurate in some cases. The following procedure may prove more desirable from the standpoint of accuracy: It will be noted that the general procedure is to determine w_3 and w_2 in terms of w_1 for equal deflections. Let us now first find the deflection of each truss for a load of, say, 1 lb., 100 lb., or 1,000 lb.—call this P . For example, suppose these deflections are found to be y_1 , y_2 , and y_3 and that y_2 is $2y_1$ and y_3 is $3y_1$. It is therefore apparent that for equal

deflections $w_2 = \frac{1}{2}w_1$ and $w_3 = \frac{1}{3}w_1$. Thus, in general, if $y_2 = k_2y_1$, $y_3 = k_3y_1$, and $y_n = k_ny_1$, we have

$$w_2 = \frac{w_1}{k_2}, \quad w_3 = \frac{w_1}{k_3}, \quad \text{and} \quad w_n = \frac{w_1}{k_n} \quad (15:21)$$

Substituting this value in equation (15:8), we have

$$\begin{aligned} x = & + \frac{w_1}{k_2} x_2 + \frac{w_1}{k} \\ & \frac{w_1}{k_3} + \frac{w_1}{k_3} + \\ & x_2 \end{aligned} \quad (15:22)$$

The deflections y_1 , y_2 , y_3 , etc., may be found by any method, for example, that illustrated in Fig. 3:24. Several values of x along the semi-span may be computed and the average value of x taken as the required value. In general, the value near the tip of the wing is misleading, as one or more of the spars may radically change sections in that neighborhood. It is reasonable in computing the deflections at various points along the semi-span to neglect the portion of the spar from the station under consideration to the tip of the wing.

15:8. Requirements for Design.—An analysis of a cantilever wing for design purpose requires that the following applied loading characteristics be available:

1. Wing loading as a function of the chord. This is for rib design only.
2. Wing loading as a function of the semi-span. Specifically this is a curve showing the load per inch of semi-span of the wing as a function of the distance in inches from the tip or from the root section.
3. Shear at all sections of the semi-span of the wing as a function of the semi-span.
4. Bending moment at all sections of the semi-span of the wing as a function of the semi-span.
5. Torsion in the wing at all sections of the semi-span as a function of the semi-span.

15:9. Distribution of Load between Wing Spars.—If the wing twists under load, the distribution of loading on the wing spars is greatly affected. This distribution is therefore a function of the torsional rigidity. If the wing is perfectly rigid in torsion or if

the load is applied so that torsion is not induced in the wing, the wing bends as a unit; that is, the deflection curves of the several spars are parallel. Under such pure bending, with identical deflection curves, the wing as a whole may be considered as a beam. The several spars may be considered as one composite spar for the purpose of calculation of stresses and division of loads. As an example, consider Fig. 15:7. The spars A , B , and

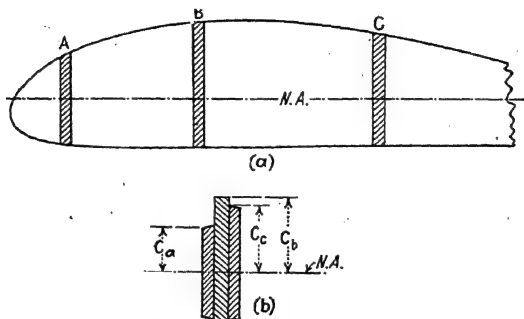


FIG. 15:7.—Distribution of stress for pure bending.

C have been brought together in b to form a composite beam. With the neutral axis computed in the usual manner for a composite beam, we have

$$\text{or} \quad (15:23)$$

where $I = I_a +$

$$J = \frac{Mc}{(I_a + I_b + I_c)} \quad (15:24)$$

We note that (Fig. 15:7)

$$f_a:f_b = c_a:c_b \quad \text{and} \quad f_c:f_b = c_c:c_b \quad (15:25)$$

Thus when f_b is the maximum allowable,

$$f_a = f_b \frac{c_a}{c_b} \quad \text{and} \quad f_c = f_b \frac{c_c}{c_b} \quad (15:26)$$

We note that the bending moment carried by each beam is

$$M_a = \frac{f_a I_a}{c_a}, \quad M_b = \frac{f_b I_b}{c_b}, \quad M_c = \frac{f_c I_c}{c_c} \quad (15:27)$$

We have

$$M = M_a + M_b + M_c \quad (15:28)$$

Equations (15:26), (15:27), and (15:28) enable us to solve for the portion of the bending moment carried by each beam. Thus, making substitutions from (15:26) into (15:27), we obtain

$$M_a = \frac{f_b I_c}{c_b} = \frac{f_b I_c}{c_b}, \quad \text{and} \quad M_c = \frac{f_b I_c}{c_b} \quad (15:29)$$

from which

$$I_a \quad (15:30)$$

Thus

$$M_a = \frac{I_a}{I_b} M_b \quad \text{and} \quad M_c = \frac{I_c}{I_b} M_b \quad (15:31)$$

Substituting these values of moments in equation (15:28), we have

$$M = M_b \frac{I_a}{I_b} + M_b + M_b \frac{I_c}{I_b} \quad (15:32)$$

from which

$$M_b = M \quad (15:33)$$

From symmetry, we write

$$M_c = M \frac{I_c}{I_b} \quad \text{and} \quad M_a = M \frac{I_a}{I_b} \quad (15:34)$$

Since the bending moment on a beam is proportional to the magnitude of the loading, assuming similar loading curves for the three beams, we may write, for any section, equations similar to (15:33) and (15:34), for the loading on each beam.

We note particularly that the design stresses are obtained from equation (15:24), in which c may be c_a , c_b , or c_c , and that we have assumed no torsion.

15:10. Cantilever Wing as a Beam.—It has been noted that, under the assumption of no torsion in a wing and no relative motion between the spars, we may consider the entire wing as a beam. This has been shown, experimentally, for a stressed-skin wing. However, for any cantilever wing with ribs of sufficient size and rigidity to cause the spars to retain the same deflection curve, the stresses caused by the bending component of the wing loading may be calculated by the modulus-of-rupture formula [see equation (15:23)].

In fact, since stresses in trussed spars and other supporting members in wings are usually below the elastic limit of the material, being designed for the compressive stress and columnar action, this formula applies with a fair degree of accuracy. It will be noted in this connection that f , the fiber stress, is also the P/A value of the chord or flange members of the wing

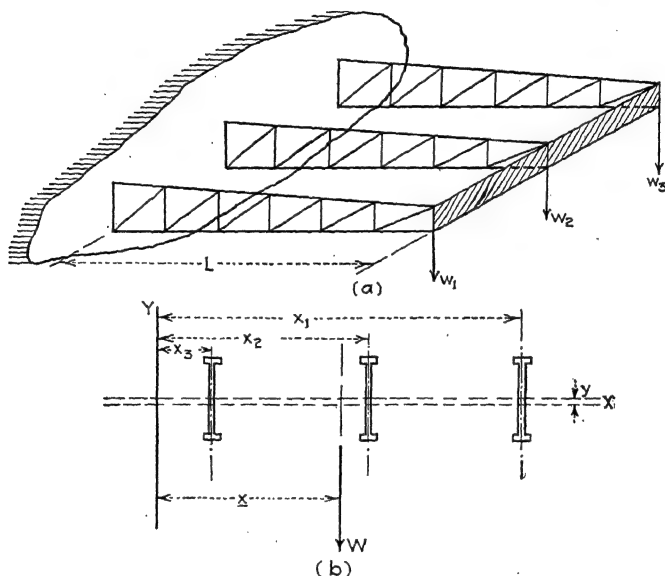


FIG. 15:8.—Bending, without torsion, in cantilever-trussed spar wing.

trussing. This P/A , allowable value, is determined from Euler's or Johnson's column formulas or by other methods appropriate to the conditions. We have thus

$$\frac{Mc}{I} \quad (15:35)$$

Let us consider a simple example, to fix ideas. In Fig. 15:9 we have represented a wing of four trussed spars 1, 2, 3, and 4. Let us assume that the allowable columnar stress value P/A for each spar has been determined for the section as for AB in Fig. 15:9b, by appropriate column formulas or by experiment. Let this value, for example, be 30,000 lb. per square inch for spar 2.

Thus,

$$30,000 = \frac{Mc_2}{(T_1 + T_2 + T_3 + T_4)} \quad (15:36)$$

from which the allowable bending moment may be found; or if the bending moment is known, the P/A value required may be found.

We note that, if c_1 is, say, one-half of c_2 , the P/A load in the chord or flange members of spar 1 will be only half that of spar 2, or 15,000 lb. per square inch. Since the failure of spar 2 would, in

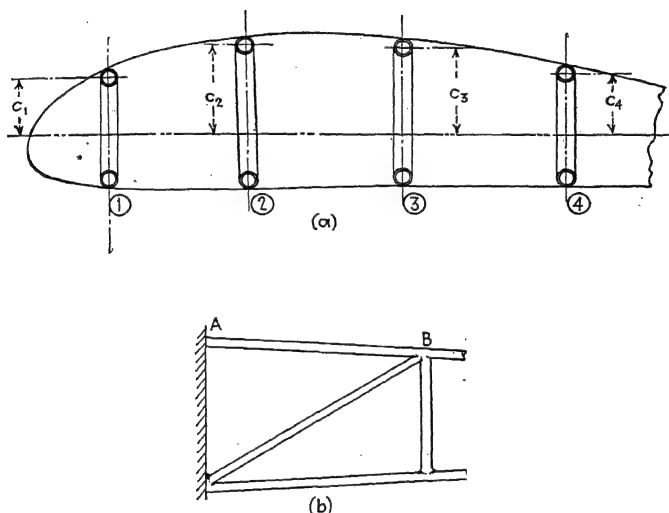


FIG. 15:9.—Wing with four trussed spars.

general, mean the failure of the wing, spar 1 has considerable excess strength if its P/A value is also 30,000 lb. per square inch.

15:11. Combination of Light and Heavy Construction.—If a light spar is inserted in a wing between two heavy spars as a former for the wing ribs, the stress in the flanges of the light spar may be computed by formula (15:35). For example, if a light spar is inserted between spars 2 and 3 in Fig. 15:9a, with c approximately equal to c_2 , the stress in the light spar must be approximately equal to the stress in spar 2. Since it is of light material, the P/A values obtainable in the light spar will be of the order, say, of half the stress of the large spar. The wing will therefore begin to fail with a very much smaller load than may be

ultimately obtained on the wing. This is the usual condition when light and heavy sections of materials are used for parallel services in a statically indeterminate structure. It is this effect which permits considerable wrinkling in the metal skin of a wing before danger of failure of the structure occurs.

15:12. Design of a Wing Beam.—Whether the wing itself is a beam or whether the wing is supported by beams, the general principles in design are approximately the same. Assuming that we have obtained loading, shear, moment, and torsion curves for the wing, we are ready to proceed with the structural design of the beams. We must first decide on the specific type of construction with respect to

1. Trussed beams.
2. Single-spar box beam; stressed skin.
3. Web beams.
4. Material—as steel, duralumin.
5. Attachment of ribs with ease and efficiency.
6. Ease in manufacture; riveting, welding, forming.
7. Availability of standard sections.

The exact type of construction will, of course, be the result of careful study by the engineering force for the specific job. The final design will be the result of successive approximations or trials, much study, ingenuity, and a large number of experiments.

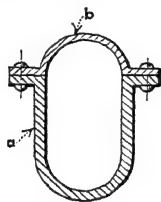


FIG. 15:10.—Types of tubular flange members.

15:13. Chord Members.—

Let us consider, for example, the chord or flange member of a trusted spar. Assume riveted construction. Assume the spar to be of composite construction

as shown in Fig. 15:10, for example, with sections *a* and *b*. Now the problem before us is to design the spar for minimum weight at each section along the spar. Since material cannot be purchased in tapered form, it is necessary to rivet successively thinner sections in place as we move outward on the spar toward the tip of the wing. It is obvious that it would not be desirable to make too many riveted joints because of the expense and additional weight, yet the spar must not be of the same heavy construction throughout its length. There is therefore a “happy

medium," or compromise, in the design of each spar concerning the location and number of joints.

15:14. Type of Joints.—The type of riveted joints depends upon the particular section under consideration. In some cases, it is more desirable and less expensive to telescope the thinner section into the thicker section and rivet as a lap joint. A butt joint with a wrapping of the plate entirely around the spar section may be desirable if construction problems permit.

If a member is composed of three, four, or more strips as *a* and *b* of Fig. 15:10, each strip may be successively decreased in size. This is the most desirable method.

15:15. Strength of the Section.—In general, the chord or flange member is designed for compression. This is true because the allowable fiber stress in compression (as a strut) is generally less than half the allowable stress in tension. Each chord member, top or bottom, will, of course, because of the inverted flight condition, be subjected to both types of loads. This condition makes the riveting problem simpler, since the design stresses of the material are rarely above the elastic limit.

In general, no data will be available for computing the strength of the chosen chord section in column action. It may be necessary to perform a series of experiments on the chosen section to obtain a column curve of P/A and a function of L/ρ as is usually done or to obtain simply a curve of P as a function of the particular section.

For preliminary design the following approximations may be found useful:

1. If the section is composed of approximately $\frac{1}{8}$ -in. plates, curved section, with width or depth of approximately 2 or 3 in., an allowable stress for duralumin of 25,000 to 30,000 lb. per square inch may be chosen.
2. If the section, as in Fig. 15:10*a*, is composed of approximately $\frac{1}{16}$ -in. plates, a stress of 15,000 to 20,000 lb. per square inch may be chosen.
3. If the section, as in Fig. 15:10*a*, is composed of approximately 0.030-in. plate, a stress of 5,000 to 10,000 lb. per square inch may be chosen.

These stresses, of course, should be used only for very rough estimates of the general size and shape of the spar. The actual allowable stresses should be determined only by experiment.

15:16. Preliminary Estimates.—To afford a visualization of the preliminary estimate in the design of the chord or flange member, a chart similar to that of Fig. 15:11 is convenient. The

abscissa of this chart is the spar; the ordinate is the load in the chord member. This load is obtained by dividing the mean depth of the spar by the bending moment at the section.

If the material were of the same thickness throughout, its strength would be indicated by a continuation of the line A. However, all strength above the "design-load" line is excess strength, and the extra material is excess material. The actual strength, however, must always be above the design-load line.

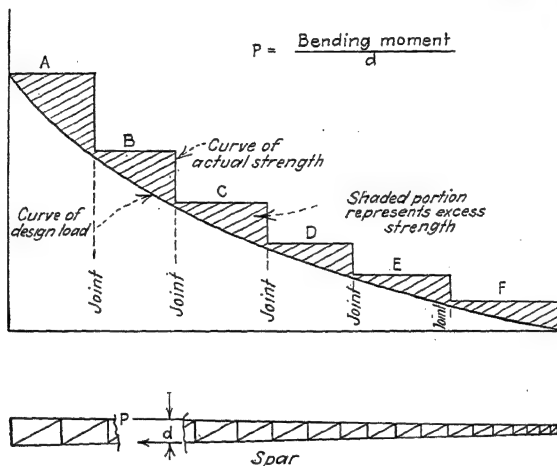


FIG. 15:11.—Preliminary design of a cantilever spar.

We are therefore able to visualize the best location of joints, the number of joints, the thickness of material, and other preliminary design items.

15:17. Vertical and Diagonal Members, Riveting.—Obviously a chart similar to that of Fig. 15:11 may be constructed for each design condition for vertical and diagonal members and for riveting. A dozen or more such charts will therefore be necessary for the complete preliminary design.

It may be necessary, if the design is to be close, to build up sections of the beam for testing with the design loads, to obtain precise data on the allowable fiber stresses.

References

1. BROWN, C. G., and CAPTAIN C. F. GREENE: Static Test and Stress Distribution Studies of the Matériel Division 55-foot Cantilever All-metal Wing. *Air Corps Information Circ.* 663, 1932.

2. BROWN, C. G.: Weight of Aluminum Cantilever Monoplane Wings, *Air Corps Information Circ.* 662, 1930.
3. HOWARD, H. B.: "The Stresses in Aeroplane Structures," Sir Isaac Pitman & Sons, Ltd., London, 1933.
4. Metal Aircraft Construction, *Aeroplane Supplement*, Vol. XXXVIII, No. 26, p. 1209, July 25, 1930. Presents descriptive accounts of the forms and methods of construction of steel spars and metal wings.
5. STIEGER, H. J.: Wing Construction, *Jour. Roy. Aeronautical Soc.*, Vol. XXXVI, No. 262, pp. 789-827, October, 1932.
6. KUHN, PAUL: Remarks on the Elastic Axis of a Shell Wing, *N.A.C.A. Tech. Note* 562, 1936.
7. KUHN, PAUL: Some Elementary Principles of Shell Stress Analysis with Notes on the Use of the Shear Center, *N.A.C.A. Tech. Note* 691, 1939.
8. SIBERT, H. W.: Shear Center of a Multi-cell Metal Wing, *Journ. Aeronautical Sciences*, Vol. VIII, No. 4, February, 1941.

CHAPTER XVI

DESIGN OF THIN-SHEET WING WEBS

16:1. Shear Buckling of a Thin-sheet Web.—As we have seen, compression causes buckling. This is true also in the case of a member transmitting a shear load. From previous discussions (Chap. III) we know that shear causes both a tensile and a compressive stress at 45 degrees from the direction of the shear stress. See, for example, Fig. 16:1a, and *b* and equations (3:22) and (3:24) in which the tensile or compressive stress is zero.

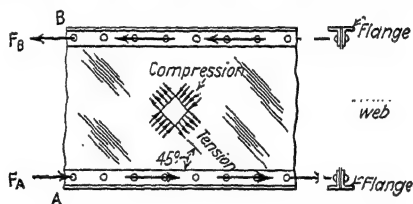


FIG. 16:1a.—Stresses in web of beam.

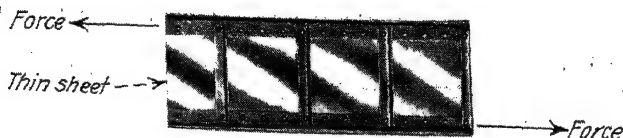


FIG. 16:1b.—Tension field web.

The magnitude, it will be noted, of the tensile and the compressive stress is the same as the shear stress.

(NOTE: s is used in this chapter for f_s to simplify writing formulas.)

The shearing stresses themselves do not cause buckling. In fact, they have very little significance, where buckling is concerned, except as a convenient means of defining the stress condition. The diagonal compressive stresses tend to buckle

the sheet. Since the condition of a flat plate transmitting shear loads is similar to that of a plate under compressive loads,

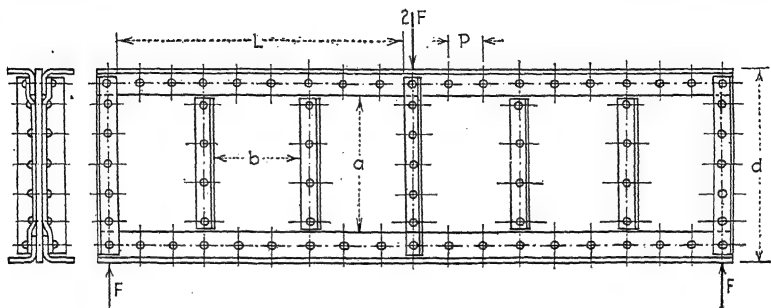


FIG. 16:2.—Riveting a thin web in a deep beam.

we should naturally expect to find the same type of formula to represent the condition. This formula is the Bryan formula, equation (11:13).

$$F_{cu} = s = \left(\frac{t}{b} \right)^2 \quad (16:2)$$

See Figs. 16:2 and 16:3 for values of K .

The coefficient K depends upon the ratio of a/b . If the beam requires no intermediate stiffeners, a/b becomes L/a (see Fig. 16:2); as L/a increases, K approaches the value $5.7 (L/a = \infty)$. The curve (Fig. 16:3) indicates the relation between L/a and K .

16:2. Stress Conditions.—

The stress condition in a tension-field web is shown in Fig. 16:4. As can be seen in the section AA, shear buckles appear as wrinkles of "washboarding" in the thin sheets. This, of course, is caused by the diagonal tensile stresses making the strips of sheet under compression behave like columns with continuous elastic support and thereby reducing the

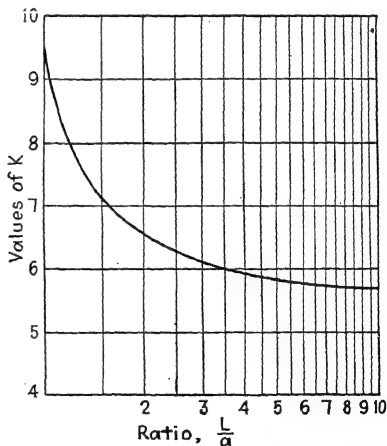


FIG. 16:3.—Constants for calculating allowable shear stress.

buckling wave length to a relatively small value. The wrinkles tend to follow the lines of tensile stress mainly because these are always normal to the maximum compressive stress, which causes the wrinkling.

This type of wrinkling web is usually called a *diagonal-tension field web*. The wrinkling, however, it must be remembered, is caused by compression and not tension.

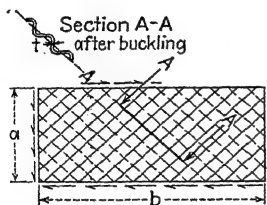


FIG. 16:4.—Flat plate under shear load.

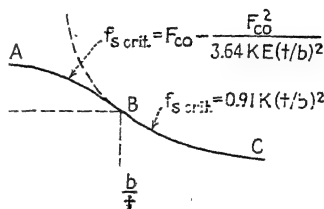


FIG. 16:5.

16:3. Stress above the Proportional Limit.—In the range of plastic failure, formula (16:2), like Euler's column formula, does not apply (see Fig. 16:5). It is therefore necessary to choose an empirical formula.

The following parabolic formula has been used with satisfactory results:

$$s = F_{co} - \frac{F_{co}^2}{3.64KE(t/b)^2} \quad (16:3)$$

where F_{co} may be taken for the F_{co} of the material as used in column formulas for tubes.

The following values are taken from the A.N.C. column formulas:

TABLE 16:1.—VALUES OF F_{co} FOR FORMULA (16:3)

Aluminum alloy	F_{ty} , lb./sq. in. yield	F_{co} , lb./sq. in.	Steel	F_{ty} , lb./sq. in. yield	F_{co} , lb./sq. in.
17ST.....	30,000	34,500	1025	36,000	36,000
17ST.....	40,000	42,500	X-4130	75,000	79,500
24ST.....	40,000 42,000	50,000	X-4130	85,000	90,100
24SRT.....	58,000	70,000	Heat-treated alloy steel	165,000	165,000

The lowest value of formula (16:3) is $\frac{1}{2}F_{co}$, for a value of

$$1.82\overline{KE} = \text{critical} \quad (16:4)$$

Below this value of b/t , (16:3) applies and above this value (16:2) applies.

16:4. Tangent Modulus Applied to Thin Webs.—Equation (16:2) should give fair results for at least preliminary design purposes for all values of t/b if \overline{E} , the *tangent modulus*, is substituted for E . Thus,

$$= 0.91K\overline{E} \left(\frac{t}{b} \right) \quad (16:5)$$

16:5. Calculation of Shear in a Web.—The longitudinal shear stress in the web of a beam is

$$\frac{F}{\bar{v}} \quad (16:6)$$

where s = shear stress, lb. per square inch.

F = total shear on the beam, at the section being considered, lb., = V .

t = thickness of web, in.

$\bar{v}A$ = static (area) moment of the area above or below the point where the shear is being determined = Q .

If the web is thin, as shown in Fig. 16:1b, we may assume A to be the area of the flange and v to be half the effective depth of the beam, which we may designate as d . I , in this case, would be approximately $2A(d/2)^2$. Thus, for a thin-webbed deep beam, equation (16:6) becomes

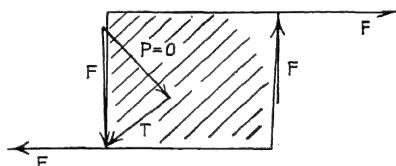


FIG. 16:6.—Stress in thin web of deep beam.

$$\frac{F}{2A(d/2)^2t} \quad (16:7)$$

16:6. Tension-field Web.—Now, as illustrated in Fig. 16:6, the shear F is the resultant of two components whose lines of action are at right angles to each other, the compressive compo-

nent P and the tensional component T . In Fig. 16:7 is represented a portion of the web, between the flanges MN and $M'N'$, subjected to the shear force F . The shearing force causes a shearing deformation δ . We shall assume the maximum tensile

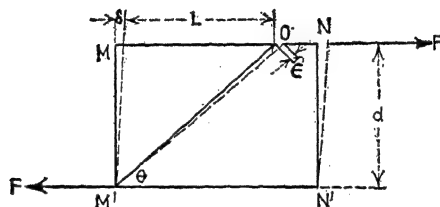


FIG. 16:7.—Direction of tension lines in a thin web.

stress f to be acting along the line $M'O$, making an angle θ with the lower flange. The length of $M'O$ is $\frac{d}{\sin \theta}$. The tensile deformation is ϵ , which may be written, approximately,

$$\epsilon = \delta \cos \theta \quad (16:8)$$

The unit strain is

$$\frac{\epsilon}{\frac{d}{\sin \theta}} = \frac{\delta}{d} \sin \theta \cos \theta \quad (16:9)$$

The unit tensile stress is f .

$$= \frac{\tau}{\sin \theta} \sin \theta \cos \theta \quad (16:10)$$

16:7. Angle of Tension Lines.—To find the maximum value of f , we equate the derivative of equation (16:10) with respect to θ to zero. Thus,

$$\frac{df}{d\theta} = -\frac{\delta E}{d} (\sin^2 \theta - \cos^2 \theta) = 0 \quad (16:11)$$

from which

$$\sin^2 \theta = \cos^2 \theta \quad \text{or} \quad \tan^2 \theta =$$

or

$$\theta = 45 \text{ degrees} \quad (16:12)$$

The angle θ is generally, from experimental data, assumed to be 42 degrees. If the web is too thin to take an appreciable amount of compression, only half the resisting shear force is available to

resist deformation. This may be introduced into our formulas of rigidity by substituting

$$(16:13)$$

16:8. Tensile Stress in Thin Web.—The unit tensile stress developed in a thin web in which the compressive stress is negligible is determined as follows:

The shear load on a length ΔL along the line of intersection of web and flange is stated as

$$\text{Shear load} = ts \Delta L \quad (16:14)$$

The tensile load T at θ degrees to the line of action of the shear load is expressed as

$$T = \frac{ts(\Delta L)}{\cos \theta} \quad (16:15)$$

The cross-sectional area subjected to the tensile load T is

$$t(\Delta L) \sin \theta \quad (16:16)$$

Hence, the unit tensile stress is obtained.

$$f = \frac{ts(\Delta L)}{\cos \theta} \frac{1}{t(\Delta L) \sin \theta} = \frac{s}{\sin \theta \cos \theta} \quad (16:17)$$

If θ is taken as 45 degrees, $\cos \theta \sin \theta = 0.5$; hence $f = 2s$.

16:9. Load on Vertical Compression Member.—If the beam is uniform in depth and the vertical stiffeners or compression

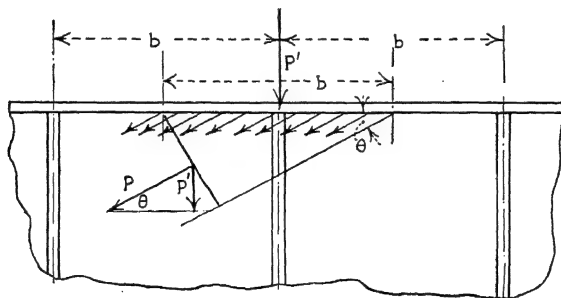


FIG. 16:8.—Loads on web stiffeners.

members may be assumed uniformly spaced for increments of length, which is generally the case, the total or design load of

the vertical member may be determined as follows (see Fig. 16:8):

$$P = ftb \sin \theta \quad (16:18)$$

and

$$P' = P \sin \theta = ftb \sin^2 \theta \quad (16:19)$$

Since, from (16:17),

$$\sin \theta \cos \theta$$

then

$$\begin{aligned} P' &= stb \tan \theta \\ &= stb \text{ (for } \theta = 45 \text{ degrees)} \\ &= 0.9stb \text{ (for } \theta = 42 \text{ degrees)} \end{aligned} \quad (16:20)$$

and since, by (16:07),

$$st = \frac{F}{d}$$

we have

$$P' = \frac{r}{d} b \tan \theta = \frac{F}{d} b \text{ (for } \theta = 45 \text{ degrees)} \quad (16:21)$$

If the compression struts are riveted to the web, failure may not occur in buckling as a column, for the tension in the web will prevent lateral buckling.

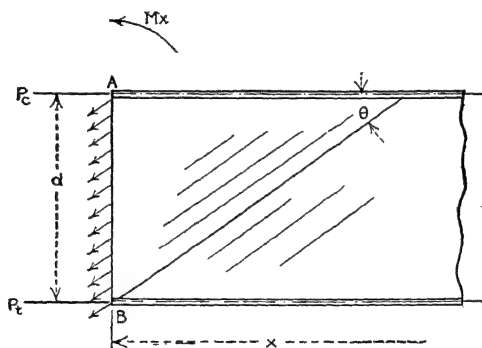


FIG. 16:9.—Loads in flanges of a thin-webbed beam.

The rivets through the stiffeners and chord members should be designed for the total load on the stiffeners as the rivets through the web serve only to prevent lateral buckling of the stiffeners.

It appears practical to assume an allowable stress of P/A not over the elastic limit of the material.

16:10. Load in the Flange Members.—With reference to the free-body diagram (Fig. 16:9), we have a beam subjected at x to

a bending moment M_x . Writing $\Sigma M_A = 0$, we have

$$M_x = P_t d + f t \frac{d^2}{2} \cos^2 \theta \quad (16:22)$$

from which

$$P_t = \frac{M_x}{d} - \frac{f t d}{2} \cos^2 \theta \quad (16:23)$$

Since $f = \frac{r}{\sin \theta \cos \theta}$ and $s = \frac{r}{dt}$, we have

$$P_t = \frac{M_x}{d} - \frac{r}{2} \cot \theta \quad (16:24)$$

The design load will probably be the compression load. In this case,

$$P_c = \frac{M_x}{d} + \frac{r}{2} \cot \theta \quad (16:25)$$

16:11. Sagging of Flange Members.—The tension field of the web of a deep and thin-webbed beam has a tendency to cause the flanges to sag as noted in Fig. 16:10. This throws an undue stress on the web and the riveting of the web at the strut (or

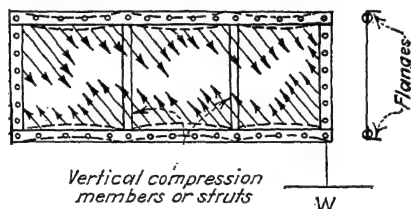


FIG. 16:10.—Shear in a thin web, and sag of flanges.

stiffener) sections of the flange. The success of a beam of this type requires that the tension field in the webs at the flanges be fairly uniform. This requires that the flange be as stiff as possible in resisting sagging. Figure 16:11 shows one method of providing this stiffness. The strip *A* is inserted to provide a large moment of inertia about the *x-x* axis and to provide sufficient rivet area for riveting the thin web to the flange.

16:12. Design of Flanges.—In general, these flanges may be considered as beam columns with the following characteristics:

1. Uniform moment of inertia of cross-sectional area between compression stiffeners.

2. Column with axial load as computed from equation (16:25).

3. Beam with a total bending load of P' as calculated from equation (16:21).

4. Column supported against buckling sideways. If the beam is sufficiently braced against sagging, a very high compressive stress may be carried. The beam is designed for the total primary bending and compressive load in sagging plus the secondary stress as a beam column.

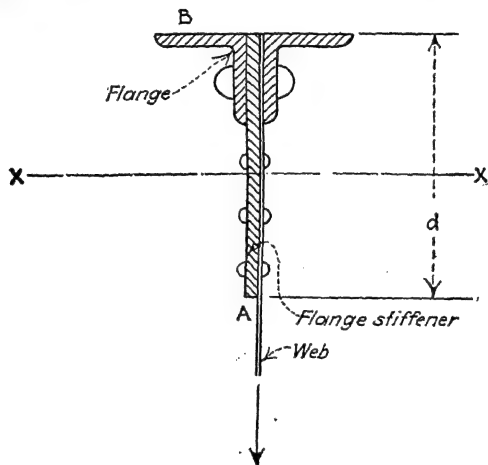


FIG. 16:11.—Stiffening a flange against sagging.

16:13. Practical Design of Rivets for Web.

1. *Rivets Attaching Web to Flanges.*—The load per rivet is

$$P_r = ftp \sin \theta \quad (16:26)$$

where f = fiber stress in tension.

t = thickness of the web.

p = pitch of the rivets.

Substituting the value of f from equation (16:17), we have

$$P_r = d \cos \bar{\theta} \quad (16:27)$$

If θ is taken as 42 degrees, equation (16:26) becomes

$$P_r = 0.669ftp \quad (16:28)$$

and equation (16:27) becomes

$$P_r = 1.338F \frac{p}{s} \quad (16:29)$$

If double rows of rivets are used, p is one-half the rivet pitch for each row.

2. *Rivets through Web Splice*.—In this case the pitch of the rivets p is measured vertically so that

$$P_r = ftp \cos \theta \quad \frac{Fp}{d \sin \theta} \quad (16:30)$$

Thus, if θ be taken as 42 degrees,

$$P_r = 0.743ftp = 1.486F \frac{p}{d} \quad (16:31)$$

3. *Loads on Rivets between Caps*.—When caps are riveted onto the chord member, the loads on rivets are given by the following formulas:

$$= \frac{S_r}{A_c} \quad \text{or} \quad \frac{P_r}{A_t} \quad (16:32)$$

where S_r = load per inch along beam between cap and chord member.

A_c = cross-sectional area of cap.

A_t = total cross-sectional area of chord member including cap.

d = mean depth of beam.

$$P_r = pS_r = p \frac{F A_c}{t} \quad \text{or} \quad P_r = pts \frac{A_c}{d} \quad (16:33)$$

where p = effective rivet pitch.

P_r = load on each rivet.

16:14. Design of Stiffeners for Nonbuckling Web.—If the distance between chord sections is too large (greater than 50 to 60 times the web thickness), intermediate stiffeners must be used. The size of these stiffeners can be determined from the equation¹

$$\frac{2.29d_{st}}{t} \quad (16:34)$$

where I_{st} = moment of inertia of stiffener.

d_{st} = rivet centerline distance between stiffeners.

t = web thickness.

F = applied shear load.

d = total depth of beam.

¹ Refer to paper presented by Herbert Wagner at the Fourth National Aeronautic Meeting of the A.S.M.E. at Dayton, Ohio, May, 1930.

16:15. Chord Loads, Beams with Stiff Webs.—The flexural stress in a plate girder is determined by the formula

$$\frac{Mc}{I} \quad (16:35)$$

Since the web of a plate girder is subjected to flexural stress, it is advisable to check the web, at the junction of the web with the flanges, for a combined flexural and shear stress.

$$f + s^2 \quad (16:36)$$

where F_c = principal buckling stress.

f = flexural stress [equation (16:35)].

s = shear stress.

This combined stress may in certain cases be higher than the extreme fiber stress.

Concentrated load stiffeners must be designed to take the total applied load and should be attached to both web and chord section. A sufficient number of rivets should be used to transmit the entire load into the web.

Intermediate stiffeners need not be attached to the chord section except in special cases as in a keelson.

The shear load per inch between the web and the chord angles is given by the equation

$$S = \frac{FQ}{I} \quad (16:37)$$

where Q is the static moment of one set of chord sections about the neutral axis of the beam.

The load on each rivet = $P_r = ps$, where p is the effective pitch.

The above formula may also be applied to rivets connecting caps to chord angles. The symbol Q will then be the static moment of the cap.

16:16. Incomplete Tension Field.—Strictly speaking, all tension-field webs are incomplete tension fields because the flanges and vertical stiffeners prevent the web from wrinkling at and near these members. Also, if the web wrinkles only slightly, it still carries approximately the critical stress. In this case, therefore, we may assume that the web carries the load as calculated for

the tension-field beam plus the load as calculated for the Bryan buckling failure.

An additional increase of total load may also be allowed owing to the supporting effect of the flanges and vertical stiffeners. This portion of the load must be determined from experiment or from empirical formulas derived from experiments.

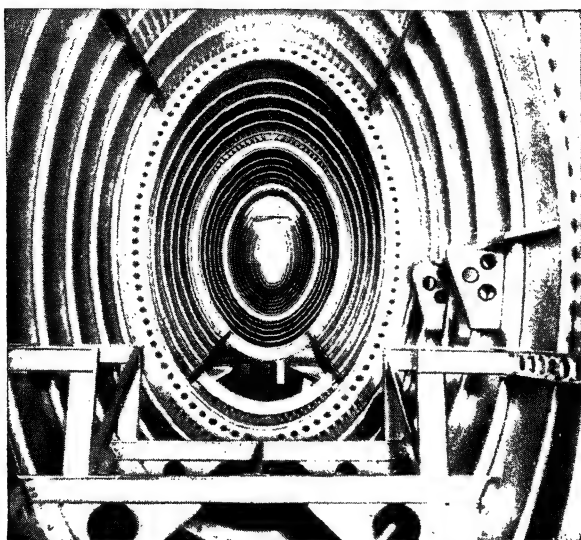


FIG. 16:12.—Model XB-10. Fuselage interior construction. Note tension and compression corrugations in top and bottom. (Courtesy of Glenn L. Martin Company.)

The same idea of “effective width” that is applied to the stringer-flat-sheet combination may be used in deriving an empirical formula.

References

1. LAHDE, R., and H. WAGNER: Tests for the Determination of the Stress Condition in Tension Fields, *N.A.C.A. Tech. Mem.* 809, 1936.
2. SCHAPITZ, E.: Contributions to the Theory of Incomplete Tension Bay, *N.A.C.A. Tech. Mem.* 831, 1937.
3. WAGNER, H.: Flat Sheet Metal Girder with Very Thin Metal Webs, *N.A.C.A. Tech. Mem.* 604, 605, 606, 1931.
4. LAHDE, R., and H. WAGNER: Tests for the Determination of the Effective Width of Bulged Sheets, “*Luftfahrtforschung*,” Vol. XI: Heft 7, S. 214, R. Oldenbourg. Munich and Berlin, 1936.
5. KUHN, PAUL: A Summary of Design Formulas for Beams Having Thin Webs in Diagonal Tension, *N.A.C.A. Tech. Note*, 469, 1933.

6. TIMOSHENKO, S.: "Theory of Elastic Stability," McGraw-Hill Book Company, Inc., New York, 1936.
7. BROWN, C. G., and CAPTAIN C. F. GREENE: Static Test and Stress Distribution Studies of the Matériel Division 55-foot Cantilever All-metal Wing, *Air Corps Information Circ.* 663, 1932.
8. GREENE, CAPTAIN C. F., and J. E. YOUNGER: Metal Wing Construction, *Air Corps Tech. Rept.* 3361, 1929.
9. ROHRBACH, A.: Materials and Methods of Construction in Light Construction, *N.A.C.A. Tech. Mem.* 515, 1929.
10. SHANLEY, F. R.: Engineering Aspects of Buckling, *Aircraft Engineering*, Vol. XI, No. 119, pp. 13-20, January, 1939.

CHAPTER XVII

INTRODUCTION TO SHEAR LAG

17:1. Definitions.—When a box beam with thin webs is bent, we may assume with little error that the bending moment is carried by compression in one flange and tension in the other. The stress is transmitted from one flange to the other in the form of shear in the webs. The tension and compression in the flanges are developed from this shear force at their edges. This, as is shown in Fig. 17:1, develops an uneven deformation in the flanges and hence likewise develops nonuniform stresses across the

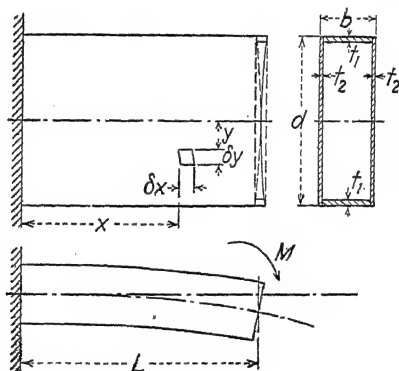


FIG. 17:1.

flanges. As a result of this, materials nearest the edges of the flanges reach their ultimate strength and fail before the ultimate strength is developed in the remainder of the flanges.

Figure 17:2 illustrates the variation of the stress across the flange. Note also that an elementary area $\delta x \delta y$ moves from *A* to *B*. We assume the motion is parallel to the *x*-axis.

The strength of the beam is thus lowered. The ratio of the lowered strength to the strength computed (within the proportional limit) under the assumption of uniform stresses throughout the flanges is called the *form factor*. The *efficiency of the flange* is defined as the ratio of the stress (allowable), shear lag being assumed, to the stress (allowable) no shear lag being assumed.

We shall first find the distribution of stresses in the flanges of the beam shown in Fig. 17:1 and 17:2. We concentrate our attention on the equilibrium of a small block of width δy , length

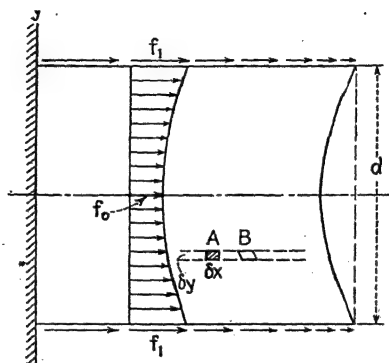


FIG. 17:2.

δx , and thickness t_2 (see Figs. 17:2 and 17:3) and define our symbols as follows:

s = unit shearing stress, lb. per square inch.

f = unit tensional or compressive stress, lb. per square inch.

t_1 = thickness of the rectangular web, in.

b = width of the rectangular web, in.

t_2 = thickness of the rectangular flange, in.

d = width of the rectangular flange, in.

L = length of the beam, in.

u = displacement of a point along the x -axis, in. (Note that, since x designates the point, it cannot also designate the displacement of the point.)

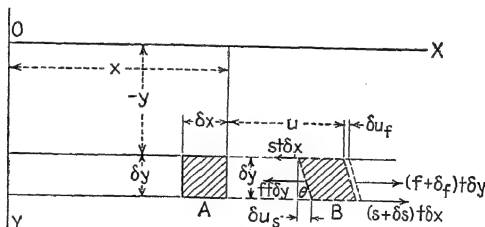


FIG. 17:3.

17:2. General Development of the Fundamental Equation.— With reference to Fig. 17:3, if s is the shearing stress on one side

of the block of dimensions δx and δy , the shearing stress on the opposite side is $(s + \delta s)$, so that the unbalanced unit force is δs . Applying Taylor's expansion to find the value of δs and discarding terms of the second degree or greater degrees, we obtain the following:

The change of shear is the rate of change of shear with respect to the change of y times the increment of change of y .

$$\delta s = \delta y \frac{\partial s}{\partial y} \quad (17:1)$$

The total unbalanced shearing force is the unit stress times the area, thus,

$$(\delta s)t \delta x = \frac{\partial s}{\partial y} t \delta y \delta x \quad (17:2)$$

Likewise, if f is the unit tensional or compressive force on one side of the block, the unbalanced unit force on the block is

$$(17:3)$$

The total unbalanced tensional or compressive force is

$$(\delta f)t \delta y = \frac{\partial f}{\partial x} t \delta y \delta x \quad (17:4)$$

Adding equations (17:2) and (17:4), equating to zero, and canceling $(t \delta y \delta x)$, we obtain our equation of equilibrium,

$$\frac{\partial s}{\partial y} + \frac{\partial f}{\partial x} = 0 \quad (17:5)$$

17:3. Stresses Expressed in Terms of Deformations.—The stresses f and s , however, are both functions of the deformation. This deformation as noted in Fig. 17:3 is u . The stresses f and s are therefore functions of u , and u is a function of both x and y . Since the modulus of elasticity is

$$E = \frac{\text{unit stress}}{\text{unit strain}} = \frac{\delta u_f}{\delta x} \quad (17:6)$$

Thus,

$$\frac{x}{\delta x} \frac{\partial u}{\partial x} = \frac{\partial u}{\delta x} \quad (17:7)$$

Also,

$$\frac{\partial f}{\partial x} = E \frac{\partial^2 u}{\partial x^2} \quad (17:8)$$

Likewise,

$$E_s = \frac{\text{unit shear stress}}{\text{unit shear strain}} = \frac{s}{\delta u_s / \delta y} \quad (17:9)$$

Thus,

$$s = E_s \frac{\delta u_s}{\delta y} = E_s \frac{\partial y}{\partial y} \frac{\partial u}{\partial y} = E_s \frac{\partial u}{\partial y} \quad (17:10)$$

Also,

$$\frac{\partial s}{\partial y} = E_s \frac{\partial^2 u}{\partial y^2} \quad (17:11)$$

Thus, letting $n^2 = E_s/E$, and substituting (17:11) and (17:8) in (17:5), we have the equation of displacement,

17:4. Solution of Equation and Evaluation of Constants.—

The solution of this equation, as may be readily verified by substitution in (17:12) and by reference to books on differential equations, is

$$u = A \cos n\beta x \cosh \beta y + B \cos n\beta x \sinh \beta y \\ + C \sin n\beta x \sinh \beta y + D \sin n\beta x \cosh \beta y \quad (17:13)$$

In this equation, β is an arbitrary constant to be determined so as to fit the physical requirement.

The boundary limits to be satisfied and to evaluate the constants of integration are

$$(a) \quad \left\{ \begin{array}{l} \text{When } x = 0, u = 0 \\ \text{When } x = 0, s = 0; \text{ thus } \frac{\partial u}{\partial y} = 0 \end{array} \right.$$

$$(b) \quad \text{When } y = 0, s = 0; \text{ thus } \frac{\partial u}{\partial y} = 0$$

$$(c) \quad \text{When } x = 2, f = 0; \text{ thus } \frac{\partial u}{\partial x} = 0$$

$$(d) \quad \text{When } y = +d/2, f = f_1 = \text{function of } x \text{ only}$$

In addition, we note that the magnitude of u and the function of u , such as f and s , must be independent of the sign of y ; that is, $f(y) = f(-y)$.

From these limits, we find that

$$u = D \sin n\beta x \cosh \beta y \quad (17:14)$$

with limits (c) and (d) still to be satisfied.

If we let

$$\beta = \frac{(2m-1)}{2} \frac{\pi}{nL} \quad (17:15)$$

where $m = 1, 2, 3$, etc., limit (c) is satisfied.

Thus

$$\frac{\pi}{nL} y \quad (17:16)$$

and

17:5. Distribution of Stress in Flange.—Letting $y = d/2$, $f = f_1$ and letting $y = 0$, $f = f_0$, and $m = 1$ for the simplest curve stress, we have

$$\frac{f_0}{f_1} = \frac{1}{\cosh \frac{\pi}{4nL} \cosh 1.25 \frac{\pi}{L}} \quad (17:18)$$

where

Thus

$$f_1 = f_0 \cosh 1.25 \frac{\pi}{L} \quad (17:19)$$

And, in general, the stress at y is

$$f_y = f_0 \cosh 2.5 \frac{\pi}{L} \quad (17:20)$$

17:6. Total Load Carried by Flange.—The total load carried by the flange is the sum of the increments of load carried by each increment of area across the flange. Thus, if P is the total load carried by the flange (letting t = thickness of flange),

$$P = 2(f_1 t \Delta y + f_2 t \Delta y +$$

Thus

$$= 2t \int_0^2 f dy \quad (17:21)$$

Substituting (17:20) in (17:21), we have

$$= 2tf_0 \int_0^2 \cosh 2.5 \frac{y}{L} dy \quad (17:22)$$

Solving, we have

$$\frac{tf_0 L}{1.25} \sinh \quad (17:23)$$

If there were no shear lag, the load P_1 would be, by equation (17:19),

$$P_1 = f_1 t d = f_0 t d \cosh 1.25 \frac{d}{L} \quad (17:24)$$

17:7. Efficiency of Flange.—The efficiency of the flange is the ratio of P to P_1 , thus letting e represent the efficiency.

$$e = \frac{P}{P_1} = \frac{f_0 t L \sinh 1.25 \frac{d}{L}}{1.25 \frac{d}{L}} \quad (17:25)$$

from which

$$\tanh 1.25 \frac{d}{L} = e \quad (17:26)$$

The total load that can be carried by the flange is the load calculated by the usual method, on the assumption of no shear lag, multiplied by e . Figure 17:4 shows a graph of equation (17:26).

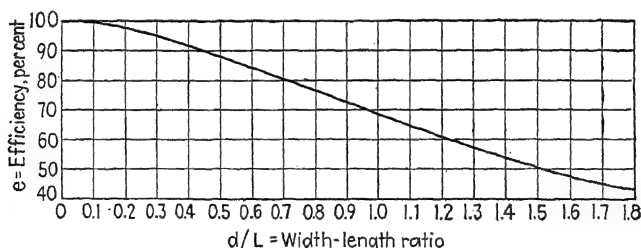


FIG. 17:4.

If the flange is corrugated sheet, the width d is the developed width of the corrugations.

17:8. Effect of Camber of Wing.—If the flange of a box beam is cambered such that C_0 is the distance from the neutral axis

of the beam to the flange at the center and C_1 is the distance at the edge, then, on the assumption of no shear lag,

$$\frac{f_0}{f_1} = \frac{C_0}{C_1} \quad \text{or} \quad f_0 \sim \quad (17:27)$$

Thus, (17:19) may be written approximately for camber,

$$f_1 = f_0 \frac{C_1}{C_0} \cosh 1.25 \frac{d}{L} \quad (17:28)$$

The ratio C_1/C_0 being less than 1 and $\cosh 1.25 \frac{d}{L}$ being greater than 1, camber therefore has a tendency to make the flange over 100 per cent efficient in spite of shear lag, that is, stronger than if there were no shear lag.

17:9. Variation of Stress along Span.—In equation (17:17), as noted, D and m are constants. Also, the sum of any number of terms in which D and m are assigned values is a solution, as may be verified by the student. Thus, equation (17:17) can be written as a Fourier series, which is quite useful for solving more complicated problems of shear lag.

For example, if we let the stress along an element of flange be

$$f = F \cos \frac{\pi}{2L} x \quad (17:29)$$

where F is the stress of the flange at the root section of the wing, we find that $m = 1$. Thus,

$$F \cos \frac{\pi}{2L} x = \cosh \frac{\pi}{2nL} y \cos \frac{\pi}{2L} x \quad (17:30)$$

Thus,

$$F = \frac{2FL}{2L} \cosh \frac{\pi}{2nL} y \quad \text{and} \quad D = \frac{2FL}{\pi E \cosh 2nL} \quad (17:31)$$

If a specific value of F is known at the root section, say, F_0 at the center ($y = 0$), we have

$$D = \frac{2F_0L}{\pi E}$$

Thus, (17:17) becomes

$$f = F_0 \cosh \frac{\pi}{2nL} y \cos \frac{\pi}{2L} x \quad (17:32)$$

Thus, the stress at any point on the flange can be found by the substitution of x and y in this equation.

17:10. Other Cases of Shear Lag.—Specific solutions and design data on shear lag are beyond the scope of this text. It is hoped however, that with this introduction the student has obtained a practical insight into the problem. From this elementary analysis, the way is paved to the study of such reports as follow in the list of references. (NOTE: This analysis is fundamentally the same as that given in Reference 1, written by the author in 1928 but not available to the public.)

17:11. Assumptions Made.—The conditions satisfied are those listed in Art. 17:4. The designation of $m = 1$ later in the paragraph is equivalent to the assumption that f_1 , the stress along the edge, is distributed proportional to $\cos \frac{\pi}{2L} x$. Any other distribution may be assumed and the constants of the Fourier series [equation (17:17)] calculated according to the mathematical methods relating to this type of series. This is done in some of the references cited at the end of this chapter.

Care should be exercised that the results of shear-lag analyses are not applied to conditions contrary to the assumptions of derivation.

References

1. YOUNGER, J. E.: Metal Wing Construction, Part II, Mathematical Investigations, *A.C.T.R. Ser. 3288, Matériel Div., U.S. Army Air Corps*, 1930.
2. WHITE, ROLAND J., and HANS M. ANTZ: Tests on the Stress Distribution in Reinforced Panels, *Jour. Aeronautical Sciences*, Vol. III, No. 6, pp. 209–212, April, 1936.
3. LOVETT, B. B. C., and W. F. RODEE: Transfer of Stress from Main Beams to Intermediate Stiffeners in Metal Sheet Covered Box Beams, *Jour. Aeronautical Sciences*, Vol. III, No. 12, pp. 426–430, October, 1936.
4. WINNY, H. F.: The Distribution of Stress in Monocoque Wings, *Air Ministry (British) R. and M. 1756*, September, 1936.
5. KUHN, PAUL: Stress Analysis of Beams with Shear Deformation of the Flanges, *N.A.C.A. Tech. Rept. 608*, 1937.
6. KUHN, PAUL: Strain Measurements on Small Duralumin Box Beams in Bending, *N.A.C.A. Tech. Note 588*, 1937.
7. KUHN, PAUL: Approximate Stress Analysis of Multi-stringer Beams with Shear Deformation of the Flanges, *N.A.C.A. Tech. Rept. 636*, 1938.
8. KUHN, PAUL: Some Notes on the Numerical Solution of Shear-lag and Mathematically Related Problems, *N.A.C.A. Tech. Note 704*, 1939.

9. KUHN, PAUL: Recurrence Formula for Shear Lag Problems, *N.A.C.A. Tech. Note* 739, 1939.
10. SIBERT, H. W.: Effect of Shear Lag on Wing Strength, *Jour. Aeronautical Sciences*, Vol. VI, No. 10, August, 1939.
11. REISSNER, ERIC: The Influence of Taper on the Efficiency of Wing Flanged Box Beams, *Jour. Aeronautical Sciences*, Vol. VII, No. 8, June, 1940.

CHAPTER XVIII

PROBLEMS IN FUSELAGE DESIGN

18:1. Fundamentals of Construction.—The present-day metal monocoque fuselage is primarily a thin-walled cylinder and as such is subjected to axial compressive, bending, and torsional loads. Chapter XII presents the fundamental methods of analyses and design data for many fuselage problems. There are, however, additional problems which should have a place in a text for students.

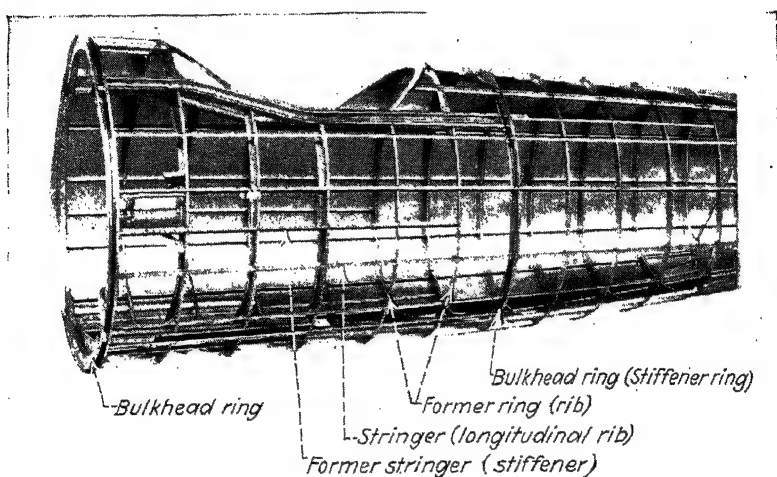


FIG. 18:1a.—Parts of a semi-monocoque fuselage.

The semi-monocoque fuselage construction (see Fig. 18:1a) consists primarily of

1. Sheet-metal covering—the skin.
2. The longitudinal stiffening members commonly referred to as *stringers*.
3. The transverse stiffening elements, commonly referred to as the *bulk-*

18:2. Functions of the Structural Parts.—(1) The functions of the sheet-metal covering are to provide a streamlined surface, to form a housing or cabin, and to constitute a primary structural

part of the fuselage. (2) The functions of the stringers are to stabilize the skin, add additional strength in resisting compressive loads, maintain the aerodynamic shape of the fuselage. (3) The functions of the bulkhead rings are to maintain the aerodynamic shape of the fuselage and to stabilize the stringers. Heavy bulkhead are used to transfer loads from the fuselage shell to other parts of the airplane (see Art. 10:14).

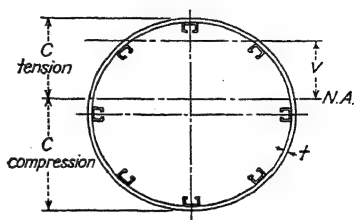


FIG. 18:1b.

18:3. Stress Calculations.—The following formulas apply up to the point of failure or buckling: the simple bending formula

$$f = \frac{Mc}{I} \quad (18:1)$$

the longitudinal shear formula

$$s = \frac{VQ}{Ib} \quad (18:2)$$

and the torsion formula

$$2At \quad (18:3)$$

The symbols are

f = stress, lb. per square inch, tension or compression.

s = shear stress, lb. per square inch.

M = bending moment, lb.-in.

T = torsional moment, lb.-in.

$Q = \int_0^c v dA$, where v (Fig. 18:1b) is the distance from the neutral axis to the point where the shear is to be calculated, in.-lb.

V = total shear, vertical, to which the fuselage is subjected, lb.

b = total thickness of the material carrying the horizontal shear, in., $= 2t$ in Fig. 18:1b.

A = area circumscribed by the skin, sq. in.

I = moment of inertia, inch units, about the neutral axis (N.A.) of the material that contributes to the load carrying. On the compression side, the skin wrinkles and does not contribute to the strength at the failure of the fuselage and hence should not be included in I . This is the reason the N.A. in Fig. 18:1b is not the axis of symmetry.

18:4. Types of Failure.—If a fuselage of semi-monocoque structure is subjected to axial compression, bending, and torsion, it may fail in one or more of four distinct ways:

1. Material rupture (see Fig. 18:2).
2. Local instability (see Fig. 18:3).
3. Panel instability (see Fig. 18:4).
4. General instability (see Fig. 18:5).

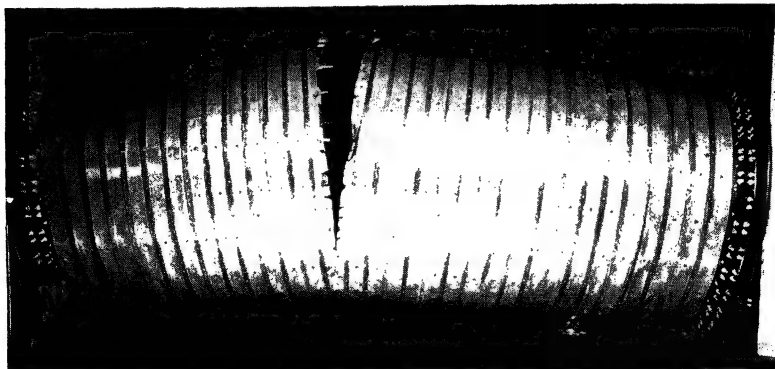


FIG. 18:2.—Material rupture failure. (Courtesy of Caltech.)

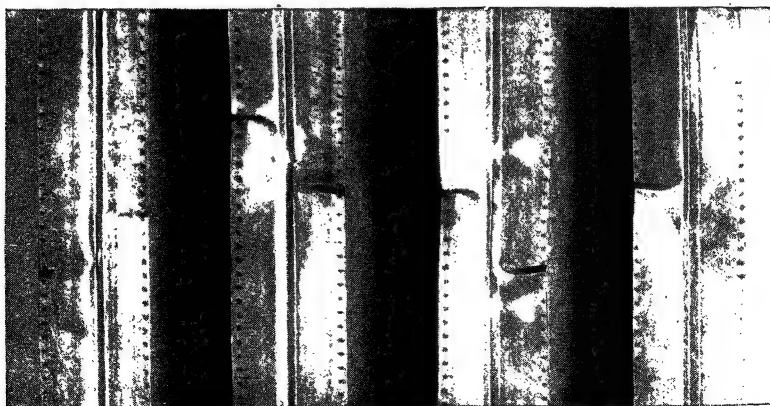


FIG. 18:3.—Local instability of stringers.

1. *Material rupture* (Fig. 18:2) is usually in tension of sheet or stringer or shear of sheet and rivets.

2. *Local instability* (Fig. 18:3) generally occurs in stringers having wide flat surfaces or unsupported flanges (see Chap. XIII, Design of Thin-walled Columns and Stringers).

This collapse of a part of a stringer may cause a failure as a column and may cause premature failure of the whole surrounding structure. The buckling stress of such sections, if they cannot be calculated, may be readily determined by tests.

3. A *panel-instability* failure (Fig. 18:4) is one that occurs between bulkhead rings. The rings of the fuselage are strong enough for support, but the sheet and stringers between the rings collapse as a column. The magnitude of the failing load depends

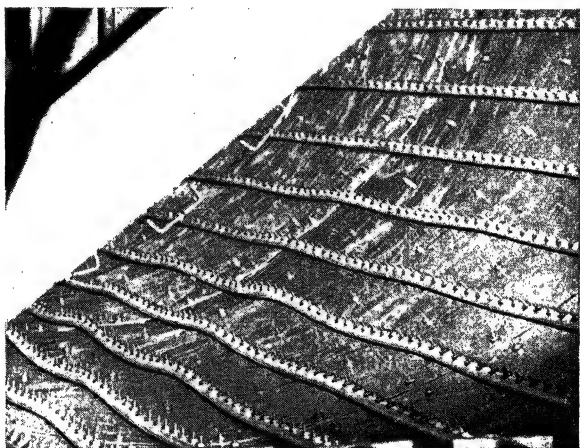


FIG. 18:4.—Panel instability of a stiffened cylinder. The bulkhead rings are on the outside of the cylinder. (Courtesy of Caltech.)

upon the column strength of the stringers, modified by the effect of the skin.

4. A *general-instability* type of failure (Fig. 18:5) will occur in a structure that has bulkhead rings and stringers of such sizes that both will fail simultaneously under the critical load. A complete collapse occurs, destroying the strength properties of all three structural elements, sheet, bulkhead rings, and stringers.

18:5. General-instability Failure.—A complete and exact theoretical treatment of this problem will probably never be attained in a practical and usable manner. It is therefore necessary, as in most other cases of airplane construction, to use approximate and empirical methods.

18:6. Equivalent-shell Method.—In this method, it is assumed that the material of the stringers and rings is distributed over

the entire cylinder, forming an unstiffened orthotropic cylinder which is then treated as a simple unstiffened cylindrical shell. The thickness and stiffness of this shell in the longitudinal direction will be different from the thickness and stiffness in the circumferential direction by amounts depending upon areas and stiffness of the stringers and rings, respectively.

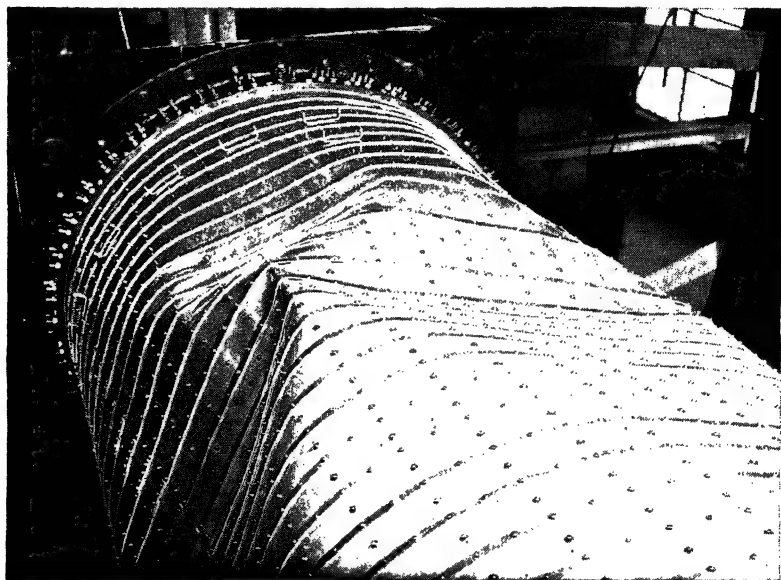


FIG. 18:5.—General instability of stiffened cylinder. (Courtesy of Caltech.)

For example, if I_s is the moment of inertia of the cross section of the stringer, p is the pitch of the stringers, and t is the thickness of the sheet, then the equivalent thickness t_e for the same thickness would be calculated as follows:

$$(18:4)$$

Likewise, if I_r is the moment of inertia of the cross section of the ring,

$$= \sqrt[3]{\frac{12I_r}{p}} \quad (18:5)$$

18:7. Equivalent-truss Method.—It is assumed in this case that the stringers and rings, each with its proper effective width of sheet acting with it, would form a statically indeterminate truss system. This truss is then solved for the collapsing loading. The method is tedious and of doubtful value.

18:8. Experimental Results.—Dunn (Ref. 1) has determined the following formula by experimentation and the method of dimensions:

$$\frac{f_{cr}}{E} = F \left(\frac{1}{R} \sqrt{\rho_x \rho_y} \sqrt[4]{\frac{\rho_x \rho_y}{bd}} \right) \quad (18:6)$$

That is, critical stress f_{cr} is a function of E , R is the radius of the fuselage, ρ_x the radius of gyration of the stringer section, and ρ_y the radius of gyration of the bulkhead-ring section, it being assumed that the entire width of sheet is effective; b is the stringer spacing, and d is the ring spacing. All units are inch-pounds.

The stringers and bulkhead rings used in the 45 or more tests are shown in Fig. 18:6.

Sample calculations are shown in Table 18:1.

Figure 18:7 shows a graph of Dunn's results.

18:9. Bulkhead-ring Design.—A bulkhead ring is a circular beam loaded by distributed and concentrated loads. The following analysis is the most practical and simple the author has been able to assemble. It is an amplification of that made by Ruffner (Ref. 6). The method is an interesting and relatively simple application of the

pe of failure

anel instability
general instability
general instability
anel instability

210
960
635
920

0.
0.
0.
0.

1723
2176
1000
633

0
0
0
0

2.50
2.12
500
998

0
0
0
0

5
5
6
6

6
8
2
6

2

0.015
0.015
0.010
0.010

41
55
56

ng

three equations of static equilibrium in a plane and the method of the theory of least work.

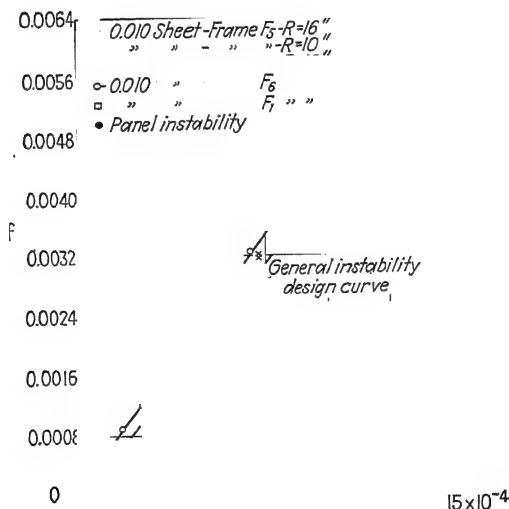
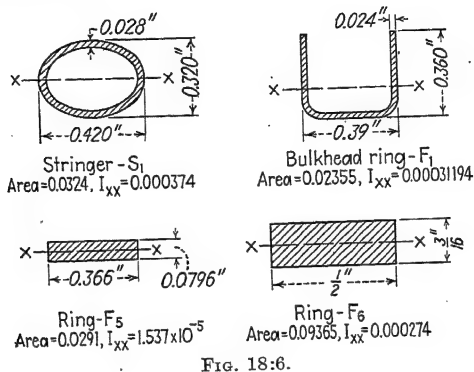


FIG. 18:7.

We have seen (Art. 10:17) that the vertical components of the skin load tend to collapse a ring (Fig. 10:24) by a force (equation 10:22)

$$dF = A \sin^2 \theta d\theta \quad (18:7)$$

and since dp , the tangential load carried by the skin, is related to dF as follows,

$$dF = dp \sin \theta \quad (18:8)$$

we have

$$dp = A \sin \theta d\theta \quad (18:9)$$

Since the vertical component of the load must equal W (Fig. 10:24), we have

$$= \int dF \sin^2 \theta d\theta \quad (18:10)$$

from which we find

$$W = \frac{A}{2} [\theta - \sin \theta \cos \theta]_0^\pi = \frac{2\pi A}{2} \quad (18:11)$$

and therefore

$$\frac{W}{\pi} \quad (18:12)$$

Thus equations (18:7) and (18:9) become

$$dF = \frac{W}{\pi} \sin^2 \theta d\theta \quad (18:13)$$

and

$$dp = \frac{W}{\pi} \sin \theta d\theta \quad (18:14)$$

18:10. Longitudinal-shear Method.—Equation (18:14)

may also be obtained by the application of the longitudinal-shear equation (18:2). In this equation, $V = W$, $I = \pi r^3 t$, $b = 2t$, and (Fig. 18:8) $Q = \int y dA$, $y = r \cos \theta$, and $dA = tr d\theta$. Thus, equation (18:2) becomes

$$(18:15)$$

and since the radial shear is equal to the longitudinal shear; $dp = \text{unit shear } s \text{ times area; thus,}$

$$dp = str d\theta = \frac{W}{\pi} \sin \theta d\theta \quad (18:16)$$

which checks equation (18:14).

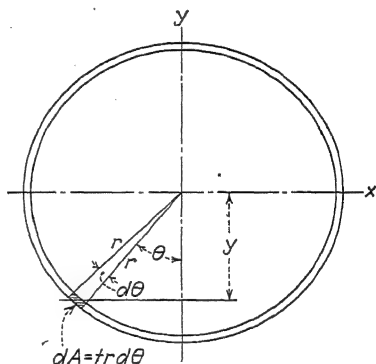


FIG. 18:8.

18:11. Equations of Equilibrium.—Figure 18:9a shows a section of the circular ring subtending an angle of θ radians. The angle θ designates the location of M , V , and P , to be found. The angle ϕ designates the location of dp , the distributed load.

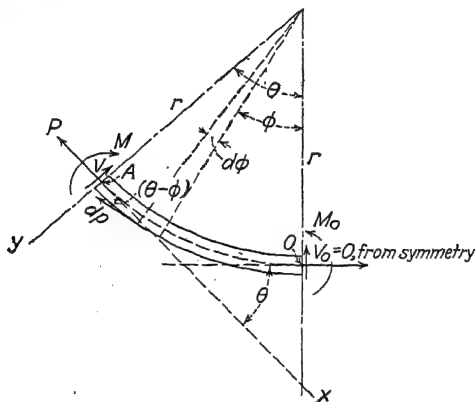


FIG. 18:9a.

At O , the lower center of the ring, due to symmetry the shear V_0 in the beam is zero. To simplify our equations, we take the x -axis and y -axis through A . For the element AO ,

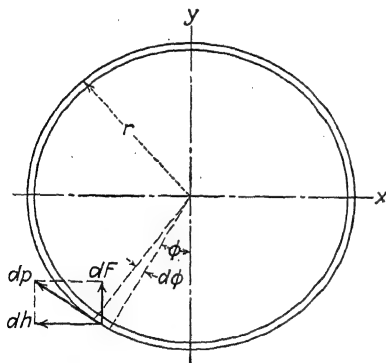


FIG. 18:9b.

$$\begin{aligned}\Sigma F_x &= 0 \\ -P - \int_0^\theta dp \cos(\theta - \phi) \\ &+ P_0 \cos \theta = 0 \quad (18:17)\end{aligned}$$

note that $dp = A \sin \phi d\phi$ [changing ϕ for θ in equation (18:9) because we wish later to sum dp from 0 to θ] (see Fig. 18:9b).

Thus, from equation (18:17), we have

$$P = P_0 \cos \theta - \frac{A}{\sin} \theta \sin \quad (18:18)$$

Also,

$$\begin{aligned}&= 0 \\ V - \int_0^\theta dp \sin(\theta - \phi) + P_0 \sin \theta &= 0 \quad (18:19)\end{aligned}$$

Solving, we have

$$\cos \quad (18:20)$$

Also,

$$= 0$$

Thus,

$$M - M_0 + dp[r - r \cos (\theta - \phi)] - P_0(r - r \cos \theta) = 0 \quad (18:21)$$

which reduces to

$$M = M_0 - Ar(\cos \theta - 1 - \sin \theta) + Pr - Pr \cos \theta + Pr(1 - \cos \theta) \quad (18:22)$$

and further reduces to

$$M = M_0 + r(P_0 - \cos \theta) + \frac{Ar}{2} \theta \sin \theta \quad (18:23)$$

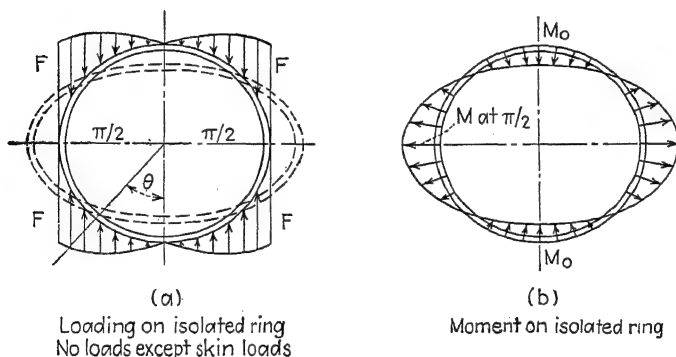


FIG. 18:10.

Thus, we have equations of P , V , and M at any location θ of the ring in terms of P_0 and M_0 at 0.

We obtain P_0 and M_0 by the method of least work, and our equations are complete.

18:12. Least-work Analysis.—The total strain energy (upon noting that $dc = r d\theta =$ a differential length of the circumference) is

$$U = 4r \int_0^{\pi/2} \frac{1}{2EI} \quad (18:24)$$

This is the equation of elastic energy in a loaded beam. Note (Fig. 18:10) that the limit is $\pi/2$.

By the theory of least work, $\partial U/\partial P_0 = 0$ and $\partial U/\partial M_0 = 0$. Thus we have, from equation (18:24),

$$\int_0^{\frac{\pi}{2}} \frac{\partial U}{\partial P_0} d\theta = 0 \quad (18:25)$$

and

$$\int_0^{\frac{\pi}{2}} M \frac{\partial M}{\partial M_0} d\theta = 0 \quad (18:26)$$

Equations (18:25) and (18:26) give two linear equations in P_0 and M_0 , which may be solved simultaneously. This is left as an exercise for the student. We now consider the more practical case shown in Fig. 18:11.

18:13. Bulkhead Ring with Concentrated Loads.—Figure 18:11 shows a bulkhead ring with skin loads dF and concentrated

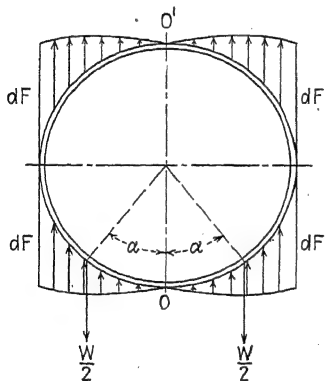


FIG. 18:11.

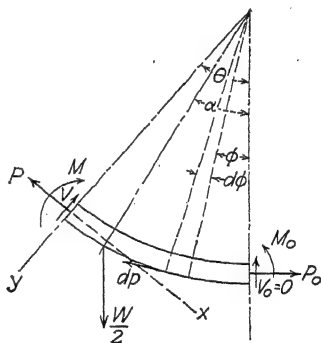


FIG. 18:12.

loads $W/2$ as attachments to wings, symmetrically spaced so that the shear at O is zero. Note that as in the case of a concentrated load on a beam the moment equation must be written in two parts, the first from the origin to the concentrated load and the second from the concentrated load to the other end of the beam, to O' in this case.

Up to the angle α , designating the location of concentrated loads, equations for P , V , and M [(18:18), (18:20), and (18:23)] hold for this case. We now derive the equations from α to π (see Fig. 18:12). To equation (18:18) we add the term $+$

$\sin \theta$ and obtain

$$P_1 = P_0 \cos \theta - \frac{A}{2} \theta \sin \theta + \frac{W}{2} \sin \theta \quad (18:27)$$

To equation (18:20) we add the term $+\frac{W}{2} \cos \theta$ and obtain

$$r_1 = A \left[\frac{3}{2} \theta - \cos \theta \left(\frac{\theta}{2} - \frac{\sin 2\theta}{4} \right) \right] - P_0 \sin \theta + \frac{W}{2} \cos \theta \quad (18:28)$$

To equation (18:23), we add the term $\frac{Wr}{2} (\sin \theta - \sin \alpha)$ and obtain

$$M_1 = M_0 + r(P_0 - A)(1 - \cos \theta) + \frac{Ar}{2} \theta \sin \theta + \frac{Wr}{2} (\sin \theta - \sin \alpha) \quad (18:29)$$

18:14. Least Work, Special Case.—Thus, we must write the energy in two integrals, the first from 0 to α and the second from α to π , as follows:

$$U = \frac{M_1^2(r d\theta)}{2EI} \quad (18:30)$$

In the first integral, we substitute M from equation (18:23), and in the second we substitute M_1 from equation (18:29).

The principle of least work states that

$$\partial U = 0 \quad (18:31)$$

and

$$(18:32)$$

which gives

and

$$(18:34)$$

These equations give two expressions involving P_0 and M_0 which when solved simultaneously give

$$= \frac{W}{2\pi} \left(\frac{3}{2} - \sin^2 \alpha \right) \quad (18:35)$$

and

$$M_0 = -\frac{Wr}{2\pi} [(\pi - \alpha) \sin \alpha - \sin^2 \alpha - \cos \alpha] + \frac{Wr}{4\pi} \quad (18:36)$$

18:15. Example of Ring Analysis.—A description of the use of equations (18:35) and (18:36) follows. Consider the case of ring loading shown in Fig. 18:13.

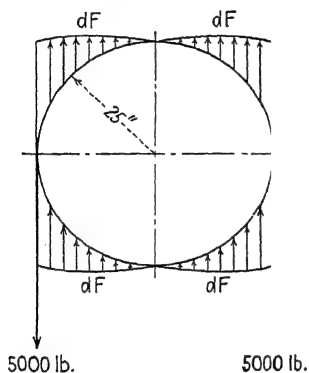


FIG. 18:13.

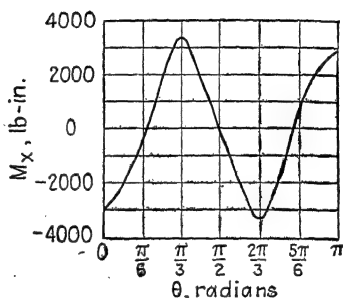


FIG. 18:14.—Loading and bending moment for ring used in example.

From equation (18:12), $A = W/\pi = 10,000/\pi = 3,183$ lb. For this case, $\alpha = \pi/2$; and so, from equation (18:35),

$$P_0 = \frac{4\pi}{4\pi} = 795.8 \text{ lb.}$$

From equation (18:36), we have $M_0 = -2,817$ in.-lb. Equations (18:23) and (18:29) then become

$$M = -2,817 - 59,680(1 - \cos \theta) + 39,788\theta \sin \theta \quad (18:37)$$

good from $\theta = 0$ to $\theta = \alpha$, and

$$M_1 = -2,817 - 59,680(1 - \cos \theta) + 39,788\theta \sin \theta - 125,000(\sin \theta - 1) \quad (18:38)$$

good from $\theta = \alpha$ to $\theta = \pi$.

If the angles θ , in radians, are substituted in these equations, the bending moments may be computed at the section under consideration. Figure 18:14 gives the results of these calculations.

18:16. Application of the Analysis.—Obviously, as in the case of several concentrated loads on a straight beam, the formulas may easily be extended to include other concentrated loads as

long as they are symmetrically located so that the shear at 0 is zero. The forces and moments may be computed for one symmetrical pair at a time and the resulting values added at corresponding points.

All calculation should be carried out to about five significant figures. This is desirable because small differences between large numbers arise in some airplanes.

It is recommended that r be taken as the outer radius of the ring. This will give conservative values for the moment.

References

1. DUNN, LOUIS G.: General Instability Criteria for Stiffened Metal Cylinders, presented at the Ninth Annual Meeting of the Institute of the Aeronautical Sciences, 1941.
2. HOFF, N. J.: Instability of Monocoque Structures in Pure Bending, *Jour. Roy. Aeronautical Soc.*, Vol. XLII, pp. 291-346, 1938.
3. TIMOSHENKO, S.: "Theory of Elastic Stability," McGraw-Hill Book Company, Inc., New York, 1936.
4. TIMOSHENKO, S.: "Strength of Materials," Vol. II, D. Van Nostrand Company, Inc., New York, 1930.
5. MILLAR, RAY A., and CARL D. WOOD: Formula for Stress Analysis of Circular Rings in a Monocoque Fuselage, *N.A.C.A. Tech. Note* 462.
6. RUFFNER, B. F., JR.: Monocoque Fuselage Circular Ring Analysis, *Jour. Aeronautical Sciences*, Vol. VI, No. 3, January, 1939.
7. NEWELL, J. S.: The Use of Symmetric and Antisymmetric Loadings, *Jour. Aeronautical Sciences*, Vol. VI, No. 6, April, 1939.
8. WISE, J. A.: Analysis of Circular Rings for Monocoque Fuselages, *Jour. Aeronautical Sciences*, Vol. VI, No. 11, September, 1939.
9. LUNDQUIST, E. E.: General Equations for the Stress Analysis of Rings, *N.A.C.A. Tech. Rept.* 509, 1934.

CHAPTER XIX

PRESSURE-CABIN STRUCTURAL DESIGN

19:1. Basic Problems.—The design of a pressure cabin suitable for high-altitude airplanes (Figs. 19:1, 1:4, and 1:5) is influenced by many factors new to aircraft structural analysis. Aside from the usual aerodynamic and landing forces, the tem-

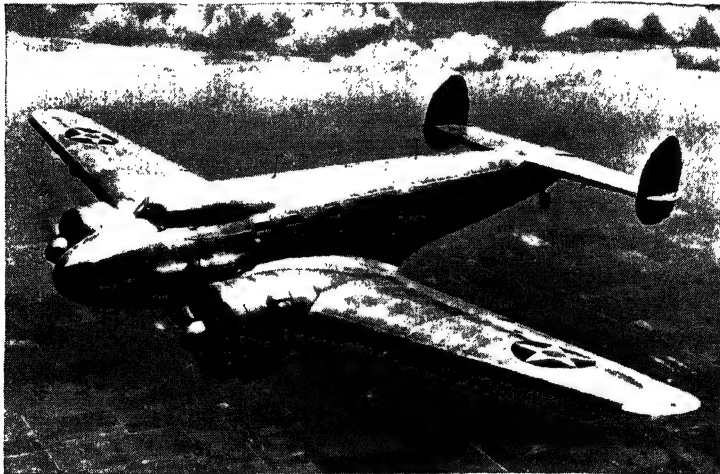


FIG. 19:1.—The world's first successful pressure-cabin airplane. For its development the U.S. Army was awarded the Collier Trophy, Col. Carl F. Greene was awarded the Distinguished Flying Cross, and the author was awarded the Spirit of St. Louis Gold Metal. (*Courtesy of U.S. Army Air Corps.*)

perature and pressure differentials must be considered in their effects on the stresses in the fuselage. The problem of temperature variation is important primarily in structures of composite materials; changes in length of various components of the cabin may introduce stresses of appreciable magnitude and affect the operation of controls that pass through the cabin walls. The most important problem, however, is the effect of the differential pressure on the cabin structure.

19:2. Temperature Effect on a Metal Fuselage.—The effect of lowering the temperature of a metal fuselage is a uniform

unit shrinkage of each dimension of the structure. If the construction embodies dissimilar metals, temperature stresses might be induced, but in a structure of a homogeneous material this effect is not present.

Within the expected range of temperature variation, the coefficient of thermal expansion of duralumin is nearly constant and equal to 12×10^{-6} per degree Fahrenheit. The change in length of any dimension of a structure is expressed by the formula

$$\Delta L = L_0(t_2 - t_1)C_t \quad (19:1)$$

where L_0 = initial length at temperature t_1 .

t_2 = new temperature.

C_t = coefficient of thermal expansion.

19:3. Temperature Change in Length of Fuselage.—Although the expected minimum air temperature is approximately -54°F ., the lowest mean temperature of the cabin walls will be probably not below 0°F ., owing to the temperature within the cabin being held at approximately $+70^\circ\text{F}$. For an example, however, let us assume that the mean metal temperature has changed from $+70$ to -30° ; for a fuselage 30 ft. long, the thermal change in length is

$$\begin{aligned} \Delta L &= L_0(t_2 - t_1)C_t, \quad L_0 = 360 \text{ in.} \\ &= 360[-30 - (70)]12 \times 10^{-6} \\ &= 360 \times (-100) \times 0.000012 \\ &= -0.43 \text{ in.} \end{aligned}$$

Temperature Diametral Change.—If the fuselage is assumed to be 6 ft. in diameter, the diametral change due to the temperature variation of -100 Fahrenheit degrees is

$$\begin{aligned} \Delta d &= 72 \times (-100) \times 0.000012 \\ &= -0.0864 \text{ in.} \end{aligned}$$

19:4. Equivalent Stresses.—To produce the same strains as those caused by the temperature change of -100°F ., the average stress would be

$$f = (t_2 - t_1)EC_t$$

where E is the modulus of elasticity, and the other terms are as previously explained.

$$\begin{aligned} f &= (-100) \times 10,500,000 \times 0.000012 \\ &= -12,600 \text{ lb. per square inch} \end{aligned}$$

This stress would be the same in both longitudinal and circumferential directions. Note that no temperature stresses occur unless the temperature deformations are opposed (see Arts. 4:24 and 4:25).

19:5. Pressure Stresses at End of Fuselage.—The total longitudinal pressure on the end of a hollow cylinder is equal to the unit pressure times the cross-sectional area of the cylinder. This total pressure is resisted by the tension stresses around the circumference of the cylinder. This is expressed by,

$$(19:2)$$

where A = cross-sectional area.

p = internal pressure.

L_c = circumferential length.

t = thickness of skin.

f_t = unit tensile stress.

Since

$$A = \pi r^2 \quad \text{and} \quad L_c = 2\pi r$$

then

$$\pi r^2 p = 2\pi r t f_t$$

Thus the tensile stress is

$$(19:3)$$

19:6. Circumferential Stresses.—The circumferential stress, or "hoop" tension, is found as follows: The total pressure on half the cylinder per unit of length is the product of the diameter times the internal pressure. This is resisted by the unit length of skin on each side of the cylinder times the unit stress. That is,

$$\begin{aligned} 2rp &= 2tf'_t \\ f'_t &= \frac{rp}{t} \end{aligned} \quad (19:4)$$

A comparison of the two formulas shows that the longitudinal stress f_t developed by the internal pressure is one-half the circumferential stress f'_t . That is,

$$f_t = \frac{1}{2}f'_t \quad (19:5)$$

If the two stresses are considered independently, the change in length or strain in either direction is given by

$$(19:6)$$

19:7. Circumferential Strain Due to Combined Stresses.—

The longitudinal strain produces an additional circumferential strain, and vice versa, relations expressed through the means of Poisson's ratio. If we call e_1 the circumferential strain due to the hoop tension f'_t , and e_2 the circumferential strain due to the longitudinal stress f_t , the following relations are found:

$$e_1 = \frac{f'_t}{E} \quad \text{and} \quad e_2 = \mu \frac{f_t}{E} \quad (19:7)$$

where μ is Poisson's ratio. The total circumferential strain is

$$e = e_1 + e_2 = \frac{f'_t}{E} + \mu \frac{f_t}{E} \quad (19:8)$$

It has been shown (19:4) that $f_t = \frac{1}{2}f'_t$. Therefore,

$$(19:9)$$

Poisson's ratio for duralumin is about 0.36; thus, the equation for total circumferential strain becomes, for that material,

19:8. Longitudinal Strain Due to Combined Stresses.—

Similarly, considering the resultant longitudinal strain e' ,

$$e' = \frac{f_t}{E} \quad \text{and} \quad e'' = \mu \frac{f'_t}{E} \quad (19:11)$$

where e' is the longitudinal strain produced by the circumferential stress. As before,

$$e - e' = \frac{f_t}{E} - \mu \frac{f'_t}{E}$$

but

$$f'_t = 2f_t \quad \text{and} \quad (19:12)$$

For duralumin,

$$= 0.28 \frac{f_t}{E} \quad (19:13)$$

e_3 and e_4 are unit strains, and the total change in length in either direction is found by multiplying the unit strain for that direction by the corresponding length affected.

Total circumferential increase = $2\pi r e_3$

Thus,

$$\Delta L_c = \frac{1.64\pi r^2 p}{tE} \quad (19:14)$$

The corresponding diametral change is

$$\frac{\Delta L}{\pi} = \Delta d = \frac{1.64r^2 p}{tE} \quad (19:15)$$

Similarly, the total change in length due to the internal pressure is $L_0 e_4$; thus,

19:9. Examples of Strain Analysis.—In our example, we choose $L_0 = 360$ in. and $r = 36$ in. Equation (19:14) gives

Diametral change due to pressure $\frac{\Delta L_c}{\pi}$

$$\begin{aligned} &= \frac{10,500,000}{10,500,000} \times \frac{p}{t} \\ &= 0.000202 \frac{p}{t} \end{aligned}$$

Equation (19:13) gives

Longitudinal change due to pressure = $\frac{0.14rp l}{tE}$

$$\begin{aligned} \Delta L_0 &= \frac{0.14 \times 36 \times 360}{10,500,000} \times \frac{p}{t} \\ &= 0.000173 \frac{p}{t} \end{aligned}$$

To continue our example, let us assume a skin thickness of 0.030 in. and compute the internal pressures necessary to balance the temperature strains.

Circumferential direction,

$$0.000202 \frac{p}{t} = 0.0864$$

$$p = \frac{0.0864 \times 0.030}{0.000202} \quad 12.8 \text{ lb. per square inch}$$

Longitudinal direction,

$$0.000173 \frac{p}{t} = 0.430$$

$$p = \frac{0.430 \times 0.030}{0.00173} = 74.6 \text{ lb. per square inch}$$

19:10. Stresses in Those Portions of the Fuselage Which Are Not Cylindrical.—Except for a small central portion, most fuselages are combinations of noncylindrical shapes; the rear is usually conical, and the forward portion is perhaps an ellipsoid of revolution. Very often these noncylindrical portions are truncated, such as at fire walls and stabilizer-spar bulkheads. The stresses induced in the various components of the fuselage depend upon their particular shape. Several cases will be investigated to indicate the possible variations in stress.

19:11. General Considerations of the Noncylindrical Cases.—To simplify the problem greatly, all the forms of “end closures” to be investigated will be assumed to be surfaces of revolution: that is, the cross section of the fuselage at any point is circular.

The skin thickness is normally very small compared with the fuselage diameter, and the amount of bending that the skin alone can resist is negligible. The skin in this case acts as a “membrane,” and so-called “membrane stresses” are induced by the internal pressure. The error introduced by neglecting the bending resistance of the skin is very small.

Figure 19:2 illustrates a surface of revolution of some general shape, with $O-O$ its axis of revolution. The area $abcd$ is any element of its surface at a point where the meridional radius of curvature is r_1 and the “latitudinal” radius (of the circle formed by cutting the surface with a plane perpendicular to $O-O$) is r_2 .

Because of symmetry, only tensile stresses act on the element. If we let

T_1 = meridional stress,

T_2 = latitudinal, or hoop, stress,

t = shell thickness,

dL_1 = meridional length of the element,

dL_2 = latitudinal length of the element,

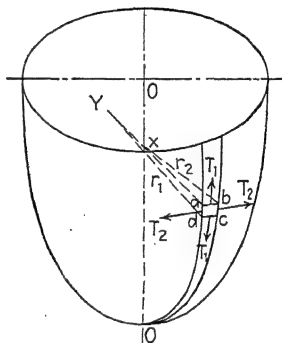


FIG. 19:2.

then the tensile force acting along the meridian is $tT_1 dL_2$, and along the latitudinal direction is $tT_2 dL_1$.

The plan view of the element $abcd$ is shown in Fig. 19:3; it may be seen that the forces acting on the sides bc and ad have components normal to the element and equal to

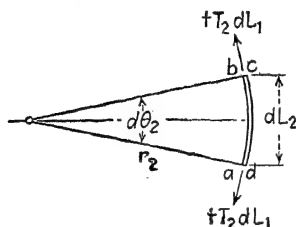


FIG. 19:3.

$$\underline{dL_2} \quad (19:16)$$

Similarly, the forces acting on the sides ab and dc have a normal component

$$dL_2 \quad tT_1 dL_2 \left(\frac{dL_1}{r_1} \right) \quad (19:17)$$

The sum of these normal components is balanced by the normal pressure on the element,

$$tT_2 dL_1 \left(\frac{dL_2}{r_2} \right) + tT_1 dL_2 \left(\frac{dL_1}{r_1} \right) = p dL_1 dL_2$$

or

$$t \quad (19:18)$$

This we shall call the *general equation*; from it we can deduce the results for some particular solutions.

19:12. Spherical End of Fuselage.—For a sphere $r_1 = r_2 = r$, by symmetry, $T_1 = T_2 = T$. The general equation (19:18) reduces to

$$T = \frac{pr}{2t} \quad (19:19)$$

which is the same as for the longitudinal stress in a cylinder of radius r and thickness t .

19:13. Conical End of Fuselage.—

If the shape is a cone, the meridional radius is infinite, and the forces acting along the meridians produce no normal components. The radius of the cone at any distance x from the apex is, as shown in Fig. 19:4,

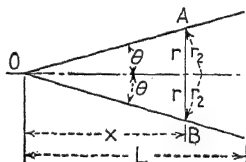


FIG. 19:4.

$$\frac{x}{\cos \theta} \tan \theta \quad (19:20)$$

The general equation then becomes

$$\frac{T_2}{x} = \frac{p}{t}, \quad \frac{T_2 \cos \theta}{x \tan \theta} = \frac{p}{t}, \quad \text{or} \quad \frac{\tan \theta}{\cos \theta}$$

p , t , and θ are constant, and so T_2 varies with x .

The T_1 stresses are found similarly to the longitudinal stresses in a cylinder [equation (19:3)].

At section AB ,

$$2\pi r t (T_1 \cos \theta) = \pi r^2 p$$

and

$$r = x \tan \theta$$

Thus,

$$2\pi x (\tan \theta) (\cos \theta) = \pi p (x \tan \theta)^2$$

and

$$T_1 = \frac{px \tan \theta}{2t \cos \theta} \quad (19:22)$$

which is one-half the value for T_2 , the hoop tension.

As before, when we consider the Poisson's ratio effect, the unit meridional strain at any point is

$$e_1' = \frac{\epsilon_1}{E} - \mu \frac{\epsilon_2}{E} = \frac{\epsilon_1}{E} (1 - 2\mu), \quad \text{for} \quad T_1 = \frac{1}{2} T_2 \quad (19:23)$$

In the hoop direction, the strain is, as previously shown,

$$(19:24)$$

19:14. Bulkhead Stresses at Junction of Cylinder and Ends.

It was assumed, because the skin is very thin, that the bending moments induced in the skin were negligible. If a bulkhead is placed at the junction of the cylindrical portion of the fuselage and the end closure, this assumption allows us to say that the outward load on the bulkhead owing to its restraining effect on the skin is very small.

In Fig. 19:5, if AB is the bulkhead and the skin on one side of it is CA , the internal pressure will move the skin to the position DEA . If the skin were not attached

FIG. 19:5.

to the bulkhead, it would expand to the position *DEF*. The only outward load on the bulkhead then is due to the "restrained" length of skin, x , and the internal pressure thereon; this load is relatively small.

If now we consider a cone *AC* of length L , as shown in Fig. 19:6, attached to the bulkhead *AB* of radius r , the meridional stress T_1 is as found previously.

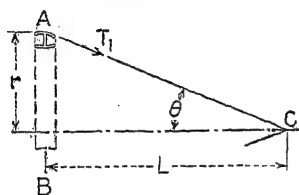


FIG. 19:6.

$$2t \cos \theta \quad (19:25)$$

The outward force on the bulkhead due to the internal pressure is, as explained above, relatively small; the major load on the ring then is due to the

inward component of T_1 ($= T_1 \sin \theta$).

For each unit width ω of skin, having an area A , the inward unit load T_n on the ring is

$$T_n = T_1 A \sin \theta, \quad \text{where} \quad A = \omega t = t$$

Thus,

$$\tan \theta \quad (19:26)$$

But

$$\tan \theta = \frac{r}{L}, \quad \text{so that} \quad \frac{pr^2}{2L} \quad (19:27)$$

It should be noted that the inward running load on the ring varies inversely with the length of the cone: the shorter the cone, the higher will be the load on the ring.

19:15. Pressure on Windows and Other Flat Surfaces.—Windows and other details that are part of, but not continuous with, the fuselage covering require a consideration of the stresses developed in them when subjected to various loadings and means of support. The derivation of the following formulas is quite involved and beyond the scope of this volume; they may be found, further discussed, however, in many treatises on the theory of elasticity.

1. *Circular plate simply supported.*

$$M = \frac{a^2}{16} (3 \quad \text{and} \quad f = \frac{3a^2}{8l^2} (3 + \mu)p \quad (19:28)$$

where M = maximum bending moment (at center of disk).

f = maximum fiber stress.

a = radius of disk.

t = thickness of disk.

μ = Poisson's ratio.

p = internal pressure.

The units are pounds and inches.

2. *Circular plate with clamped edges.*—The maximum moment and fiber stress occur at the rim.

$$M = \frac{\alpha^2 p}{8}, \quad = \frac{1}{14.2} p \quad (19:29)$$

3. *Rectangular plate simply supported.*—The solution for a rectangular plate is not exact but is solved by approximate methods. If the plate is square,

$$M(\text{at center}) = 0.0368a^2p(1 + \mu) \quad (19:30)$$

where a is the length of either side.

When b , the length of the longer side, is twice a , the shorter side, and $\mu = 0.25$, the particular solution gives

$$M = 0.0992a^2p \quad (19:31)$$

where M is the moment at the center across a unit width parallel to the longer sides.

When b/a is very great, the effect of the supporting of the short sides is very small, and the plate may be treated as a beam.

$$M = \frac{1}{8}pa^2 \quad (19:32)$$

where M is the moment at the center across a unit width parallel to the shorter sides (see Fig. 19:7). The maximum bending moment for other values of b/a is given by

$$M = Kpa^2 \quad (19:33)$$

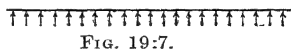


FIG. 19:7.

The value of K is a maximum of approximately 0.12, taking $\mu = 0.3$. K is a minimum of 0.048 approximately for square plates, taking $\mu = 0.3$.

4. *Rectangular plate with clamped edges.*—The solution of this condition is also an approximate one and is given by equation (19:33) in a coefficient form as indicated above. Values of K are

$$\text{For } \frac{\nu}{a} = 0.1, \quad K = 0.051$$

$$\frac{\nu}{a} = 0.2, \quad K = 0.083$$

$$\text{For } \frac{\nu}{a} = \quad K = 0.083$$

5. *Elliptic plate with clamped edges*.—This solution is precise,¹ the moment at the center of the plate being

$$\frac{1}{b^2} + \frac{\mu}{a^2} \quad (19:34)$$

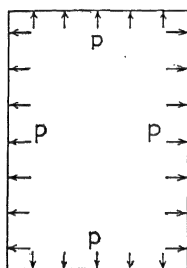


FIG. 19:8.

when the equation for the ellipse is $\frac{x^2}{a^2} + \frac{y^2}{b^2} = 1$. This moment is for the unit

strip in the y -direction. The maximum moment in the plate occurs at the ends of the $2b$ axes and is given by

$$M'_2 = \frac{P}{b^2} \left(\frac{1}{\frac{3}{a^4} + \frac{3}{b^4} + \frac{2}{a^2 b^2}} \right)$$

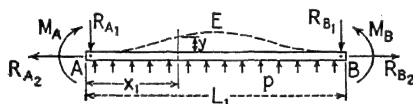


FIG. 19:9.

19:16. Rectangular Section Subject to Internal Pressure.—Let $ABCD$ in Fig. 19:8 be a rectangular tube with sides of length L_1 and L_2 , subjected to internal pressure p . The corners are continuous; each side is therefore subject to restraining moments from the adjacent sides. In Fig. 19:9, we have isolated the side AB and have shown it with the various applied forces for equilibrium. \overline{AB} is the unstrained position of the side, and \overline{AEB} is its deformed shape.

¹ See Prescott, John, "Applied Elasticity," p. 416. Longmans, Green and Company, New York, 1924.

From symmetry, it is seen that $M_A = M_B$ and $R_{A_1} = R_{B_1} = \frac{1}{2}(pL_1)$. The moment at any point x_1 is then given by

$$(19:35)$$

The last term in this expression is the moment about the point x_1 of the force or reaction from the adjacent side $= R_{A_4} = R_{B_2} = \frac{1}{2}(pL_2)$ (see Fig. 19:10).

Taking the second derivative of M_1 with respect to x_1 , we find

$$\frac{d^2 M_1}{dx_1^2} = p$$

But

$$\frac{d^2 M_1}{dx_1^2} = \frac{EI}{EI}$$

and so we have

$$(19:36)$$

Letting $pL_2/2EI_1 = n_1^2$, we arrive at the differential form

$$p = \frac{EI}{EI} \quad (19:37)$$

19:17. Solution of the General Equation.—The general solution of equation (19:36) is

$$M_1 = A_1 \sinh n_1 x_1 + B_1 \cosh n_1 x_1 - \frac{p}{n_1^2} \quad (19:38)$$

In a similar manner, we can write the equation for the moment at any point in the side L_2 .

$$M_2 = A_2 \sinh n_2 x_2 + B_2 \cosh n_2 x_2 - \frac{p}{n_2^2} \quad (19:39)$$

To evaluate the constants A and B , we have

(a) By symmetry the shear $\frac{dM}{dx} = 0$, when $x = \frac{L}{2}$

(b) When $x_1 = 0$, $M_1 = M_A$

From (a) and (b), we find

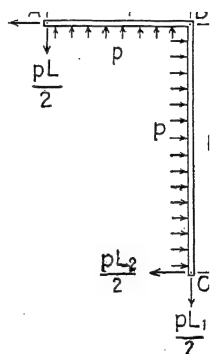


FIG. 19:10.

$$1 \frac{L_1}{2} \quad (19:40)$$

and

$$\beta_1 = M_A + \frac{P}{n_2} \quad (19:41)$$

Corresponding results for A_2 and B_2 may be similarly found.

TABLE 19:1.—PRECISE THREE-MOMENT-EQUATION FUNCTIONS FOR AXIAL TENSION

jL	α	β	γ
0.00	1.0000	1.0000	1.0000
0.50	0.9716	0.9837	0.9756
1.00	0.8945	0.9391	0.9092
1.10	0.8748	0.9276	0.8922
1.20	0.8542	0.9155	0.8743
1.30	0.8328	0.9028	0.8557
1.40	0.8107	0.8897	0.8364
1.50	0.7881	0.8762	0.8167
1.60	0.7652	0.8625	0.7967
1.70	0.7421	0.8485	0.7766
1.80	0.7189	0.8344	0.7560
1.90	0.6958	0.8202	0.7355
2.00	0.6728	0.8060	0.7152
2.10	0.6501	0.7918	0.6950
2.20	0.6278	0.7777	0.6750
2.30	0.6058	0.7637	0.6555
2.40	0.5843	0.7499	0.6360
2.50	0.5633	0.7362	0.6170
2.60	0.5429	0.7228	0.5985
2.70	0.5230	0.7097	0.5803
2.80	0.5037	0.6967	0.5627
2.90	0.4851	0.6840	0.5457
3.00	0.4670	0.6716	0.5288
3.10	0.4496	0.6595	0.5125
3.20	0.4328	0.6476	0.4968

19:18. Moments at the Corners.—If we consider one side and one end as a continuous beam, as in Fig. 19:10, the conditions of symmetry allow us to solve for M_A by the use of the precise three-moment equation.

$$L_1 \quad \backslash \quad L_1 \quad L_2 \quad (19:42)$$

By symmetry,

$$M_A = M_B = M_C$$

Thus

$$(19:43)$$

It must be noted that the values for α , β , and γ are those for beams with axial tension (see Table 19:1).

The moment in the middle of the side L_1 , ($x_1 = L_1/2$), is given by the expression

$$\frac{M_L}{2} \cosh \frac{n_1^2}{m^2} \frac{p}{m^2} \quad (19:44)$$

References

1. YOUNGER, J. E., and G. D. BOGERT: Pressure Cabin Investigation, Phase 1, *Air Corps Tech. Rept.* 4220, 1936.
2. Textbooks on advanced applied elasticity.
3. ENGELHARDT, L. F.: Some Structural Problems Pertaining to Pressurized Fuselages, *Jour. Aeronautical Sciences*, Vol. VI, No. 8, pp. 319-322, June, 1939.
4. MONESS, E.: Flat Plates under Pressure, *Jour. Aeronautical Sciences*, Vol. V, No. 11, pp. 421-425, September, 1938.

CHAPTER XX

WING FLUTTER AND OTHER STRUCTURAL VIBRATIONS

20:1. Contributing Causes.—The conditions in modern airplane structures are ideal for the development of excessive vibrations. These basic conditions are

1. An elastic structure.
2. Augmenting impulses such as are contributed by the engines and air stream.

The combination of conditions may be expressed in a fundamental equation

$$M \frac{d^2y}{dt^2} + Ky = P_0 \sin \frac{2\pi}{T} t \quad (20:1)$$

where M = mass of the vibrating structure.

K = elasticity, or spring constant, of the structure.

$P_0 \sin \frac{2\pi}{T} t$ = periodic augmenting force.

T = period of the augmenting force.

To fix ideas, let us assume a weight suspended from a spring. In this case, M is the mass of the weight, and K is the spring constant in pounds per foot of stretch. Now if the weight is vibrating freely (with no augmenting force), the equation is

$$M \frac{d^2y}{dt^2} + Ky = 0 \quad (20:2)$$

which is the equation of *simple harmonic motion*, the natural period of which is

$$(20:3)$$

Now, applying a periodic force, we express the conditions by equation (20:1).

20:2. Resonant Vibration.—The solution of equation (20:1) is

$$y = A \sin \sqrt{\frac{K}{M}} t \sin \left(\frac{\omega \pi}{T} \right) \quad (20:4)$$

Now from equation (20:3) we note that

Thus, with reference to the third term of equation (20:4), when $T_0 = T$, the denominator of the term becomes zero; hence, y becomes infinite. Therefore, *when $T_0 = T$, that is, when the period of the augmenting force becomes equal to the natural period of vibration of the structure, the system is said to be in resonance.* In the prevention of dangerous structural vibration, the first principle is to avoid resonance. It will be observed [equation (20:3)] that the magnitude of P_0 affects ordinary vibration, but it does not affect resonant vibrations.

20:3. Transverse Vibration of Engine Mounts.—The frequency of impulsive forces of the engine, in general, is proportional to the r.p.m. and hence cannot be changed. It is easy, however, to fix the natural frequency (or period) of the structure, so that resonance will not occur. The frequency may be *raised* by making the structure more rigid. This may be accomplished by the use of more members, of heavier members, or of material with higher modulus of elasticity or by an inherently rigid type of structure, such as monocoque. The natural frequency may be lowered by making the structure more flexible. Rubber or spring pads for mounting the engine are convenient for this purpose.

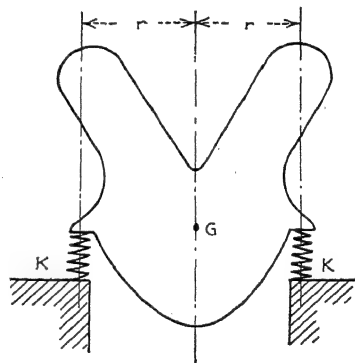


FIG. 20:1.—Flexible engine mount.

In calculating the natural frequency, equation (20:3) is used. M is the mass of the engine—the weight in pounds divided by 32.2. y is measured at the center of gravity of the engine in feet. K is the spring constant of the engine mount, that is, the force that would be required to deflect the structure 1 ft. For example, calculate the deflection of the structure due to a weight of 1,000 lb. If this is, say, 0.1 ft., then $K = 10,000$ lb. per foot. The deflection y may be simply computed as noted in Art. 6:13.

20:4. Torsional Vibration of Engine Mount.—The equation of motion for this condition is (Fig. 20:1),

$$(20:6)$$

where I = mass moment of inertia of the engine about its center of oscillation, which may be assumed the center of gravity.

K = spring constant of the mounting.

M_0 = applied torque.

The solution is

$$\theta = A \sin \sqrt{\frac{2Kr^2}{I} - \left(\frac{2\pi}{T}\right)^2} t + B \cos \sqrt{\frac{2Kr^2}{I} - \left(\frac{2\pi}{T}\right)^2} t + \frac{M_0/1}{\frac{2Kr^2}{I} - \left(\frac{2\pi}{T}\right)^2} \frac{2\pi}{T} t \quad (20:7)$$

The natural period of oscillation is

$$T_0 = 2\pi \sqrt{\frac{I}{2Kr^2}} \quad (20:8)$$

Resonance occurs when $T_0 = T$.

The units are pounds, feet, and seconds.

20:5. Damping Vibrations.—The usual methods of eliminating vibrations are as follows:

1. Remove, if possible, the source of the augmenting force. In the case of the engine, this would imply perfect balancing.
2. Change the natural frequency of the structure so that resonance with augmenting forces is not probable.
3. Dissipate the energy of the vibrating system by means of dry friction or viscous friction. Fibrous packing for joints in the structure is available commercially. Such packing between the engine mount and the structure and between the fuselage and wing is advantageous.
4. Set up opposing vibrating system by means of a dynamical vibration damper (see Ref. 6).

Methods (2) and (3) are most adaptable to aircraft.

20:6. Nature of Wing Flutter.—Wing flutter may occur in the overhanging tip of a braced wing or in a monoplane wing. The phenomenon is a vibration of the wing in approximately its own *natural frequency* and *mode*. The augmenting force is supplied by the air stream, controlled by the action of the wing. The resulting amplitudes of vibration *build up* to alarming proportions, and generally the result is a destruction of the wings

A wing has two principal modes of vibration. If the *elastic axis* coincides with the *gravity axis*, the modes are *pure bending* and *pure torsion*. If the elastic axis and the gravity axis do not coincide, the axes of vibration are inclined to the pure-bending and pure-torsional axes. For practical designs, it is probably accurate enough to assume vibration in pure torsion and pure bending.

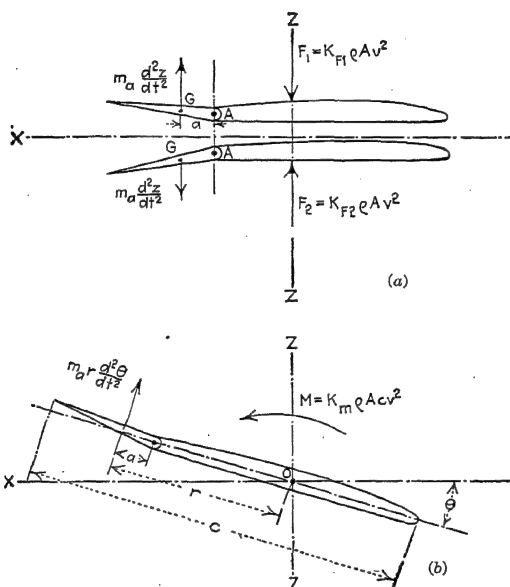


FIG. 20:2.—Modes of wing flutter.

20:7. Wing Flutter in Bending.—In Fig. 20:2a, we have represented the cross section of a cantilever monoplane wing near the tip of the wing. We assume, first, a free vibration of the wing in bending. Thus the *reversed effective force* acting on each mass particle is $m \frac{d^2 z}{dt^2}$ acting away from the x -axis. Hence, the moment tending to turn the aileron about its hinge is

$$(20:9)$$

in which m_a is the mass of the aileron, assumed concentrated at the center of gravity G .

Now if the aileron is free or if the elastic restraints (control wires) are flexible enough, the aileron is deflected as noted in the figure. If the wing is moving forward at a velocity V , the camber of the wing in its up-and-down position causes air impulses F_1 and F_2 , respectively, where

$$F = K_F \rho A v^2 \quad (20:10)$$

where the magnitude of K_F is unknown.

This augmenting impulse F causes the amplitude to build up to excessive values.

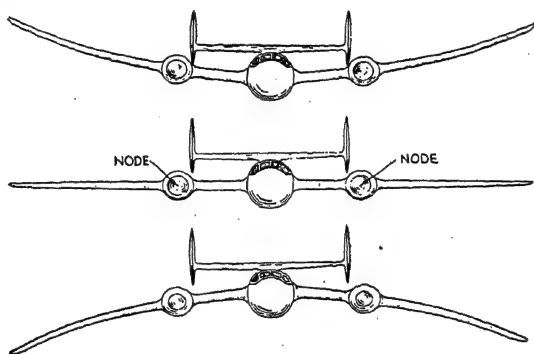


FIG. 20:3.—Primary wing flexure.

Experiments show that, when the natural frequency of the aileron about its hinge A is the same as the natural frequency of the wing in bending, this type of flutter is certain to occur. This is, in general, true also if the ailerons are free.

20:3. Wing Flutter in Torsion.—Figure 20:2*b* shows that the moment which tends to deflect the aileron is

$$(20:11)$$

where θ is the angular displacement of the wing. A restoring aerodynamic moment

$$M = K_m \rho A C v^2 \quad (20:12)$$

is induced which augments the oscillations. If the aileron is free or if it has the same natural frequency in vibration about its hinge as that of the torsional oscillation of the wing, the amplitude will readily build up.

20:9. Aileron-wing Flutter.—It is readily obvious that the two types of flutter represented in Fig. 20:2 may occur simultaneously. In most cases, this is probably what actually occurs. In this case, the point *O*, the center of oscillation, would be forward of

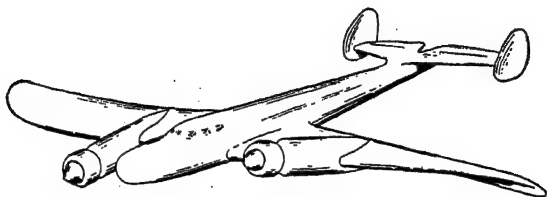


FIG. 20:4.

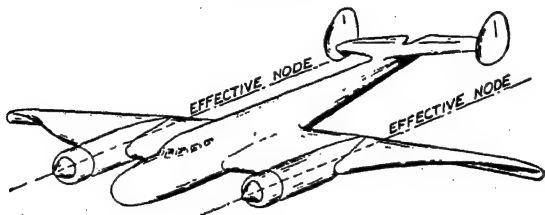


FIG. 20:5.

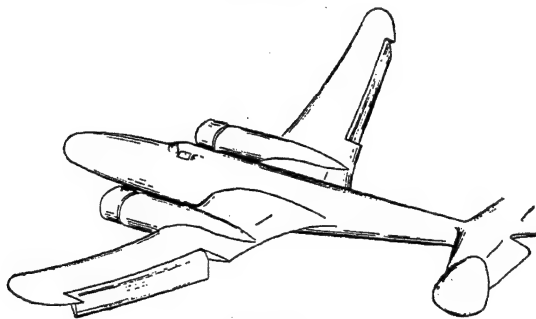


FIG. 20:6.

the leading edge. Figures 20:3 to 20:6 show types of wing flutter that may occur on wings of a monoplane with two motors.

20:10. Recommendations for the Prevention of Wing Flutter.

In general, the structure of the wing should be as rigid as possible, though this alone will not preclude wing flutter. It is especially desirable that the wing be rigid in torsion. This is one of the most outstanding advantages of the stressed-skin wing—it is the most rigid in torsion of all types yet developed.

. With reference to Fig. 20:2 and the discussion thereof, we may make the following recommendations relative to the ailerons:

1. The ailerons should be made as light as possible to decrease the deflecting moment [see equations (20:9) and (20:11)]. Some find it desirable in "all-metal" airplanes to cover the ailerons with fabric for lightness.

2. Make a in Fig. 20:2 zero or negative; that is, the hinge of the aileron should coincide with the center of gravity of the aileron or be slightly to the rear of it.

3. The control rods or wires should be made as rigid as possible. From this standpoint, push rods or tubes are highly desirable. Long wires allow the ailerons considerable elastic movement with a low natural frequency, both of which are conducive to flutter.

4. Irreversibility of aileron controls prevents free oscillations of the ailerons, thus affording a damping tendency. Pilots, however, offer serious objections to this feature, as forces on the ailerons cannot be felt on the control wheel.

5. Frictional damping of the aileron has a decided effect in preventing aileron flutter, but it interferes with the smooth operation of the aileron.

The first three items of this list are the most effective in preventing wing flutter and are under the control of the structural designer. The designer will find that item 4 is also quite effective if the aileron is made partially irreversible and the mechanism is installed immediately adjacent to the ailerons. The principle of the screw or inclined plane may be used effectively in this respect. The installation of the irreversible mechanism near the aileron makes the aileron quite rigid in torsion about its hinges.

20:11. Elevator Flutter.—Elevator flutter manifests itself as a torsional oscillation about the axis of the fuselage. Figure 20:2 may well represent the tip of a horizontal stabilizer with its elevator. In this case the forces and moments are of the same nature as those of the wings and ailerons.

Recommendations for the prevention of this type of flutter may be listed as follows:

1. Great torsional rigidity of the fuselage.
2. The elevators should be constructed on the same torsion tube. This tube between the elevators should be very rigid in torsion.
3. The five recommendations of the last article for ailerons apply equally well for elevators.

These rules will also apply for rudders.

20:12. Airfoil Flutter.—Airfoil flutter is the flutter of an airfoil such as a propeller or wing when not influenced by an aileron or

other auxiliaries. Airfoil flutter may be either bending or torsion or a combination.

It has been shown (Ref. 3) that an airfoil flutters with a frequency approximately its own natural frequency and that the critical speed is proportional to the natural frequency of the wing or propeller blade (see, for example, Fig. 20:7).

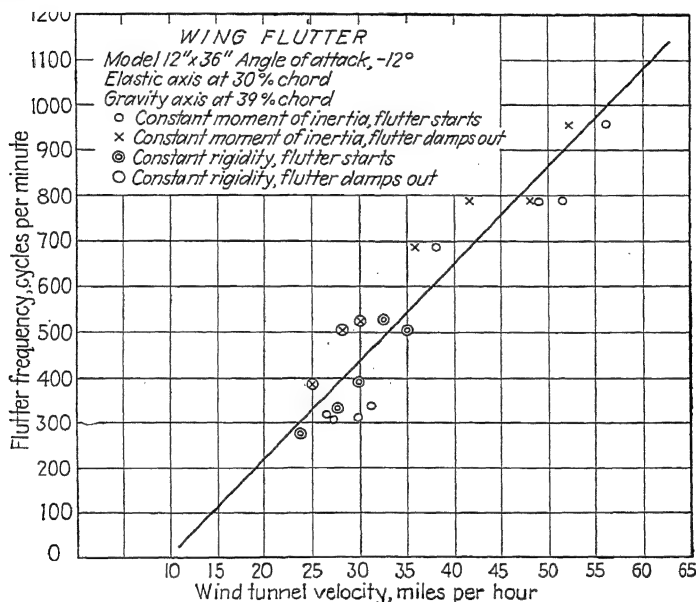


FIG. 20:7.

20:13. Natural Frequency in Bending and in Torsion.—The natural frequency of a propeller blade or a wing may be determined by the method of successive approximations. See for example, Reference 6, for bending-frequency-formula derivation and sample calculations and Chap. XXI for torsional-frequency-formula derivation and sample calculations.

References

1. DEN HARTOG, J. P.: "Mechanical Vibrations," McGraw-Hill Book Company, Inc., New York, 1934.
2. FRAZER, R. A., and W. J. DUNCAN: The Flutter of Monoplanes, Biplanes, and Tail Units, *British Advisory Committee Aeronautics, Repts. and Mem.* 1255, January, 1931.

3. GREENE, CAPTAIN C. F., and J. E. YOUNGER: Study of Wing Flutter, *Air Corps Information Circ.*, Part I, Vol. VII, No. 635, Sept. 15, 1929; Part II, Vol. VII, No. 653, Aug. 30, 1930.
4. GREENE, CAPTAIN C. F.: An Introduction to the Problem of Wing Flutter, June 28, 1928, 8 pages, *Trans. A.S.M.E.*, AER-50-10 May-August, 1928.
5. VON BAUMHAUER, A. G., and C. KONING: On the Stability of Oscillations of an Aeroplane Wing, paper presented to the International Air Congress, London, June, 1923.
6. YOUNGER, J. E., and B. M. WOODS: "Dynamics of Airplanes and Airplane Structures," John Wiley & Sons, Inc., New York, 1931.
7. THEODORSEN, THEO.: General Theory of Aerodynamic Instability, and the Mechanism of Flutter, *N.A.C.A. Tech. Rept.* 496, 1934.
8. THEODORSEN, THEO., and I. E. GARRICK: Mechanism of Flutter, a Theoretical and Experimental Investigation on the Flutter Problem, *N.A.C.A. Confidential Rept.*, November, 1938.
9. WYLIE, JEAN: Flexure Torsion Binary Flutter, *C.A.A. Dept. Commerce, Aircraft Airworthiness Sec.*, *Rept.* 22, 1941.
10. BERGEN, W. B., and LEE ARNOLD: Graphical Solution of the Bending Aileron Case of Flutter, *Jour. Aeronautical Science*, Vol. VII, No. 12, Oct. 1940.

CHAPTER XXI

RIVETING IN AIRCRAFT CONSTRUCTION

21:1. Kinds of Riveted Joints.—Two general types of riveted joints in aircraft construction are (1) *lap joints* (Fig. 21:1), and (2) *butt joints* (Fig. 21:2).

It is seldom that two very thin sheets (less than 0.050 in. thick) are spliced except where a structural member backs up the joint

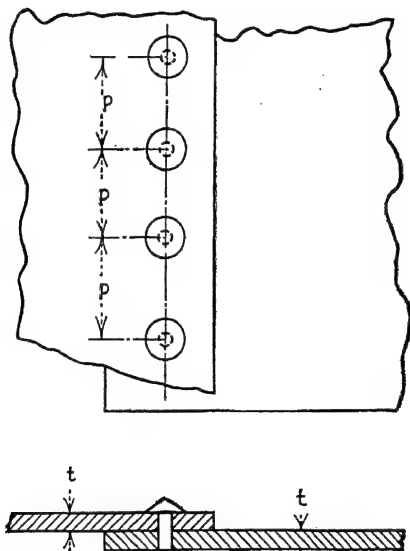


FIG. 21:1.—Lap joint.

as shown in Fig. 21:3. The designer is mostly concerned with the design of joints in strength members, gusset plates, etc.

Either type of riveted joint may have one or more rows of rivets as shown in Figs. 21:4 and 21:5.

In the double-riveted lap joint (Fig. 21:6), the rivets in the second row may be placed directly behind the rivets in the first row, or they may be arranged zigzag as shown in the figure. The two rows must not be placed too closely together or the sheets

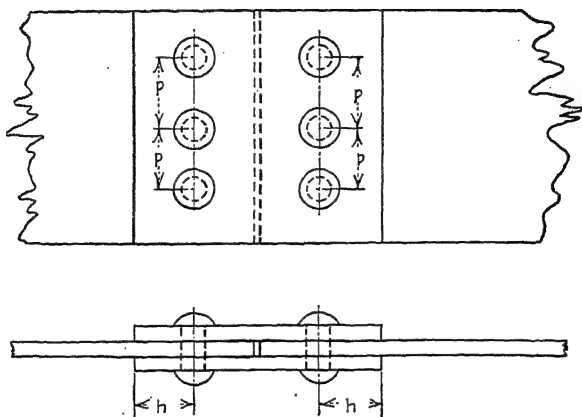


FIG. 21:2.—Butt joint.

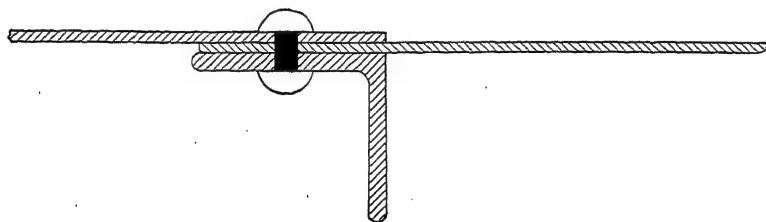


FIG. 21:3.—Riveted seam in thin material.

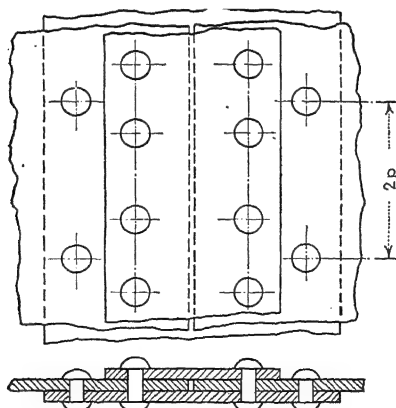


FIG. 21:4.—Multiple-riveted butt joint, with two rows of rivets.

of thin metal may fail along the diagonal lines joining the rivets of the two rows. This is also true for all multiple-riveted joints. The total distance a or b should be over 20 per cent greater than d . The rivets should be far enough away from the edge to prevent shearing out the plate. The pitch p depends upon the purpose of the joint. In a gas tank the pitch is made quite small to prevent leakage. In a strength member the pitch, together with diameters of rivets, etc., should be calculated to give a joint of approximately the same strength in *tension*, *compression*, and *shear*.

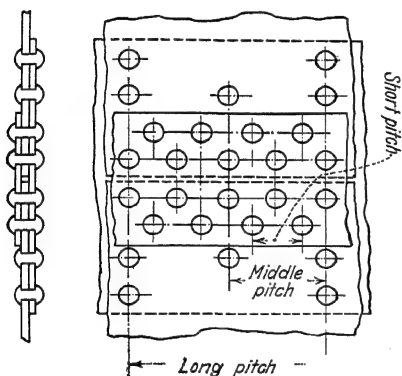


FIG. 21:5.—Multiple-riveted butt joint with four rows of rivets.

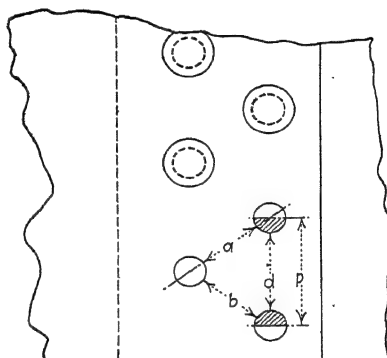


FIG. 21:6.—Spacing of rivets.

21:2. General Rules for Design of Riveted Joints.—The designer should bear in mind, in the design of riveted joints, the following rules:

1. The joint should be designed so that the rivets are in shear. Tension in rivets should be avoided.
2. In general, the rivets should be regularly and equally spaced.
3. Where butt straps are used, as in the butt joints, the straps should *not* be of less thickness than the main plate.
4. The thickness of the plates should regulate the size of the rivets (see Table 21:1).
5. The rivet holes should have smooth and regular sides, without burrs or cracks. A drilled hole usually meets this requirement.
6. Rivets should be dipped into a good quality of bituminous paint or other preparation before inserting to prevent corrosion.
7. The sheets are bolted together with small bolts that fit the rivet holes before, and while, rivets are driven.

8. In general, rivets should not be nearer to butts or edges of the plating, straps, or bars than a space equal to $1\frac{1}{2}$ times the diameter of rivet.

9. In general, in edge riveting, the space between any two consecutive rows of rivets should not be less than two rivet diameters.

21:3. Heat-treating Aluminum-alloy Rivets.—Rivets of 2S and 3S do not need heat-treating before driving, although they do "work-harden" in driving. This is a desirable feature to prevent permanent deformation under load and loosening as a result. It is imperative that 17S rivets be heat-treated before driving as they are too hard normally and, if driven untreated, are very apt to split around the edge of the head. The hard rivet will also swell the hole in the sheet, causing the sheet to wave between rivets.

The heat treatment of duralumin rivets is a comparatively simple operation, but the temperature must be properly controlled to obtain satisfactory results. Although there are several types of furnaces used for the treatment of rivets and small duralumin parts, the salt-tank type is the most widely used. This consists of a steel tank of sufficient capacity to handle the desired volume of work, with some means of heating (electricity, gas, etc.). The salt bath, which is a half-and-half mixture of pure sodium nitrate and potassium nitrate, is heated to from 940 to 960°F. in the heat-treatment process and is maintained at this temperature through the use of a pyrometer. The rivets are left in the solution 10 to 20 min., depending upon the size of the rivets. After the rivets have been in the salt bath for the required period, they should be taken out and quenched in cold water and then washed off. Two tanks should be used for the quenching and washing operations.

The rivets should be driven within $\frac{1}{2}$ hr. after quenching; otherwise, they will become excessively hard and re-treatment will be necessary.

After they have been quenched, the rivets are soft but start aging immediately, obtaining their maximum hardness in about 4 days. This feature is very advantageous as it allows sufficient time for the job to be finished before the maximum hardness is developed. If, for any reason, it is desired to keep the rivets soft after heat-treatment, they may be placed in an atmosphere below 32°F., as in containers surrounded by dry ice (solid carbon dioxide). In this way the rivets may be kept soft enough for driving for several hours.

21:4. Riveting of Stainless-steel Sheets.—Riveting of stainless steel is done either hot or cold. Small rivets may be drawn cold and set by comparatively few heavy blows. Hot rivets should be heated out of contact with the furnace flame or in electric resistance heaters, which use the rivet as the circuit between two electrodes of low electrical resistance, to a temperature of 2100°F. These hot rivets must be set so that mechanical deformation is finished before they cool below 1750°F. Riveting is of doubtful economy in structural joints. The holes are readily torn. Stainless rivets harden rapidly and are difficult to handle.

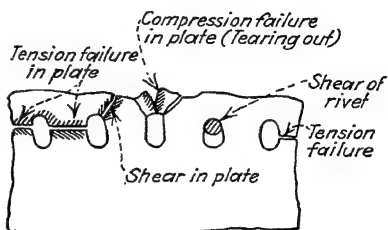


FIG. 21:7.—Types of failures in riveted joint.

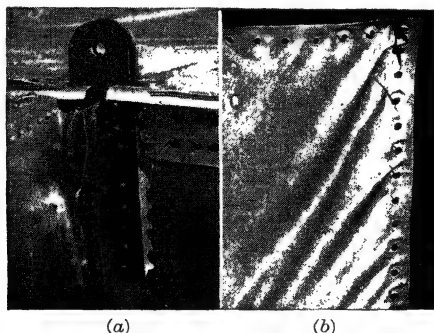


FIG. 21:8.—Types of failures in riveted joints. (a) Tearing and shear of sheet, (b) tension and crushing of sheet.

21:5. Rivet Stress Calculations.—Figures 21:7 and 21:8 show the three types of failures in a riveted joint, in tension, in compression, and in shear. Figure 21:9 shows a free-body diagram of the types of stress in a riveted joint to be provided for in design. These may be listed as follows:

1. Shear in rivet.
2. Shear in plate.
3. Compression in plate.
4. Compression in rivet.
5. Tension in plate.
6. Tension in rivet (if designed for tension; this, in general is poor practice).

In stress calculations it is assumed that a group of rivets in a joint will carry their full shear-stress value. If the joint is not properly designed, this assumption does not hold. The proper consideration must be given to the elasticity of the plates or straps. The stretch or strain in a strap is proportional to the stress; hence, the first row of rivets is subjected to a greater shear stress than are the remaining rivets. In a compact joint this condition does not affect the strength appreciably.

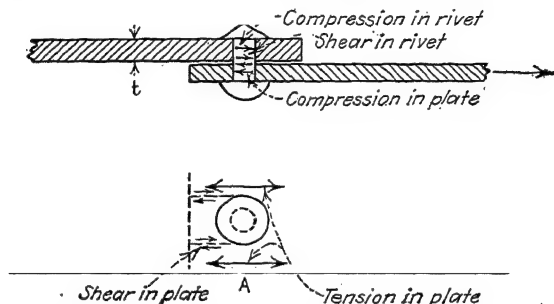


FIG. 21:9.—Types of stresses in riveted joint.

Care must also be exercised in grouping the rivets so that the centroid of the rivet areas coincides with the intersection of the neutral axes of the members connected; otherwise, because of the flexibility of the members, undue stress will be thrown upon some of the rivets by the bending moment developed by eccentricity. Experiments show that an error in design of this nature produces considerable loss in the strength of the joint.

21:6. Joints of Equal Strength in Shear, Tension, and Compression.—If we designate s as the unit shearing strength of the rivets, f_c the unit crushing or compressive strength of the plate, f_t the unit tensile strength of the plate, t the thickness of the plate, d the diameter of the rivets, and p the pitch of the rivets, we have for a single-row riveted lap joint, by equating the compressive strength to the tensile strength of the plate,

$$- d) \quad (21:1)$$

or

$$p = \quad (21:2)$$

If we define the efficiency as

$$(21:3)$$

we have, by substituting equation (21:2) in equation (21:3),

$$e = \overline{f_c + f_t} \quad (21:4)$$

If we equate the shearing strength and the compressive strength, we have

$$f_c t d = \frac{\pi d^2}{4} \quad (21:5)$$

or

$$d = \frac{\pi J c t}{\pi s} \quad (21:6)$$

Thus, if the values of f_s , s , and t are known, the diameter and pitch of the rivets may be determined from equations (21:2) and (21:6).

For a single-riveted butt joint the relation between compression of plate and tension in the plate section is the same as in a single-riveted lap joint; hence, equation (21:2) holds for this case.

Since each rivet is in double shear, equation (21:5) becomes

$$(21:7)$$

from which

$$\pi s \quad (21:8)$$

In a double-riveted lap joint two rivets are in compression in unit width, so that

$$2 f_c t d = f_t (p - d) \quad (21:9)$$

Thus

$$p = \frac{2 f_c t}{f_t} d \quad (21:10)$$

The relation between shear and compression is the same as in a single-riveted lap joint so that equation (21:6) holds.

21:7. Eccentric Loads on Riveted Joints.—The following procedure should be followed when calculating rivet and bolt stresses in eccentrically loaded joints:

1. *Calculate the centroid of the rivet group.*—This is done in the same way as finding centroids of composite sections except that the rivet values are used instead of areas. Either the *shear* or the *bearing* values should be used, depending on which is the smaller.

$$\bar{r} = \frac{\quad}{+ V_2 +} \quad (21:11)$$

where V = bearing or shear value of rivet.

d = distance of rivet from reference axis.

2. Calculate the moment of the applied load about the centroid of the rivet group.

3. Calculate the moment of inertia of the rivet group about the centroid.—This is done by taking the sum of the product of the rivet value and the square of the distance to the centroid.

$$I = \Sigma V_1 r_1^2 + V_2 r_2^2 + \dots \quad (21:12)$$

4. Calculate the resultant load on each rivet due to the moment.

$$\text{Load on rivet 1} = \quad (21:13)$$

The direction of this load on each rivet is perpendicular to a line passing through the rivet and the centroid of the section.

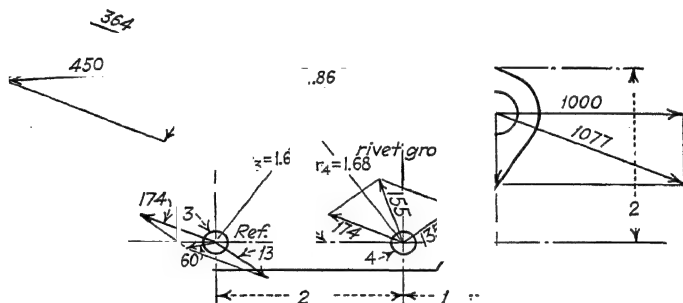


FIG. 21:10.—Centroid rivet group.

5. Calculate the load on each rivet due to the direct load.—This is equal to the resultant applied load times the value of the rivet in question divided by the sum of all the rivet values.

$$\text{Direct load on rivet 1} = \text{resultant load} \times \frac{V_1}{\Sigma V} \quad (21:14)$$

6. From inspection determine which rivets are most highly loaded, and find the resultant load on these rivets; this is the vector sum of the load due to moment and the load due to direct load.

The following example is given to show how the method is applied to a typical joint (see Fig. 21:10). The plate is aluminum

alloy of 0.064 in. thickness. The two upper aluminum-alloy rivets are $\frac{3}{16}$ in. in diameter and the two lower ones $\frac{1}{8}$ in. in diameter.

Bearing value of $\frac{3}{16}$ -in. rivets on 0.064-in. plate = 900 lb.

Shear value of $\frac{1}{8}$ -in. rivets = 431 lb. (assumed data).

It should be noted that in figuring the rivet values the critical value should be used. For example, the $\frac{1}{8}$ -in. rivet is weaker in shear than in bearing in this case.

It is generally more convenient to arrange the calculations in tabular form as shown below:

Tabulated Results

Rivet number	Critical value, V	d^*	Vd	r	Vr^2	Vr	Moment load	Direct load
(1)	(2)	(3)	(4)	(5)	(6)	(7)	(8)	(9)
1	900	2.0	1,800	1.19	1,274	1,071	199	364
2	900	2.0	1,800	1.19	1,274	1,071	199	364
3	431	0	0	1.68	1,216	724	135	174
4	431	0	0	1.68	1,216	724	135	174

* The reference axis is taken to be the horizontal line through the two lower rivets.

$\Sigma V = 2,662$; $\Sigma Vd = 3,500$; $\Sigma Vr^2 = 4,980$.

$$\bar{r} = \frac{3,600}{2,662} = 1.35 \text{ in.}$$

M = applied moment = $1,077 \times 0.86 = 926$ in.-lb.

The loads in column (8) were determined by multiplying the applied moment by the corresponding value in column (7) and dividing by the sum total of column (6). Thus,

$$\text{Moment load} = \frac{M(Vr)}{\Sigma Vr^2} \quad (21:15)$$

The loads in column (9) were determined by multiplying the resultant applied load by the corresponding rivet value given in column (2) and dividing by the sum total of the rivet values. Thus,

$$\text{Direct load} = P \frac{V}{\Sigma V} \quad (21:16)$$

The vectorial sums of the rivet loads are shown in Fig. 21:10.

21:8. Strength of Plate versus Strength of Rivet.—We should not use $\frac{1}{8}$ -in. rivets to join $\frac{1}{4}$ -in. plates, nor should we use $\frac{1}{4}$ -in.

TABLE 21:1.—ANC SPECIFICATIONS FOR SHEAR AND BEARING STRENGTHS
OF ALUMINUM-ALLOY RIVETS AND SHEET
(October, 1940)

Allowable Single Shear Strength of Aluminum-alloy Rivets, Lb.

Aluminum alloy	Dia. of rivet or pin, in.							
	$\frac{1}{16}$	$\frac{3}{32}$	$\frac{1}{8}$	$\frac{5}{32}$	$\frac{3}{16}$	$\frac{1}{4}$	$\frac{5}{16}$	$\frac{3}{8}$
A17ST & 56SH ($F_{su} = 27,000$ lb./sq. in.)	83	186	331	518	745	1,325	2,071	2,984
17ST ($F_{su} = 30,000$ lb./sq. in.)	92	206	366	574	828	1,472	2,300	3,313
24ST ($F_{su} = 35,000$ lb./sq. in.)	107	241	429	670	966	1,718	2,684	3,865

TABLE 21:1.—ANC SPECIFICATIONS FOR SHEAR AND BEARING STRENGTHS
OF ALUMINUM-ALLOY RIVETS AND SHEET.—(Continued)

Allowable Bearing* Strength of 17ST Aluminum-alloy Sheet, Lb.
($F_{br} = 75,000$ lb./sq. in.)

Sheet thick- ness	Dia. of rivet or pin, in.							
	$\frac{1}{16}$	$\frac{3}{32}$	$\frac{1}{8}$	$\frac{5}{32}$	$\frac{3}{16}$	$\frac{1}{4}$	$\frac{5}{16}$	$\frac{3}{8}$
0.014	65							
0.016	75							
0.018	84	126						
0.020	93	140						
0.025	117	175	234					
0.032	150	224	300	375				
0.036	168	253	337	421	506			
0.040	187	281	375	468	562			
0.045	210	316	422	527	632			
0.051	239	358	478	597	717	956		
0.064	300	449	600	749	900	1,200	1,500	
0.072	337	506	675	843	1,012	1,350	1,687	2,025
0.081	379	569	759	949	1,139	1,518	1,898	2,278
0.091	426	639	853	1,066	1,279	1,706	2,132	2,559
0.102	478	716	956	1,195	1,434	1,912	2,390	2,868
0.128	600	899	1,200	1,499	1,800	2,499	3,000	3,600
$\frac{5}{32}$	732	1,097	1,464	1,829	2,196	2,928	3,661	4,393
$\frac{3}{16}$	878	1,317	1,757	2,196	2,636	3,515	4,394	5,473
$\frac{1}{4}$	1,171	1,756	2,343	2,928	3,515	4,687	4,859	7,031

* For D/t values greater than 5.5 the allowable bearing strengths must be substantiated by tests covering both yield and ultimate strength of the joint.

rivets to join 0.020-in. plate. In the first case the rivet would shear off at a low plate stress, and in the second case the plate would tear out at a low rivet stress. It is probably desirable to design the joint so that the rivets will fail in shear before the plate fails by crushing, tearing, or shearing. Table 21:1, gives the data required to select the proper size of rivet for an assumed plate thickness.

TABLE 21:1.—ANC SPECIFICATIONS FOR SHEAR AND BEARING STRENGTHS OF ALUMINUM-ALLOY RIVETS AND SHEET.—(Continued)

Allowable Bearing* Strength of 24ST Aluminum-alloy Sheet, Lb.
($F_{br} = 90,000$ lb./sq. in.)

Sheet thickness	Dia. of rivet or pin, in.							
	$\frac{1}{16}$	$\frac{3}{32}$	$\frac{1}{8}$	$\frac{5}{32}$	$\frac{3}{16}$	$\frac{1}{4}$	$\frac{5}{16}$	$\frac{3}{8}$
0.014	78							
0.016	90							
0.018	101	151						
0.020	112	168						
0.025	140	210	281					
0.032	180	269	360	449				
0.036	202	303	405	506	607			
0.040	225	337	450	562	675			
0.045	253	379	506	632	759			
0.051	286	430	573	716	860	1,147		
0.064	360	539	720	899	1,080	1,440	1,800	
0.072	405	607	810	1,012	1,215	1,620	2,025	2,430
0.081	455	683	910	1,138	1,366	1,822	2,278	2,733
0.091	511	767	1,023	1,279	1,535	2,047	2,559	3,071
0.102	573	860	1,147	1,434	1,721	2,295	2,868	3,442
0.128	720	1,079	1,440	1,799	2,160	2,880	3,600	4,320
$\frac{5}{32}$	878	1,317	1,757	2,195	2,635	3,514	4,393	5,271
$\frac{3}{16}$	1,054	1,581	2,109	2,635	3,164	4,218	5,273	6,328
$\frac{1}{4}$	1,406	2,108	2,812	3,514	4,218	5,625	7,031	8,437

* For D/t values greater than 5.5 the allowable bearing strengths must be substantiated by tests covering both yield and ultimate of the joint.

21:9. Types and Dimensions of Rivets.—Figure 21:11 shows various types of aluminum and aluminum-alloy rivets in general use. The use and sometimes the appearance will determine the type. For example, the mushroom-head rivet would be desirable

where the head is exposed to the air stream and where the sheet is very thin. The buttonhead would be more applicable where the rivet is subjected to a tensile load. The countersunk flat-head is applicable for thick plates over which other plates must fit snugly and for outer wing smoothness.

TABLE 21:1.—ANC SPECIFICATIONS FOR SHEAR AND BEARING STRENGTHS OF ALUMINUM-ALLOY RIVETS AND SHEET.—(Continued)

Allowable Bearing* Strength of 17ST Alclad Aluminum-alloy Sheet, Lb.
($F_{br} = 68,000$ lb./sq. in.)

Sheet thickness	Dia. of rivet or pin, in.							
	$\frac{1}{16}$	$\frac{3}{32}$	$\frac{1}{8}$	$\frac{5}{32}$	$\frac{3}{16}$	$\frac{1}{4}$	$\frac{5}{16}$	$\frac{3}{8}$
0.014	59							
0.016	68							
0.018	76	114						
0.020	85	127						
0.025	106	159	212					
0.032	136	203	272	339				
0.036	153	229	306	382	459			
0.040	170	254	340	424	510			
0.045	191	286	382	478	573			
0.051	216	325	433	541	650	867		
0.064	272	407	544	679	816	1,088	1,360	
0.072	306	458	612	764	918	1,224	1,530	1,836
0.081	344	516	688	860	1,032	1,377	1,721	2,065
0.091	386	579	773	966	1,160	1,547	1,933	2,320
0.102	433	650	867	1,083	1,300	1,734	2,167	2,601
0.128	544	815	1,088	1,359	1,632	2,176	2,720	3,268
$\frac{5}{32}$	663	995	1,327	1,659	1,991	2,655	3,319	3,983
$\frac{3}{16}$	796	1,194	1,593	1,991	2,390	3,187	3,984	4,781
$\frac{1}{4}$	1,062	1,593	2,125	2,655	3,187	4,250	5,312	6,375

* For D/t values greater than 5.5 the allowable bearing strengths must be substantiated by tests covering both yield and ultimate of the joint.

21:10. Types of Riveting.—The types of riveting may be classified as follows:

1. Hand peening.
2. Automatic hammer riveting.
 - a. Electric hammer.
 - b. Air hammer.
 - c. Mechanical hammer.

TABLE 21:1.—ANC SPECIFICATIONS FOR SHEAR AND BEARING STRENGTHS
OF ALUMINUM-ALLOY RIVETS AND SHEET
(October, 1940)

Allowable Single Shear Strength of Aluminum-alloy Rivets, Lb.

Aluminum alloy	Dia. of rivet or pin, in.							
	$\frac{1}{16}$	$\frac{3}{32}$	$\frac{1}{8}$	$\frac{5}{32}$	$\frac{3}{16}$	$\frac{1}{4}$	$\frac{5}{16}$	$\frac{3}{8}$
A17ST & 56SH ($F_{su} = 27,000$ lb./sq. in.)	83	186	331	518	745	1,325	2,071	2,984
17ST ($F_{su} = 30,000$ lb./sq. in.)	92	206	366	574	828	1,472	2,300	3,313
24ST ($F_{su} = 35,000$ lb./sq. in.)	107	241	429	670	966	1,718	2,684	3,865

TABLE 21:1.—ANC SPECIFICATIONS FOR SHEAR AND BEARING STRENGTHS
OF ALUMINUM-ALLOY RIVETS AND SHEET.—(Continued)

Allowable Bearing* Strength of 17ST Aluminum-alloy Sheet, Lb.
($F_{br} = 75,000$ lb./sq. in.)

Sheet thick- ness	Dia. of rivet or pin, in.							
	$\frac{1}{16}$	$\frac{3}{32}$	$\frac{1}{8}$	$\frac{5}{32}$	$\frac{3}{16}$	$\frac{1}{4}$	$\frac{5}{16}$	$\frac{3}{8}$
0.014	65							
0.016	75							
0.018	84	126						
0.020	93	140						
0.025	117	175	234					
0.032	150	224	300	375				
0.036	168	253	337	421	506			
0.040	187	281	375	468	562			
0.045	210	316	422	527	632			
0.051	239	358	478	597	717	956		
0.064	300	449	600	749	900	1,200	1,500	
0.072	337	506	675	843	1,012	1,350	1,687	2,025
0.081	379	569	759	949	1,139	1,518	1,898	2,278
0.091	426	639	853	1,066	1,279	1,706	2,132	2,559
0.102	478	716	956	1,195	1,434	1,912	2,390	2,868
0.128	600	899	1,200	1,499	1,800	2,499	3,000	3,600
$\frac{5}{32}$	732	1,097	1,464	1,829	2,196	2,928	3,661	4,393
$\frac{3}{16}$	878	1,317	1,757	2,196	2,636	3,515	4,394	5,473
$\frac{1}{4}$	1,171	1,756	2,343	2,928	3,515	4,687	4,859	7,031

* For D/t values greater than 5.5 the allowable bearing strengths must be substantiated by tests covering both yield and ultimate strength of the joint.

rivets to join 0.020-in. plate. In the first case the rivet would shear off at a low plate stress, and in the second case the plate would tear out at a low rivet stress. It is probably desirable to design the joint so that the rivets will fail in shear before the plate fails by crushing, tearing, or shearing. Table 21:1, gives the data required to select the proper size of rivet for an assumed plate thickness.

TABLE 21:1.—ANC SPECIFICATIONS FOR SHEAR AND BEARING STRENGTHS OF ALUMINUM-ALLOY RIVETS AND SHEET.—(Continued)

Allowable Bearing* Strength of 24ST Aluminum-alloy Sheet, Lb.
($F_{br} = 90,000$ lb./sq. in.)

Sheet thickness	Dia. of rivet or pin, in.							
	$\frac{1}{16}$	$\frac{3}{32}$	$\frac{1}{8}$	$\frac{5}{32}$	$\frac{3}{16}$	$\frac{1}{4}$	$\frac{5}{16}$	$\frac{3}{8}$
0.014	78							
0.016	90							
0.018	101	151						
0.020	112	168						
0.025	140	210	281					
0.032	180	269	360	449				
0.036	202	303	405	506	607			
0.040	225	337	450	562	675			
0.045	253	379	506	632	759			
0.051	286	430	573	716	860	1,147		
0.064	360	539	720	899	1,080	1,440	1,800	
0.072	405	607	810	1,012	1,215	1,620	2,025	2,430
0.081	455	683	910	1,138	1,366	1,822	2,278	2,733
0.091	511	767	1,023	1,279	1,535	2,047	2,559	3,071
0.102	573	860	1,147	1,434	1,721	2,295	2,868	3,442
0.128	720	1,079	1,440	1,799	2,160	2,880	3,600	4,320
$\frac{5}{32}$	878	1,317	1,757	2,195	2,635	3,514	4,393	5,271
$\frac{3}{16}$	1,054	1,581	2,109	2,635	3,164	4,218	5,273	6,328
$\frac{1}{4}$	1,406	2,108	2,812	3,514	4,218	5,625	7,031	8,437

* For D/t values greater than 5.5 the allowable bearing strengths must be substantiated by tests covering both yield and ultimate of the joint.

21:9. Types and Dimensions of Rivets.—Figure 21:11 shows various types of aluminum and aluminum-alloy rivets in general use. The use and sometimes the appearance will determine the type. For example, the mushroom-head rivet would be desirable

where the head is exposed to the air stream and where the sheet is very thin. The buttonhead would be more applicable where the rivet is subjected to a tensile load. The countersunk flat-head is applicable for thick plates over which other plates must fit snugly and for outer wing smoothness.

TABLE 21:1.—ANC SPECIFICATIONS FOR SHEAR AND BEARING STRENGTHS OF ALUMINUM-ALLOY RIVETS AND SHEET.—(Continued)

Allowable Bearing* Strength of 17ST Alclad Aluminum-alloy Sheet, Lb.
($F_{br} = 68,000$ lb./sq. in.)

Sheet thickness	Dia. of rivet or pin, in.							
	$\frac{1}{16}$	$\frac{3}{32}$	$\frac{1}{8}$	$\frac{5}{32}$	$\frac{3}{16}$	$\frac{1}{4}$	$\frac{5}{16}$	$\frac{3}{8}$
0.014	59							
0.016	68							
0.018	76	114						
0.020	85	127						
0.025	106	159	212					
0.032	136	203	272	339				
0.036	153	229	306	382	459			
0.040	170	254	340	424	510			
0.045	191	286	382	478	573			
0.051	216	325	433	541	650	867		
0.064	272	407	544	679	816	1,088	1,360	
0.072	306	458	612	764	918	1,224	1,530	1,836
0.081	344	516	688	860	1,032	1,377	1,721	2,065
0.091	386	579	773	966	1,160	1,547	1,933	2,320
0.102	433	650	867	1,083	1,300	1,734	2,167	2,601
0.128	544	815	1,088	1,359	1,632	2,176	2,720	3,268
$\frac{5}{32}$	663	995	1,327	1,659	1,991	2,655	3,319	3,983
$\frac{3}{16}$	796	1,194	1,593	1,991	2,390	3,187	3,984	4,781
$\frac{1}{4}$	1,062	1,593	2,125	2,655	3,187	4,250	5,312	6,375

* For D/t values greater than 5.5 the allowable bearing strengths must be substantiated by tests covering both yield and ultimate of the joint.

21:10. Types of Riveting.—The types of riveting may be classified as follows:

1. Hand peening.
2. Automatic hammer riveting.
 - a. Electric hammer.
 - b. Air hammer.
 - c. Mechanical hammer.

3. Squeezing rivets in place.

a. Hydraulic power.

b. Air power.

c. Mechanical power.

Very little hand peening is done in aircraft work. There are various sizes of automatic hammers to fit the various sizes of

TABLE 21:1.—ANC SPECIFICATIONS FOR SHEAR AND BEARING STRENGTHS OF ALUMINUM-ALLOY RIVETS AND SHEET.—(Continued)

Allowable Bearing* Strength of 24ST Alclad Aluminum-alloy Sheet, Lb.
($F_{br} = 82,000$ lb./sq. in.)

Sheet thick- ness	Dia. of rivet or pin, in.							
	$\frac{1}{16}$	$\frac{3}{32}$	$\frac{1}{8}$	$\frac{5}{32}$	$\frac{3}{16}$	$\frac{1}{4}$	$\frac{5}{16}$	$\frac{3}{8}$
0.014	71							
0.016	82							
0.018	92	138						
0.020	102	153						
0.025	128	192	256					
0.032	164	245	328	409				
0.036	184	276	369	461	553			
0.040	205	307	410	512	615			
0.045	230	345	461	576	691			
0.051	261	391	522	653	784	1,045		
0.064	328	491	656	819	894	1,312	1,640	
0.072	369	553	738	922	1,107	1,476	1,845	2,214
0.081	415	622	830	1,037	1,245	1,660	2,075	2,490
0.091	466	699	932	1,165	1,399	1,865	2,331	2,798
0.102	522	783	1,045	1,306	1,568	2,091	2,613	3,136
0.128	656	983	1,312	1,639	1,968	2,624	3,280	3,936
$\frac{5}{32}$	800	1,200	1,601	2,000	2,401	3,202	4,002	4,803
$\frac{3}{16}$	960	1,440	1,921	2,401	2,882	3,843	4,804	5,765
$\frac{1}{4}$	1,281	1,920	2,562	3,202	3,843	5,125	6,406	7,687

* For D/t values greater than 5.5 the allowable bearing strengths must be substantiated by tests covering both yield and ultimate strength of the joint.

rivets. The hammer is usually applied to the head of the rivet with the rivet in position through a block, stationary with respect to the rivet but attached to the hammer, while the dolly bar forms the cap on the shank end of the rivet. This practice makes riveting possible in places that would otherwise be inaccessible.

The squeeze-type riveter is quite generally used in connection with very accessible work, such as in riveting small parts that may be readily moved. This type of riveting is quite rapid and generally satisfactory.

21:11. Design for Accessibility in Riveting.—In designing a riveted structure, especially of the stressed-skin type, care must

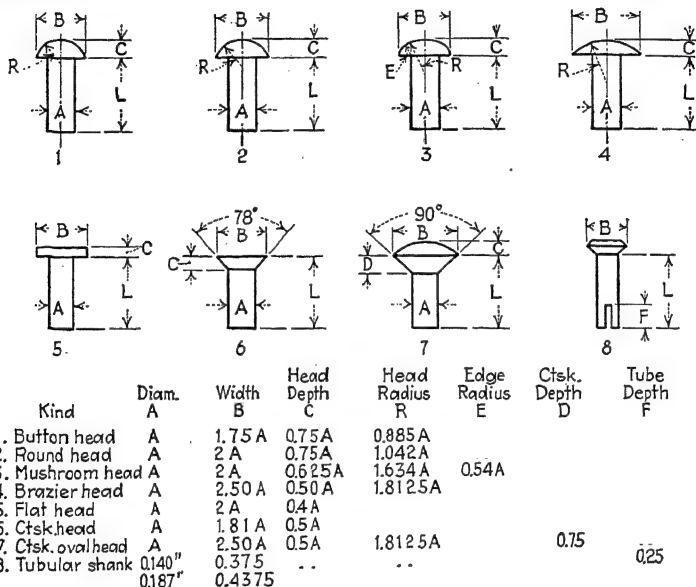


FIG. 21:11.—Common types of rivets that may be made from aluminum and aluminum alloys. (Courtesy of Aluminum Company of America; from *The Riveting of Aluminum*.)

be used that the resulting design is sufficiently simple for efficient fabrication. Riveted joints should be made as simple and accessible as possible, consistent with reasonable efficiency in strength characteristics.

In the construction of closed sections, access must be provided to the inside for bucking the rivets that close the last opening.

21:12. Riveting to Small-diameter Tube.—The strength efficiency of a tube in thin sheet-metal construction, especially where torsion is involved, outweighs the inefficiency of fabrication. Figure 21:12 shows the most common method of bucking rivets inside a tube. The steel blocks *A* and *B* slide on each other at the inclined surfaces *MN* when actuated by the rods *C* and *D*

extending from the end of the tube. This sliding action causes the shank h to decrease as the cap is formed on the rivet.

While there are many other devices for this purpose, it is sufficient for the designer to realize the possibilities so that he not be handicapped in his design.

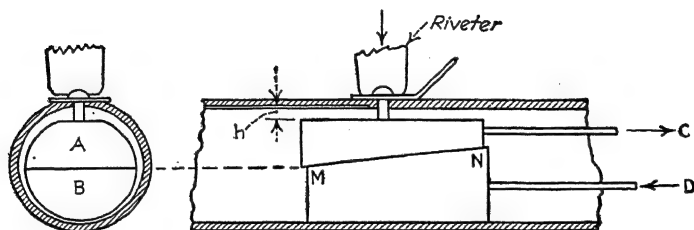


FIG. 21:12.—Riveting to the walls of a tube.

21.13. Allowance for Forming Rivetheads.—The length of shank required for forming a rivethead depends upon the type of head and size of the rivet hole. The average is specified at about twice the diameter of the shank of the rivet.

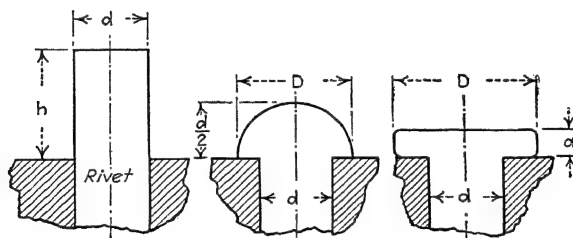


FIG. 21:13.—Shank required to form rivet head.

Upon the assumption of the size of the rivet hole and the size and type of rivethead to be made, the length of shank required may be calculated by the application of solid geometry. For example, in Fig. 21:13, the volume of the cylinder (shank) of diameter d and height h must equal the volume of the semi-sphere of diameter D . Thus

$$\frac{1}{12} \pi D^3 = \frac{\pi d^2}{4} h \quad (21:17)$$

If we require D to be $2d$, then, solving for h , we have

$$h = 2.6d \quad (21:18)$$

On the other hand, if the head is to be flat as in *c*, we have

$$\frac{\pi D^2}{4} a = \frac{\pi d^2}{4} h \quad (21:19)$$

If we require *D* to be $2d$ and *a* to be $\frac{1}{2}d$, we have

$$h = 2d$$

We have assumed that the rivet exactly fits the rivet hole and that the shank does not swell in driving except at the head.

References

1. HILBES, W.: Riveted Joints in Thin Plates (translated from the German), *N.A.C.A. Tech. Mem.* 590, November, 1930.
2. PLEINES, W.: Riveting in Metal Airplane Construction (translated from the German), *N.A.C.A. Tech. Mem.* 596, 597, 598, and 599, 1930.
3. "Structural Aluminum Handbook," Aluminum Company of America, Pittsburgh, Pa.
4. "The Riveting of Aluminum," Aluminum Company of America, Pittsburgh, Pa.

Parallel axis theorem, 88
 Performance, estimate of, 15
 Plastics, 28
 table of properties of, 29
 Plates, curved, 197, 241
 (See also Curved plate)
 flat, 232
 (See also Flat plates)
 Plywood, 28
 constructions of, 80-82
 Poisson's ratio, 34
 Polar moment of inertia, 89
 Power plant, 12
 Pressure cabin, 7
 strain analysis of, 356
 structural analysis of, 352
 window design of, 360

R

Research, structural, 59
 Rivet, shear and bearing strength of,
 tables of, 384-387
 Rivet stress calculations, 379
 Riveted butt joint, 376
 Riveted joints, eccentric load on, 381
 kinds of, 375
 Riveted lap joint, 375
 Riveting in aircraft construction,
 375
 Riveting stainless steel, 379
 Riveting web of beam, 324
 Rivets, aluminum alloy, 378
 Round tube sections, table of prop-
 erties of, 98
 Rupture, modulus of, 38

 Secondary stress, 45
 Shear, in beam, sign of, 47
 on beam, 159
 in beam web, 41
 due to tension, 35
 in skin of fuselage, 345
 in web, allowable, 44

Shear equations, table of, 182
 Shear lag, equation of, 330
 introduction to, 329
 Shear modulus of elasticity, 178
 Shear stress, in solid shaft, 180
 in various cross sections, 181
 in walls of tube, 180
 Sheet, aluminum alloy, 23
 curved (see Curved plates)
 Sheet metal construction, 196
 Shell wing, angle of twist of, 183
 Simple columns, 143
 Simple struts, 143
 Spars, distribution of load between,
 308
 trussed, 306
 Specifications of airplane, 2, 12
 Speed, high, 8
 Stainless steel, 24
 riveting of, 379
 table of, 26
 Stainless-steel columns, 281
 Static equilibrium, equations of, 102
 Statically indeterminate structure,
 107
 Steel, stainless, 24
 Steel alloy, chrome-molybdenum, 24
 table of, 25
 Steel construction, 80-82
 Steels, S.A.E. numbering of, 23
 Stiffener spacing, flat pannel, 231
 Stiffeners (see Stringers)
 Stratoliner, Boeing, 7
 Streamline tubes, properties of sec-
 tions of, 100
 Strength, design, 5
 Strength criterion of design, 9
 Stress, allowable, 34
 calculated, 34
 combined, in tubes, 262
 division of, in composite struc-
 tures, 74
 above proportional limit, 129, 150
 secondary, 45
 and strain, proportionality of, 108
 temperature, 75
 Stress formulas, basic, summary of,
 32

- Stressed-skin wing structure, design of, 224
- Stringers, angle section used as, 285
 application of, 218
 application of load to, 281
 buckling of, 219
 curved-sheet combination of, 264
 equation of, 264
 failure of, by twisting, 282
 mutual support of, with sheet, 220
 stress in, allowable, 234
 critical, 279
 stressed-skin combination, 223
 support given to, by curved sheet, 265
 with thin flat walls, 275
 types of, 219
- Structural analysis, fundamentals of, 102
- Structural flexibility, 5
- Structural research, 59
- Structural sections, properties of, 83
- Structures, composite, 74
 methods of analysis of, 114
 statically indeterminate, 107
- Strut, strength of, with bending load, 134
 with variable cross section, 152
- Supercharged cabins, 7, 352
 (*See also* Pressure cabin)
- Tangent modulus, applied to beam web design, 193
 of elasticity, 235
- Temperature stresses, 75
- Tension field, incomplete, in beam web, 326
- Tension-field web, of beam, 319
 design of, 316
- Thin-walled tubes as columns, 269
- Three-moment equation, 163, 165
 for beam column, 174
- Three-view drawing, 15
- Torsion, basic theory of, 178
 in box beam, 186, 193
 of connected cylinders, 188
- Torsion, members, analysis of, 178
 rigidity of shell wing, 183
 in round steel tubes, 259
 in round tubes, 259
 of shaft, 181
 in shell wing, 188
 of streamlined tubes, 259
 in tubes, 254-256
- Torsion equation of box wing beam, 290
- Torsion equations, table of, 182
- Torsional stress, in solid round rod, 180
 in various cross sections, 181
 in walls of tube, 179
- Tubes, bending, correction of data on, 251
 chrome-molybdenum, bending of, 251
 combined allowable stress in, 139-142
 elliptical, combined stress in, 262
 large size, thin walls (*see* Curved plates)
 mild steel, bending of, 254
 steel, column formulas for, 271
 effect of welding of, on column strength, 273
 torsion in, 259
 strength in bending of, 203
 thin walled, as columns, 269
 torsional failure of, 254
 torsional stress in walls of, 179
- V
- Vibration, damping of, 368
 of engine mount, 367
 structural, 366
- W
- Web, of beam, design of, 316
 design of rivets for, 324
 shear in, 41
 calculation of, 319
 tension stress in, 321
 nonbuckling, 325

- Flat plates, reinforced structures of,
 design of, 227
 shear in, 229
 short column range of, 228
 stiffened, 234
 stiffener combination of, 230
 stress above buckling in, 231
- Flat sheets (*see* Flat plates)
- Flexibility of structure, 5
- Flexure of a beam, 46
- Flutter, airfoil, 372
 elevator, 372
 wing, 369
- Free-body diagram, 103
- Function for three-moment equation
 for axial tension, 364
- Functions, α , β , and γ for beam columns, formulas for, 175
 table of, 176
- Fuselage, change in length of, due to
 temperature, 353
 circumferential stress due to pressure in, 354
 design, problems in, 338
 general instability failure of, 341
 monocoque, stress calculations in, 339
 pressure stress at end of, 354
 structural parts of, 338
 temperature effect on, 352
 types of failure of, 340
- Fuselage bulkhead ring, design of, 343
 least work applied to, 347

H

- H-section of extruded aluminum alloy, column strength of, 277

I

- Indeterminate structures, 107
 general equations of, 124
- Inertia, ellipse of, 92
 moment of, 87
 polar, 89
- Initial stresses in a structure, 110

- Joints, empennage to fuselage, 216
 motor mount to fuselage, 216
 riveted, 375
 wing to fuselage, 210

- Least work, analysis by, 347, 349
 applied to beams, 162
 example of, 123
 first theorem of, 118
 second theorem of, 120
 steps in method of, 122
- Load curve, integration of, 51
- Load factors, 10
- Loads on structure, 8

M

- Magnesium alloys, 26
 construction of, 80-82
 table of, 27
- Materials, comparison of properties
 of, table of, 30
 of fabrication, 17
 structural, use of, 57
- Method of successive approximations, 157
- Modulus, of elasticity, 33
 effective, 277
 of rupture, 38
- Moment, bending, on beam, 159
- Moment distribution, Hardy Cross
 method of, 160
- Moment equation, 51
 general, 50
- Moments of inertia, 83, 87
 of an airfoil section, 95
 of wing section, 63
- Monocoque, distribution of stress in, 206
- Monocoque structures, fittings in, 204
- Motor mount, 216